Authors: Beno, Carl J[1]., Bowman, John R[1]., Kitajima, Kouki[2], Valley, John W[2]., Loury, Patrick C[3]., Tapanila, Lorraine M[4]

Title: Asynchronous infiltration-driven growth of forsterite and periclase during metamorphism in marbles of the inner Alta aureole, Utah: $\delta^{18}O$ and textural records of oxygen isotope disequilibrium, rapid forsterite growth and permeability evolution

Affiliations:

1) Department of Geology and Geophysics, University of Utah, Salt Lake City, UT, USA
2) Department of Geoscience, University of Wisconsin, Madison, WI, USA
3) Prime Mining Corp., Vancouver, BC, Canada
4) Department of Geosciences, Idaho State University, Pocatello, ID, USA

Corresponding Author Email: carl.beno@utah.edu

ORCID ID: 0000-0001-7611-1602

Abstract:

Infiltration-driven metamorphism has produced the widespread development of forsterite in the siliceous dolomites of the Alta, Utah contact aureole. SIMS (secondary ion mass spectrometry) $\delta^{18}O$ analyses show that in most of the middle to outer forsterite zone samples, forsterite, calcite and dolomite are homogenous in $\delta^{18}O$ at the grain-scale, but forsterite and calcite exhibit minor intergranular heterogeneities of <1‰ on the thin-section to hand sample scales. Within ~300m of the igneous contact (inner forsterite and periclase zones), grain-scale $\delta^{18}O$ heterogeneities in forsterite are as large as 3.0‰, but forsterite crystals do not exhibit systematic center-to-edge decreases in $\delta^{18}O$ due to skeletal growth and infilling. With one exception, forsterite, calcite and dolomite in all samples analyzed yield disequilibrium fractionations. The trend of increasing numbers of progressively smaller forsterite crystals and the increase in temperature toward the contact with the Alta stock is interpreted to record increased reaction overstepping, and an increased role of nucleation rate relative to growth rate during the formation of forsterite, toward the igneous contact. The oxygen isotope disequilibrium commonly recorded among forsterite, calcite and dolomite may reflect the rapid growth of forsterite or result from $^{18}O/^{16}O$ depletion in the matrix carbonate minerals during continued fluid infiltration after forsterite crystallization was complete, during the initial stages of cooling in the forsterite zone.

In a traverse across the boundary between forsterite- and periclase-bearing marble layers in the periclase zone, forsterite and calcite SIMS $\delta^{18}O$ profiles combined with the trend in forsterite textures indicate that both layers were not infiltrated simultaneously, nor continuously during both prograde reactions responsible for forsterite and periclase. Rather, the texture and SIMS data require infiltration and formation of forsterite first in the forsterite marble layer, followed by infiltration and formation of periclase in the periclase marble layer. As a consequence, the $\delta^{18}O$ profile recorded by forsterite formed earlier than the $\delta^{18}O$ profile recorded by calcite, but both profiles are prograde features—that is, both profiles formed in response to prograde reactions forming first forsterite and then periclase. These grain-scale $\delta^{18}O$ profiles further suggest that these layers experienced significant changes in permeability that are linked to their sequential infiltration-reaction history.

Keywords: forsterite, calcite, dolomite, oxygen isotopes, SIMS, asynchronous growth

DECLARATIONS:

Funding: University of Utah Geological Studies; National Science Foundation Grant EAR-1853806. WiscSIMS is supported by NSF (EAR-2004618) and the University of Wisconsin-Madison).

Conflict of Interest: The authors declare that they have no conflict of interest.
Availability of data and material: Additional data available in electronic supplementary files.
Code availability: Not Applicable
Acknowledgements: The authors thank Mike Spicuzza for assistance with laser fluorination data collection; Mike Spicuzza and Brian Hess for assistance with sample preparation prior to SIMS analysis; Clay Jones and Joseph Moore for access to the SEM at the Energy and Geoscience Institute; Barbara Nash and Wil Mace for assistance with EMPA work. Support from National Science Foundation Grant EAR-1853806 and the Miller-Uffens fund are gratefully acknowledged.

INTRODUCTION

Contact metamorphic environments provide important natural laboratories to investigate fundamental processes related to infiltration driven metamorphism of carbonate rocks (Kerrick 1991). Reaction and transport kinetics may be especially important during contact metamorphism because changes in temperature (T) and $X(CO_2)$ are important drivers of reaction overstepping for decarbonation reactions (multiple references in Kerrick 1991). In particular, large and rapid changes in $X(CO_2)$ is expected to accompany fluid infiltration episodes and drive significant reaction overstepping (Ferry et al. 2011).

Textures and isotopic compositions of product and reactant phases involved in metamorphic decarbonation reactions record the roles of reaction kinetics and rates of isotope redistribution during contact metamorphism. Several studies have documented textural evidence for rapid, kinetically-influenced crystallization of forsterite in contact metamorphic marbles (Holness et al. 1991; Roselle et al. 1997; Beno et al. 2020). Beno et al. (2020) documented crystal habit, crystal surface features and aggregate texture evidence consistent with dendritic crystallization and skeletal infilling of forsterite crystals in marbles of the Alta, Utah contact aureole. On a mm, multi-grain scale, a number of studies have found that reaction products are out of oxygen isotope exchange equilibrium with reactants (Eppel and Abart 1997; Graham et al. 1998; Matthews et al. 1999; Roselle et al. 1999; Valley 2001; Lackey and Valley 2004; Müller et al. 2004; Pollington et al. 2005; Ferry et al. 2010; Ferry et al. 2014). Müller et al. (2004) documented oxygen isotope equilibrium between the reaction products forsterite and calcite, and disequilibrium of both phases with the reactant dolomite in marbles of the Ubehebe Peak, CA aureole. Using this isotope evidence together with mass balance considerations, they proposed that forsterite formed from the metastable reaction: dolomite + SiO_2 = forsterite + calcite + CO_2. At this time, only a few studies (particularly Ferry et al. 2011) have combined both textures and SIMS stable isotope data to investigate the interplay between reaction rates and the rates of oxygen transport and isotope exchange during infiltration-driven metamorphism of carbonate rocks.

In this study, we use high-resolution secondary ion mass spectrometry (SIMS) to analyze the oxygen isotope compositions of forsterite, calcite, and dolomite in marbles across the forsterite and periclase zones in the Alta aureole. We use these results to evaluate the extent of grain-scale heterogeneity of oxygen isotopes in variably refractory phases (forsterite vs. carbonates), and to evaluate the degree of oxygen isotope exchange equilibrium among these minerals. Combination

of these SIMS $\delta^{18}O$ analyses and forsterite textural data (Loury 2014; Beno et al. 2020; Chadwell 2020; this study) provide insights into forsterite growth rates relative to rates of oxygen transport and isotope exchange during forsterite petrogenesis in the Alta aureole and the possibility of continued isotope exchange of the carbonate phases after completion of forsterite crystallization.

Determining the relative timing of decarbonation reactions—and hence formation of index minerals—particularly at the bedding-scale, at which textural and reaction progress measurements are made, is important to improve quantitative understanding of infiltration-driven contact metamorphic processes. The distribution of index mineral zones developed in marbles in a contact aureole can be understood to result from a combination of increase in temperature (T) and fluid infiltration-induced decrease in $X(CO_2)$ toward the igneous contact over time. The relative timing of the decarbonation reactions responsible for these index mineral zones at the aureole-scale does not necessarily follow in the order predicted by an equilibrium phase diagram from these changes in T and $X(CO_2)$. Heat flow modeling of contact aureoles (Furlong et al. 1991; Cook et al. 1997; Cui et al. 2001; Nabelek et al. 2012) has shown that maximum temperatures are achieved at progressively later times at progressively greater distances into the aureole; that is, the T-time(t) paths for the different mineral zones making up the aureole will be different. As a result, the highest-grade reaction (i.e., to form periclase) could complete development of the periclase zone and this zone could be cooling, as lower-grade reactions (i.e., to develop forsterite, tremolite or talc) are still advancing or have yet to start in the outer aureole.

However, at the scale of an outcrop, the thermal histories (T-time paths) of two adjacent and compositionally-distinct bedding layers (cm to m scale)—for example, adjacent layers of periclase + calcite marble and forsterite + calcite marble within the inner aureole—will be the same. Hence whether periclase or forsterite forms first in their respective lithologies is a function of the fluid infiltration histories of the adjacent layers—which may be different. The default assumption is that both layers had the same permeability and were infiltrated at the same time. However, it is not apparent that the periclase + calcite and forsterite + calcite marble layers, which have distinct bulk composition and reaction history, necessarily have the same permeability. A reasonable assumption could be that the forsterite marble layer, because it may have experienced previous reactions to create talc and tremolite, possible pre-cursor reactants to form forsterite, may have the higher permeability. However, Brennan (1991) has emphasized the transient nature of permeability at the timescales of aureole petrogenesis, as permeability enhanced by a decarbonation reaction is substantially and rapidly reduced after the reaction ceases by compaction and recrystallization of the carbonate rock matrix at elevated water pressure and increasing T. Hence it is not clear which layer has the greater permeability, and therefore which layer is infiltrated first.

Consideration of mineralogy and reaction progress based on the appropriate phase equilibrium topology alone is not sufficient to resolve the timing of mineral reactions, as will be demonstrated later in the Discussion. The extent of $^{18}O/^{16}O$ depletion of a marble layer is a measure of the total fluid flux of lower $\delta^{18}O$ fluid experienced by that layer (Bowman et al. 1994), but $\delta^{18}O$ values alone do not provide constraints on the relative timing of this infiltration-induced $^{18}O/^{16}O$ depletion. In this study, we document forsterite textures and SIMS $\delta^{18}O$ profiles from forsterite, and utilize the SIMS $\delta^{18}O$ profile defined by calcite from Bowman et al. (2009) on a cm-scale traverse across the boundary between adjacent periclase + calcite and forsterite + calcite marble layers in the periclase zone of the Alta aureole. The combination of textural and SIMS $\delta^{18}O$ data

allow reconstruction of the infiltration and reaction history in the periclase zone, and highlight the connection between infiltration-driven decarbonation reactions and transient permeability.

Geologic Setting and Previous Work

The Alta granodiorite stock is one of several Mid-Tertiary intrusive rocks that make up the Wasatch Igneous Belt exposed in an east-west trending sequence in north-central Utah (Fig. 1; Wilson 1961; Baker et al. 1966; John 1989; Vogel et al. 2001; Stearns et al. 2020). The stock has intruded and contact metamorphosed a series of Precambrian to Paleozoic sedimentary rocks. The carbonate wallrock strata (Maxfield, Fitchville, Deseret, and Gardison formations) primarily consist of siliceous dolomites with sparsely disseminated quartz, or chert nodules in a dolomite matrix. Metamorphism of the siliceous dolomites has produced the prograde isograd sequence: talc, tremolite, forsterite, and periclase toward the igneous contact with the Alta stock (Moore and Kerrick 1976; Cook 1992).

Previous studies (Moore and Kerrick 1976; Cook and Bowman 2000) have shown that a combination of prograde heating and infiltration of water-rich fluids has driven the formation of forsterite and calcite in the Alta aureole by either the breakdown of tremolite and dolomite, which is predicted by equilibrium phase petrology (Skippen 1974; Berman 1988), or by the metastable breakdown of dolomite and quartz, if overstepping of the tremolite forming reaction is large (Müller et al. 2004). A variety of field observations and data indicate that the formation of the periclase zone is closely linked to infiltration of water-rich fluids near the thermal peak of metamorphism. Some of these features are illustrated qualitatively in a schematic cross-section in Fig. 2a and quantitative constraints for different locations within the aureole are also listed in Fig. 2b (Cook et al. 1997; Cook and Bowman 2000). Thermometry applied to coexisting calcite-dolomite pairs in the south aureole have defined peak metamorphic temperatures of ~575ºC at the periclase isograd to ~625ºC at the igneous contact (Cook and Bowman 1994). Periclase formation in dolomite-bearing marbles is always accompanied by large $^{18}O/^{16}O$ depletion of the marbles which requires infiltration of significant amounts of both H_2O-rich and low-$\delta^{18}O$ fluids. The periclase-forming reaction goes to completion in these rocks which is recorded by the lack of remaining primary dolomite and the low-$\delta^{18}O$ values preserved in matrix calcite from these marbles (Bowman et al. 1994; Cook et al. 1997). Field observations and $\delta^{18}O$ analyses show that lenses of high $\delta^{18}O$ dolomite marble are interlayered with low $\delta^{18}O$ periclase marble within the periclase zone (Fig. 2). As these m-scale interlayers at the same distance from the igneous contact have the same thermal history, their interlayering and the connection between periclase formation and significant $^{18}O/^{16}O$ depletion demonstrate that without the infiltration of both H_2O-rich and lower $\delta^{18}O$ fluid, periclase does not form in the dolomite-bearing marble wallrocks. The close correlation between development of periclase directly from dolomite and $^{18}O/^{16}O$ depletion in the periclase marbles of the inner Alta aureole (Cook et al., 1997; Cook and Bowman, 2000) demonstrates that the formation of periclase is controlled primarily by the infiltration of low $\delta^{18}O$, H_2O-rich fluids while the marbles were hot (at least ~575ºC), based on calcite-dolomite thermometry (Cook and Bowman 1994).

Periclase marbles record isotopic and textural evidence for retrograde reaction and continued fluid flow during cooling. Secondary dolomite rims brucite pseudomorphs of periclase and occurs as micro-veins (Cook and Bowman 2000). Optically 'turbid' calcite (porous and containing dolomite exsolution blebs) replaces optically 'clear' (primary) calcite along fractures, cleavages and grain

margins. This turbid calcite and the secondary dolomite have highly variable and lower oxygen isotope ratios compared to 'clear' calcite (Bowman et al. 2009). The Mg contents of calcite in some periclase zone marbles near the igneous contact also suggest retrograde reaction during cooling (Cook and Bowman 1994). Forsterite in both the periclase and forsterite zone marbles is commonly serpentinized to varying degrees along fractures and grain margins (Beno et al. 2020). All of these retrograde features were avoided in locating SIMS spot analyses for this study.

METHODS

Sampling, textures, and imaging

Marble samples were selected from an existing collection of samples from the southern aureole to create a traverse through the periclase and forsterite zones (Fig. 1). Both polished thin sections and forsterite grain mounts were prepared for ion microprobe (SIMS) oxygen isotope analysis of forsterite, calcite and dolomite. Forsterite grain mounts were prepared by first isolating forsterite crystals from their carbonate host by acid digestion (2-5% HCl) followed by gentle sieving. Both thin sections and grain mounts were imaged on the SEM. All SEM images shown in this study were collected on a JEOL JSM-IT300 located at the Energy and Geoscience Institute at the University of Utah. Textural data were collected from QEMSCAN (Loury, 2014) and electron microprobe (EMPA) Ca Kα X-ray maps (Chadwell 2020). The CAMECA SX-50 microprobe and QEMSCAN instruments are both housed in the Geology and Geophysics department at the University of Utah.

Bulk oxygen isotope analyses

Millimeter-scale samples of carbonate matrix were collected using a dental drill. Approximately 100 μg aliquots from each powdered sample were placed in sample vials, which were flushed with Ultra High Purity (UHP) Helium for approximately 5 minutes at 50 ml/min He to remove atmospheric CO_2 before analysis. The samples were then reacted with anhydrous phosphoric acid (H_3PO_4) at 75°C to generate CO_2 gas for mass spectrometric analysis. The $\delta^{18}O$ and $\delta^{13}C$ (see electronic supplement 1 for the $\delta^{13}C$ values) values of these samples were measured using the Finnigan-MAT Gas Bench II interface coupled with a Delta Plus gas source mass spectrometer (GSMS) in the University of Utah's Stable Isotope Ratio Facility for Environmental Research (SIRFER). A detailed description of the Gas Bench II interface analysis method for carbonate samples is provided by Breitenbach and Bernasconi (2011). NBS19, NBS18, LSVEC, and Carrara marble were used as standards for these isotope analyses.

Bulk forsterite $\delta^{18}O$ data were collected using the mineral separates generated from Alta marbles. The HCl-insoluble material (mostly forsterite with minor but variable amounts of sulfide, phlogopite, and serpentine) were cleaned and sieved into five different crystal size fractions (>853 μm, 853-420 μm, 420-178 μm, 178-106 μm, and 106-75 μm). Each size fraction was then subjected to a reagent grade HF treatment (48%) for ~6 minutes at ~25°C to remove retrograde serpentine. Laser fluorination techniques (Sharp 1990; Valley et al. 1995) were used to liberate O_2 from the forsterite separates at the Department of Geoscience Stable Isotope Laboratory, University of Wisconsin-Madison. The O_2 gas was converted to CO_2 by reaction with graphite at 800 °C and the oxygen isotope ratio of the CO_2 was analyzed with a Finnigan-MAT 251 mass spectrometer. The $\delta^{18}O$ values of forsterite samples were determined with a reproducibility of better than $\pm$0.1‰ (2SD) by regular analysis of the UWG-2 garnet reference material ($\delta^{18}O$ = 5.80% VSMOW; Valley et al. 1995).

Grain-scale oxygen isotope analyses

Forsterite, calcite, and dolomite $\delta^{18}O$ values were measured on a CAMECA IMS-1280 large-radius, multi-collector secondary ion mass spectrometer (SIMS) at the University of Wisconsin-Madison WiscSIMS laboratory using sample preparation and analysis procedures outlined elsewhere (Kita et al. 2009; Valley and Kita 2009; Wang et al. 2014). The SIMS analysis was performed in two separate analytical sessions under the same conditions. The $^{133}Cs^{+}$ primary ion beam (20 keV total impact energy) was focused to a 10 µm diameter on the sample surface. Charge neutralization was achieved using an electron flood gun and an ~50 nm gold coat on the sample surface. Sputtered O^{-} secondary ions are accelerated into a double-focusing mass spectrometer at 10 kV where they are sorted by mass/charge before reaching the detector array. Three Faraday cups were used for $\delta^{18}O$ and "water" measurements ($^{16}O^{-}$, $^{18}O^{-}$, and $^{16}O^{1}H^{-}$). UWG-2 garnet ($\delta^{18}O$ = 5.80‰, VSMOW; Valley et al. 1995) and UWC-3 calcite ($\delta^{18}O$ = 12.49‰, VSMOW; Kozdon et al., 2009) reference materials were included in forsterite grain mounts or face mounted into thin section rounds prior to analysis. All unknowns analyzed were within 5 mm of the associated reference material and the center of the mount. The running standard was analyzed four times before and after every 7-12 unknown analyses to correct for any small amounts of instrumental drift during the analytical runs. Analytical precision is reported as two standard deviations of the bracketing standard analyses (typically N = 8) and averaged ±0.3‰ across all analytical sessions.

Matrix effects (Hervig et al. 1992; Eiler et al. 1997) cause systematic instrumental mass fractionation (IMF) which were evaluated with a suite of standards at the beginning of each session to generate a calibration curve relative to the running standards (Kita et al. 2010; Page et al. 2010; Śliwiński et al. 2016). Corrections applied throughout the runs based on evaluation of these running standards were: Fo = ~4 to 4.5‰, Cal = ~-6.5‰, Dol = ~-11.5‰. EMPA analyses performed after SIMS data acquisition revealed that all three phases analyzed have very low iron contents; less than 2 mole % in olivine, 0 mole % in calcite and <<0.005 mole % in dolomite, so no corrections for iron were applied on a spot-by-spot basis. In the first session, all forsterites were corrected against San Carlos olivine (Fo_{89}) because there was no resolvable difference between Fo_{89} and Fo_{100}. A few analyses were excluded based on large increases in the $^{16}O^{1}H^{-1}$ ion counts relative to counts on the running standards and the norm for the unknowns; these increases occurred mostly in forsterite, and were attributed to contributions from serpentine minerals intersected on fractures below the polished surface, or inadvertent analysis of clinohumite. Additional quality control was conducted post analysis by imaging individual SIMS pits to identify any intersection with mineral inclusions or serpentinized fractures (in the case of forsterite). All sample and standard data, including excluded data and the reasons for their exclusion, are reported in electronic supplementary material 2 and 3. Isotope ratios are normalized relative to VSMOW and are reported in standard $\delta^{18}O$ notation.

$\delta^{18}O$ population statistics

A focus of this study was to document grain-scale $\delta^{18}O$ heterogeneities in samples from the aureole, as well as any intergranular variability within samples. Consequently, the terms "homogeneous" and "heterogeneous" were defined quantitatively using statistical approaches outlined by Mahon (1996). A sample, or grain, was judged to be "homogeneous" if all analyses from a given sample, or grain, were consistent with a single oxygen isotope ratio within a 95% confidence interval defined by the mean square weighted deviate (MSWD; Wendt and Carl, 1991;

Mahon 1996). This approach may produce spurious results from populations when n (number of analyses) < 4 (Mahon 1996) so these parameters were only applied on grains with n > 4. Grains with four or fewer spot analyses were evaluated within each given sample, and can only be assessed as "homogeneous" or "heterogeneous" based on the calculated SIMS value and the uncertainty associated with the measurement. Statistical calculations were performed using Microsoft Excel and IsoplotR (Vermeesch 2018).

RESULTS

Aureole- and bedding-scale textural variability

Forsterite textures (Fig. 3) vary generally across the inner Alta aureole from abundant small crystals in marbles close to the igneous contact to fewer and larger crystals in marbles near the forsterite-in isograd (Loury 2014; Beno et al. 2020). At any given lateral distance from the contact, there is variation in the abundance and average size of forsterite crystals in different stratigraphic horizons (e.g., Fig. 3a and b; Fig. 3e and f). Even within a single stratigraphic or bedding layer, textures can vary significantly. Additionally, the morphology of individual forsterite crystals can vary widely from euhedral grains to tabular crystal centers with skeletal margins (see Beno et al. 2020 for details) within any given stratigraphic horizon (Fig 3f).

Dolomite and calcite in the rock matrix generally increase in grain size toward the igneous contact owing to recrystallization induced by heat and fluid infiltration. The abundance of organic matter in the carbonate protolith also progressively decreases. These textural changes are quite distinct by the transition into the forsterite zone and are suggestive of pervasive fluid-infiltration on the scale of individual grains. Dolomite generally decreases in abundance as the contact is approached (Fig. 3) as it is a reactant phase for the production of the index minerals defining the metamorphic zones of the Alta aureole (Cook and Bowman 2000). Dolomite abundance at any given distance from the igneous contact can vary widely between individual stratigraphic units in the periclase and inner forsterite zones (Fig. 3a-b; Fig. 3e-f) as a result of both original variations in the bulk composition (principally SiO_2 content) of these marble protoliths and also owing to variation in the infiltration histories of individual stratigraphic horizons (Cook and Bowman 2000; Bowman et al. 2009). Calcite in samples >300m from the contact commonly occurs as coronas rimming forsterite crystals (Fig. 3c-f), while in forsterite-bearing samples at ~300m from the igneous contact and closer, calcite dominates and little or no primary dolomite remains (Fig. 3a-b).

Oxygen isotope ratios of forsterite, calcite and dolomite

The $\delta^{18}O$ values of forsterite were determined by SIMS in this study and by laser fluorination (LF) techniques in Loury (2014); forsterite was analyzed by both techniques in eight samples (Table 1) and results from four are highlighted in Fig. 4. Forsterite SIMS analyses from grain mounts are summarized in Fig. 5, while coexisting forsterite, calcite, and dolomite measurements performed in three thin-sections from the forsterite zone are summarized in Fig. 6.

Forsterite from two samples investigated (B-7-1 [Fig. 5] and 99V-3 [Fig. 6]) show slight variability in their $\delta^{18}O$ value (~1‰) when all analyses are considered from all grains. However, when population statistics (Mahon 1996) are performed on individual grains from each sample, all grains are internally consistent with a single $\delta^{18}O$ value within the 95% confidence interval (Fig. 5; Fig. 6). Thus, forsterite crystals in these samples have small intergranular $\delta^{18}O$ heterogeneities but

exhibit intragranular $\delta^{18}O$ homogeneity. Both samples are from marbles that have not experienced significant $^{18}O/^{16}O$ depletion (>>20‰ carbonate $\delta^{18}O$ value; Tables 2, 3).

Samples with homogeneous forsterite oxygen isotope ratios are also found in the forsterite zone (88-7, FZ7-6, A-4-1, FZ9-18, FZ4-5a; Fig. 5; Fig. 6). All of these samples are from marbles that are located at and beyond 230m from the igneous contact, have not experienced significant $^{18}O/^{16}O$ depletion (>>20‰ carbonate $\delta^{18}O$ value; Tables 2, 3), and have a significant percentage of primary dolomite remaining in the host rock.

In three forsterite bearing marbles covering most of the width of the Fo zone, coexisting calcite and dolomite were analyzed in polished thin section with SIMS to constrain the grain-scale $\delta^{18}O$ behavior of the two carbonate phases with respect to forsterite (Fig. 6). Dolomite was found to be homogeneous in two of these three samples (A-4-1 and 99V-3; Table 3; Fig. 6) while the third (FZ4-5a) shows only minor $\delta^{18}O$ variation (0.7‰; Table 3, Fig. 6). Calcite in all three samples exhibits small (≤1‰ variation within any sample; Table 3; Fig. 6) intergranular heterogeneities at the thin section-scale, but most crystals analyzed exhibit intragranular $\delta^{18}O$ homogeneity.

In sample 99V-3 (615m from contact), a SIMS analytical traverse was made from the interior of a forsterite crystal through the surrounding calcite corona and into the dolomite matrix (Fig. 7; Traverse 1). All three phases are homogeneous in $\delta^{18}O$ along this traverse, and yield local oxygen isotope fractionation factors of $\Delta^{18}O_{Cal\text{-}Fo}$ = 3.2‰, $\Delta^{18}O_{Dol\text{-}Fo}$ = 3.0‰, and $\Delta^{18}O_{Dol\text{-}Cal}$ = -0.2‰.

Two crystals that show large grain-scale heterogeneities are highlighted in Fig. 8. The edges of heterogenous crystals documented in this study generally have lower $\delta^{18}O$ values (Fig. 8a, sample 94I-9-2b; Fig. 8d, sample 88-8). However, these crystals commonly do not exhibit systematic heavy-to-light $\delta^{18}O$ zoning from center to edge. For example, the crystal illustrated in figure 8a exhibits a complex pattern of increases and decreases in $\delta^{18}O$ along the traverse A-A' (Fig. 8b). Both these samples are from within 230m of the igneous contact and have experienced moderate to significant $^{18}O/^{16}O$ depletion.

Interstratigraphic textural and $\delta^{18}O$ variability in the periclase zone

Bowman et al. (1994) and Cook et al. (1997) showed that at any given location within the periclase zone, the $\delta^{18}O$ values of calcite in individual bedding layers within the marbles could vary considerably (from ~11 to 21‰). This isotopic variation was ascribed to variable infiltration histories for these adjacent marble layers resulting from the bedding-controlled, down temperature flow regime operating within the inner aureole. As an example, sample 94I-9-2d, a periclase (brucite) + calcite marble located ~150m from the igneous contact, contains no primary dolomite and has a low $\delta^{18}O$(Cal) value (~12‰; Bowman et al. 2009), evidence for extensive fluid infiltration. In contrast, sample 23-B is located only 25m from the contact but preserves primary dolomite and has a high $\delta^{18}O$ (23.2‰) approaching those of outer forsterite zone samples with abundant primary dolomite (Table 1), indicating that this sample has experienced substantially less infiltration of lower-$\delta^{18}O$ fluids than other marble beds within the periclase zone.

Bowman et al. (2009) documented with SIMS analyses that the $\delta^{18}O$ values of calcite within the upper ~6 cm of a calcite + forsterite marble (layer 8, $\delta^{18}O$ = ~18‰; sample 94I, 150m to contact) decreased systematically along a traverse toward the boundary with overlying layer 9 (lower $\delta^{18}O$;

~12‰), a periclase (brucite) + calcite marble (Fig. 9a). Forsterite SIMS data were collected along this same traverse to complement this calcite SIMS dataset (sample 94I-9-2; Fig. 9a). Forsterite crystals were analyzed from three intervals along this traverse (2a, 2b and 2c, Fig. 9a) to get a nearly complete profile of forsterite oxygen isotope ratios. No forsterite remains in the marble within ~2.5 cm of the layer 8/9 boundary, as it is replaced by humite (i.e., between the humite-in boundary and the overlying layer 9 periclase marble; Fig. 9). Forsterite crystal locations were precisely measured and superimposed on the existing calcite zoning profile to identify any systematic variation in forsterite $\delta^{18}O$ values with respect to the $\delta^{18}O$ values of spatially-correlated calcite along this traverse (Fig. 9a).

Both forsterite oxygen isotope ratios and forsterite textures vary systematically as the layer 8/9 boundary is approached. Forsterite textures vary considerably across the short distance (~4 cm) between horizons 2a (Fig. 10a) and 2c (Fig. 10b). Forsterite becomes coarser and there are fewer forsterite crystals/mole forsterite (a decrease in crystal number density; Ferry et al. 2011) in horizons closer to the layer 8/9 boundary. Forsterite in all three intervals (2a, 2b, 2c) is characterized by grain-scale isotopic heterogeneity of as much as 3.0‰ (Fig. 11b-f), but relatively homogeneous grains were also identified in all three horizons. In many cases the grain-scale zoning is highly irregular with no clear systematic variation in $\delta^{18}O$ from grain interior to grain edge (Fig. 11c-d). In general, the average $\delta^{18}O$ values of the forsterite crystals increase across this traverse, opposite the significant decrease in $\delta^{18}O$ values of the calcite (Fig. 9a). As a result, the range of calcite-forsterite fractionation factors calculated as the layer 8/9 boundary is approached go from values slightly less than +4‰ in sample 2a (near the expected equilibrium value of +4.5‰ at the estimated T = 570°C; Fig. 9b; Chiba et al. 1989) to much lower, even negative (reversed) values down to -4.2‰ in sample 2c (Fig 9b).

Aureole-scale variations in $\delta^{18}O$ values and mineral fractionation factors

The carbonate $\delta^{18}O$ values determined by both SIMS and GSMS for the forsterite and periclase zone samples (Fig. 12a) are consistent with values determined by conventional acid digestion methods for these zones by previous studies (Bowman et al. 1994; Cook et al. 1997). Within ~300m of the igneous contact the $\delta^{18}O$ values of the carbonate minerals are less than ~24‰, ranging to as low as 11.7‰. Bulk carbonate samples beyond 300m from the igneous contact normally fall within the $\delta^{18}O$ range of ~23‰ to 26‰. These values are ~0 to 4‰ lower than the $\delta^{18}O$ values of dolomite (+26 to +30‰) from dolostones in the outermost aureole (Cook et al. 1997) and from the unmetamorphosed protoliths of the marbles (Brenner 2018; Brenner et al. 2021; Bowman and Beno, unpublished data). With the exception of sample 94I, SIMS $\delta^{18}O$ values of forsterite generally mirror the $\delta^{18}O$ values of carbonate minerals on the aureole-scale (Fig. 12a). Beyond ~300m from the igneous contact, the $\delta^{18}O$ values of forsterite vary over a narrow range of 21.4‰ to 22.9‰. Within 300m, forsterite $\delta^{18}O$ values are generally lower and much more variable, ranging from 13.0‰ to 22.7‰ (Table 3).

In three samples covering most of the width of the Fo zone (Fig. 6), SIMS analyses show that at the scale of a thin section, forsterite, calcite and dolomite crystals can be at least slightly heterogenous in $\delta^{18}O$ from grain to grain (< 1‰). Accordingly, the resulting fractionation factors can vary. For example, in sample FZ4-5a, the SIMS results record the following ranges: $\Delta^{18}O_{Cal-Fo}$ = 2.6 to 3.5‰, $\Delta^{18}O_{Dol-Fo}$ = 2.4 to 3.1‰, $\Delta^{18}O_{Dol-Cal}$ = -1.1 to 0.5‰. Fractionation factors calculated from SIMS data from homogeneous crystals of forsterite, calcite and dolomite along a

single traverse in a thin section (sample 99V-3, Figs. 6, 7) yield similar values for these fractionation factors: $\Delta^{18}O_{Cal-Fo}$ = 3.2‰, $\Delta^{18}O_{Dol-Fo}$ = 3.0‰, $\Delta^{18}O_{Dol-Cal}$ = - 0.2‰.

To evaluate the behavior of mineral-mineral oxygen isotope fractionation at the aureole-scale, the fractionation factors for forsterite-calcite(dolomite) pairs are plotted as a function of distance in Figure 12b. Forsterite is consistently out of oxygen isotope exchange equilibrium with associated carbonate minerals in the middle to outer Fo zone, regardless of the dominant carbonate mineralogy (Fig. 12b). In the three samples where SIMS data are available for all three minerals (A-4-1, FZ4-5a and 99V-3; Fig. 6), all three measured fractionation factors are smaller than those expected from exchange equilibrium values (Chiba et al. 1989; Zheng et al. 1994), based on their distance from the contact and existing calcite-dolomite geothermometry data from the aureole (Cook and Bowman 1994). In addition, the $\Delta^{18}O_{Dol-Cal}$ factor can be negative or reversed (e.g., in 99V-3, Fig. 7). Across the entire Fo zone and into the Per zone, $\Delta^{18}O_{Carb-Fo}$ values are generally much smaller than expected equilibrium values, and often exhibit significant variations, especially within ~300m of the igneous contact (Fig. 12b). Variations in the fractionation factors result primarily from isotopic heterogeneities in the forsterite crystals (see sample 88-8; Fig. 8d, Fig. 12a). In only two samples (94I-9-2 [horizon 2a] and 88-8; Fig. 12b) do the measured ranges of fractionation factors approach closely or reach values corresponding to oxygen isotope exchange equilibrium with the surrounding carbonate matrix. Both of these samples are located within 300m of the igneous contact, have experienced significant depletion of the calcite matrix, lack any primary dolomite, and exhibit grain-scale $\delta^{18}O$ heterogeneities in forsterite. As a result, only one sample (88-8) gives calculated temperatures from $\Delta^{18}O_{Cal-Fo}$ that are consistent with calcite-dolomite solvus thermometry results (Cook and Bowman 1994; Table 3).

DISCUSSION

Mechanisms of infiltration and the nature of permeability

Regarding the mechanisms of fluid infiltration into these marbles, several lines of evidence suggest that fluid propagated along grain boundaries because of grain boundary wetting, rather than propagation of fractures due to fluid overpressure. The former mechanism further implies the existence of interconnected porosity at the grain scale to produce the necessary permeability for fluid infiltration. There is very limited evidence at outcrop or bedding/layering scale for fracture induced permeability—the existence of small (<1-2 cm wide) micro-veinlets of calcite originating in one layer and penetrating for a short distance (a few cm's) into an adjacent layer. However, the vast majority of rocks in the inner aureole show evidence for pervasive infiltration at the grain-scale, which implies the existence of interconnected porosity at the grain scale. These lines of evidence include: 1) the common occurrence of oxygen isotope homogenization—or near-homogenization—of matrix calcite and dolomite throughout the periclase and forsterite zones; 2) the presence of coherent $\delta^{18}O$ gradients in matrix calcite at layer boundaries—the ~6‰ $\delta^{18}O$ gradient at the layer 8/9 boundary at site 94I (Fig. 9) is an example; 3) recrystallization and coarsening of matrix carbonates, and wholesale disappearance of disseminated graphite as the igneous contact is approached. In addition, the combination of reaction progress calculations and results of calcite-dolomite thermometry indicate infiltration of substantial fluxes of H_2O-rich fluids into the inner aureole (Cook and Bowman, 2000). These H_2O-rich fluids would have favorable wetting characteristics consistent with infiltration via interconnected porosity at the grain scale.

Origins of aureole-scale textural variation

In the Alta aureole, the average grain size of forsterite decreases and forsterite crystals change from tabular to more equigranular toward the igneous contact (Loury 2014; Beno et al. 2020; Chadwell 2020; Fig. 3, this study), and as temperature increased as recorded by calcite-dolomite thermometry (Cook and Bowman, 1994). These systematic aureole-scale changes observed in Alta forsterite textures are similar to textural variations of forsterite documented in other contact metamorphic environments (Hoersch 1981; Roselle et al. 1997; Ferry et al. 2011). In the Ubehebe peak aureole (Roselle et al. 1997) sparse, coarse, tabular forsterite in the outer aureole transitions to abundant, fine-grained, equigranular forsterite crystals preserved in inner aureole marbles. Roselle et al. (1997) interpreted this trend to be the result of increased overstepping of the forsterite forming reaction as the igneous contact is approached, based on kinetic formulations by Ridley and Thompson (1986). Beno et al. (2020) also interpreted the observed decrease in average grain size of forsterite and the measured increase in temperature toward the igneous contact in the Alta aureole to result from increased reaction overstepping. Based on kinetic formulations by Ridley and Thompson (1986), such an increase in reaction overstepping indicates an increased role of nucleation rate relative to growth rate in the formation of the Alta forsterite toward the igneous contact. Ferry et al. (2011) also ascribed analogous textural variation in forsterite from the Twin Lakes pendant (Davis and Ferry 1993) and the Beinn an Dubhaich aureole (Ferry and Rumble 1997) to be the result of variable overstepping of the forsterite forming reaction.

Beno et al. (2020) concluded that nucleation and growth kinetics induced by reaction overstepping play an important role in the observed change in forsterite habit (equigranular → tabular) across the Alta aureole. At all lateral distances, crystal morphologies, forsterite surface features (e.g., abundant hopper structures and terraces) as well as trace element and cathodoluminescence patterns, are all consistent with a period of skeletal crystal growth followed by textural maturation toward euhedral morphologies. Roselle et al. (1997) suggest that equigranular crystals in the inner Ubehebe Peak aureole may have been promoted at high degrees of overstepping due to kinetic roughening (Bennema and van der Eerden 1987). Additionally, small crystals attain textural equilibrium faster than larger crystals (Holness and Siklos 2000), suggesting that rapid textural equilibration of fine-grained forsterite may allow the rapid approach of forsterite to a rounded habit due to the 165° Fo-Cal-Cal equilibrium dihedral angle (Holness et al. 1991). Dilissen et al. (2020) suggest that tabular forsterite may be favored during fluid-driven metamorphic crystallization due to the formation of surfactants (Bakshi 2016) that inhibit growth on specific crystal interfaces (i.e. (100) and to a lesser extent (010) interfaces), promoting the development of c-axis (001) elongate tabular forsterite. Regardless of the mechanism of formation of specific forsterite habits, the observed change in forsterite texture across the forsterite and periclase zones in the Alta aureole is consistent with an increase in overstepping of the forsterite forming reaction as the igneous contact is approached.

Aureole-scale oxygen isotopic fractionations

Constraints on mineral textures (Loury 2014; Beno et al. 2020; Chadwell 2020; preceding section, this study), mineral chemistry (Cook and Bowman 2000), and the characteristics of infiltration-driven metamorphism in the inner aureole (Bowman et al. 1994; Cook et al. 1997; Cook and Bowman 2000) allow evaluation of possible pathways responsible for the development of disequilibrium oxygen isotope ratios recorded by most of the coexisting forsterite and carbonate mineral pairs measured in the Alta aureole.

Oxygen isotope disequilibrium in the outer forsterite zone

In both samples analyzed from the outer forsterite zone (samples FZ4-5a [475m] and 99V-3 [615m]), forsterite, calcite and dolomite are all out of oxygen isotope exchange equilibrium. Both of these samples are characterized by tabular forsterite, and associated coronal calcite, in a dolomite matrix (Figs. 3 and 7). The only textural difference between these samples being the presence of larger, sparser forsterite in 99V-3 (Loury 2014), suggesting lower overall reaction affinity in this sample consistent with its downstream location in the aureole (either lower T [Cook and Bowman 1994] or higher $X(CO_2)$ [Cook and Bowman 2000], or both). In addition, there is some intergranular heterogeneity in $\delta^{18}O$ in forsterite and calcite, but very little heterogeneity observed in outer aureole dolomite (<0.7‰; sample FZ4-5a [Table 3]).

Matrix carbonate $\delta^{18}O$ values in samples FZ4-5a and 99V-3 (Fig. 6, Fig. 12) fall within the range of values reported for the lower grade tremolite and talc zones reported by Cook et al. (1997), but are ~0-4‰ lower than those of stratigraphically-equivalent, unmetamorphosed dolostone protoliths outside of the aureole (~26-30‰; Brenner 2018; Brenner et al. 2021). The lower $\delta^{18}O$ values of these outer Fo zone marbles suggest they have experienced some $^{18}O/^{16}O$ depletion resulting from the cumulative effects of decarbonation reactions (forming forsterite, and possibly from earlier talc- and tremolite-forming reactions) and from at least modest influxes of lower $\delta^{18}O$ fluid driving these reactions. The disappearance of organic matter from the dolomitic protolith, along with the coarsening of the dolomitic matrix also suggests that the primary dolomite was modified to some degree by infiltration-driven recrystallization over the timescale of aureole petrogenesis. The homogeneity in $\delta^{18}O$ of dolomite at the grain-scale in these two samples indicates that any infiltration-driven recrystallization of the dolomite matrix was pervasive. Further, the lack of significant grain-scale $\delta^{18}O$ heterogeneity in dolomite from outer forsterite zone samples rules out the possibility of initial intrastratigraphic variation in $\delta^{18}O$ as the cause of observed intergranular isotopic heterogeneities in forsterite and calcite pairs from samples A-4-1 and 99V-3 (Table 3).

$\Delta^{18}O_{Dol\text{-}Cal}$ values are locally reversed in both samples (FZ4-5a, 99V-3) from the outer forsterite zone (Fig. 6; Fig. 12). In addition, values of both $\Delta^{18}O_{Cal\text{-}Fo}$ and $\Delta^{18}O_{Dol\text{-}Fo}$ in both samples are also smaller than the expected equilibrium values, demonstrating that both products and reactants in this portion of the flow regime are out of oxygen isotopic equilibrium. This is inconsistent with conventional models of isotope redistribution that require isotopic equilibrium be maintained between all phases during prograde decarbonation reactions (Rumble 1982; Valley 1986; Bowman 1998). The lack of equilibrium between products (forsterite and calcite) is also inconsistent with the Müller et al. (2004) model that demonstrated the feasibility for formation of forsterite from the metastable reaction of dolomite + SiO_2 = forsterite + calcite + CO_2 in the Ubehebe Peak aureole, but also documented oxygen isotopic equilibrium between the forsterite and calcite products of this metastable reaction.

Rubie (1998) noted that nucleation can be much slower for any reactions involving two product phases, such as the reaction producing forsterite and calcite in the Alta aureole. This delay of nucleation can lead to high degrees of reaction overstepping, potentially leading to rapid growth rates and the development of metastable phases when barriers to nucleation are overcome. Isotopic disequilibrium has also been reproducibly obtained experimentally (Zheng et al. 1999; Zheng et al. 2003). Zheng et al. (1999) documented disequilibrium oxygen isotope exchange between

calcite-forsterite pairs due to rapid dissolution-reprecipitation processes that led to negative, or "crossed-over," fractionations for this pair when compared to the expected equilibrium values.

Ferry et al. (2011) documented similar textures to those of the forsterite marbles at Alta, and similar oxygen isotope disequilibrium among product and reactant minerals at the grain-scale, in a forsterite marble from the Beinn an Dubhaich aureole, Scotland (i.e., sample B4L in Ferry and Rumble 1997; see Fig. 4 and Fig. 8b in Ferry et al. 2011). Besides these Alta and Beinn an Dubhaich examples, the lack of isotopic exchange equilibrium between cogenetic mineral assemblages at the grain-scale has been documented in carbonate-bearing metamorphic rocks from a variety of other natural systems (Ferry et al. 2010). Ferry et al. (2011) acknowledged that the Rumble (1982) and Müller et al. (2004) models for isotope redistribution during prograde forsterite formation fail to explain the oxygen isotopic disequilibrium observed between calcite, dolomite, and forsterite from the Beinn an Dubhaich marbles.

The pervasive lack of oxygen isotope equilibrium among product (forsterite and calcite) and reactant (dolomite) phases in the Alta marbles must either result from kinetic factors that prevent attainment of grain-scale equilibrium during growth of forsterite and calcite or from post-growth exchange of the less refractory carbonate phases. We discuss these alternative possibilities in the following two sub-sections.

Reaction overstepping driving high ratio of growth rate to the rate of oxygen transport

Ferry et al. (2011) explained the observed forsterite textures, and grain-scale isotopic characteristics of coexisting products and reactants in the Beinn an Dubhaich marble, primarily as a result of the interplay between variable reaction affinity (overstepping) and local differences in transport mechanisms (interplay between advective and diffusive transport or Péclet number; Bowman and Willet 1991). This interpretation proposes that overstepping drives the development of tabular forsterite, and suggests that if overstepping is sufficiently great, crystal growth rate could become sufficiently rapid relative to transport of oxygen to induce both the intergranular and intragranular variations in $\delta^{18}O$ observed at Beinn an Dubhaich, as well as oxygen isotope disequilibrium between both product and reactant phases (Watson and Müller 2009; Fig. 5, Fig. 6, Table 3, this study).

There is widespread textural evidence throughout the forsterite and periclase zones in the Alta aureole for dendritic/skeletal crystallization of forsterite, implying its rapid growth (Beno et al., 2020; Fig. 3, this study). Depending on the rates of oxygen isotope exchange at the interface of the growing crystal, the rapid kinetics of forsterite growth suggested by the textural evidence could produce isotopic disequilibrium among product and reactant phases, and intergranular $\delta^{18}O$ heterogeneities in forsterite and calcite at the thin section-scale, as measured in this study. Even in the outermost forsterite zone, (i.e., sample 99V-3; Fig. 7) where overstepping is presumably the smallest, there are significant departures from isotope equilibrium between products and reactants. These isotopic characteristics suggest that throughout the inner Alta aureole either rapid heating rates or more likely rapid and significant changes in fluid composition or fluid fluxes, or both, are driving significant overstepping of the forsterite-forming reaction. Such significant overstepping could lead to rapid growth of forsterite relative to transport of oxygen, consistent with the evidence from forsterite morphologies and textures (Beno et al. 2020).

Reaction progress calculations (Cook and Bowman, 2000) indicate the reaction forming forsterite in the Alta marbles was driven by infiltration of H_2O-rich fluid, implying that the transport of oxygen to forsterite growth surfaces was also infiltration-controlled. Accordingly, the development of a high ratio of growth rate to transport requires either very rapid growth of forsterite or fluid infiltration over an extended time period. If oxygen transport kinetics are rate-limiting, the net effects of $\Delta^{18}O_{Cal\text{-}Fo}$ (>0) and $\Delta^{18}O_{Dol\text{-}Cal}$ (~0) could create $^{18}O/^{16}O$-enriched boundary layers surrounding the growing forsterite crystals (Watson and Müller 2009). Continued rapid growth of forsterite, by variably incorporating these $^{18}O/^{16}O$-enriched domains (Ferry et al. 2011), could induce the oxygen isotope disequilibrium and intergranular heterogeneities observed in the forsterite zone marbles at Alta. Another possible kinetic effect is that sufficiently rapid devolatilization and product mineral growth driven by large reaction overstepping may produce non-equilibrium (reduced) fractionations between released volatiles (CO_2, H_2O) and both reactant and product minerals. Further, variations in the extent of this disequilibrium fractionation could result from variations in overstepping at the thin section-scale. Variations in both the extent of reaction overstepping and accompanying variations in the size of CO_2-mineral fractionation factors, may explain the minor intergranular variation in $\delta^{18}O$ of the product minerals forsterite and calcite in these outer Fo zone samples. Such variations in overstepping could be prompted by spatial and/or temporal variations in fluid flux—with accompanying changes in the oxygen isotope ratio of the infiltrating fluid—at the thin section-scale.

Continued carbonate exchange in the outer forsterite zone

An alternative explanation for the observed departure from $\Delta^{18}O_{Carb\text{-}Fo}$ equilibrium values is that the carbonate matrix was further depleted by ~2-3‰ during continued exchange between the carbonates and infiltrating fluids after formation of the refractory forsterite. This extent of depletion is compatible with the 0-4‰ depletion in the bulk carbonate matrix within the outer Fo zone compared to the $\delta^{18}O$ values of the dolostone protoliths beyond the talc zone. Heat and fluid flow modeling of the Alta aureole (Cook et al. 1997) indicate that prograde infiltration-driven metamorphism occurs in the more distal tremolite and talc zones after cooling begins in the higher-grade forsterite zone. The similarity of the $\delta^{18}O$ values of the bulk carbonate matrix in the outer forsterite, tremolite and talc zones (~23-26‰) is consistent with continued (retrograde) infiltration in the forsterite zone during its initial stages of cooling contemporaneous with infiltration-driven prograde metamorphism throughout the middle and outer Alta aureole.

Regardless of whether or not continued exchange occurred, the calcite and dolomite in the outer forsterite zone are clear (non-porous) and exhibit only minor (<1‰) grain-scale $\delta^{18}O$ heterogeneity in calcite and grain-scale $\delta^{18}O$ homogeneity in dolomite, indicating that this carbonate matrix has experienced pervasive recrystallization and extensive isotope homogenization. These characteristics are quite distinct from those of the turbid and isotopically heterogenous calcite that records distinctly "retrograde" alteration in the periclase zone. Although minor turbid calcite is observed in these outer forsterite zone samples at Alta, areas of turbid calcite were specifically avoided during this study.

Record of fluid infiltration from grain-scale $\delta^{18}O$ heterogeneity in inner forsterite and periclase zone marbles

Most of the marbles from within ~300m from the contact have bulk carbonate $\delta^{18}O$ values less than +20, indicating infiltration and exchange with variable fluxes of low-$\delta^{18}O$ fluids (Table 2, this

study; Bowman et al. 1994). Grain-scale heterogeneities in single crystals of forsterite from samples 88-8 and 94I are as large as 3‰ (Fig. 5; Fig 8). Maximum measured $\Delta^{18}O_{Cal-Fo}$ factors, based on minimum forsterite $\delta^{18}O$ values, suggest some stage(s) of forsterite growth in sample 88-8 occurred at, or at least near, equilibrium (Table 3), at the estimated temperature of formation (~550ºC; Cook and Bowman 1994). We interpret the large grain-scale variation recorded by forsterite single crystals in this sample to be the result of growth in response to the progressive depletion of the carbonate matrix (88-8 carbonate $\delta^{18}O$ = 19.2‰; Table 2) during fluid infiltration-driven reaction, rather than the result of temperature-driven changes to the equilibrium fractionation factor. A 3‰ change in $\Delta^{18}O_{Cal-Fo}$, if grown in a closed-system carbonate reservoir of constant $\delta^{18}O$ value, requires temperature changes exceeding 500ºC (Chiba et al. 1989; Zheng et al. 1994). However, due to this sample's location within the water-dominated portion of the oxygen isotope exchange front in the aureole (Bowman et al. 1994; Cook et al. 1997), the evolution of fluid composition towards more H_2O-rich and lower $\delta^{18}O$ values with continued fluid flux is a possible driver of significant isotopic change.

The $\delta^{18}O$ zoning patterns in these forsterite crystals can be complex, and are not simple center-to-edge decreases in $\delta^{18}O$ (Figs. 8, 11). Generally, growth of single crystals is interpreted with a conventional "tree-ring" model where the cores of individual crystals are thought to be older than the corresponding rims (Welsch et al. 2014). This model is inappropriate for Alta forsterite based on the observations of Beno et al. (2020). Dendritic/skeletal crystallization followed by infilling produces highly complex 2D isotopic profiles (i.e., high to low $\delta^{18}O$ [Fig. 8e, Fig. 11b, d] and low to high $\delta^{18}O$ [Fig. 8b, Fig 11c, e]). We interpret these complex zoning profiles in forsterite to result from early dendritic/skeletal crystallization (high $\delta^{18}O$ domains) and subsequent infilling of the dendritic/skeletal scaffolding (low $\delta^{18}O$ domains) as the carbonate reservoir is being progressively depleted by infiltration of progressively lower $\delta^{18}O$ fluids over the timescales of forsterite petrogenesis.

Reaction history in the periclase zone

Impact of infiltration history on the order of decarbonation reactions

As noted in the Introduction, at the scale of an outcrop, the thermal histories (T-time paths) of two adjacent and compositionally-distinct bedding layers (cms to m scale)—for example, adjacent layers of periclase + calcite marble and forsterite + calcite marble within the inner aureole—are the same. Hence, the sequence of decarbonation reactions producing the index minerals forsterite and periclase in these layers is a function of the relative timing of fluid infiltration of these individual layers. These different sequences are illustrated in the set of schematic T-X(CO_2) diagrams in figure 13.

In this first case, layers one (L1; Fig 13) and two (L2; Fig 13) are infiltrated simultaneously and at equal flux. Infiltration of H_2O-rich fluid begins at t_1 and in response, the pore fluid composition decreases in X(CO_2) simultaneously in both layers (Fig. 13a); assuming a reasonable approach to equilibrium, this first leads to the production of the calcite + forsterite assemblage in L2 at t_2 (Fig. 13a). With continued fluid infiltration and decrease in X(CO_2) over time to t_3, dolomite then reacts to form periclase + calcite in layer L1. For this case of simultaneous infiltration of both layers, the reaction sequence follows the order of reactions defined by all T-X(CO_2) paths for prograde, infiltration-driven metamorphism in the equilibrium phase diagram; that is, forsterite forms in L2 before periclase forms in L1 (Fig. 13a).

However, it is not apparent that L1 and L2, which have distinct bulk composition and reaction history, would necessarily have had the same permeability. The situation where the dolomite-rich L1 is infiltrated first is illustrated in figure 13b. In this case, periclase forms first in L1 (at t_2) and because infiltration does not start in L2 until after t_2, forsterite forms second in L2 (at t_3), opposite the order predicted by all T- $X(CO_2)$ paths for prograde, infiltration-driven metamorphism in the equilibrium phase diagram.

A third possibility is that L2, because it may have experienced previous reactions to create talc and tremolite, possible pre-cursor reactants to form forsterite, has the higher permeability. If so, then L2 is infiltrated first, the scenario illustrated in figure 13c. In this situation, fluid infiltration commences in L2 at t_1, and by t_2, pore fluid $X(CO_2)$ composition is sufficiently lower that forsterite forms. As L1 is not infiltrated, its pore fluid composition does not change, until after t_2 when fluid infiltration in L1 commences and pore fluid composition decreases to sufficiently low $X(CO_2)$ values by t_3 that dolomite breaks down to periclase + calcite in L1. In this scenario forsterite forms in L2 first and periclase forms in L1 later; the same order that results from simultaneous fluid infiltration.

These schematics demonstrate that infiltration history determines the order of metamorphic reactions occurring in two compositionally distinct stratigraphic horizons with identical T-t histories that are experiencing infiltration driven metamorphism. However, it is difficult to identify the relative timing of decarbonation reactions occurring in contact metamorphic systems using only mineralogy or only stable isotope data. Here we present quantitative forsterite textural measurements and paired calcite-forsterite SIMS isotopic analyses that suggest that a combined textural and isotopic approach may be used to identifying the order of metamorphic reactions occurring in these systems on the outcrop-scale.

Combined textural and isotopic model

In this section, the oxygen isotope profiles defined by the $\delta^{18}O$ values of spatially-coordinated calcite-forsterite pairs across the layer 8/9 boundary in the 94I traverse (Fig. 9) are combined with forsterite textural constraints in layer 8 (Fig. 10) to reconstruct the history of prograde formation of forsterite and periclase in the periclase zone. Oxygen diffusion is much slower in forsterite than in calcite or dolomite (Fissler and Cygan 1999; Cole and Chakraborty 2001; Dohmen et al. 2002) and both carbonates are vulnerable to recrystallization during retrograde processes (Heberling et al. 2016). Therefore, SIMS $\delta^{18}O$ values of forsterite crystals provide a "snapshot" of the nature and extent of fluid infiltration during forsterite petrogenesis. Further, comparison of the SIMS $\delta^{18}O$ values of spatially-correlated crystals of forsterite and calcite –two phases of contrasting refractory nature—along the traverse provides the opportunity to address some additional, fundamental questions about infiltration-driven metamorphism of these marbles: 1) What is the relative timing of fluid infiltration and petrogenesis in layer 8 and in layer 9?; and 2) Is the $^{18}O/^{16}O$ depletion and oxygen isotope homogenization in calcite within the uppermost section of layer 8 a prograde or retrograde feature with respect to forsterite and periclase petrogenesis? In the following paragraphs we evaluate various scenarios of fluid infiltration and exchange kinetics (Fig. 14) to see which scenarios are consistent with the isotopic and textural data available from forsterite and calcite along the 94I traverse.

The scenarios illustrated in Fig. 14 utilize a planar cross-section representing the analyzed traverse across the boundary between marble layers 8 and 9 at sample location 94I (Fig. 14b). Both marble layers in this model start with the same initial $\delta^{18}O$ value (~25‰; Fig. 14a). Layer 9 is initially all dolomite and layer 8 is initially a mix of dolomite, calcite and a SiO_2-bearing phase (tremolite or quartz) that reacts with dolomite to form forsterite. Fluid infiltration is normal to (into or out of) the plane of the cross-section and the infiltrating fluids are H_2O-rich and have low $\delta^{18}O$ values out of exchange equilibrium with the marble layers. These fluids are flowing laterally away, and down-temperature, from the adjacent Alta stock. The dominant mode of infiltration in all models presented here is horizontal bedding-concordant flow. All of these characteristics and modes of fluid flow geometry are well-constrained by previous studies (Bowman et al. 1994; Cook and Bowman 1994, 2000; Cook et al. 1997; Bowman et al. 2009), as noted earlier in the section on Geologic Setting and Previous Work. The model has three parameters that are varied to produce the final oxygen isotope profiles for forsterite and calcite in each scenario. First, cumulative fluid flow is shown by the size of the fluid flow symbol (circle in Fig. 14a). In all four scenarios, as calcite from layer 9 (<12‰) has a significantly lower measured $\delta^{18}O$ value than calcite from the interior of layer 8 (~18‰; Fig. 14b), layer 9 experiences significantly more cumulative fluid flow than layer 8. Second, fluid infiltration starts simultaneously in both layers in the first three scenarios; in scenario 4, layer 8 is infiltrated first. Third, decreasing reaction overstepping is reflected by increasing size of the schematic forsterite crystal symbols. The demonstrable increase in forsterite grain-size and decrease in numbers of forsterite crystals/mole forsterite as the layer 8/9 boundary is approached (Fig. 10, this study; Loury 2014; Beno et al. 2020) is interpreted to reflect a decrease in the overstepping of the forsterite-forming reaction in that direction. In all scenarios, reaction overstepping is driven by decreases in $X(CO_2)$ of the infiltrating fluid, as significant differences in temperature between the layers are unlikely to be maintained at the cm-scale of the 94I traverse being modeled.

Scenarios 1, 2, and 3

The first three scenarios illustrated in figure 14 do not reproduce the $\delta^{18}O$ profiles and textural changes in forsterite recorded in the uppermost section of layer 8. The reasons these models are unsuccessful are summarized below, and discussed in detail in appendix A.

In the simplest infiltration-reaction scenario 1 (Fig. 14c), both layers 8 and 9 have the same initial permeability and experience simultaneous infiltration of equal fluxes of fluid with the same $X(CO_2)$ composition. In response, the carbonate matrix of layer 8 experiences declining, but uniform $\delta^{18}O$ values, and because $X(CO_2)$ pore fluid compositions are uniform within layer 8, reaction overstepping is constant within layer 8 during forsterite petrogenesis (from time t_1 to t_2). As a result, the $\delta^{18}O$ value of the crystallizing forsterite and the texture of these forsterite crystals within layer 8 remains the same toward the layer 8/9 boundary in scenario 1 (Fig. 14c), in contrast with the observed changes in these characteristics (Fig. 14b).

In all of the first three scenarios, after forsterite petrogenesis ceases in layer 8 (by time t_2), fluid infiltration continues in layer 9, driving the periclase reaction and producing significant, additional $^{18}O/^{16}O$ depletion in layer 9 (time t_3, Fig. 14c-e). As discussed further in appendix A, limited cross-stratal influx of the low $\delta^{18}O$ fluids from layer 9 into layer 8 during periclase petrogenesis can produce in all three models the steep gradient of decreasing $\delta^{18}O$ values of the matrix calcite observed in the uppermost margin (~8 cm) of layer 8.

In scenario 2, both layers 8 and 9 also experience simultaneous infiltration of equal fluid fluxes with the same $X(CO_2)$ composition, but forsterite reaction overstepping decreases within layer 8 toward the layer 8/9 boundary. In response to this uniform infiltration, the carbonate matrix in both layers 8 and 9 experience uniform and equal decreases in $\delta^{18}O$ during forsterite petrogenesis (time t_1 to t_2, Fig. 14d). The increase in reaction overstepping into the interior of layer 8 reproduces the observed decrease in forsterite grain size into the interior of layer 8 but also leads to progressively higher $\delta^{18}O$ forsterite into the interior of layer 8 (Fig. 14d). This increase in $\delta^{18}O$ is opposite of the measured trend of decreasing forsterite $\delta^{18}O$ values into the interior of layer 8 (Fig. 14b).

In scenario 3, both layers again experience simultaneous fluid infiltration, but because layer 9 has a much lower final $\delta^{18}O(Cal)$ value, it is assigned a greater fluid flux and its carbonate matrix experiences greater $^{18}O/^{16}O$ depletion during forsterite petrogenesis (t_1 to t_2, Fig. 14e). Because no reaction occurs in layer 9 during forsterite petrogenesis in layer 8, fluids in layer 9 have lower $X(CO_2)$ and $\delta^{18}O$ values than fluids in layer 8. As a consequence, and explained further in appendix A, limited cross-stratal transport of these lower $\delta^{18}O$ and lower $X(CO_2)$ pore fluids from layer 9 into the uppermost margin of layer 8 during forsterite petrogenesis in layer 8 produces, respectively, decreasing $\delta^{18}O$ values of forsterite and progressive increase in reaction overstepping in layer 8 toward the 8/9 boundary (Fig. 14e). This significant decrease in the model $\delta^{18}O$ values of forsterite in uppermost layer 8 is opposite of the observed trend (Fig. 14b). Further, the decrease in grain size resulting from the increase in reaction overstepping toward the layer 8/9 boundary in this scenario 3 is the opposite of the observed changes (Figs. 10, 14b).

Scenario 4: Non-simultaneous infiltration (layer 8 before layer 9), unequal fluxes (layer 8<layer 9), variable reaction overstepping (Fig. 14f):
In scenario 4, fluid infiltration and the forsterite-forming reaction are initially confined to layer 8 (t_1 to t_2), with little or no infiltration into layer 9. Because H_2O-rich fluids are not infiltrating layer 9 at this time, pore fluids in layer 9 have higher $X(CO_2)$ values, and as a consequence, their limited cross-stratal transport into layer 8 sets up a gradient of increasing $X(CO_2)$ toward the top of layer 8. This increase in $X(CO_2)$ leads to a progressive decrease in reaction overstepping within layer 8 toward the layer 8/9 boundary. Such a decrease leads to the observed trend of decreasing number of forsterite crystals/mole forsterite and an increase in their size toward the layer 8/9 boundary. During the infiltration-driven forsterite reaction, layer 8 experiences significant $^{18}O/^{16}O$ depletion to values near its present $\delta^{18}O$ value (~+18‰) and layer 9 ($\delta^{18}O_i$ = +25‰) experiences little to no depletion. As a consequence, cross-stratal mixing with the significantly higher $\delta^{18}O$ pore fluids from layer 9 also sets up a gradient of increasing $\delta^{18}O$ of the carbonate matrix toward the layer 8/9 boundary in the uppermost margin of layer 8 during forsterite petrogenesis. Layer 8 must experience infiltration and $^{18}O/^{16}O$ depletion first so that cross-stratal influx and mixing of $^{18}O/^{16}O$-enriched fluids from layer 9 can progressively increase the $\delta^{18}O$ of the uppermost part of layer 8 during forsterite petrogenesis. This increase in $\delta^{18}O$ of the carbonate matrix of layer 8 toward the layer 8/9 boundary is much larger than the modest increase in the $\Delta^{18}O_{Cal\text{-}Fo}$ fractionation factor induced by the decrease in reaction overstepping toward the layer 8/9 boundary. As a result, the $\delta^{18}O$ composition of model forsterite increases toward the layer 8/9 boundary (Fig. 14f), as observed (Fig. 14b). The orientations of the gradients in $X(CO_2)$ and $\delta^{18}O$ produced at the top of layer 8 in this scenario are the consequence of the direction of cross-stratal fluid flux (from layer

9 into layer 8); this flux direction is in turn the consequence of layer 8 being infiltrated before layer 9. After the prograde forsterite reaction is complete (t_2), fluid infiltration ceases within layer 8.

After time t_2 fluid infiltration begins in layer 9, and dolomite begins to react to form calcite and periclase in layer 9 in response to this fluid infiltration, inducing permeability enhancement and promoting further fluid infiltration in layer 9. Continued fluid infiltration leads to extensive $^{18}O/^{16}O$ depletion of calcite in layer 9 and further prograde periclase formation. Layer 9 now has the lower $\delta^{18}O$ (Cal) value (t_3). Calcite in the upper part of layer 8 is then progressively depleted in $^{18}O/^{16}O$ and recrystallized in response to limited, cross-stratal infiltration of low $\delta^{18}O$ and H_2O-rich fluids from layer 9, eventually leading to the observed isotope gradient of decreasing $\delta^{18}O$ values preserved in calcite in layer 8 at the layer 8/9 boundary (Fig. 9 or 14b). This infiltration-driven recrystallization of calcite also leads to oxygen isotope homogenization at the grain-scale along this $\delta^{18}O$ gradient (Bowman et al., 2009).

In this scenario 4, the spatial $\delta^{18}O$ profile defined by forsterite forms earlier than the spatial $\delta^{18}O$ profile defined by calcite because fluid infiltration occurs first in layer 8 and later in layer 9. Because of the refractory nature of forsterite, the forsterite $\delta^{18}O$ profile is preserved during the subsequent development of the calcite $\delta^{18}O$ profile. Although forsterite and calcite in the uppermost portion of layer 8 acquire and retain their final $\delta^{18}O$ values at different times, their spatial $\delta^{18}O$ profiles are both prograde features—that is, both form in response to prograde reactions forming first forsterite and then periclase. The asynchronous infiltration of these two layers and the resulting asynchronous development of the preserved forsterite and calcite isotope profiles can explain the coarsening of forsterite AND the general increase in $\delta^{18}O$ values observed in forsterite from the interior of layer 8 toward the layer 8/9 boundary (Fig. 14f, b). We coin the term asynchronous growth to describe the process of temporally decoupled infiltration-driven decarbonation reactions, leading to decoupled development of these preserved isotope profiles. Insight into this process has required using a combination of textural analysis and in-situ stable isotope analysis.

Interrogation of these models demonstrates the utility of combined textural and isotopic studies that utilize variably refractory phases. These models allow reconstruction of the isotopic evolution of individual lithologies and thus provide important insights into their corresponding infiltration and reaction histories. Only one of the suggested scenarios (#4) reproduces both the spatial isotope profiles preserved in forsterite and calcite and the observed change in forsterite texture along the 94I traverse as the layer 8/9 boundary is approached (Fig. 14b, f). This scenario requires moderate $^{18}O/^{16}O$ depletion coupled with prograde forsterite formation in layer 8 in response to infiltration of H_2O-rich and low $\delta^{18}O$ fluids prior to significant infiltration-driven periclase reaction and extensive $^{18}O/^{16}O$ depletion in layer 9.

The integration of texture trends and multi-mineral $\delta^{18}O$ profiles, by providing insights into the temporally-distinct infiltration and reaction histories of these two marble layers, suggests in addition that these layers experienced significant changes in permeability over time that are linked to their sequential reaction histories. The temporal evolution of reaction-driven permeability and recrystallization in these marble layers could have in turn influenced their infiltration histories and helped define the $\delta^{18}O$ profiles recorded by both forsterite and calcite.

CONCLUSIONS

Pervasive infiltration of hydrothermal fluids into siliceous dolomites surrounding the Alta stock has caused the widespread development of forsterite. Throughout most of the forsterite zone (>250m from the contact), the $\delta^{18}O$ values are high: forsterite (16.0-23.1‰); calcite (23.3-26.5‰); dolomite (23.2-26.1‰). These minerals are either homogeneous in $\delta^{18}O$ at the grain-scale (dolomite) or sometimes exhibit small (<1.0‰) grain-scale heterogeneity. Inner forsterite and periclase zone samples have lower and more variable $\delta^{18}O$ values: forsterite (13.0-22.7‰); calcite (12.2-18.4‰). These forsterite single crystals exhibit grain-scale heterogeneities as large as 3‰ and the patterns of isotopic variation on the grain-scale are complex. Complex zoning patterns are interpreted to be the result of initially rapid growth of skeletal grains followed by the subsequent infilling of the skeletal scaffolding as the carbonate matrix is being depleted in $^{18}O/^{16}O$ during fluid infiltration-driven forsterite petrogenesis.

With one exception (sample 88-8), forsterite, calcite and dolomite in all samples analyzed throughout the aureole yield smaller than expected (i.e., equilibrium) fractionation factors, and $\Delta_{Cal\text{-}Dol}$ factors are often reversed. Additionally, the general trend of decreasing numbers of progressively larger forsterite crystals and decreasing temperature away from the igneous contact to the forsterite isograd requires progressively greater degrees of reaction overstepping, and an increased role of nucleation rate relative to growth rate in the formation of forsterite, as the igneous contact is approached. The nucleation and growth of forsterite may have been sufficiently rapid to overwhelm rates of oxygen transport and perturb isotope exchange between evolved CO_2 and both reactant and product phases, inducing intergranular variations in mineral $\delta^{18}O$ values and disequilibrium isotope fractionations among mineral products (forsterite and calcite) as well as reactants (dolomite). Alternatively, the $\delta^{18}O$ values of calcite and dolomite could have been lowered 2-3‰ after forsterite crystallization was complete by continued and pervasive fluid infiltration driving prograde reactions (tremolite, talc) in the outer aureole as the forsterite zone underwent the initial stages of (retrograde) cooling.

Combined textural characteristics of forsterite and SIMS $\delta^{18}O$ analyses of forsterite and calcite on a traverse across the boundary between a forsterite + calcite marble (layer 8) and a periclase(brucite) + calcite marble (layer 9) within the periclase zone provide important insights into the infiltration and reaction history in the periclase zone (94I, 150m to contact). These data are used to evaluate various infiltration-reaction scenarios for petrogenesis of forsterite (in layer 8) and periclase (in layer 9). The model results indicate that the observed trends of increasing $\delta^{18}O$ of forsterite, decreasing $\delta^{18}O$ of calcite, progressively larger forsterite crystals, and decreasing numbers of forsterite crystals/mole forsterite across the upper part of layer 8 toward the overlying layer 9 are consistent with initial infiltration and forsterite formation in layer 8 followed by infiltration and formation of periclase in layer 9. The $\delta^{18}O$ profile recorded in forsterite forms earlier than the $\delta^{18}O$ profile recorded in calcite, but both profiles are prograde features—that is, both profiles form in response to prograde reactions forming first forsterite and then periclase. Combination of the changes in forsterite texture and SIMS $\delta^{18}O$ profiles indicate that both layers cannot have been significantly infiltrated at the same time, nor continuously during both prograde reactions. This asynchronous growth, which can only be demonstrated by combination of textural analysis and in situ stable isotope analysis by SIMS, may be a common process during fluid-driven metamorphism.

Integration of forsterite textures and grain-scale SIMS $\delta^{18}O$ analyses along this traverse suggest that these layers experienced dramatic changes in permeability that are linked to their sequential reaction history, over the timescale of prograde infiltration-driven metamorphism in the periclase zone. We interpret the observed isotope profiles and forsterite textural variation at 94I to reflect significant changes in permeability in these layers over the timescales of prograde infiltration driven metamorphism. Marbles have significant permeability to maintain fluid infiltration only when undergoing active decarbonation reactions—and experiencing associated negative changes in the volumes of solids. This interpretation suggests that once these prograde reactions stop, compaction and recrystallization of the carbonate matrix, accelerated by elevated pressure and temperature, rapidly reduces permeability and inhibits further fluid flow.

Appendix A: Detailed discussion of Scenario 1, 2, and 3 (Fig. 14)

Scenario 1: Simultaneous infiltration, equal fluxes, constant reaction overstepping (Fig. 14c)

The simplest infiltration-reaction scenario is outlined in Fig. 12c. In this scenario, both layers 8 and 9 have the same initial permeability and experience simultaneous infiltration of equal fluxes of fluid with the same $X(CO_2)$ composition. As a result, the bulk carbonate reservoirs in both layers initially experience homogeneous, and equal $^{18}O/^{16}O$ depletion during forsterite petrogenesis (from t_1 to t_2). In this model, as the $X(CO_2)$ composition of the fluid infiltrating both layers is the same, reaction overstepping is constant within layer 8 as the layer 8/9 boundary is approached. Given homogeneous $\delta^{18}O$ values of the carbonate matrix and constant reaction overstepping within layer 8 in this scenario, the $\delta^{18}O$ value of the crystallizing forsterite remains the same toward the layer 8/9 boundary, in contrast with the observed increase (Fig. 14b). In addition, forsterite textures also remain the same along this profile in this scenario, in contrast to the observed change of fewer numbers of larger crystals/mole forsterite. After forsterite petrogenesis ceases in layer 8 (by time t_2), infiltration slows and ceases in this layer as porosity is no longer being created by the forsterite reaction and the calcite matrix compacts and recrystallizes. As a result, no further $^{18}O/^{16}O$ depletion occurs in the interior of layer 8 as suggested by the near equilibrium fractionation factors preserved in sample 94I-9-2a (Fig. 9b).

After time (t_2), infiltration continues in layer 9, and by time (t_3) reaction of dolomite to periclase and calcite has begun in layer 9. The significant negative volume change associated with periclase + calcite replacing dolomite enhances permeability in this layer, promoting continued fluid infiltration and further, extensive $^{18}O/^{16}O$ depletion of calcite in layer 9 (eventually down to <12‰). Limited cross-stratal influx of the low $\delta^{18}O$ fluids from layer 9 into layer 8 produces the steep gradient of decreasing $\delta^{18}O$ values of the matrix calcite in the uppermost margin (~8 cm) of layer 8 and drives extensive recrystallization and grain-scale oxygen isotope homogenization (Bowman et al., 2009) of this calcite. Infiltration within layer 9 ceases after all dolomite has reacted to periclase and calcite and permeability is sufficiently reduced by subsequent compaction and calcite recrystallization in layer 9 (t_f).

This scenario reproduces the observed spatial $\delta^{18}O$ profile recorded by calcite but not the increase in $\delta^{18}O$ toward layer 9 recorded by forsterite in the 94I traverse. In addition, this scenario also does not produce the observed change to smaller, more numerous forsterite crystals into the layer 8 marble.

Scenario 2: Simultaneous infiltration, equal fluxes, variable reaction overstepping (Fig. 14d)

Similar to scenario 1, both layers 8 and 9 in scenario 2 also experience simultaneous infiltration of equal fluid fluxes (both layers have the same permeability). However, in scenario 2 reaction overstepping decreases toward the layer 8/9 boundary. In response to this uniform infiltration, the carbonate matrices in both layers 8 and 9 experience uniform and equal deceases in $\delta^{18}O$ during forsterite petrogenesis (from time t_1 to t_2). As in scenario 1, after forsterite petrogenesis is complete in layer 8 (time t_2), infiltration ceases in layer 8 and it experiences no further $^{18}O/^{16}O$ depletion. After time (t_2), fluid infiltration continues in layer 9 and from t_3 to t_f drives formation of periclase and further $^{18}O/^{16}O$ depletion in layer 9. Limited cross-stratal flow of the low $\delta^{18}O$ fluids from layer 9 into layer 8 produces the steep gradient of decreasing $\delta^{18}O$ values of the matrix calcite preserved in the uppermost margin (~8 cm) of layer 8 by time t_f (Fig. 14b, d). The increased kinetic control into the interior of layer 8 reproduces the observed decrease in forsterite grain size into the interior of layer 8. However, increased kinetic control (decreased $\Delta^{18}O_{(Cal-Fo)}$) toward the interior of layer 8 leads to progressively higher $\delta^{18}O$ forsterite into the interior of layer 8 (Fig. 14d), opposite of the measured trend of increasing forsterite $\delta^{18}O$ values as the layer 8/9 boundary is approached (Fig. 14b).

Scenario 3: Simultaneous infiltration, unequal fluxes (layer 8<layer9), variable reaction overstepping (Fig. 14e)

In scenario 3, both layers again experience simultaneous fluid infiltration, but because layer 9 has a much lower final $\delta^{18}O(Cal)$ value, it is assigned a higher initial permeability. Therefore layer 9 experiences greater fluid flux and its carbonate matrix experiences greater $^{18}O/^{16}O$ depletion during forsterite petrogenesis (t_1 to t_2). Because of this greater fluid flux and that no reaction occurs in layer 9 during forsterite petrogenesis in layer 8, fluids in layer 9 have lower $X(CO_2)$ and $\delta^{18}O$ values than fluids in layer 8. During forsterite petrogenesis in layer 8 (t_1 to t_2), limited cross-stratal transport of lower $\delta^{18}O$ and lower $X(CO_2)$ pore fluids from layer 9 into the uppermost margin of layer 8 sets up gradients of decreasing $\delta^{18}O$ and $X(CO_2)$ values of pore fluids in layer 8 toward the layer 8/9 boundary. These gradients produce, respectively, decreasing $\delta^{18}O$ of the carbonate matrix and progressive increase in reaction overstepping in layer 8 toward the 8/9 boundary. This significant decrease in $\delta^{18}O$ in uppermost layer 8 overwhelms the modest decrease in $\Delta^{18}O_{(Cal-Fo)}$ produced by the increase in reaction overstepping, so the model $\delta^{18}O$ values of forsterite in layer 8 decreases toward layer 9, opposite of the observed trend (Fig. 14b). Further, the decrease in grain size and increase in numbers of forsterite crystals resulting from the increase in reaction overstepping toward the layer 8/9 boundary is the opposite of the observed changes in these texture parameters. After forsterite petrogenesis ceases in layer 8 (t_2), the dolomite in layer 9 reacts to produce periclase + calcite (t_2 to t_3). This continued infiltration further reduces the oxygen isotope ratio of the matrix calcite in layer 9 and in the uppermost ~8 cm of layer 8 to their present values. This scenario fails to reproduce either the oxygen isotope profile preserved in forsterite or the observed changes in texture of forsterite (i. e., fewer, larger crystals) in the upper part of layer 8.

REFERENCES

Bakshi MS (2016) How surfactants control crystal growth of nanomaterials. Cryst Growth Des 16:1104-1133

Baker AA, Calkins FC, Crittenden MD, Bromfield CS (1966) Geologic map of the Brighton quadrangle, Utah. U.S. Geological Survey Map GQ-535

Bennema P, van der Eerden JP (1987) Crystal graphs, connected nets, roughening transition and the morphology of crystals, In: Sunagawa I (ed) Morphology of crystals: Part A: Tokyo,

Japan, Terra Scientific, p. 1-75
Beno CJ, Bowman JR, Loury PC, Tapanila LM, Fernandez DP (2020) Evidence for dendritic crystallization of forsterite olivine during contact metamorphism of siliceous dolostones, Alta stock aureole, Utah. Contrib Mineral Petrol 175:93
Berman RG (1988) Internally-consistent thermodynamic data for minerals in the system Na_2O-K_2O-CaO-MgO-FeO-Fe_2O_3-Al_2O_3-SiO_2-TiO_2-H_2O-CO_2. J Petrol 29:445-522
Bowman JR (1998) Stable isotope systematics of skarns. In: Lentz DR (ed) Mineralized intrusion-related skarn systems (1a ed.) Ottawa, Ont., Canada: Mineralogical Association of Canada
Bowman JR, Willett SD, Cook SJ (1994) Oxygen isotopic transport and exchange during fluid flow: one-dimensional models and applications. Am J Sci 294:1–55
Bowman JR, Kita NT, Valley JW (2009) Mechanisms of oxygen isotopic exchange and isotopic evolution of $^{18}O/^{16}O$-depleted periclase zone marbles in the Alta aureole, Utah: insights from ion microprobe analysis of calcite. Contrib Mineral Petrol 157:77–93
Bowman JR, Willet SD (1991) Spatial patterns of oxygen isotope exchange during one-dimensional fluid infiltration. Geophys Res Lett 18:971-974
Breitenbach SF, Bernasconi SM (2011) Carbon and oxygen isotope analysis of small carbonate samples (20 to 100 µg) with a GasBench II preparation device. Rapid Commun Mass Spectrom 25:1910-1914
Brenan JM (1991) Development of metamorphic permeability: implications for fluid transport Processes. In: Kerrick DM (ed) Contact metamorphism. Rev Mineral Geochem 26:291-319
Brenner DC (2018) Controls on solid-state kinetics of carbonate clumped isotope geothermometry and implication for metamorphic reactions. Dissertation, John Hopkins University
Brenner DC, Passey BH, Holder RM, Viete DR (2021) Clumped-isotope geothermometry and carbonate U-Pb geochronology of the Alta stock metamorphic aureole, Utah, USA: Insights on the kinetics of metamorphism in carbonates. Geochem Geophy Geosy 22
Chadwell LM (2020) Crystallization kinetics of forsterite in the Alta contact aureole, Utah: insights from quantitative textural analysis. MS Thesis, University of Utah
Chiba H, Chaco T, Clayton RN, Goldsmith JR (1989) Oxygen isotope fractionations involving diopside, forsterite, magnetite, and calcite: Application to geothermometry. Geochim Cosmochim Acta 53:2985-2995
Cole DR, Chakraborty S (2001) Rates and mechanisms of isotopic exchange. In: Valley JW, Cole DR (eds) Stable isotope geochemistry. Rev Mineral Geochem 43:83-191
Cook SJ (1992) Contact metamorphism surrounding the Alta stock, Little Cottonwood Canyon, Utah. Dissertation, University of Utah, Salt Lake City
Cook SJ, Bowman JR, Forster CB (1997) Contact metamorphism surrounding the Alta stock: finite element model simulation of heat- and $^{18}O/^{16}O$ mass transport during prograde metamorphism. Am J Sci 297:1–55
Cook SJ, Bowman JR (1994) Contact metamorphism surrounding the Alta stock: thermal constraints and evidence of advective heat transport from calcite + dolomite geothermometry. Am Miner 79:513–525
Cook SJ, Bowman JR (2000) Mineralogical evidence for fluid–rock interaction accompanying prograde contact metamorphism of siliceous dolomites: Alta Stock Aureole, Utah, USA. J Pet 41:739–757
Cui X, Nabelek PI, Liu M (2001) Heat and fluid flow in contact metamorphic aureoles with

layered and transient permeability, with application to the Notch Peak aureole, Utah. J Geophys Res 106:6477-6491
Davis SR, Ferry JM (1993) Fluid infiltration during contact metamorphism of interbedded marble calc-silicate hornfels, Twin Lakes area, central Sierra Nevada, California. J Metamorph Geol 11:71-88
Dilissen N, Hidas K, Garrido CJ, Sánchez-Vizcaíno VL, Kahl WA (2020) Morphological transition during prograde olivine growth formed by high-pressure dehydration of antigorite-serpentinite to chlorite-harzburgite in a subduction setting. Lithos 105949:382-383
Dohmen R, Chakraborty S, Becker HW (2002) Si and O diffusion in olivine and implications for characterizing plastic flow in the mantle. Geophys Res Lett 29:(26-1)-(26-4)
Eiler, J. M., Graham, C., and Valley, J. W. (1997) SIMS analysis of oxygen isotopes: matrix effects in complex minerals and glasses. Chemical Geol. 138: 221-244.
Eppel H, Abart R (1997) Grain-scale stable isotope disequilibrium during fluid-rock interaction. 2: An example from the Penninic-Austroalpine tectonic contact in eastern Switzerland. Am J Sci 297:707-728
Ferry JM, Ushikubo T, Kita NT, Valley JW (2010) Assessment of grain-scale homogeneity and equilibration of carbon and oxygen isotope compositions of minerals in carbonate-bearing metamorphic rocks by ion microprobe. Geochim Cosmochim Acta 74:6517–6540
Ferry JM, Ushikubo T, Valley JW (2011) Formation of forsterite by silicification of dolomite during contact metamorphism. J Pet 52:1619–1640
Ferry JM, Kitajima K, Strickland A. Valley JW (2014) Ion microprobe survey of the grain-scale oxygen isotope geochemistry of minerals in metamorphic rocks. Geochim. Cosmochim. Acta, 144: 403-433
Ferry JM, Rumble D (1997) Formation and destruction of periclase by fluid flow in two contact aureoles. Contrib Mineral Petrol 128:313-334
Fissler DK, Cygan RT (1999) Diffusion of Ca and Mg in calcite. Am Miner 84:1392-1399
Furlong KP, Hanson RB Bowers JR (1991) Modeling thermal regimes In: Kerrick DM (ed) Contact Metamorphism. Rev Mineral Geochem 26:437-506
Gerdes ML, Baumgartner LP, Person M (1995) Stochastic permeability models of fluid flow during contact metamorphism. Geology 23:945-948
Gerdes ML, Baumgartner LP, Person M (1998) Convective fluid flow through heterogeneous country rocks during contact metamorphism. J Geophys Res 103:23983-24003
Graham CM, Valley JW, Eiler JM, Wada H (1998) Timescales and mechanism of fluid infiltration in a marble: an ion microprobe study. Contrib Mineral Petrol 132:371-389
Heberling F, Paulig L, Nie Z, Schild D, Finck N (2016) Morphology controls on calcite recrystallization. Environ Sci Technol 50:11735-11741
Hervig RL Williams P, Thomas RM, Schauer SN, Steele IM (1992) Microanalysis of oxygen isotopes in insulators by secondary ion mass spectrometry. Int J Mass Spectrom Ion Process 120:45-63
Hoersch AL (1981) Progressive metamorphism of the chert-bearing Durness limestone in the Beinn an Dubhaich aureole, Isle of Skye, Scotland: A reexamination. Am Miner 66:491-506
Holness MB, Bickle MJ, Graham CM (1991) On the kinetics of textural equilibration in forsterite marbles. Contrib Mineral Petrol 108:356–367
Holness MB, Siklos STC (2000) The rates and extent of textural equilibrium in high-temperature

fluid-bearing systems. Chem Geol 162:137-153
John DA (1989) Geologic setting, depths of emplacement, and regional distribution of fluid inclusions in intrusions of the central Wasatch Mountains, Utah. Econ Geol 84:386–409
Kerrick DM (1991) Overview of contact metamorphism. In: Kerrick DM (ed) Contact Metamorphism. Rev Mineral Geochem 26:1-12
Kita NT, Ushikubo T, Fu B, Valley JW (2009) High precision SIMS oxygen isotope analysis and the effect of sample topography. Chem Geol 264:43-57
Kita NT, Nagahara H, Tachibana S, Tomomura S, Spicuzza MJ, Fournelle JH and Valley JW (2010) High precision SIMS oxygen three isotope study of chondrules in LL3 chondrites: Role of ambient gas during chondrule formation. Geochim. Cosmochim. Acta, 74: 6610-6635.
Kozdon R, Ushikubo T, Kita NT, Spicuzza M, Valley JW (2009) Intratest oxygen isotope variability in the planktonic foraminifer *N. pachyderma*: Real vs. apparent vital effects by ion microprobe. Chem Geol 258:327-337
Lackey JS, Valley JW (2004) Complex patterns of fluid flow during wollastonite formation in calcareous sandstones at Laurel Mountain, Mt. Morrison Pendant, California. Geol Soc Am Bull 116:76-93
Loury P (2014) Metamorphism and fluid–rock interaction in the Alta, Utah contact aureole: identification of forsterite reaction path- ways, evaluation of reaction overstepping, and trace element characterization. MS Thesis, University of Utah
Mahon KI (1996) The new "York" regression: application of an improved statistical method to geochemistry. International Geol Rev 38:293-303
Matthews A, Lieberman J, Avigad D, Garfunkel Z (1999) Fluid-rock interaction and thermal evolution during thrusting of an alpine metamorphic complex (Tinos Island, Greece). Contrib Mineral Petrol 135:212-224
Moore JN, Kerrick DM (1976) Equilibria in siliceous dolomites of the Alta aureole, Utah. Am J Sci 276:502–524
Müller T, Baumgartner LP, Forster CT, Vennemann TW (2004) Metastable prograde mineral reactions in contact aureoles. Geology 32:821–824
Müller T, Baumgartner LP, Foster CT, Bowman JR (2009) Crystal size distribution of periclase in contact metamorphic dolomite marbles from the southern Adamello Massif, Italy. J Pet 50:451-465
Nabelek PI, Hofmeister AM, Whittington AG (2012) The influence of temperature-dependent thermal diffusivity on the conductive cooling rates of plutons and temperature-time paths in contact aureoles. Earth Planet. Sci. Let. 317-318:157-164
Page FZ, Kita, NT, Valley JW (2010) Ion microprobe analysis of oxygen isotopes in garnets of complex chemistry. Chem Geol 270:9-19
Pollington AD, Bowman JR, Kaszuba JP (2005) Heterogeneous fluid flow, reaction progress, and isotope distribution in the talc zone, outer Alta aureole, Utah (abst): Geol. Soc. Amer. Mtg., Salt Lake City, UT
Ridley J, Thompson AB (1986) The role of mineral kinetics in the development of metamorphic microtextures. In: Walther JV, Wood BJ (eds) Fluid–rock interactions during metamorphism. Springer, Berlin, pp 154–193
Roselle GT, Baumgartner LP, Chapman JA (1997) Nucleation-dominated crystallization of forsterite in the Ubehebe Peak contact aureole, California. Geology 25:823–826
Roselle GT, Baumgartner LP, Valley JW (1999) Stable isotope evidence of heterogeneous fluid

infiltration at the Ubehebe Peak contact aureole, Death Valley National Park, California. Am J Sci 299:93-138
Rubie DC (1998) Disequilibrium during metamorphism: the role of nucleation kinetics. In: Treloar PJ, O'Brien PJ (eds) What drives metamorphism and metamorphic reactions? Geological Society, London, Special publications 138:199-214
Rumble D (1982) Stable isotope fractionation during metamorphic devolatilization reactions. In: Ferry JM (ed) Characterization of Metamorphism through Mineral Equilibria. Mineralogical Society of America, Rev Mineral Geochem 10:327-353.
Sharp ZD (1990) A laser-based microanalytical method for the in-situ determination of oxygen isotope ratios of silicates and oxides. Geochim Cosmochim Acta 54:1353-1357
Skippen GB (1974) An experimental model for low pressure metamorphism of siliceous dolomitic marble. Am J Sci 274:487-509
Śliwiński MG, Kitajima K, Kozdon R, Spicuzza MJ, Fournelle JH, Denny A, Valley JW (2016) Secondary ion mass spectrometry bias on isotope ratios in dolomite-ankerite, Part I: $\delta^{18}O$ matrix effects. Geostand Geoanal Res 40:157-172
Stearns MA, Bartley JM, Bowman JR, Forster CW, Beno CJ, Riddle DD, Callis SJ, Udy ND (2020) Simultaneous magmatic and hydrothermal regimes in the Alta—Little Cottonwood stocks, Utah, USA, recorded by multiphase U-Pb petrochronology. Geosciences 10:129–150
Valley JW (1986) Stable Isotope Geochemistry of Metamorphic Rocks. In Stable Isotope in High Temperature Geological Processes. JW Valley, JR O'Neil, and HP Taylor (eds.), M.S.A. Rev Mineral 16: 445-489.
Valley JW, Kitchen N, Kohn MJ, Niendorf CR, and Spicuzza MJ (1995) UWG- 2, a garnet standard for oxygen isotope ratios: strategies for high precision and accuracy with laser heating: Geochim Cosmochim Acta 59:5223-5231.
Valley JW, Kita NT (2009) In situ oxygen isotope geochemistry by ion microprobe. In: M. Fayek (ed) Secondary Ion Mass Spectrometry in the Earth Sciences, Mineralogical Association of Canada Short Course 41:19-63
Valley JW (2001) Stable isotope thermometry at high temperatures: In: Valley JW, Cole DR (eds) Stable isotope geochemistry. Rev Mineral & Geochem 43:365-414
Vermeesch P (2018) IsoplotR: a free and open toolbox for geochronology. Geosci Front 9:1479-1493
Vogel TA, Cambray FW, Constenius KN (2001) Origin and emplacement of igneous rocks in the central Wasatch Mountains, Utah. Rocky Mt. Geol. 36:119–162
Wang X-L, Coble MA, Valley JW, Shu X-J, Kitajima K, Spicuzza MJ, Sun T (2014) Influence of radiation damage on late Jurassic zircon from southern China: Evidence from in situ measurement of oxygen isotopes, laser Raman, U-Pb ages, and trace elements. Chem. Geol., 389: 122-136.
Watson EB, Müller T (2009) Non-equilibrium isotopic and elemental fractionation during diffusion-controlled crystal growth under static and dynamic conditions. Chem Geol 267:111-124
Welsch B, Hammer J, Hellebrand E (2014) Phosphorus zoning reveals dendritic architecture of olivine. Geology 42:867–870
Wendt I, Carl C (1991) The statistical distribution of the mean square weighted deviation. Chem Geol 86:275-285
Wilson JC (1961) Geology of the Alta Stock, Utah. Ph.D. Thesis, California Institute of

Technology
Zheng YF, Metz P, Satir M, Sharp ZD (1994) An experimental calibration of oxygen isotope fractionation between calcite and forsterite in the presence of a CO_2-H_2O fluid. Chem Geol 116:17-27
Zheng YF, Satir M, Metz P, Sharp ZD (1999) Oxygen isotope exchange processes and disequilibrium between calcite and forsterite in an experimental C-O-H fluid. Geochim Cosmochim Acta 63:1781-1786
Zheng YF, Satir M, Metz P (2003) Oxygen isotope exchange and disequilibrium between calcite and tremolite in the absence and presence of an experimental C–O–H fluid. Contrib Mineral Petrol 146:683-695

FIGURE CAPTIONS

Fig. 1 Geologic map of the study area showing the Alta stock and its surrounding contact aureole after Baker et al. (1966), Moore and Kerrick (1976), and Chadwell (2020). Locations of isograds for the metamorphic index minerals talc, tremolite, forsterite, clinohumite, and periclase are shown with the jagged purple lines. Inset shows the southern aureole and the sampling locations of forsterite-bearing marbles discussed in this study.

Fig. 2 (a) A simplified schematic cross section through the periclase and forsterite zones showing the compositional heterogeneity in this section of marble wallrocks. Dolomite-rich (light blue) and dolomite-poor (purple) lithologies are shown below the Alta-Grizzly thrust (labeled A-G Thrust; solid horizontal black line). Dolomite-poor lithologies lack reactant dolomite and do not experience periclase formation, while lithologies with dolomite remaining after the forsterite reaction has gone to completion do experience the periclase forming reaction (dark blue). The average location of periclase isograd is labeled with the grey dashed line, while the black dashed lines that separate periclase-bearing lithologies from periclase absent lithologies demonstrate some of the complexity observed at the periclase reaction front. White arrows indicate the source and direction of fluid flow: lateral, bedding concordant down temperature fluid flow. (b) The range of measured oxygen isotopic values from Cook et al. (1997) and the estimates of time integrated fluid flux (q_{TIFF}) from reaction progress calculations of Cook and Bowman (2000) are listed for each lithology.

Fig. 3 Ca Kα X-ray maps of forsterite zone marbles at different distances from the igneous contact: forsterite (black), dolomite (dark gray), calcite (light grey). From Chadwell (2020). Samples from the inner aureole (a-b) are generally characterized by fine-grained forsterite with little to no remaining primary dolomite in the matrix. Middle (c-d) and outer (e-f) aureole forsterite takes on a more tabular habit, becomes coarser with increasing distance from the contact, and is commonly surrounded by calcite coronas. All areas shown here are at the same scale. Forsterite in the outer forsterite zone can have skeletal margins—arrays of numerous, small and physically separate forsterite grains in parallel extinction with the central forsterite tablet (f).

Fig. 4 Comparison of $\delta^{18}O$ forsterite values determined by both LF-GSMS and SIMS techniques from four samples across the periclase and middle forsterite zones. SIMS data (in red) from three homogenous forsterite zone samples are presented as weighted averages of all spots analyzed while the range of SIMS $\delta^{18}O$ values measured is shown for one heterogeneous sample from the periclase zone (23B). SIMS $\delta^{18}O$ values are consistently higher than values determined by LF (up to ~1.7‰

higher; FZ9-18). The LF results show no clear dependence on the grain-size and may include traces of serpentine.

Fig. 5 SIMS $\delta^{18}O$ data for forsterite mineral separates from the forsterite and periclase zones, cast in 25.4 mm diameter epoxy rounds. Each cross shows the reported SIMS $\delta^{18}O$ value (vertical line) and the 2SD precision on the analysis (horizontal band). The color of each cross identifies the location of the spot analysis within a forsterite crystal (red = center, purple = interior, and blue = edge). Light grey boxes group all spot analyses from a single forsterite crystal, while larger clear boxes with solid black outlines group crystals from individual samples. Sample identification and locations within the aureole are also included. The calculated weighted mean (WM; vertical black line), 95% confidence interval (associated darker grey band) and MSWD values are included for the three homogeneous samples (88-7, FZ7-6, and FZ9-18). MSWD values are included for B-7-1 to demonstrate that although the sample is heterogeneous (MSWD = 3.01), individual crystals pass both the quantitative (for ex., grain 1: MSWD = 0.53) and semiquantitative definitions for homogeneity defined in the Methods section.

Fig. 6 Compilation of SIMS $\delta^{18}O$ data from samples where touching grains of forsterite, calcite and dolomite were analyzed. These samples come from 300m (A-4-1), 475m (FZ4-5a) and 615m (99V-3) from the contact. Brackets on the left side of each sample grouping separate analyses of individual phases. Analyses within a single crystal are identified by brackets on the right side of each sample group. Each cross shows the reported SIMS $\delta^{18}O$ value (short vertical line) and the 2SD precision of the analysis (crossing horizontal band). The color of each cross identifies the location of the spot analysis (red = center, purple = interior, and blue = edge). Statistical analysis (see Methods section) shows that forsterite and dolomite from A-4-1, forsterite from FZ4-5a and dolomite from 99V-3 are homogeneous in $\delta^{18}O$ and their weighted mean (WM; vertical dark grey line) and 95% confidence interval (associated lighter-grey band) are plotted as well. All other phases have an associated grey box that represents the range of reported SIMS $\delta^{18}O$ values for that phase. SIMS values (either sample weighted average or the range of values) were used to calculate mineral-mineral fractionation factors (black horizontal bars).

Fig. 7 (a) Plot of forsterite (top), calcite (middle), and dolomite (bottom) SIMS data from Traverse 1 in sample 99V-3. All phases are locally homogeneous in $\delta^{18}O$ within analytical uncertainty and allow calculation of local mineral-mineral fractionation factors. (b) BSE-SEM image of traverse 1 with spot locations and $\delta^{18}O$ values superimposed.

Fig. 8 BSE-SEM images and multiple transects through two forsterite single crystals from two samples from the outer periclase (94I-9-2b [a-c]; 150m from contact) and inner forsterite zones (88-8 [d-f]; 220m from contact). Serpentine (lighter grayscale) has replaced forsterite along fractures in both crystals. The A-A' transect (b) through the crystal in (a) shows relatively abrupt changes in $\delta^{18}O$ (Fo) from an isotopically light center, to isotopically heavier zones in the interior, and back to isotopically light edges. The rim on this crystal is consistently low in $\delta^{18}O$ on both traverses (a-c). The B-B' transect through this grain establishes that the significant retrograde serpentinization that this grain has experienced (serpentine veins shown by grey bars in plots) does not perturb the $\delta^{18}O$ values of adjacent domains of primary forsterite. Transects through the crystal in (d) show more gradational changes and absence of systematic decreases (f) in $\delta^{18}O$ values from center-to-edge, although the edges tend to have lower $\delta^{18}O$ values (e-f). The precision of all

individual measurements plotted in this figure is ±0.2 to 0.3‰. Haloes around SIMS are surface contamination from ion sputtering and are not internal to the olivine crystal.

Fig. 9 (a) Traverse I (site 94I; 150m from contact) from Bowman et al. (2009) demonstrating the systematic decrease in $\delta^{18}O$ values of calcite traversing the boundary from a calcite + forsterite marble (layer 8) to an overlying calcite + periclase(brucite) +/- humite marble (layer 9). White diamonds = SIMS calcite data; grey line = bulk calcite data; see Bowman et al. (2009) for detailed discussion of the calcite SIMS data. The locations of all forsterite crystals from the 2a, 2b, and 2c horizons analyzed in this study were measured with respect to the 8/9 boundary and superimposed on this traverse. Within ~2.5 cm of the 8/9 boundary, humite completely replaces forsterite [i.e., Hum (in); dashed line]. SIMS $\delta^{18}O$ data for forsterite are presented as a grain average (black squares) with the associated vertical line representing the range of $\delta^{18}O$ values measured in each crystal. The precision of individual forsterite measurements across all horizons is 0.2-0.3‰. (b) Plot of calculated $\Delta^{18}O_{Cal\text{-}Fo}$ values (white circles) along traverse I. These $\Delta^{18}O_{Cal\text{-}Fo}$ values are based on the average of the measured SIMS $\delta^{18}O$ values for each forsterite crystal and the SIMS $\delta^{18}O$ values from the calcite at the same stratigraphic level (from Bowman et al., 2009). The corresponding vertical lines represent the ranges of calculated $\Delta^{18}O_{Cal\text{-}Fo}$ based on grain-scale isotopic heterogeneities preserved in individual forsterite crystals. Also included is the expected equilibrium $\Delta^{18}O_{Cal\text{-}Fo}$ value of +4.5‰ at 570ºC (Chiba et al. 1989). The measured $\Delta^{18}O_{Cal\text{-}Fo}$ values range from near equilibrium values in horizon 2a (max. value at 3.7) down to reversed, or crossed over, values in horizon 2c (min. value at -4.2).

Fig. 10 BSE-SEM images of forsterite marble sample 94I (layer 8; Fig. 8) from horizon 2a (a) and 2c (b). Greyscale can be used to identify the minerals calcite (Cal; light grey matrix), phlogopite (Phl; grey), and forsterite (Fo; dark grey) in 2a (a) and calcite and forsterite in 2b (b). Void space and serpentinized fractures and rims in forsterite crystals (black) are also visible in both scans. Both visual inspection and statistical data (lower right box in both images) show that forsterite crystals become on average larger and fewer in number, and the number of forsterite crystals/mole of forsterite decreases, from horizon 2a to 2c—toward the layer 8/9 boundary (Fig. 8a).

Fig. 11 Detailed SIMS $\delta^{18}O$ characterization of representative forsterite crystals along traverse I at site 94I in the periclase zone. Two crystals from each of the three horizons investigated in detail (Fig. 8) are presented [(a-b) 94I-9-2a, (c-d) 94I-9-2b, (e-f) 94I-9-2c]. The degree of grain-scale zoning recorded in all three horizons is as much as 2.5-3.0‰, but relatively homogeneous grains were also identified in all three horizons. Zoning patterns are generally not systematic, and $\delta^{18}O$ values both decrease (b, d, f) and increase (c) along center-to-edge traverses. Haloes around SIMS pits are surface contamination from ion sputtering and are not internal to the olivine crystal.

Fig. 12 (a) Average $\delta^{18}O$ values and $\delta^{18}O$ ranges (vertical solid lines) of carbonate minerals and forsterite plotted against distance from the igneous contact. Symbols are: bulk carbonate analyzed by GSMS (blue triangles); SIMS calcite (green square); SIMS dolomite (red hexagon); and SIMS forsterite (black diamond). Results for each of the nine samples are plotted in boxes for clarity; the actual sample locations are shown by vertical dashed lines. Samples A-4-1 and B-7-1 are from the same outcrop location. Sample A-4-1 and 94I demonstrate the consistency of bulk carbonate and SIMS $\delta^{18}O$ data. Lowest calcite values in 94I from both GSMS (11.7‰) and SIMS (12.2‰) are off this chart and are listed numerically. (b) Measured $\Delta^{18}O_{Cal\text{-}Fo}$ and $\Delta^{18}O_{Dol\text{-}Fo}$ values plotted

against distance from the contact. Variations in the expected equilibrium $\Delta^{18}O_{Cal\text{-}Fo}$ and $\Delta^{18}O_{Dol\text{-}Fo}$ values with distance from the igneous contact (based on calcite-dolomite solvus thermometry, Cook and Bowman, 1994) are shown for comparison. Two samples (88-7 and FZ9-18) plot as spots because of the homogeneity in $\delta^{18}O$ of forsterite in these two samples. All other samples exhibit ranges of calculated $\Delta^{18}O_{Cal\text{-}Fo}$ because of heterogeneity in $\delta^{18}O$ for carbonate minerals and/or forsterite. Negative values of $\Delta^{18}O_{Cal\text{-}Fo}$ at 94I are not included, but the low value is listed numerically. With two exceptions (88-8, 94I), forsterite is significantly out of oxygen isotope exchange equilibrium with calcite and dolomite throughout the periclase and forsterite zones of the aureole.

Fig. 13 Schematic T-X(CO_2) phase diagrams showing evolution pathways for two compositionally distinct layers (L1 and L2) and their prograde evolution pathways under three infiltration regimes: (a) simultaneous infiltration, (b) L1 infiltrated before L2, and (c) L2 infiltrated before L1.

Fig. 14 (a) The initial unmetamorphosed condition of sample 94I (carbonate $\delta^{18}O$ profile—red line) and the symbols for the parameters (fluid flux and forsterite grain-size) used in the one-dimensional (1D) infiltration-reaction models. (b) The existing $\delta^{18}O$ profiles measured by SIMS in forsterite and calcite along a traverse normal to the layer 8/9 interface (see Fig. 9). Four scenarios (c-f) are proposed as testable models to explain measured data in (b) (in light of existing constraints from this traverse) that allow interrogation of the development of both the calcite and forsterite isotope profiles preserved along this traverse. The left box (time interval t_1 to t_2) in each scenario highlights the range of forsterite isotope ratios (black band from t_1 to t_2) expected from growth in response to the carbonate reservoir in layer 8 that is being progressively depleted (range in red lines from t_1 to t_2). The middle box (t_3) in each scenario represents a period of time where layer 9 experiences continued or the onset (scenario 4) of fluid flow as a result of periclase petrogenesis and carbonates in layer 9 experience additional $\delta^{18}O$ depletion relative to carbonate in the interior of layer 8. At this stage forsterite $\delta^{18}O$ values that developed from t_1 to t_2 are fixed due to the refractory nature of this phase. The right box (t_f) in each scenario represents the final condition of the system where by varying parameters from t_o to t_f, the measured calcite $\delta^{18}O$ profile is reproduced. Each scenario is discussed in the text, with more detailed discussions of scenario's 1-3 found in appendix A.

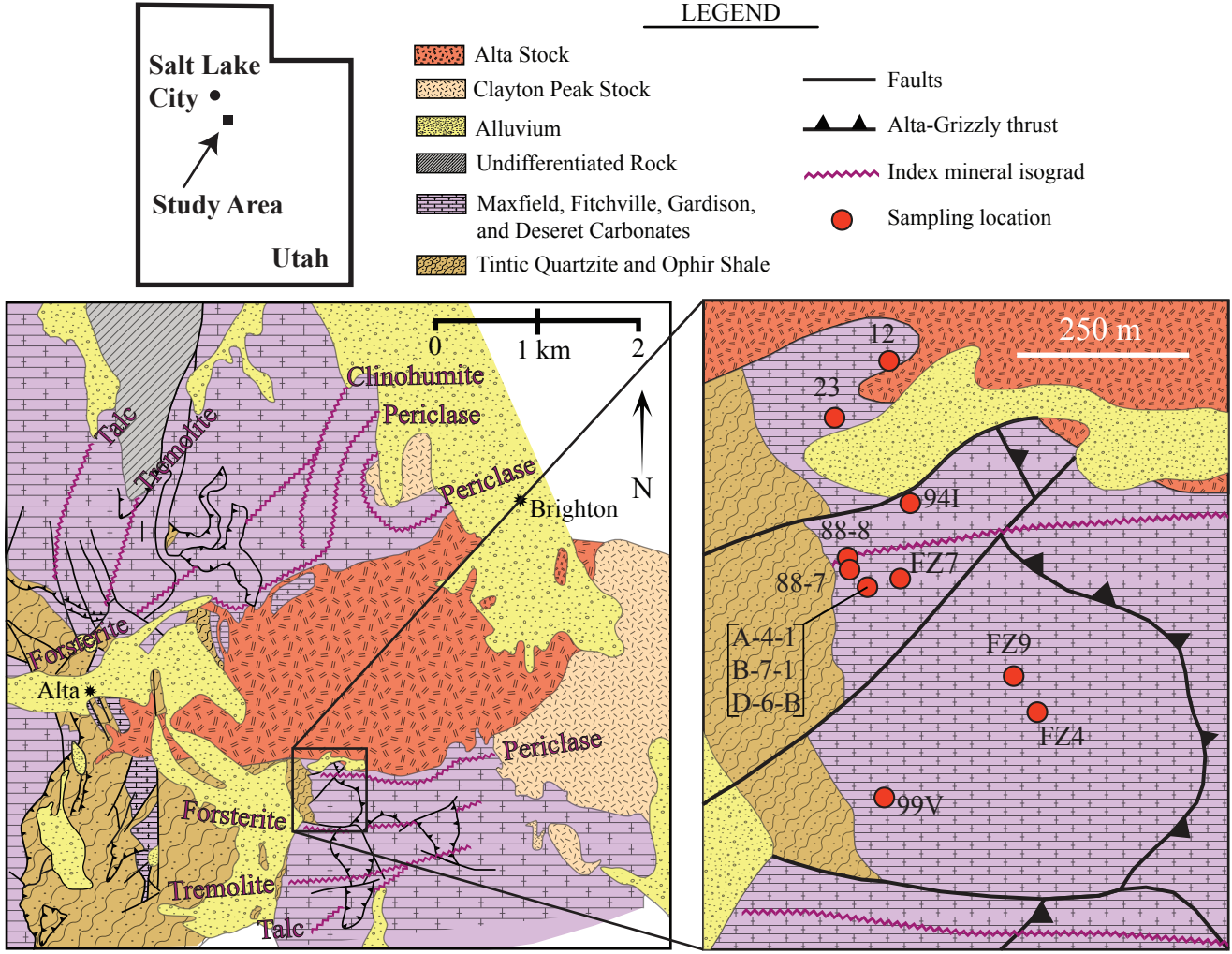
Salt Lake City
Study Area
Utah
LEGEND
Alta Stock
Clayton Peak Stock
Alluvium
Undifferentiated Rock
Maxfield, Fitchville, Gardison, and Deseret Carbonates
Tintic Quartzite and Ophir Shale
Faults
Alta-Grizzly thrust
Index mineral isograd
Sampling location
0
1 km
2
N
Clinohumite
Periclase
Periclase
Brighton
Talc
Tremolite
Forsterite
Alta
Periclase
Forsterite
Tremolite
Talc
250 m
12
23
94I
88-8
88-7
FZ7
A-4-1
B-7-1
D-6-B
FZ9
FZ4
99V

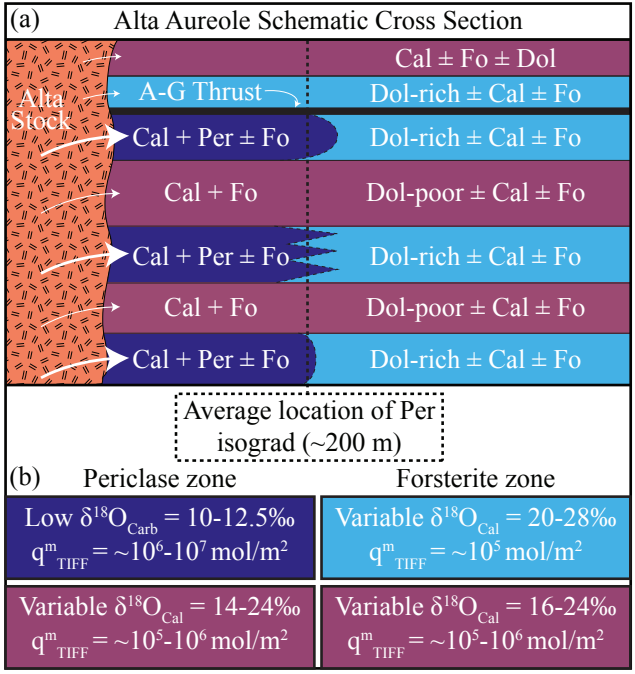
(a)
Alta Aureole Schematic Cross Section
Alta Stock
Cal ± Fo ± Dol
A-G Thrust
Dol-rich ± Cal ± Fo
Cal + Per ± Fo
Dol-rich ± Cal ± Fo
Cal + Fo
Dol-poor ± Cal ± Fo
Cal + Per ± Fo
Dol-rich ± Cal ± Fo
Cal + Fo
Dol-poor ± Cal ± Fo
Cal + Per ± Fo
Dol-rich ± Cal ± Fo
Average location of Per isograd (~200 m)
(b)
Periclase zone
Forsterite zone
Low $\delta^{18}O_{Carb}$ = 10-12.5‰
q^m_{TIFF} = ~10^6-10^7 mol/m^2
Variable $\delta^{18}O_{Cal}$ = 20-28‰
q^m_{TIFF} = ~10^5 mol/m^2
Variable $\delta^{18}O_{Cal}$ = 14-24‰
q^m_{TIFF} = ~10^5-10^6 mol/m^2
Variable $\delta^{18}O_{Cal}$ = 16-24‰
q^m_{TIFF} = ~10^5-10^6 mol/m^2

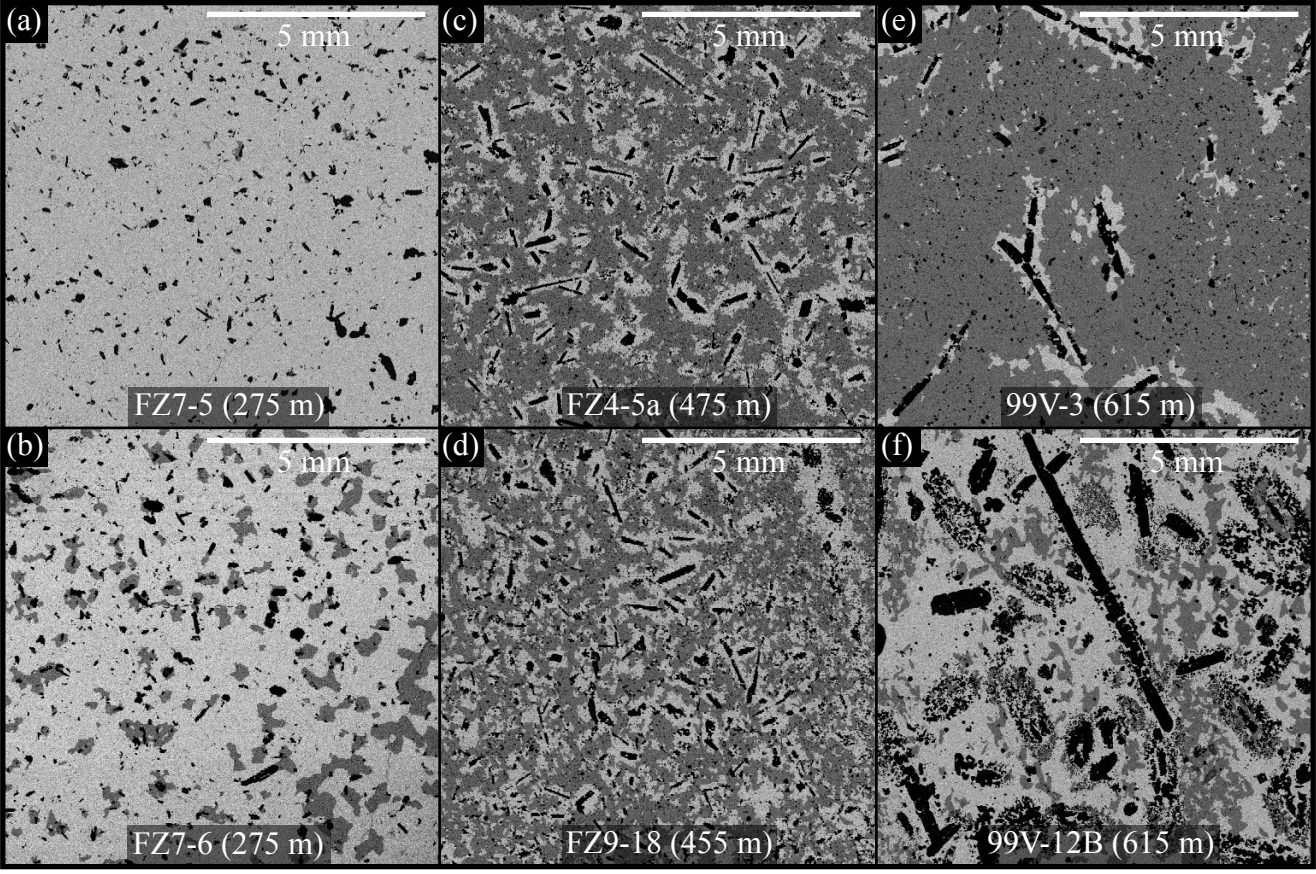
(a)
5 mm
FZ7-5 (275 m)
(c)
5 mm
FZ4-5a (475 m)
(e)
5 mm
99V-3 (615 m)
(b)
5 mm
FZ7-6 (275 m)
(d)
5 mm
FZ9-18 (455 m)
(f)
5 mm
99V-12B (615 m)

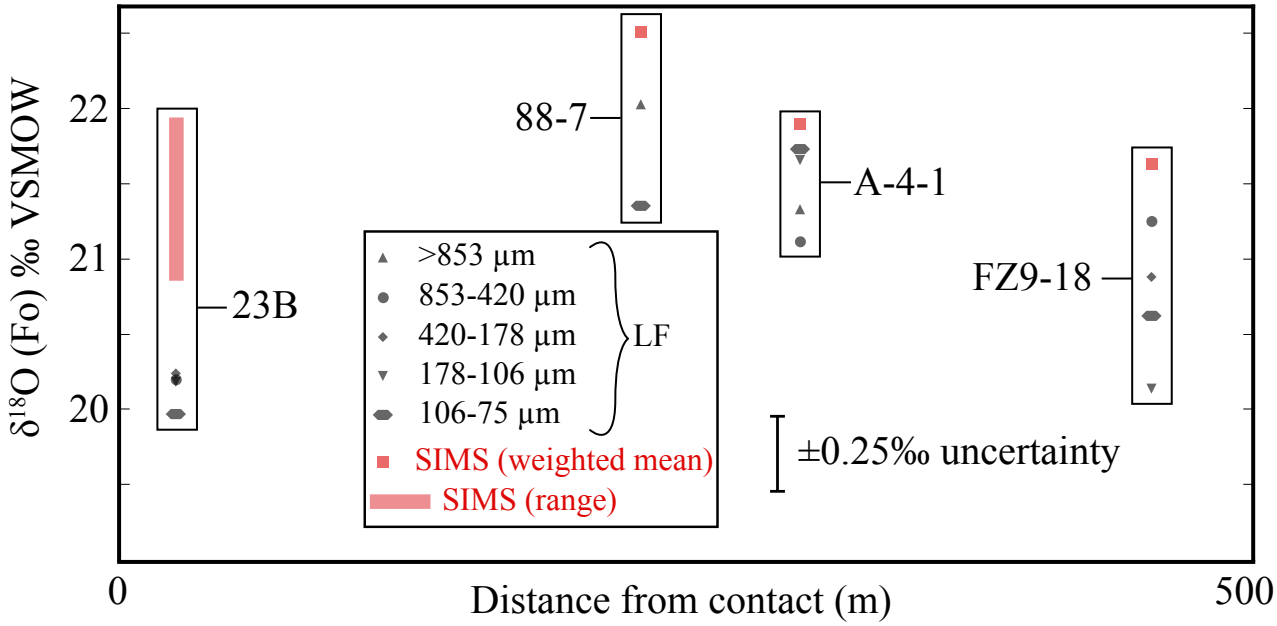
δ18O (Fo) ‰ VSMOW
22
21
20
23B
88-7
A-4-1
FZ9-18
>853 µm
853-420 µm
420-178 µm
178-106 µm
106-75 µm
LF
SIMS (weighted mean)
SIMS (range)
±0.25‰ uncertainty
0
Distance from contact (m)
500

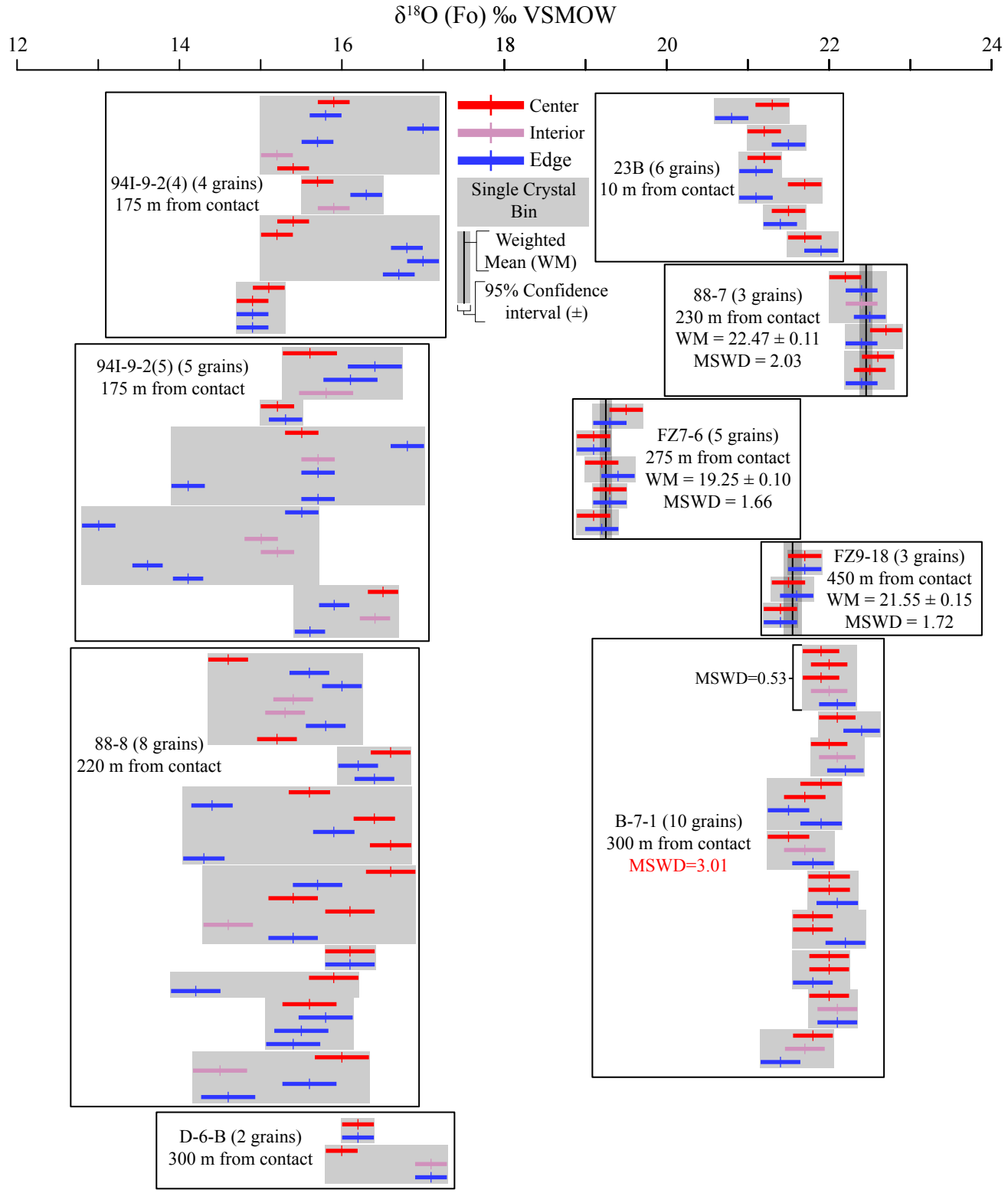
δ18O (Fo) ‰ VSMOW
12
14
16
18
20
22
24
Center
Interior
Edge
Single Crystal Bin
Weighted Mean (WM)
95% Confidence interval (±)
94I-9-2(4) (4 grains)
175 m from contact
23B (6 grains)
10 m from contact
88-7 (3 grains)
230 m from contact
WM = 22.47 ± 0.11
MSWD = 2.03
94I-9-2(5) (5 grains)
175 m from contact
FZ7-6 (5 grains)
275 m from contact
WM = 19.25 ± 0.10
MSWD = 1.66
FZ9-18 (3 grains)
450 m from contact
WM = 21.55 ± 0.15
MSWD = 1.72
MSWD=0.53
B-7-1 (10 grains)
300 m from contact
MSWD=3.01
88-8 (8 grains)
220 m from contact
D-6-B (2 grains)
300 m from contact

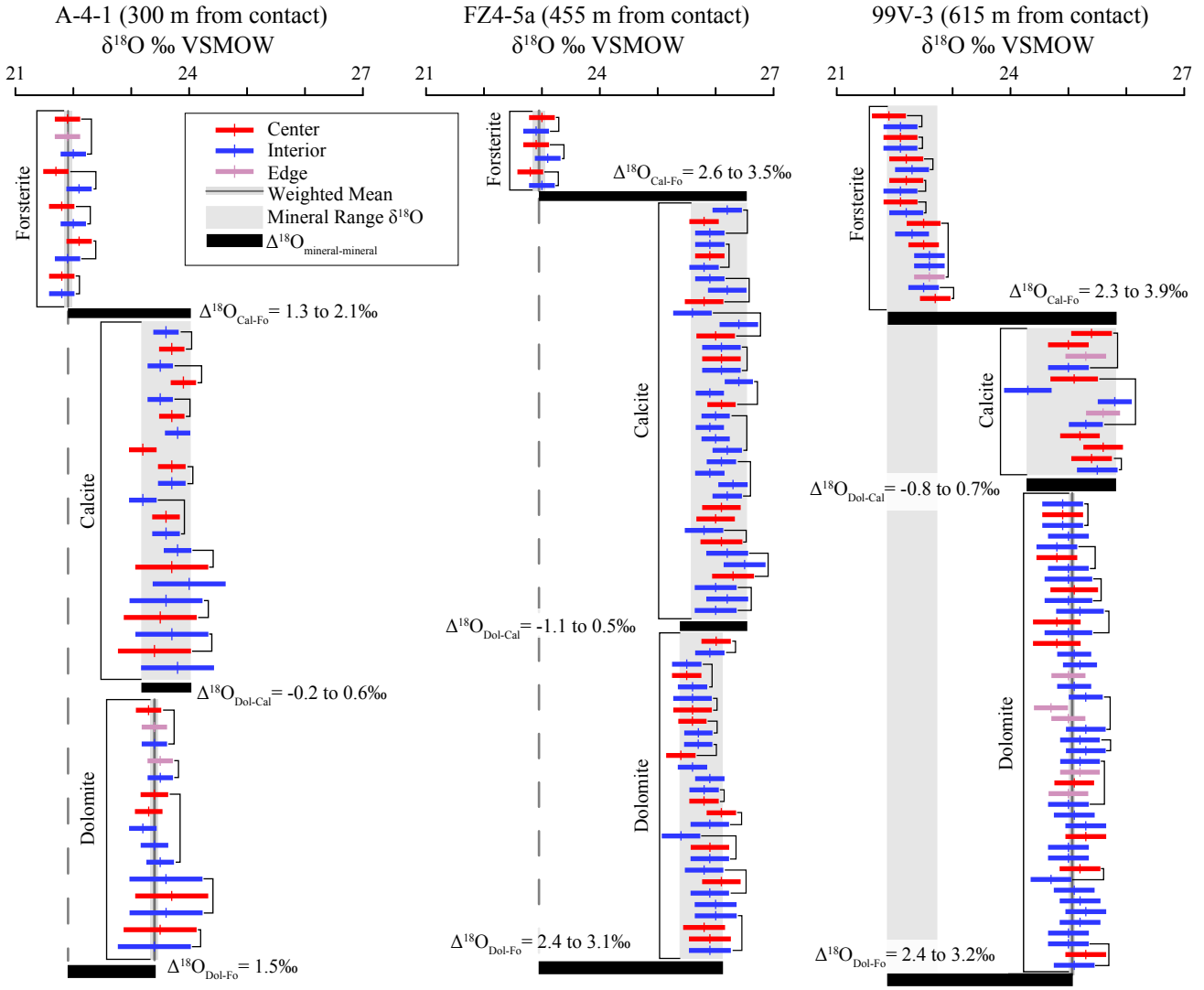
A-4-1 (300 m from contact)
δ18O ‰ VSMOW
FZ4-5a (455 m from contact)
δ18O ‰ VSMOW
99V-3 (615 m from contact)
δ18O ‰ VSMOW
21
24
27
Center
Interior
Edge
Weighted Mean
Mineral Range δ18O
Δ18Omineral-mineral
Forsterite
Calcite
Dolomite
Δ18OCal-Fo= 1.3 to 2.1‰
Δ18ODol-Cal= -0.2 to 0.6‰
Δ18ODol-Fo= 1.5‰
Δ18OCal-Fo= 2.6 to 3.5‰
Δ18ODol-Cal= -1.1 to 0.5‰
Δ18ODol-Fo= 2.4 to 3.1‰
Δ18OCal-Fo= 2.3 to 3.9‰
Δ18ODol-Cal= -0.8 to 0.7‰
Δ18ODol-Fo= 2.4 to 3.2‰

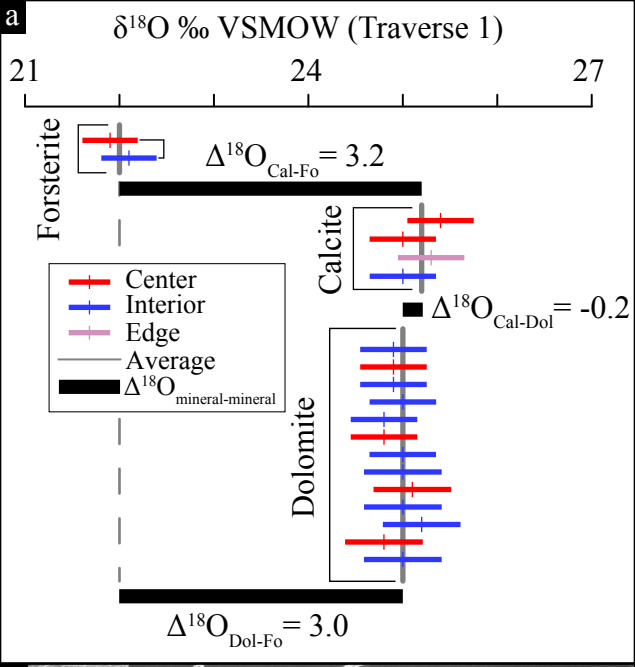
a
δ18O ‰ VSMOW (Traverse 1)
21
24
27
Forsterite
Δ18O Cal-Fo = 3.2
Calcite
Δ18O Cal-Dol = -0.2
Center
Interior
Edge
Average
Δ18O mineral-mineral
Dolomite
Δ18O Dol-Fo = 3.0

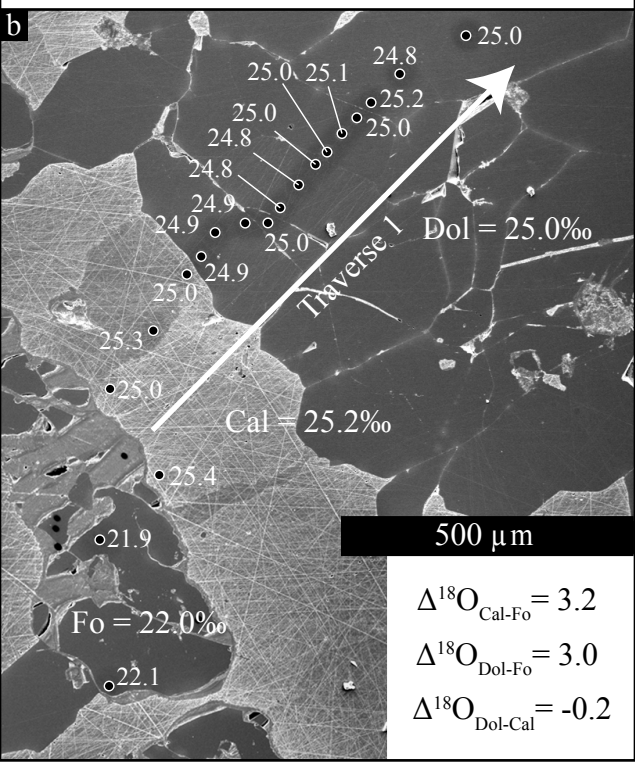
b
25.0
24.8
25.0
25.1
25.2
25.0
25.0
24.8
24.8
24.9
24.9
25.0
24.9
25.0
Traverse 1
Dol = 25.0‰
25.3
25.0
Cal = 25.2‰
25.4
21.9
Fo = 22.0‰
22.1
500 µm
Δ18O Cal-Fo = 3.2
Δ18O Dol-Fo = 3.0
Δ18O Dol-Cal = -0.2

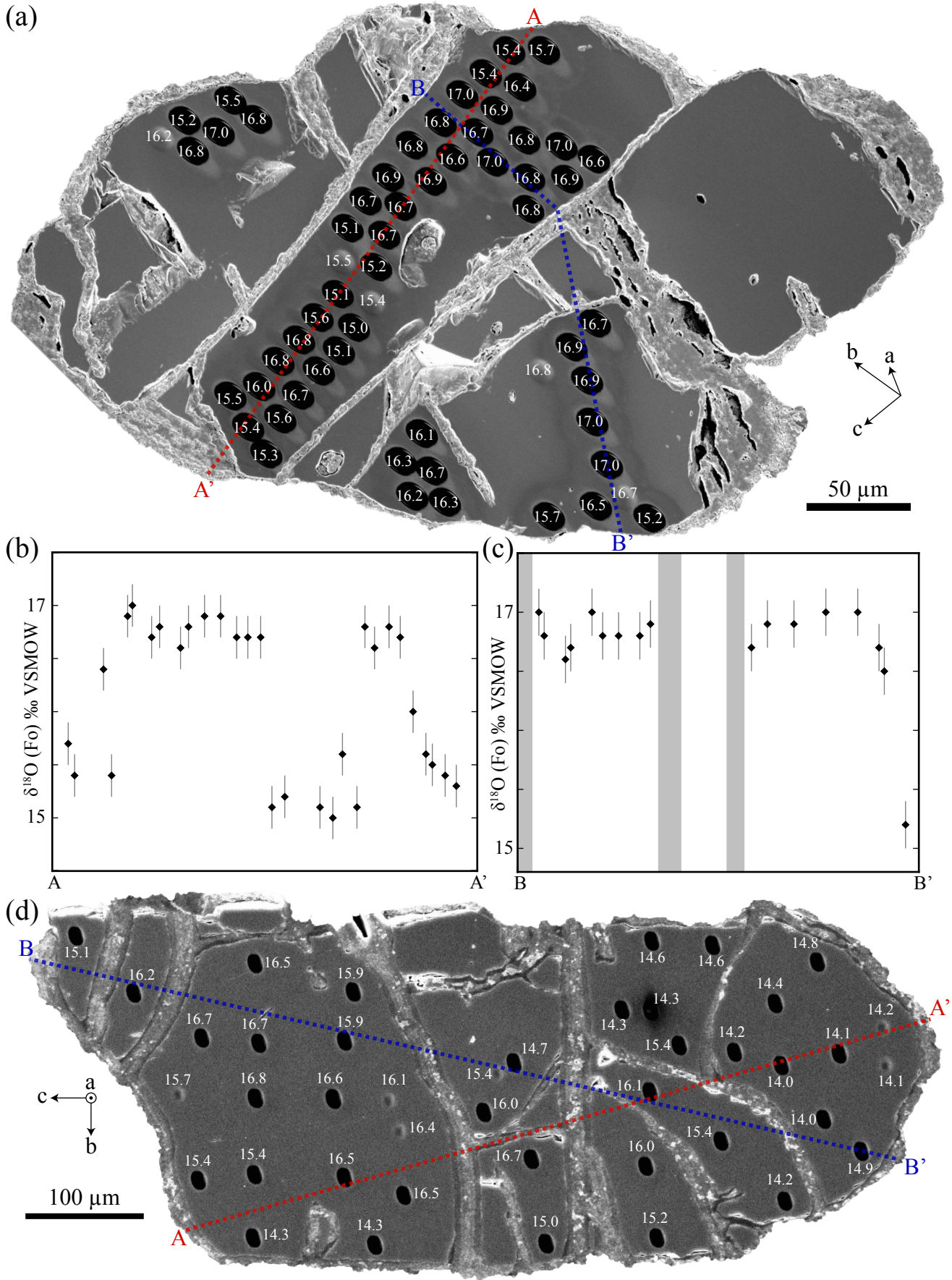
(a)
A
A'
B
B'
15.4 15.7
15.4
16.4
17.0
16.9
16.8
16.7
16.8
17.0
16.6
16.6
17.0
16.8
16.9
16.9
16.9
16.8
16.7
16.7
16.8
15.1
16.7
15.5
15.2
15.1
15.4
15.6
15.0
16.8
15.1
16.8
16.6
16.0
16.7
15.5
15.6
15.4
15.3
16.1
16.3
16.7
16.2
16.3
15.7
16.5
15.2
16.7
16.9
16.8
16.9
17.0
17.0
16.7
15.5
15.2
16.2
17.0
16.8
b
a
c
50 µm
(b)
17
15
δ18O (Fo) ‰ VSMOW
A
A'
(c)
17
15
δ18O (Fo) ‰ VSMOW
B
B'
(d)
B
A'
A
B'
15.1
16.2
16.5
15.9
14.6
14.6
14.8
14.4
14.3
14.3
14.2
16.7
16.7
15.9
14.2
14.1
15.4
14.7
15.7
16.8
16.6
16.1
15.4
16.1
14.0
14.1
16.0
16.4
14.0
15.4
15.4
15.4
16.5
16.7
16.0
14.9
14.2
16.5
14.3
14.3
15.0
15.2
a
c
b
100 µm

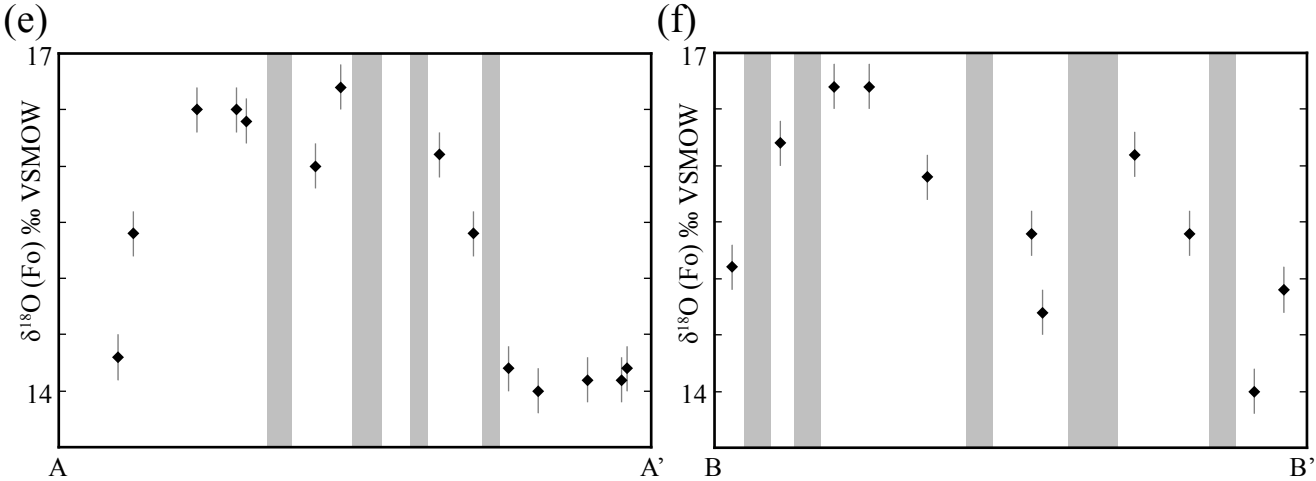
(e)
17
14
δ18O (Fo) ‰ VSMOW
A
A'
(f)
17
14
δ18O (Fo) ‰ VSMOW
B
B'

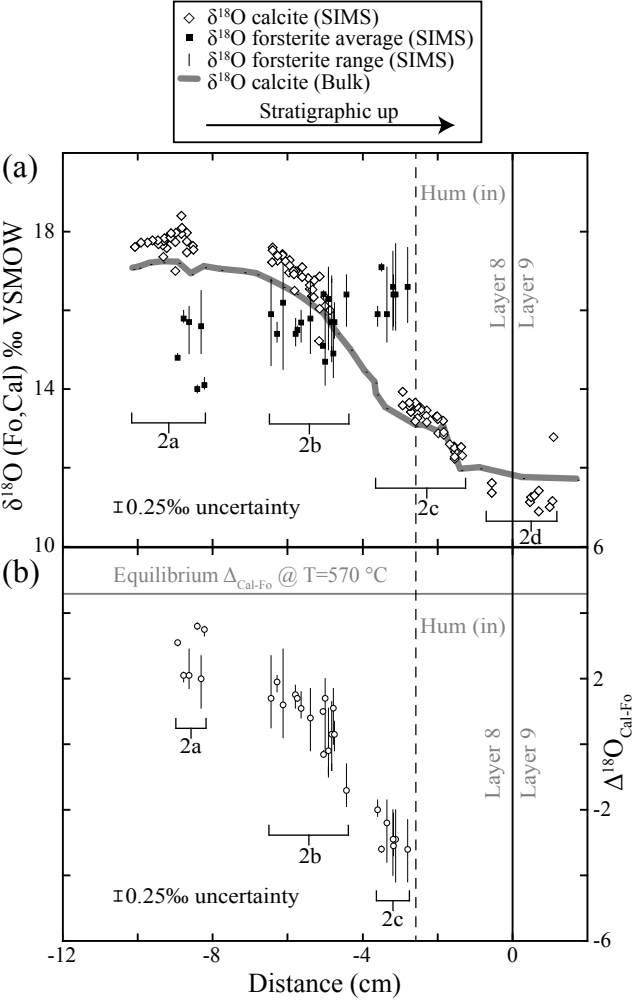
δ18O calcite (SIMS)
δ18O forsterite average (SIMS)
δ18O forsterite range (SIMS)
δ18O calcite (Bulk)
Stratigraphic up
(a)
Hum (in)
Layer 8
Layer 9
δ18O (Fo,Cal) ‰ VSMOW
18
14
10
2a
2b
2c
2d
±0.25‰ uncertainty
(b)
Equilibrium Δ Cal-Fo @ T=570 °C
Hum (in)
Layer 8
Layer 9
Δ18O Cal-Fo
6
2
-2
-6
2a
2b
2c
±0.25‰ uncertainty
-12
-8
-4
0
Distance (cm)

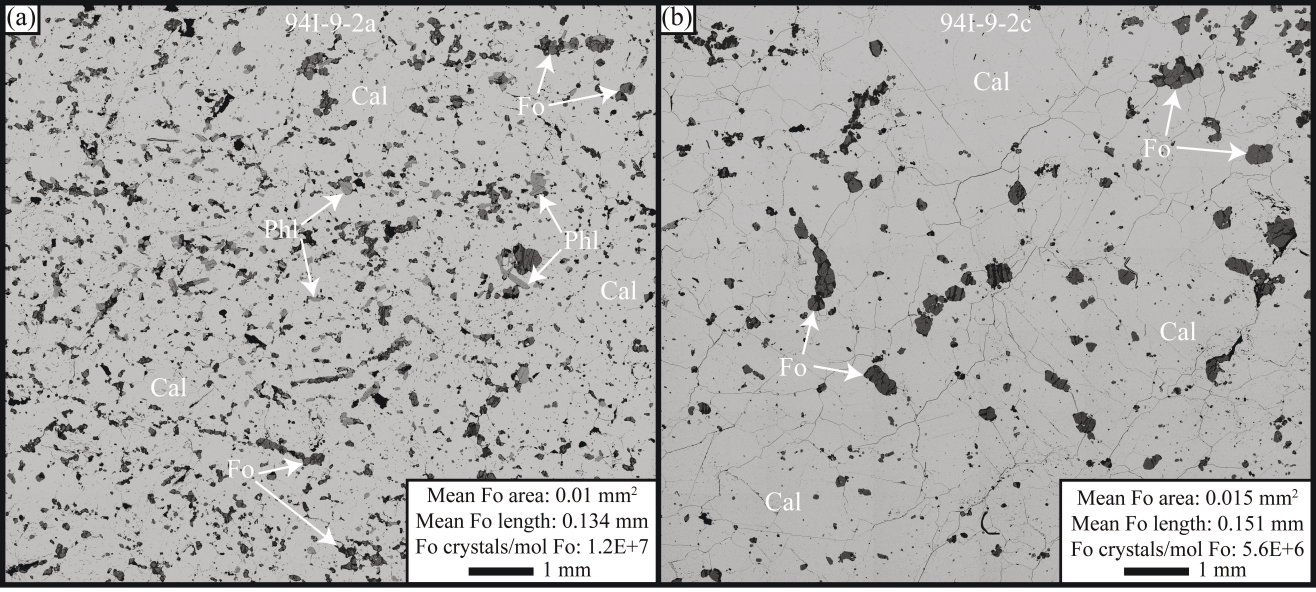
(a)
94I-9-2a
Cal
Fo
Phl
Phl
Cal
Cal
Fo
Mean Fo area: 0.01 mm²
Mean Fo length: 0.134 mm
Fo crystals/mol Fo: 1.2E+7
1 mm
(b)
94I-9-2c
Cal
Fo
Cal
Fo
Cal
Mean Fo area: 0.015 mm²
Mean Fo length: 0.151 mm
Fo crystals/mol Fo: 5.6E+6
1 mm

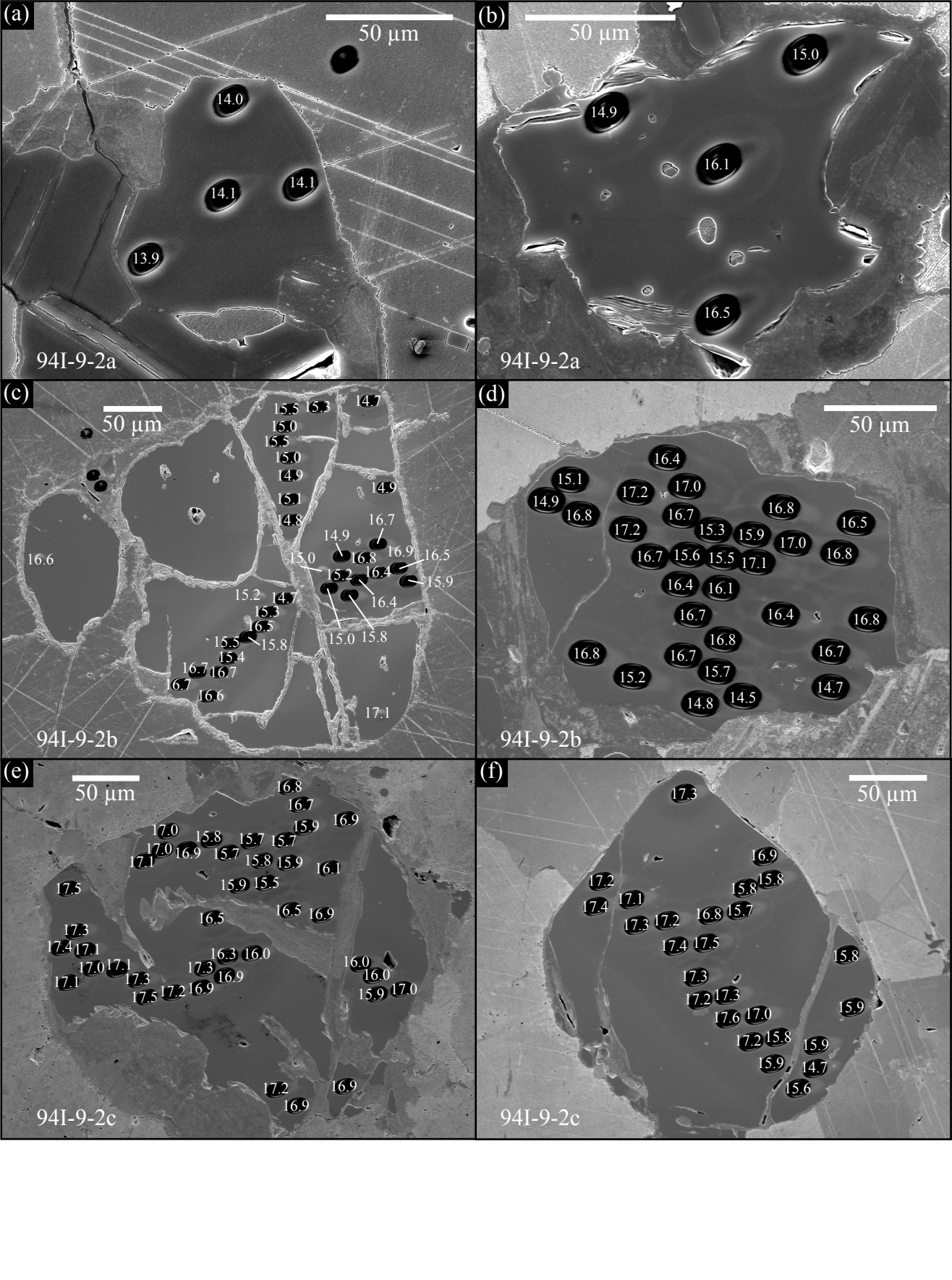
(a)
50 µm
14.0
14.1
14.1
13.9
94I-9-2a
(b)
50 µm
15.0
14.9
16.1
16.5
94I-9-2a
(c)
50 µm
15.5 15.3 14.7
15.0
15.5
15.0
14.9
14.9
15.1
14.8
16.7
14.9
16.9
16.5
15.0
16.8
15.2
16.4
15.9
16.6
15.2 14.7
16.4
15.3
16.5
15.5
15.8
15.0 15.8
15.4
16.7 16.7
16.7
16.6
17.1
94I-9-2b
(d)
50 µm
16.4
15.1
17.2
17.0
14.9
16.8
16.7
16.8
16.5
17.2
15.3
15.9
17.0
16.7
15.6
15.5
17.1
16.8
16.4
16.1
16.7
16.4
16.8
16.8
16.8
16.7
16.7
15.2
15.7
14.7
14.8
14.5
94I-9-2b
(e)
50 µm
16.8
16.7
15.9
16.9
17.0
15.8
15.7
15.7
17.0
16.9
15.7
17.1
15.8
15.9
16.1
15.9
15.5
17.5
16.5
16.5
16.9
17.3
17.4
17.1
16.3
16.0
17.0
17.1
17.3
16.9
16.0
17.1
17.3
16.0
17.5
17.2
16.9
15.9
17.0
17.2
16.9
16.9
94I-9-2c
(f)
50 µm
17.3
16.9
17.2
15.8
15.8
17.4
17.1
17.3
17.2
16.8
15.7
17.4
17.5
15.8
17.3
17.2
17.3
15.9
17.6
17.0
17.2
15.8
15.9
15.9
14.7
15.6
94I-9-2c

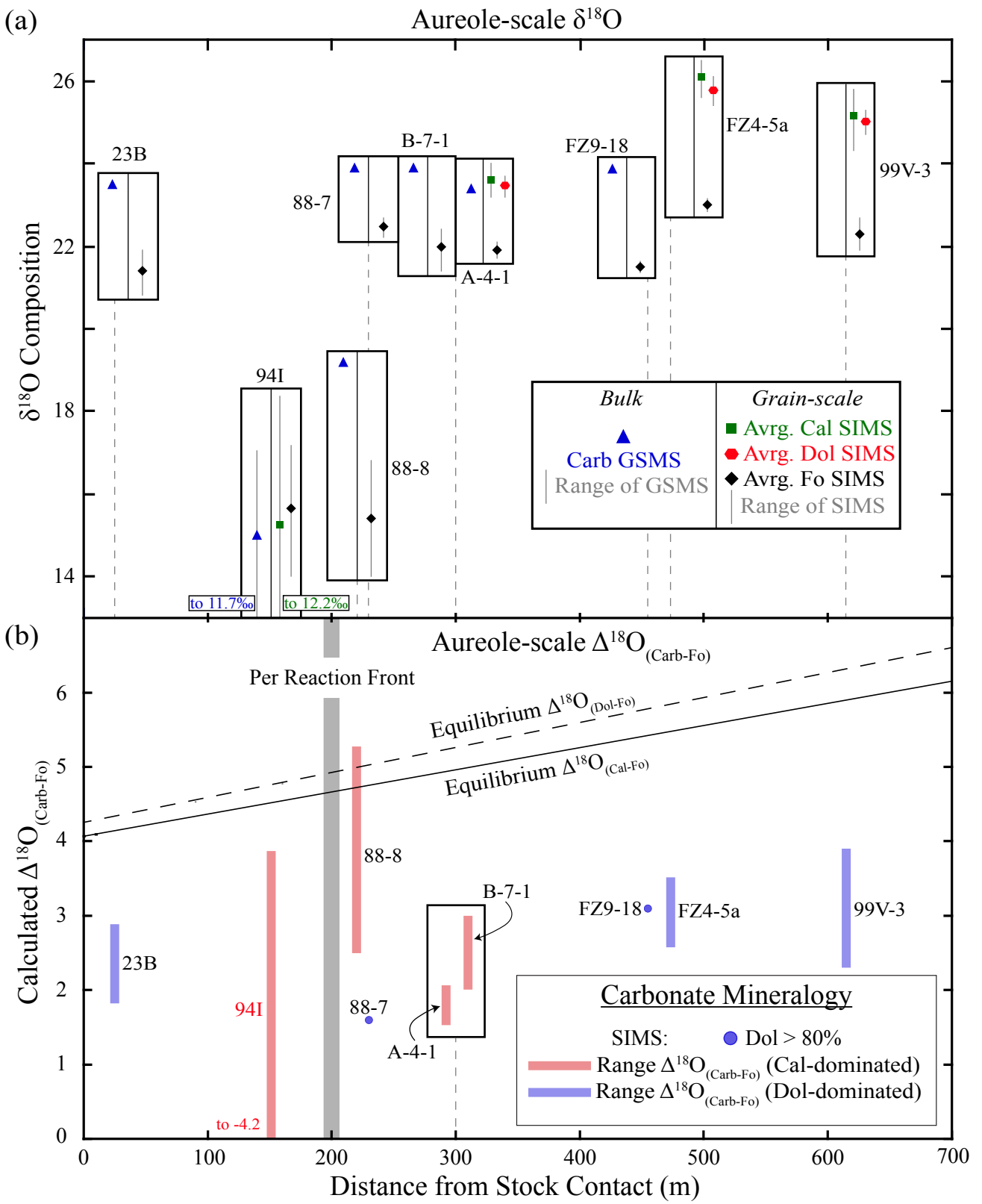
(a)
Aureole-scale δ18O
δ18O Composition
26
22
18
14
23B
94I
88-7
B-7-1
A-4-1
88-8
FZ9-18
FZ4-5a
99V-3
to 11.7‰
to 12.2‰
Bulk
Carb GSMS
Range of GSMS
Grain-scale
Avrg. Cal SIMS
Avrg. Dol SIMS
Avrg. Fo SIMS
Range of SIMS
(b)
Aureole-scale Δ18O(Carb-Fo)
Per Reaction Front
Equilibrium Δ18O(Dol-Fo)
Equilibrium Δ18O(Cal-Fo)
Calculated Δ18O(Carb-Fo)
6
5
4
3
2
1
0
23B
94I
to -4.2
88-8
88-7
B-7-1
A-4-1
FZ9-18
FZ4-5a
99V-3
Carbonate Mineralogy
SIMS:
Dol > 80%
Range Δ18O(Carb-Fo) (Cal-dominated)
Range Δ18O(Carb-Fo) (Dol-dominated)
0
100
200
300
400
500
600
700
Distance from Stock Contact (m)

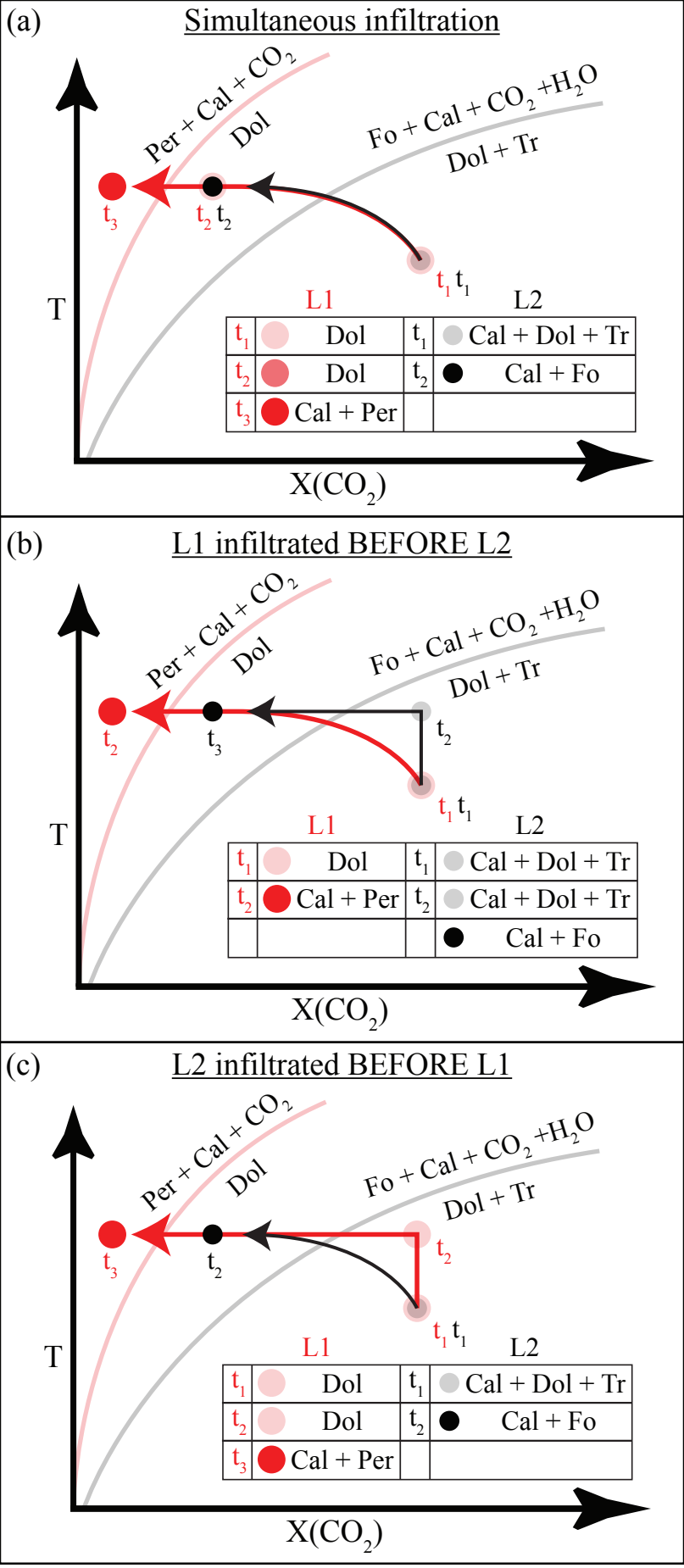
(a)
Simultaneous infiltration
Per + Cal + CO2
Dol
Fo + Cal + CO2 +H2O
Dol + Tr
t3
t2 t2
t1 t1
T
L1
L2
t1 Dol
t2 Dol
t3 Cal + Per
t1 Cal + Dol + Tr
t2 Cal + Fo
X(CO2)
(b)
L1 infiltrated BEFORE L2
Per + Cal + CO2
Dol
Fo + Cal + CO2 +H2O
Dol + Tr
t2
t3
t2
t1 t1
T
L1
L2
t1 Dol
t2 Cal + Per
t1 Cal + Dol + Tr
t2 Cal + Dol + Tr
Cal + Fo
X(CO2)
(c)
L2 infiltrated BEFORE L1
Per + Cal + CO2
Dol
Fo + Cal + CO2 +H2O
Dol + Tr
t3
t2
t2
t1 t1
T
L1
L2
t1 Dol
t2 Dol
t3 Cal + Per
t1 Cal + Dol + Tr
t2 Cal + Fo
X(CO2)

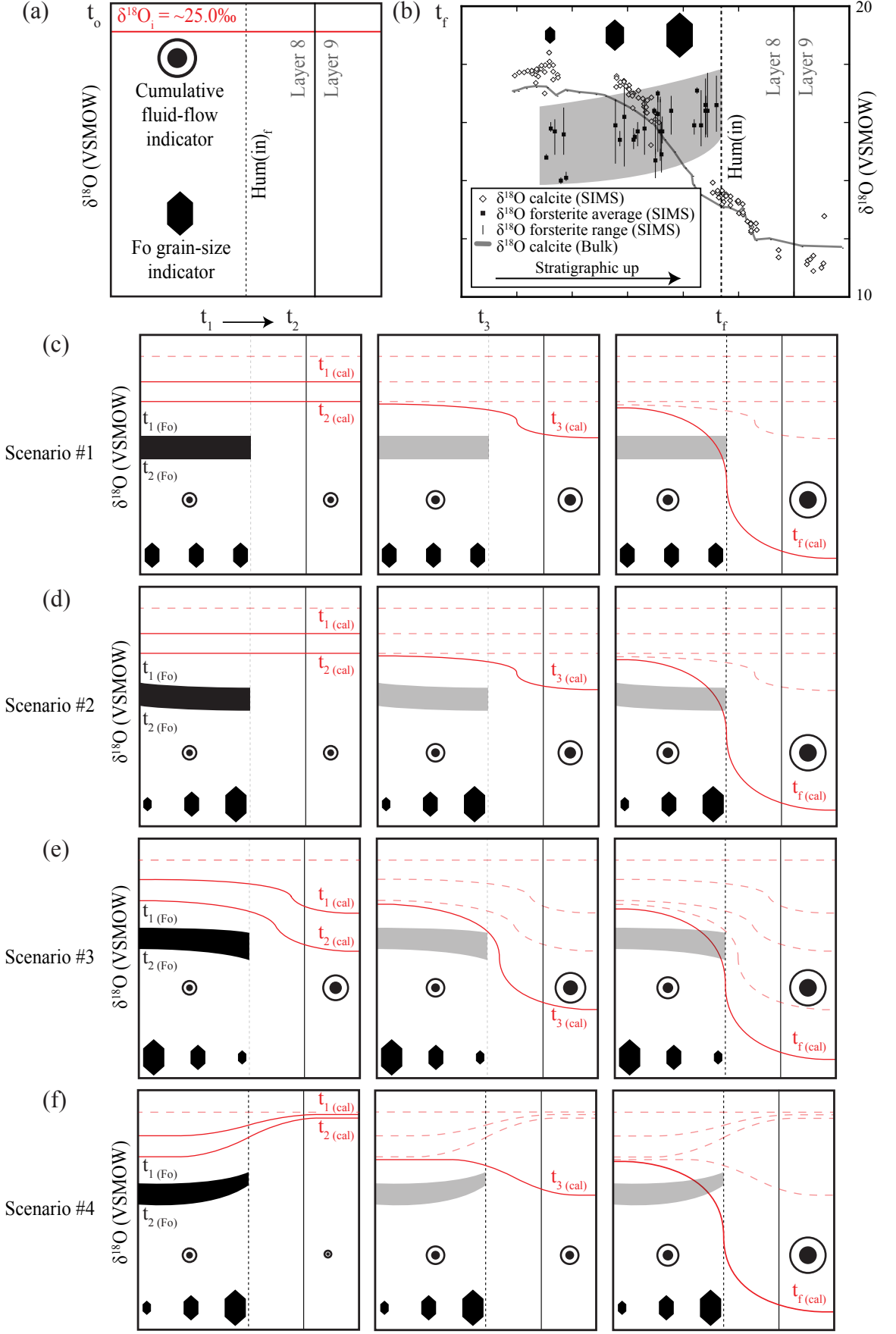
(a)
t_o
$\delta^{18}O_i$ = ~25.0‰
Cumulative fluid-flow indicator
Fo grain-size indicator
$\delta^{18}O$ (VSMOW)
$Hum(in)_f$
Layer 8
Layer 9
(b)
t_f
20
10
$\delta^{18}O$ (VSMOW)
Hum(in)
Layer 8
Layer 9
$\delta^{18}O$ calcite (SIMS)
$\delta^{18}O$ forsterite average (SIMS)
$\delta^{18}O$ forsterite range (SIMS)
$\delta^{18}O$ calcite (Bulk)
Stratigraphic up
t_1 → t_2
t_3
t_f
(c)
Scenario #1
(d)
Scenario #2
(e)
Scenario #3
(f)
Scenario #4
$t_{1\,(cal)}$
$t_{2\,(cal)}$
$t_{3\,(cal)}$
$t_{f\,(cal)}$
$t_{1\,(Fo)}$
$t_{2\,(Fo)}$

Table 1: Comparison of forsterite $\delta^{18}O$ (VSMOW) compositions determined by LF and SIMS techniques

Sample ID	**Distance (m)**	**>853 µm $\delta^{18}O$[a]**	**853-420 µm $\delta^{18}O$[a]**	**420-178 µm $\delta^{18}O$[a]**	**178-106 µm $\delta^{18}O$[a]**	**106-75 µm $\delta^{18}O$[a]**	**LF Mean $\delta^{18}O$[a]**	**SIMS Mean $\delta^{18}O$**
12-1b	10	11.4	11.3	11.3	11.4	11.0	11.3	-
23B	25	-	20.3	20.0	20.0	20.1	20.1	21.4
94I-9-2b	150	-	15.5	14.6	13.7	13.7	14.4	15.8
94I-9-2a	150	-	14.7	15.5	15.2	14.8	15.0	15.4
88-8	220	15.5	-	-	-	15.4	15.4	15.4
88-7	230	22.0	-	-	-	21.4	21.7	22.5
FZ7-6	275	-	-	-	-	-	-	19.3
A-1-1	300	21.0	21.0	21.0	20.9	20.8	20.9	-
A-1-4	300	21.9	-	-	-	21.9	21.9	-
A-3-1	300	20.2	20.0	20.1	20.4	19.9	20.1	-
A-4-1	300	21.3	21.1	-	21.7	21.7	21.5	21.9
B-7-1	300	20.7	20.4	21.2	20.9	19.9	20.6	21.9
B-8-1	300	20.1	20.3	20.2	19.8	19.5	19.9	-
B-8-3A	300	21.3	-	-	-	21.4	21.3	-
D-6-B	300	15.2	15.9	-	15.9	15.4	15.6	16.5
88-60	315	16.3	-	-	-	15.9	16.1	-
88-55	370	20.1	-	-	-	-	20.1	-
88-D8	455	19.7	-	-	-	19.6	19.6	-
FZ9-18	455	-	21.3	20.9	20.1	20.6	20.7	21.6
FZ4-5a	475	-	-	-	-	-	-	22.9
FZ4-4a	475	21.1	21.6	21.7	20.9	20.9	21.2	-
88-C5	550	21.8	20.2	20.3	20.4	19.9	20.5	-
88-20	570	19.8	-	-	-	21.2	20.5	-
99V-12c	615	18.9	19.1	18.4	18.2	18.4	18.6	-
99V-3	615	-	-	-	-	-	-	22.3
99V-5a	615	20.2	20.0	20.4	20.4	20.0	20.2	-

[a]Data from Loury (2014)

Table 2: Comparison of carbonate $\delta^{18}O$ (VSMOW) compositions determined by GC-MS and SIMS techniques

Sample ID	Carbonate Mineralogy	Distance (m)	$\delta^{18}O$ GC-MS[a]	Mean $\delta^{18}O$ SIMS Cal	Mean $\delta^{18}O$ SIMS Dol
12-1b	Cal-Dol Mix	10	15.3	-	-
23B	Dol-Dominated	25	23.2	-	-
94I-9-2b	Cal-Dominated	150	15.9	17.7[b]	-
94I-9-2a	Cal-Dominated	150	17.2	16.4[b]	-
88-8	Cal-Dominated	220	19.2	-	-
88-7	Dol-Dominated	230	23.9	-	-
A-1-1	Cal-Dominated	300	23.1	-	-
A-1-4	Cal-Dominated	300	23.9	-	-
A-3-1	Cal-Dominated	300	22.8	-	-
A-4-1	Cal-Dominated	300	23.9	23.6	23.5
B-7-1	Cal-Dominated	300	24.4	-	-
B-8-1	Cal-Dominated	300	23.4	-	-
B-8-3A	Cal-Dominated	300	24.6	-	-
D-6-B	Cal-Dominated	300	20.0	-	-
88-60	Cal-Dominated	315	18.8	-	-
88-55	Cal-Dol Mix	370	24.0	-	-
88-D8	Cal-Dol Mix	455	22.2	-	-
FZ9-18	Dol-Dominated	455	24.4	-	-
FZ4-5a	Dol-Dominated	475	-	26.1	25.8
FZ4-4a	Dol-Dominated	475	25.3	-	-
88-C5	Dol-Dominated	550	24.5	-	-
88-20	Cal-Dominated	570	22.6	-	-
99V-12c	Dol-Dominated	615	24.1	-	-
99V-3	Dol-Dominated	615	-	25.3	25.1
99V-5a	Dol-Dominated	615	24.0	-	-

[a]Data from Loury (2014)
[b]Data from Bowman et al. (2009)

Table 3: SIMS $\delta^{18}O$ (VSMOW) summary, population statistics, and calculated temperatures based on $\Delta_{Carb-Fo}$

Sample	**23B**	**94I-9-2a**	**94I-9-2an**	**94I-9-2b**	**94I-9-2bo**	**94I-9-2(b)**	**94I-9-2(4)**
Mineral	Fo	Cal	Fo	Cal	Fo	Fo	Fo
Distance (m)	25	150	150	150	150	150	150
Peak T[a]	618	580	580	580	580	580	580
No. of analyses	12	26	34	30	113	21	18
Range of $\delta^{18}O$‰	20.8-21.9	17.0-18.4	13.8-16.5	15.2-17.6	14.1-17.0	15.0-17.1	14.9-17.0
2SD ($\delta^{18}O$‰)	0.21	0.52	0.20-0.21	0.20-0.49	0.20-0.27	0.33-0.39	0.2
Sample MSWD[b]	Inhomog	Inhomog	Inhomog	Inhomog	Inhomog	Inhomog	Inhomog
Weighted mean[c]	Inhomog	Inhomog	Inhomog	Inhomog	Inhomog	Inhomog	Inhomog
Intragranular variation	Hetero	Homo	Hetero	Homo	Hetero	Hetero	Hetero
No. of grains analyzed	6	27	13	30	6	6	4
Calculated T (Cal-Fo)[d]	998	622	622	745	745	1069	1069
Sample	**94I-9-2(5)**	**94I-9-2bbo**	**94I-9-2c**	**94I-9-2ccn**	**88-8**	**88-7**	**FZ7-6**
Mineral	Fo	Fo	Cal	Fo	Fo	Fo	Fo
Distance (m)	150	150	150	150	220	230	275
Peak T[a]	580	580	580	580	561	558	546
No. of analyses	22	90	33	120	70	9	10
Range of $\delta^{18}O$‰	13.0-16.8	14.5-17.2	12.2-13.9	15.4-17.7	14.0-16.8	22.2-22.7	19.1-19.5
2SD ($\delta^{18}O$‰)	0.20-0.35	0.20-0.32	0.20-0.49	0.20-0.40	0.20-0.35	0.2	0.21
Sample MSWD[b]	Inhomog	Inhomog	Inhomog	Inhomog	Inhomog	2.03	1.66
Weighted mean[c]	Inhomog	Inhomog	Inhomog	Inhomog	Inhomog	22.47±0.11	19.25±0.10
Intragranular variation	Hetero	Hetero	Homo	Hetero	Hetero	Homo	Homo
No. of grains analyzed	5	6	32	9	8	3	5
Calculated T (Cal-Fo)[d]	645	819	crossed-over	crossed-over	543	1313	-
Sample	**A-4-1**	**A-4-1**	**A-4-1**	**B-7-1**	**D-6-B**	**FZ9-18**	**FZ4-5a**

Mineral	Cal	Dol	Fo	Fo	Fo	Fo	Cal
Distance (m)	300	300	300	300	300	455	475
Peak T[a]	540	540	540	540	540	505	501
No. of analyses	21	15	11	32	5	6	36
Range of $\delta^{18}O$‰	23.2-24.0	23.2-23.7	21.7-22.1	21.4-22.4	16.0-17.1	21.4-21.7	25.6-26.5
2SD ($\delta^{18}O$‰)	0.20-0.62	0.20-0.62	0.2	0.23-0.26	0.2	0.21	0.24-0.35
Sample MSWD[b]	Inhomog	0.70	1.69	Inhomog	Inhomog	1.72	Inhomog
Weighted mean[c]	Inhomog	23.4±0.058	21.91±0.09	Inhomog	Inhomog	21.55±.15	Inhomog
Intragranular variation[d]	Homo	Homo	Homo	Homo	Hetero	Homo	Homo
No. of grains analyzed	12	5	5	10	2	3	13
Calculated T (Cal-Fo)[e]	1032	1032	1032	1152	671	840	713

Sample	**FZ4-5a**	**FZ4-5a**	**99V-3**	**99V-3**	**99V-3**
Mineral	Dol	Fo	Cal	Dol	Fo
Distance (m)	475	475	615	615	615
Peak T[a]	501	501	475	475	475
No. of analyses	26	6	12	44	18
Range of $\delta^{18}O$‰	25.4-26.1	22.8-23.1	24.3-25.8	24.7-25.3	21.9-22.7
2SD ($\delta^{18}O$‰)	0.24-0.35	0.21	0.28-0.40	0.28-0.40	0.25-0.28
Sample MSWD[b]	Inhomog	1.00	Inhomog	1.04	Inhomog
Weighted mean[c]	Inhomog	22.95±0.11	Inhomog	25.07±0.52	Inhomog
Intragranular variation	Homo	Homo	Homo	Homo	Homo
No. of grains analyzed	13	3	5	25	7
Calculated T (Cal-Fo)[d]	713	713	999	999	999

[a]Data from Cook and Bowman (1994)
[b]Mean square weighted deviate (Mahon 1996). Inhomog = inhomogeneous sample.
[c]Weighted mean and 95% confidence interval (uncertainty) calculated following Mahon (1996).
[d]Homo, no intragranular variation; Hetero, some intragranular variation.
[e]Calculated using the calibration outlined in Chiba et al. (1989).

Sample	$\delta^{18}O_{carbonate}$	$\delta^{13}C_{carbonate}$	Distance (m)	Zone
12-2	12.2	2.4	10	Per
12-1b	15.3	-1.0	10	Per
A-1-1	23.1	5.2	300	Fo
A-1-4 (1)	23.9	5.5	300	Fo
A-1-4 (4)	24.5	5.6	300	Fo
A-3-1	22.75	5.9	300	Fo
A-4-1 (2)	23.9	6.0	300	Fo
A-4-1 (4)	23.9	6.1	300	Fo
B-7-1 coarse	23.4	5.9	300	Fo
B-8-1 lower	22.3	5.1	300	Fo
B-8-1 mid	22.5	5.1	300	Fo
B-8-3A	24.6	5.3	300	Fo
D-6-B coarse	20	5.2	300	Fo
D-6-B fine	19.4	5.1	300	Fo
23-B(l)	23.2	4.0	25	Per
23-B(u)	23.7	4.0	25	Per
99V-12c	24.1	4.8	615	Fo
99V-5a	24	4.5	615	Fo
FZ4-4a	25.3	4.6	475	Fo
FZ9-18	24.4	4.3	455	Fo

File	Comment	$\delta^{18}O$ ‰ VSMOW	2SD (ext.)	Mass Bias (‰)
	WI-STD-18			
20140929@1.as	WI-STD-18 SC-Ol #1			
20140929@2.as	WI-STD-18 SC-Ol #2 cam-open			
20140929@3.as	WI-STD-18 SC-Ol #3 Cs-Res=140			
20140929@4.as	WI-STD-18 SC-Ol #4			
20140929@5.as	WI-STD-18 SC-Ol #5			
20140929@6.as	WI-STD-18 SC-Ol #6			
	average and 2SD			
20140929@7.as	WI-STD-18 HN-Ol g4			
20140929@8.as	WI-STD-18 HN-Ol g2			
20140929@9.as	WI-STD-18 HN-Ol g1			
20140929@10.a	WI-STD-18 HN-Ol g3			
	average and 2SD	**8.90**		**4.49**
	bias relative to SC-Ol			**0.20**
20140929@11.a	WI-STD-18 OR-Ol g37			
20140929@12.a	WI-STD-18 OR-Ol g34			
~~20140929@13.a~~	~~WI-STD-18 OR-Ol g33~~			
20140929@14.a	WI-STD-18 OR-Ol g35			
20140929@15.a	WI-STD-18 OR-Ol g36			
	average and 2SD	**5.88**		**3.62**
	bias relative to SC-Ol			**-0.66**
20140929@16.a	WI-STD-18 SC-Ol			
20140929@17.a	WI-STD-18 SC-Ol			
20140929@18.a	WI-STD-18 SC-Ol			
20140929@19.a	WI-STD-18 SC-Ol			
	average and 2SD			
	bracket average and 2SD	**5.32**		**4.29**
	WI-STD-74			
20140929@20.a	WI-STD-74 UWG-2 g1			
20140929@21.a	WI-STD-74 UWG-2 g2			
~~20140929@22.a~~	~~WI-STD-74 UWG-2 g3~~			
20140929@23.a	WI-STD-74 UWG-2 g5			
20140929@24.a	WI-STD-74 UWG-2 g4			
20140929@25.a	WI-STD-74 UWG-2 g3#2			
	average and 2SD			
20140929@26.a	WI-STD-74 SC-Ol g1			
20140929@27.a	WI-STD-74 SC-Ol g2			
20140929@28.a	WI-STD-74 SC-Ol g1			
20140929@29.a	WI-STD-74 SC-Ol g2			
	average and 2SD	**5.32**		**4.27**
	bias relative to UWG-2			**1.60**

20140929@30.a	WI-STD-74 UWG-2 g1			
20140929@31.a	WI-STD-74 UWG-2 g2			
20140929@32.a	WI-STD-74 UWG-2 g4			
20140929@33.a	WI-STD-74 UWG-2 g5			
	average and 2SD			
	bracket average and 2SD	**5.80**		**2.67**
20140929@34.a	WI-STD-74 UWC-3 g1			
	9/30/14			
20140930@35.a	WI-STD-74 UWG-2 g1			
20140930@36.a	WI-STD-74 UWG-2 g2			
20140930@37.a	WI-STD-74 UWG-2 g4			
20140930@38.a	WI-STD-74 UWG-2 g5			
	average and 2SD	**5.80**		**2.52**
	Mount 8			
20140930@39.a	8-uwg2			
20140930@40.a	8-uwg2			
20140930@41.a	8-uwg2			
20140930@42.a	8-uwg2			
	average and 2SD			
20140930@43.a	8-g4c	**21.86**	**0.23**	3.93
20140930@44.a	8-g4oc	**22.02**	**0.23**	3.93
20140930@45.a	8-g4oc2	**21.92**	**0.23**	3.93
20140930@46.a	8-g4ir	**22.02**	**0.23**	3.93
20140930@47.a	8-g4r	**22.14**	**0.23**	3.93
20140930@48.a	8-g5c	**22.15**	**0.23**	3.93
20140930@49.a	8-g5c	**22.39**	**0.23**	3.93
20140930@50.a	8-g6c	**22.03**	**0.23**	3.93
20140930@51.a	8-g6ir	**22.07**	**0.23**	3.93
20140930@52.a	8-g6or	**22.15**	**0.23**	3.93
20140930@53.a	8-uwg2			
20140930@54.a	8-uwg2			
20140930@55.a	8-uwg2			
20140930@56.a	8-uwg2			
	average and 2SD			
	bracket average and 2SD	**5.80**		**2.32**
20140930@57.a	8-g8c	**21.92**	**0.26**	4.01
20140930@58.a	8-g8oc	**21.73**	**0.26**	4.01
20140930@59.a	8-g8r	**21.48**	**0.26**	4.01
20140930@60.a	8-g8r2	**21.89**	**0.26**	4.01
20140930@61.a	8-g9c	**21.52**	**0.26**	4.01
20140930@62.a	8-g9oc	**21.74**	**0.26**	4.01
20140930@63.a	8-g9r	**21.81**	**0.26**	4.01
20140930@64.a	8-g12c	**22.03**	**0.26**	4.01
20140930@65.a	8-g12oc	**22.04**	**0.26**	4.01

20140930@66.a	8-g12r	**22.11**	**0.26**	4.01
20140930@67.a	8-uwg2			
20140930@68.a	8-uwg2			
20140930@69.a	8-uwg2			
20140930@70.a	8-uwg2			
	average and 2SD			
	bracket average and 2SD	**5.80**		**2.41**
20140930@71.a	8-g13c	**21.77**	**0.25**	4.09
20140930@72.a	8-g13oc	**21.82**	**0.25**	4.09
20140930@73.a	8-g13r	**22.16**	**0.25**	4.09
20140930@74.a	8-g14c	**21.97**	**0.25**	4.09
20140930@75.a	8-g14oc	**21.97**	**0.25**	4.09
20140930@76.a	8-g14r	**21.84**	**0.25**	4.09
20140930@77.a	8-g21c	**21.97**	**0.25**	4.09
20140930@78.a	8-g21oc	**22.07**	**0.25**	4.09
20140930@79.a	8-g21r	**22.15**	**0.25**	4.09
20140930@80.a	8-g30c	**21.85**	**0.25**	4.09
20140930@81.a	8-g30oc	**21.72**	**0.25**	4.09
20140930@82.a	8-g30r	**21.39**	**0.25**	4.09
20140930@83.a	8-uwg2			
20140930@84.a	8-uwg2			
20140930@85.a	8-uwg2			
20140930@86.a	8-uwg2			
	average and 2SD			
	bracket average and 2SD	**5.80**		**2.49**
20140930@87.a	8-g33c	**21.92**	**0.13**	4.11
20140930@88.a	8-g33oc	**21.92**	**0.13**	4.11
20140930@89.a	8-g33r	**21.96**	**0.13**	4.11
20140930@90.a	8-g48c	**21.71**	**0.13**	4.11
20140930@91.a	8-g48r	**22.13**	**0.13**	4.11
20140930@92.a	8-g47c	**21.78**	**0.13**	4.11
20140930@93.a	8-g47r	**22.03**	**0.13**	4.11
20140930@94.a	8-g46br	**22.08**	**0.13**	4.11
20140930@95.a	8-g46dk	**21.94**	**0.13**	4.11
20140930@96.a	8-g45c	**21.76**	**0.13**	4.11
20140930@97.a	8-g45r	**21.83**	**0.13**	4.11
20140930@98.a	8-uwg2			
20140930@99.a	8-uwg2			
20140930@100.	8-uwg2			
20140930@101.	8-uwg2			
	average and 2SD			
	bracket average and 2SD	**5.80**		**2.51**
20140930@102.	8-60c	**19.50**	**0.21**	4.12
20140930@103.	8-60r	**19.35**	**0.21**	4.12
20140930@104.	8-65c	**19.12**	**0.21**	4.12
20140930@105.	8-65r	**19.06**	**0.21**	4.12

20140930@106.	8-67c	**19.23**	**0.21**	4.12
20140930@107.	8-67r	**19.37**	**0.21**	4.12
20140930@108.	8-70c	**19.30**	**0.21**	4.12
20140930@109.	8-70r	**19.26**	**0.21**	4.12
20140930@110.	8-71c	**19.14**	**0.21**	4.12
20140930@111.	8-71c	**19.19**	**0.21**	4.12
20140930@112.	8-uwg2			
20140930@113.	8-uwg2			
20140930@114.	8-uwg2			
20140930@115.	8-uwg2			
	average and 2SD			
	bracket average and 2SD	**5.80**		**2.52**
	Mount 6			
20140930@116.	6-uwg2			
20140930@117.	6-uwg2			
20140930@118.	6-uwg2			
20140930@119.	6-uwg2			
	average and 2SD			
20140930@120.	6-g5c	**23.00**	**0.21**	3.99
20140930@121.	6-g5r	**22.85**	**0.21**	3.99
20140930@122.	6-g6c	**22.92**	**0.21**	3.99
20140930@123.	6-g6r	**23.12**	**0.21**	3.99
20140930@124.	6-g4c	**22.82**	**0.21**	3.99
20140930@125.	6-g4r	**22.96**	**0.21**	3.99
20140930@126.	6-g12c	**21.73**	**0.21**	3.99
20140930@127.	6-g12r	**21.71**	**0.21**	3.99
20140930@128.	6-g13c	**21.48**	**0.21**	3.99
20140930@129.	6-g13r	**21.62**	**0.21**	3.99
20140930@130.	6-g14c	**21.38**	**0.21**	3.99
20140930@131.	6-g14r	**21.40**	**0.21**	3.99
20140930@132.	6-uwg2			
20140930@133.	6-uwg2			
20140930@134.	6-uwg2			
20140930@135.	6-uwg2			
	average and 2SD			
	bracket average and 2SD	**5.80**		**2.39**
	99V-3			
20140930@136.	99V-3-uwg2			
20140930@137.	99V-3-uwg2			
20140930@138.	99V-3-uwg2			
20140930@139.	99V-3-uwg2			
	average and 2SD			

20140930@140.	99V-3- G1_1	**21.94**	**0.28**	4.08
20140930@141.	99V-3- G1_2	**22.13**	**0.28**	4.08
20140930@142.	99V-3- G3_1	**22.10**	**0.28**	4.08
20140930@143.	99V-3- G3_2	**22.10**	**0.28**	4.08
20140930@144.	99V-3- G7_1	**22.16**	**0.28**	4.08
20140930@145.	99V-3- G7_2	**22.29**	**0.28**	4.08
20140930@146.	99V-3- G8_1	**22.21**	**0.28**	4.08
20140930@147.	99V-3- G8_2	**22.12**	**0.28**	4.08
20140930@148.	99V-3- G10_1	**22.15**	**0.28**	4.08
20140930@149.	99V-3- G10_2	**22.16**	**0.28**	4.08
20140930@150.	99V-3- G11_1	**22.53**	**0.28**	4.08
20140930@151.	99V-3- G11_2	**22.27**	**0.28**	4.08
20140930@152.	99V-3- uwg2			
20140930@153.	99V-3- uwg2			
20140930@154.	99V-3- uwg2			
20140930@155.	99V-3- uwg2			
	average and 2SD			
	bracket average and 2SD	**5.80**		**2.48**
20140930@156.	99V-3- G11_3	**22.47**	**0.25**	3.96
20140930@157.	99V-3- G11_4	**22.56**	**0.25**	3.96
20140930@158.	99V-3- G11_5	**22.58**	**0.25**	3.96
20140930@159.	99V-3- G11_6	**22.55**	**0.25**	3.96
20140930@160.	99V-3- G9_1	**22.48**	**0.25**	3.96
20140930@161.	99V-3- G9_2	**22.71**	**0.25**	3.96
20140930@162.	99V-3- uwg2			
20140930@163.	99V-3- uwg2			
20140930@164.	99V-3- uwg2			
20140930@165.	99V-3- uwg2			
	average and 2SD			
	bracket average and 2SD	**5.80**		**2.36**
	Mount 10			
20140930@166.	10-uwg2			
20140930@167.	10-uwg2			
20140930@168.	10-uwg2			
20140930@169.	10-uwg2			
	average and 2SD			
20140930@170.	10-23B-9c	**21.33**	**0.21**	3.84
20140930@171.	10-23B-9r	**20.79**	**0.21**	3.84
20140930@172.	10-23B-8c	**21.20**	**0.21**	3.84
20140930@173.	10-23B-8c	**21.51**	**0.21**	3.84
20140930@174.	10-23B-10c	**21.19**	**0.21**	3.84
20140930@175.	10-23B-10r	**21.08**	**0.21**	3.84
20140930@176.	10-23B-11c	**21.66**	**0.21**	3.84

20140930@177.	10-23B-11r	**21.09**	**0.21**	3.84
20140930@178.	10-23B-15c	**21.46**	**0.21**	3.84
20140930@179.	10-23B-15c	**21.40**	**0.21**	3.84
20140930@180.	10-23B-18c	**21.68**	**0.21**	3.84
20140930@181.	10-23B-18r	**21.94**	**0.21**	3.84
20140930@182.	10-uwg2			
20140930@183.	10-uwg2			
20140930@184.	10-uwg2			
20140930@185.	10-uwg2			
	average and 2SD			
	bracket average and 2SD	**5.80**		**2.24**
20140930@186.	10-88-8-15c	**14.56**	**0.25**	3.92
20140930@187.	10-88-8-15r	**15.56**	**0.25**	3.92
20140930@188.	10-88-8-15r(se)	**16.03**	**0.25**	3.92
20140930@189.	10-88-8-15oc(nw)	**15.40**	**0.25**	3.92
20140930@190.	10-88-8-15oc(se)	**15.31**	**0.25**	3.92
20140930@191.	10-88-8-15r(sw)	**15.82**	**0.25**	3.92
20140930@192.	10-88-8-15c(e)	**15.21**	**0.25**	3.92
20140930@193.	10-88-8-18c	**16.56**	**0.25**	3.92
20140930@194.	10-88-8-18r	**16.21**	**0.25**	3.92
20140930@195.	10-88-8-18r(se)	**16.40**	**0.25**	3.92
20140930@196.	uwg2			
20140930@197.	uwg2			
20140930@198.	uwg2			
20140930@199.	uwg2			
	average and 2SD			
	bracket average and 2SD	**5.80**		**2.32**
20140930@200.	10-88-8-g10c	**15.56**	**0.26**	4.01
20140930@201.	10-88-8-g10r	**14.39**	**0.26**	4.01
20140930@202.	10-88-8-g10c(n)	**16.35**	**0.26**	4.01
20140930@203.	10-88-8-g10r(n)	**15.90**	**0.26**	4.01
20140930@204.	10-88-8-g10c(l)	**16.61**	**0.26**	4.01
20140930@205.	10-88-8-g10r(l)	**14.27**	**0.26**	4.01
20140930@206.	10-uwg2			
20140930@207.	10-uwg2			
20140930@208.	10-uwg2			
20140930@209.	10-uwg2			
	average and 2SD			
	bracket average and 2SD	**5.80**		**2.41**
20140930@210.	10-88-8-g6c	**16.58**	**0.31**	3.85
20140930@211.	10-88-8-g6r(n)	**15.68**	**0.31**	3.85
20140930@212.	10-88-8-g6oc(n)	**15.43**	**0.31**	3.85
20140930@213.	10-88-8-g6c(w)	**16.11**	**0.31**	3.85

20140930@214.	10-88-8-g6oc(e)	**14.64**	**0.31**	3.85
20140930@215.	10-88-8-g6r(e)	**15.43**	**0.31**	3.85
20140930@216.	10-88-8-g1c	**16.14**	**0.31**	3.85
20140930@217.	10-88-8-g1r	**16.07**	**0.31**	3.85
20140930@218.	10-88-8-g2c	**15.89**	**0.31**	3.85
20140930@219.	10-88-8-g2r(s)	**14.22**	**0.31**	3.85
20140930@220.	10-uwg2			
20140930@221.	10-uwg2			
20140930@222.	10-uwg2			
20140930@223.	10-uwg2			
	average and 2SD			
	bracket average and 2SD	**5.80**		**2.25**
	Adjusted Cs res			
20140930@224.	10-uwg2			
20140930@225.	10-uwg2			
20140930@226.	10-uwg2			
20140930@227.	10-uwg2			
	average and 2SD			
20140930@228.	10-88-8-g3c	**15.60**	**0.34**	3.76
20140930@229.	10-88-8-g3r(e)	**15.85**	**0.34**	3.76
20140930@230.	10-88-8-g3r(ne)	**15.46**	**0.34**	3.76
20140930@231.	10-88-8-g3r(s)	**15.44**	**0.34**	3.76
20140930@232.	10-88-8-g4c	**15.96**	**0.34**	3.76
20140930@233.	10-88-8-g4r	**14.52**	**0.34**	3.76
20140930@234.	10-88-8-g4oc(e)	**15.59**	**0.34**	3.76
20140930@235.	10-88-8-g4r(ne)	**14.57**	**0.34**	3.76
20140930@236.	10-94I9-2(5)-g4c	**15.61**	**0.34**	3.76
20140930@237.	10-94I9-2(5)-g4r(s)	**16.37**	**0.34**	3.76
20140930@238.	10-94I9-2(5)-g4r(n)	**16.13**	**0.34**	3.76
20140930@239.	10-94I9-2(5)-g4oc(s)	**15.81**	**0.34**	3.76
20140930@240.	10-uwg2			
20140930@241.	10-uwg2			
20140930@242.	10-uwg2			
20140930@243.	10-uwg2			
	average and 2SD			
	bracket average and 2SD	**5.80**		**2.15**
20140930@244.	10-94I9-2(5)-g1c	**15.17**	**0.21**	3.84
20140930@245.	10-94I9-2(5)-g1r(n)	**15.30**	**0.21**	3.84
20140930@246.	10-94I9-2(5)-g3c	**15.52**	**0.21**	3.84
20140930@247.	10-94I9-2(5)-g3r(s)	**16.84**	**0.21**	3.84
20140930@248.	10-94I9-2(5)-g3oc(s)	**15.68**	**0.21**	3.84
20140930@249.	10-94I9-2(5)-g3r(sw)	**15.72**	**0.21**	3.84
20140930@250.	10-94I9-2(5)-g3r(n)	**14.13**	**0.21**	3.84
20140930@251.	10-94I9-2(5)-g3r(ne)	**15.72**	**0.21**	3.84
20140930@252.	10-94I9-2(5)-g7c	**15.49**	**0.21**	3.84

20140930@253.	10-94I9-2(5)-g7r	**13.04**	**0.21**	3.84
20140930@254.	10-94I9-2(5)-g7oc	**14.98**	**0.21**	3.84
20140930@255.	10-94I9-2(5)-g7ir	**15.19**	**0.21**	3.84
20140930@256.	10-uwg2			
20140930@257.	10-uwg2			
20140930@258.	10-uwg2			
20140930@259.	10-uwg2			
	average and 2SD			
	bracket average and 2SD	**5.80**		**2.24**
20140930@260.	10-94I9-2(5)-g7r	**13.57**	**0.19**	3.85
20140930@261.	10-94I9-2(5)-g7r(s)	**14.06**	**0.19**	3.85
20140930@262.	10-94I9-2(5)-g11c	**16.48**	**0.19**	3.85
20140930@263.	10-94I9-2(5)-g11r(e)	**15.87**	**0.19**	3.85
20140930@264.	10-94I9-2(5)-g11c(s)	**16.37**	**0.19**	3.85
20140930@265.	10-94I9-2(5)-g11r(se)	**15.59**	**0.19**	3.85
20140930@266.	10-94I9-2(4)-g12c	**15.91**	**0.19**	3.85
20140930@267.	10-94I9-2(4)-g12r(n)	**15.77**	**0.19**	3.85
20140930@268.	10-94I9-2(4)-g12r(s)	**16.99**	**0.19**	3.85
20140930@269.	10-94I9-2(4)-g12r(se)	**15.72**	**0.19**	3.85
20140930@270.	10-94I9-2(4)-g12ir(s)	**15.21**	**0.19**	3.85
20140930@271.	10-94I9-2(4)-g12oc(s)	**15.45**	**0.19**	3.85
20140930@272.	10-uwg2			
20140930@273.	10-uwg2			
20140930@274.	10-uwg2			
20140930@275.	10-uwg2			
	average and 2SD			
	bracket average and 2SD	**5.80**		**2.25**
20140930@276.	10-94I9-2(4)-g13c	**15.67**	**0.18**	3.89
20140930@277.	10-94I9-2(4)-g13r	**16.29**	**0.18**	3.89
20140930@278.	10-94I9-2(4)-g13oc	**15.85**	**0.18**	3.89
20140930@279.	10-94I9-2(4)-g5c	**15.37**	**0.18**	3.89
20140930@280.	10-94I9-2(4)-g5oc	**15.23**	**0.18**	3.89
20140930@281.	10-94I9-2(4)-g5r	**16.85**	**0.18**	3.89
20140930@282.	10-94I9-2(4)-g5r(w)	**16.97**	**0.18**	3.89
20140930@283.	10-94I9-2(4)-g5r(sw)	**16.70**	**0.18**	3.89
20140930@284.	10-94I9-2(4)-g1dkc	**15.09**	**0.18**	3.89
20140930@285.	10-94I9-2(4)-g1lt ir	**14.94**	**0.18**	3.89
20140930@286.	10-94I9-2(4)-g1lt r(s)	**14.91**	**0.18**	3.89
20140930@287.	10-94I9-2(4)-g1lt r(n)	**14.86**	**0.18**	3.89
20140930@288.	10-uwg2			
20140930@289.	10-uwg2			
20140930@290.	10-uwg2			
20140930@291.	10-uwg2			
	average and 2SD			

	bracket average and 2SD	**5.80**		**2.29**
	Adjusted Cs reservoir			
20140930@292.	10-uwg2			
20140930@293.	10-uwg2			
20140930@294.	10-uwg2			
20140930@295.	10-uwg2			
	average and 2SD			
20140930@296.	10-88-7-g7c	**22.25**	**0.19**	3.90
20140930@297.	10-88-7-g7r	**22.41**	**0.19**	3.90
20140930@298.	10-88-7-g7sat c	**22.35**	**0.19**	3.90
20140930@299.	10-88-7-g7sat r	**22.55**	**0.19**	3.90
20140930@300.	10-88-7-g6c	**22.67**	**0.19**	3.90
20140930@301.	10-88-7-g6r	**22.44**	**0.19**	3.90
20140930@302.	10-88-7-g6 sat c	**22.64**	**0.19**	3.90
20140930@303.	10-88-7-g1c	**22.55**	**0.19**	3.90
20140930@304.	10-88-7-g1r	**22.36**	**0.19**	3.90
20140930@305.	10-D-6-B-g5c	**16.16**	**0.19**	3.90
20140930@306.	10-D-6-B-g5r	**16.16**	**0.19**	3.90
20140930@307.	10-D-6-B-g8c	**16.01**	**0.19**	3.90
20140930@308.	10-D-6-B-g8c	**17.14**	**0.19**	3.90
20140930@309.	10-D-6-B-g8oc	**17.13**	**0.19**	3.90
20140930@310.	10-uwg2			
20140930@311.	10-uwg2			
20140930@312.	10-uwg2			
20140930@313.	10-uwg2			
	average and 2SD			
	bracket average and 2SD	**5.80**		**2.29**
	94I-9-2(b)			
20140930@314.	94I-9-2(b)-uwg2			
20140930@315.	94I-9-2(b)-uwg2			
20140930@316.	94I-9-2(b)-uwg2			
20140930@317.	94I-9-2(b)-uwg2			
	average and 2SD			
20140930@318.	94I-9-2(b)-G1_1	**15.15**	**0.39**	4.30
20140930@319.	94I-9-2(b)-G1_2	**15.06**	**0.39**	4.30
20140930@320.	94I-9-2(b)-G1_3	**15.19**	**0.39**	4.30
20140930@321.	94I-9-2(b)-G6_1	**16.49**	**0.39**	4.30
20140930@322.	94I-9-2(b)-G6_2	**16.48**	**0.39**	4.30
20140930@323.	94I-9-2(b)-G6_3	**16.32**	**0.39**	4.30
20140930@324.	94I-9-2(b)-G8_1	**15.47**	**0.39**	4.30
20140930@325.	94I-9-2(b)-G8_2	**16.71**	**0.39**	4.30
20140930@326.	94I-9-2(b)-G8_3	**16.20**	**0.39**	4.30
20140930@327.	94I-9-2(b)-G8_4	**15.43**	**0.39**	4.30
20140930@328.	94I-9-2(b)-G8_5	**16.84**	**0.39**	4.30

20140930@329.	94I-9-2(b)-uwg2			
20140930@330.	94I-9-2(b)-uwg2			
20140930@331.	94I-9-2(b)-uwg2			
20140930@332.	94I-9-2(b)-uwg2			
20140930@333.	94I-9-2(b)-uwg2			
	average and 2SD			
	bracket average and 2SD	**5.80**		**2.70**
20140930@334.	94I-9-2(b)-G9_1	**15.25**	**0.33**	4.22
20140930@335.	94I-9-2(b)-G9_2	**16.97**	**0.33**	4.22
20140930@336.	94I-9-2(b)-G9_3	**15.03**	**0.33**	4.22
20140930@337.	94I-9-2(b)-G9_4	**17.07**	**0.33**	4.22
20140930@338.	94I-9-2(b)-G9_5	**16.55**	**0.33**	4.22
20140930@339.	94I-9-2(b)-G10_1	**16.79**	**0.33**	4.22
20140930@340.	94I-9-2(b)-G10_2	**17.11**	**0.33**	4.22
20140930@341.	94I-9-2(b)-G5_1	**15.31**	**0.33**	4.22
20140930@342.	94I-9-2(b)-G5_2	**16.21**	**0.33**	4.22
20140930@343.	94I-9-2(b)-G5_3	**15.71**	**0.33**	4.22
20140930@344.	94I-9-2(b)-uwg2			
20140930@345.	94I-9-2(b)-uwg2			
20140930@346.	94I-9-2(b)-uwg2			
20140930@347.	94I-9-2(b)-uwg2			
	average and 2SD			
	bracket average and 2SD	**5.80**		**2.62**
	2014_MGS_Carb_02			
20140930@348.	2014_MGS_Carb_02 UWC-3			
20140930@349.	2014_MGS_Carb_02 UWC-3			
20140930@350.	2014_MGS_Carb_02 UWC-3			
20140930@351.	2014_MGS_Carb_02 UWC-3			
	average and 2SD			
20140930@352.	2014_MGS_Carb_02 UW6220			
20140930@353.	2014_MGS_Carb_02 UW6220			
20140930@354.	2014_MGS_Carb_02 UW6220			
20140930@355.	2014_MGS_Carb_02 UW6220			
	average and 2SD	**22.72**		**-11.48**
	relative to UWC-3			**-5.09**
20140930@356.	2014_MGS_Carb_02 NMNH 93418-08 Ankerite (Ank-4) #1			
20140930@357.	2014_MGS_Carb_02 NMNH 93418-08 Ankerite (Ank-4) #2			
20140930@358.	2014_MGS_Carb_02 NMNH 93418-08 Ankerite (Ank-4) g8			
20140930@359.	2014_MGS_Carb_02 NMNH 93418-08 Ankerite (Ank-4) g14			
	average and 2SD	**9.22**		**-4.39**
	relative to UWC-3			**2.05**
	relative to UW6220			**7.17**
20140930@360.	2014_MGS_Carb_02 UWC-3			

20140930@361.	2014_MGS_Carb_02 UWC-3			
20140930@362.	2014_MGS_Carb_02 UWC-3			
20140930@363.	2014_MGS_Carb_02 UWC-3			
	average and 2SD			
	bracket average and 2SD	**12.49**		**-6.43**
	99V-3			
20140930@364.	99V-3_UWC-3			
20140930@365.	99V-3_UWC-3			
20140930@366.	99V-3_UWC-3			
20140930@367.	99V-3_UWC-3			
	average and 2SD			
20140930@368.	99V-3_T1_1	**25.42**	**0.34**	-6.21
20140930@369.	99V-3_T1_2	**25.00**	**0.34**	-6.21
20140930@370.	99V-3_T1_3	**25.27**	**0.34**	-6.21
20140930@371.	99V-3_T1_4	**25.03**	**0.34**	-6.21
20140930@372.	99V-3_T1_5	**24.88**	**0.34**	-11.26
20140930@373.	99V-3_T1_6	**24.93**	**0.34**	-11.26
20140930@374.	99V-3_T1_7	**24.88**	**0.34**	-11.26
20140930@375.	99V-3_T1_8	**25.00**	**0.34**	-11.26
20140930@376.	99V-3_T1_9	**24.82**	**0.34**	-11.26
20140930@377.	99V-3_T1_10	**24.76**	**0.34**	-11.26
20140930@378.	99V-3_T1_11	**24.98**	**0.34**	-11.26
20140930@379.	99V-3_UWC-3			
20140930@380.	99V-3_UWC-3			
20140930@381.	99V-3_UWC-3			
20140930@382.	99V-3_UWC-3			
	average and 2SD			
	bracket average and 2SD	**12.49**		**-6.21**
20140930@383.	99V-3_T1_12	**25.03**	**0.40**	-11.43
20140930@384.	99V-3_T1_13	**25.07**	**0.40**	-11.43
20140930@385.	99V-3_T1_14	**25.04**	**0.40**	-11.43
20140930@386.	99V-3_T1_15	**25.24**	**0.40**	-11.43
20140930@387.	99V-3_T1_16	**24.83**	**0.40**	-11.43
20140930@388.	99V-3_T1_17	**24.99**	**0.40**	-11.43
~~20140930@389.~~	~~99V-3_Fo~~	~~**32.85**~~	~~**0.40**~~	~~-6.37~~
20140930@390.	99V-3_T2_1	**25.09**	**0.40**	-6.37
20140930@391.	99V-3_T2_2	**24.26**	**0.40**	-6.37
20140930@392.	99V-3_T2_3	**24.84**	**0.40**	-11.43
20140930@393.	99V-3_UWC-3			
20140930@394.	99V-3_UWC-3			
20140930@395.	99V-3_UWC-3			
20140930@396.	99V-3_UWC-3			
	average and 2SD			

	bracket average and 2SD	**12.49**		**-6.37**
20140930@397.	99V-3_T2_4	**25.77**	**0.28**	-6.56
20140930@398.	99V-3_T2_5	**25.65**	**0.28**	-6.56
20140930@399.	99V-3_T2_6	**25.33**	**0.28**	-6.56
20140930@400.	99V-3_T2_7	**25.06**	**0.28**	-11.62
20140930@401.	99V-3_T2_8	**25.20**	**0.28**	-11.62
20140930@402.	99V-3_T2_9	**25.05**	**0.28**	-11.62
20140930@403.	99V-3_T2_10	**25.12**	**0.28**	-11.62
20140930@404.	99V-3_T2_11	**25.29**	**0.28**	-11.62
20140930@405.	99V-3_T2_12	**24.73**	**0.28**	-11.62
20140930@406.	99V-3_T2_13	**24.96**	**0.28**	-11.62
20140930@407.	99V-3_UWC-3			
20140930@408.	99V-3_UWC-3			
20140930@409.	99V-3_UWC-3			
20140930@410.	99V-3_UWC-3			
20140930@411.	99V-3_UWC-3			
	average and 2SD			
	bracket average and 2SD	**12.49**		**-6.56**
20140930@412.	99V-3_T2_14	**25.31**	**0.33**	-11.63
20140930@413.	99V-3_T2_15	**25.20**	**0.33**	-11.63
20140930@414.	99V-3_T2_16	**25.33**	**0.33**	-11.63
~~20140930@415.~~	~~99V-3_T2_17~~	~~**28.60**~~	~~**0.33**~~	~~-11.63~~
20140930@416.	99V-3_T2_18	**25.17**	**0.33**	-11.63
20140930@417.	99V-3_T2_19	**25.21**	**0.33**	-11.63
20140930@418.	99V-3_T2_20	**25.22**	**0.33**	-6.58
20140930@419.	99V-3_T2_21	**25.55**	**0.33**	-6.58
20140930@420.	99V-3_T2_22	**25.06**	**0.33**	-11.63
20140930@421.	99V-3_T2_23	**25.01**	**0.33**	-11.63
20140930@422.	99V-3_UWC-3			
20140930@423.	99V-3_UWC-3			
20140930@424.	99V-3_UWC-3			
20140930@425.	99V-3_UWC-3			
20140930@426.	99V-3_UWC-3			
	average and 2SD			
	bracket average and 2SD	**12.49**		**-6.58**
20140930@427.	99V-3_T2_24	**25.01**	**0.34**	-11.55
20140930@428.	99V-3_T2_25	**25.09**	**0.34**	-11.55
20140930@429.	99V-3_T2_26	**25.35**	**0.34**	-11.55
20140930@430.	99V-3_T2_27	**25.27**	**0.34**	-11.55
20140930@431.	99V-3_T2_28	**25.00**	**0.34**	-11.55
20140930@432.	99V-3_T2_29	**25.03**	**0.34**	-11.55
20140930@433.	99V-3_T2_30	**25.20**	**0.34**	-11.55
20140930@434.	99V-3_T2_31	**24.74**	**0.34**	-11.55
20140930@435.	99V-3_T2_32	**25.09**	**0.34**	-11.55

~~20140930@436.~~	~~99V-3_T2_33 cal~~	~~**26.63**~~	~~**0.34**~~	~~-6.49~~
20140930@437.	99V-3_T2_34 cal	**25.38**	**0.34**	-6.49
20140930@438.	99V-3_T2_35 cal	**25.52**	**0.34**	-6.49
20140930@439.	99V-3_UWC-3			
20140930@440.	99V-3_UWC-3			
20140930@441.	99V-3_UWC-3			
20140930@442.	99V-3_UWC-3			
	average and 2SD			
	bracket average and 2SD	**12.49**		**-6.49**
20140930@443.	99V-3__T2_36	**25.24**	**0.34**	-11.39
20140930@444.	99V-3__T2_37	**25.25**	**0.34**	-11.39
20140930@445.	99V-3__T2_38	**25.22**	**0.34**	-11.39
20140930@446.	99V-3__T2_39	**24.97**	**0.34**	-11.39
20140930@447.	99V-3__T2_40	**25.02**	**0.34**	-11.39
20140930@448.	99V-3__T2_41	**25.34**	**0.34**	-11.39
20140930@449.	99V-3__T2_42	**25.14**	**0.34**	-11.39
20140930@450.	99V-3__UWC-3			
20140930@451.	99V-3__UWC-3			
20140930@452.	99V-3__UWC-3			
20140930@453.	99V-3__UWC-3			
	average and 2SD			
	bracket average and 2SD	**12.49**		**-6.34**

20140930@454.	4-5a__UWC-3			
20140930@455.	4-5a__UWC-3			
20140930@456.	4-5a__UWC-3			
20140930@457.	4-5a__UWC-3			
	average and 2SD			
20140930@458.	4-5a__T1-1	**25.83**	**0.24**	-11.67
20140930@459.	4-5a__T1-2	**25.88**	**0.24**	-11.67
20140930@460.	4-5a__T1-3	**26.21**	**0.24**	-6.61
20140930@461.	4-5a__T1-4	**25.82**	**0.24**	-6.61
20140930@462.	4-5a__T1-5	**25.91**	**0.24**	-6.61
20140930@463.	4-5a__T1-6	**25.89**	**0.24**	-6.61
20140930@464.	4-5a__T1-7	**25.85**	**0.24**	-6.61
20140930@465.	4-5a__T1-8	**25.85**	**0.24**	-6.61
20140930@466.	4-5a__T1-9	**25.53**	**0.24**	-11.67
20140930@467.	4-5a__T1-10	**25.54**	**0.24**	-11.67
20140930@468.	4-5a__T1-11	**25.58**	**0.24**	-11.67
20140930@469.	4-5a__T1-12	**25.89**	**0.24**	-6.61
20140930@470.	4-5a__UWC-3			
20140930@471.	4-5a__UWC-3			

20140930@472.	4-5a__UWC-3			
20140930@473.	4-5a__UWC-3			
20140930@474.	4-5a__UWC-3			
	average and 2SD			
	bracket average and 2SD	**12.49**		**-6.61**
20140930@475.	4-5a__T1-13	**26.21**	**0.32**	-6.59
20140930@476.	4-5a__T1-14	**25.79**	**0.32**	-6.59
20140930@477.	4-5a__T1-15	**25.65**	**0.32**	-6.59
20140930@478.	4-5a__T1-16	**26.44**	**0.32**	-6.59
20140930@479.	4-5a__T1-17	**25.99**	**0.32**	-6.59
20140930@480.	4-5a__T1-18	**25.60**	**0.32**	-11.64
20140930@481.	4-5a__T1-19	**26.15**	**0.32**	-6.59
20140930@482.	4-5a__T1-20	**26.12**	**0.32**	-6.59
20140930@483.	4-5a__T1-21	**26.06**	**0.32**	-6.59
20140930@484.	4-5a__T1-22	**25.64**	**0.32**	-11.64
20140930@485.	4-5a__UWC-3			
20140930@486.	4-5a__UWC-3			
20140930@487.	4-5a__UWC-3			
20140930@488.	4-5a__UWC-3			
	average and 2SD			
	bracket average and 2SD	**12.49**		**-6.59**
20140930@489.	4-5a__T1-23 cal	**26.38**	**0.23**	-6.52
20140930@490.	4-5a__T1-24 cal	**25.89**	**0.23**	-6.52
20140930@491.	4-5a__T1-25 cal	**26.14**	**0.23**	-6.52
20140930@492.	4-5a__T1-26	**25.56**	**0.23**	-11.58
20140930@493.	4-5a__T1-27	**25.68**	**0.23**	-11.58
~~20140930@494.~~	~~4-5a__T1-28~~	~~**27.99**~~	~~**0.23**~~	~~-11.58~~
20140930@495.	4-5a__T1-29	**25.67**	**0.23**	-11.58
20140930@496.	4-5a__T1-30 cal	**25.98**	**0.23**	-6.52
20140930@497.	4-5a__T1-31 cal	**25.90**	**0.23**	-6.52
20140930@498.	4-5a__T1-32 cal	**25.97**	**0.23**	-6.52
20140930@499.	4-5a__UWC-3			
20140930@500.	4-5a__UWC-3			
20140930@501.	4-5a__UWC-3			
20140930@502.	4-5a__UWC-3			
	average and 2SD			
	bracket average and 2SD	**12.49**		**-6.52**
20140930@503.	4-5a__T1-33 cal	**26.20**	**0.24**	-6.60
20140930@504.	4-5a__T1-34	**25.37**	**0.24**	-11.65
20140930@505.	4-5a__T1-35	**25.61**	**0.24**	-11.65
20140930@506.	4-5a__T2-1	**25.91**	**0.24**	-11.65
20140930@507.	4-5a__T2-2 cal	**26.06**	**0.24**	-6.60
~~20140930@508.~~	~~4-5a__T2-3~~	~~**30.71**~~	~~**0.24**~~	~~-6.60~~
20140930@509.	4-5a__T2-4 cal	**25.93**	**0.24**	-6.60

20140930@510.	4-5a__T2-5 cal	**26.28**	**0.24**	-6.60
20140930@511.	4-5a__T2-6 cal	**26.22**	**0.24**	-6.60
20140930@512.	4-5a__T2-7	**25.76**	**0.24**	-11.65
20140930@513.	4-5a__T2-8	**25.82**	**0.24**	-11.65
20140930@514.	4-5a__T2-9	**26.14**	**0.24**	-11.65
20140930@515.	4-5a__UWC-3			
20140930@516.	4-5a__UWC-3			
20140930@517.	4-5a__UWC-3			
20140930@518.	4-5a__UWC-3			
	average and 2SD			
	bracket average and 2SD	**12.49**		**-6.60**
20140930@519.	4-5a__T2-10	**25.85**	**0.32**	-11.77
20140930@520.	4-5a__T2-11	**25.42**	**0.32**	-11.77
20140930@521.	4-5a__T2-12	**25.89**	**0.32**	-11.77
20140930@522.	4-5a__T2-13	**25.89**	**0.32**	-11.77
20140930@523.	4-5a__T2-14 cal	**26.05**	**0.32**	-6.71
20140930@524.	4-5a__T2-15 cal	**25.96**	**0.32**	-6.71
20140930@525.	4-5a__T2-16	**25.79**	**0.32**	-11.77
20140930@526.	4-5a__T2-17	**26.06**	**0.32**	-11.77
20140930@527.	4-5a__T2-18	**25.87**	**0.32**	-11.77
20140930@528.	4-5a__T2-19 cal	**25.75**	**0.32**	-6.71
20140930@529.	4-5a__UWC-3			
20140930@530.	4-5a__UWC-3			
20140930@531.	4-5a__UWC-3			
20140930@532.	4-5a__UWC-3			
	average and 2SD			
	bracket average and 2SD	**12.49**		**-6.71**
20140930@533.	4-5a__T2-20 cal	**26.08**	**0.35**	-6.74
20140930@534.	4-5a__T2-21 cal	**26.17**	**0.35**	-6.74
20140930@535.	4-5a__T2-22 cal	**26.50**	**0.35**	-6.74
20140930@536.	4-5a__T2-23 cal	**26.29**	**0.35**	-6.74
20140930@537.	4-5a__T2-24	**26.04**	**0.35**	-11.79
20140930@538.	4-5a__T2-25 cal	**26.00**	**0.35**	-6.74
20140930@539.	4-5a__T2-26 cal	**26.23**	**0.35**	-6.74
20140930@540.	4-5a__T2-27	**26.03**	**0.35**	-11.79
20140930@541.	4-5a__T2-28	**25.80**	**0.35**	-11.79
20140930@542.	4-5a__T2-29	**25.90**	**0.35**	-11.79
20140930@543.	4-5a__T2-30	**25.94**	**0.35**	-11.79
20140930@544.	4-5a__T2-31 cal	**26.02**	**0.35**	-6.74
20140930@545.	4-5a__UWC-3			
20140930@546.	4-5a__UWC-3			
20140930@547.	4-5a__UWC-3			
20140930@548.	4-5a__UWC-3			
	average and 2SD			

	bracket average and 2SD	**12.49**		**-6.74**

20140930@549.	A-4-1__UWC-3			
20140930@550.	A-4-1__UWC-3			
20140930@551.	A-4-1__UWC-3			
20140930@552.	A-4-1__UWC-3			
	average and 2SD			
20140930@553.	A-4-1__1-1	**23.31**	**0.18**	-11.37
20140930@554.	A-4-1__1-2	**23.44**	**0.18**	-11.37
20140930@555.	A-4-1__1-3	**23.45**	**0.18**	-11.37
20140930@556.	A-4-1__1-4 cal	**23.64**	**0.18**	-6.32
20140930@557.	A-4-1__1-5 cal	**23.67**	**0.18**	-6.32
20140930@558.	A-4-1__1-6	**23.49**	**0.18**	-11.37
20140930@559.	A-4-1__1-7	**23.51**	**0.18**	-11.37
20140930@560.	A-4-1__1-8 cal	**23.55**	**0.18**	-6.32
20140930@561.	A-4-1__1-9 cal	**23.85**	**0.18**	-6.32
20140930@562.	A-4-1__1-10 cal	**23.48**	**0.18**	-6.32
20140930@563.	A-4-1__1-11 cal	**23.73**	**0.18**	-6.32
20140930@564.	A-4-1__1-12 cal	**23.84**	**0.18**	-6.32
20140930@565.	A-4-1__UWC-3			
20140930@566.	A-4-1__UWC-3			
20140930@567.	A-4-1__UWC-3			
20140930@568.	A-4-1__UWC-3			
	average and 2SD			
	bracket average and 2SD	**12.49**		**-6.32**
20140930@569.	A-4-1__6-1	**23.38**	**0.22**	-11.29
20140930@570.	A-4-1__6-2	**23.25**	**0.22**	-11.29
20140930@571.	A-4-1__6-3 cal	**23.16**	**0.22**	-6.24
20140930@572.	A-4-1__6-4	**23.24**	**0.22**	-11.29
20140930@573.	A-4-1__6-5	**23.43**	**0.22**	-11.29
20140930@574.	A-4-1__6-6 cal	**23.74**	**0.22**	-6.24
20140930@575.	A-4-1__6-7 cal	**23.67**	**0.22**	-6.24
20140930@576.	A-4-1__6-8	**23.50**	**0.22**	-11.29
20140930@577.	A-4-1__6-9 cal	**23.21**	**0.22**	-6.24
20140930@578.	A-4-1__6-10 cal	**23.58**	**0.22**	-6.24
20140930@579.	A-4-1__6-11 cal	**23.60**	**0.22**	-6.24
20140930@580.	A-4-1__6-12 cal	**23.80**	**0.22**	-6.24
20140930@581.	A-4-1__UWC-3			
20140930@582.	A-4-1__UWC-3			
20140930@583.	A-4-1__UWC-3			
20140930@584.	A-4-1__UWC-3			
	average and 2SD			
	bracket average and 2SD	**12.49**		**-6.24**

20140930@585.	A-4-1__6-13 cal	**23.70**	**0.62**	-6.45
20140930@586.	A-4-1__7-1 cal	**24.04**	**0.62**	-6.45
20140930@587.	A-4-1__7-2	**23.65**	**0.62**	-11.50
20140930@588.	A-4-1__7-3	**23.71**	**0.62**	-11.50
20140930@589.	A-4-1__7-4	**23.64**	**0.62**	-11.50
20140930@590.	A-4-1__7-5 cal	**23.55**	**0.62**	-6.45
20140930@591.	A-4-1__7-6 cal	**23.53**	**0.62**	-6.45
20140930@592.	A-4-1__13-1	**23.54**	**0.62**	-11.50
20140930@593.	A-4-1__13-2	**23.37**	**0.62**	-11.50
20140930@594.	A-4-1__13-3 cal	**23.72**	**0.62**	-6.45
20140930@595.	A-4-1__13-4 cal	**23.43**	**0.62**	-6.45
20140930@596.	A-4-1__13-5 cal	**23.76**	**0.62**	-6.45
20140930@597.	A-4-1__UWC-3			
20140930@598.	A-4-1__UWC-3			
20140930@599.	A-4-1__UWC-3			
20140930@600.	A-4-1__UWC-3			
	average and 2SD			
	bracket average and 2SD	**12.49**		**-6.45**

$\delta^{18}O$ ‰ raw	2SE (int.)	16O (Gcps)	IP (nA)	Yield (Gcps/nA)	Date	Time	X	Y	DTFA-X
9.509	0.228	2.687	1.971	1.363	9/29/14	14:19	132	324	0
9.449	0.194	2.703	1.970	1.372	9/29/14	14:23	242	237	1
9.521	0.192	2.803	2.043	1.372	9/29/14	14:28	450	129	0
9.501	0.181	2.818	2.063	1.366	9/29/14	14:31	21	-284	3
9.796	0.208	2.823	2.069	1.365	9/29/14	14:36	154	-352	3
9.542	0.260	2.839	2.072	1.370	9/29/14	14:39	190	-71	2
9.590	**0.277**								
13.283	0.187	2.536	2.069	1.225	9/29/14	14:44	1290	2741	4
13.376	0.281	2.549	2.069	1.232	9/29/14	14:48	3077	2954	2
13.478	0.204	2.534	2.066	1.227	9/29/14	14:51	3664	1624	0
13.568	0.185	2.538	2.065	1.229	9/29/14	14:55	1879	958	-5
13.426	**0.247**								
9.640	0.198	3.086	2.061	1.497	9/29/14	14:59	-1553	2148	8
9.471	0.223	3.076	2.059	1.494	9/29/14	15:03	-1483	2635	6
~~9.056~~	~~0.240~~	~~3.089~~	~~2.059~~	~~1.500~~	~~9/29/14~~	~~15:06~~	~~-1520~~	~~3031~~	~~6~~
9.266	0.176	3.088	2.059	1.500	9/29/14	15:10	-934	2638	5
9.708	0.180	3.088	2.057	1.501	9/29/14	15:14	-993	2201	6
9.521	**0.394**								
9.670	0.115	2.814	2.055	1.369	9/29/14	15:18	-538	452	4
9.835	0.238	2.814	2.055	1.369	9/29/14	15:21	-291	446	3
9.583	0.252	2.812	2.053	1.369	9/29/14	15:24	-211	652	2
9.578	0.171	2.794	2.054	1.360	9/29/14	15:28	176	273	5
9.667	**0.240**								
9.628	**0.253**								
8.342	0.218	2.776	2.061	1.347	9/29/14	15:56	191	-1972	19
8.419	0.146	2.790	2.065	1.352	9/29/14	15:59	-138	-3032	22
~~8.920~~	~~0.192~~	~~2.784~~	~~2.063~~	~~1.349~~	~~9/29/14~~	~~16:03~~	~~375~~	~~-3583~~	~~18~~
8.687	0.197	2.769	2.071	1.337	9/29/14	16:13	-33	-4521	25
8.471	0.160	2.776	2.068	1.343	9/29/14	16:17	68	-3835	24
8.240	0.169	2.775	2.068	1.342	9/29/14	16:20	564	-3428	23
8.454	**0.334**								
9.507	0.126	2.864	2.066	1.386	9/29/14	16:25	-1825	-113	13
9.700	0.160	2.859	2.064	1.385	9/29/14	16:28	-3375	-478	11
9.684	0.210	2.836	2.063	1.375	9/29/14	16:32	-2191	-72	13
9.573	0.216	2.823	2.060	1.371	9/29/14	16:40	-3559	-756	20
9.616	**0.184**								

8.425	0.203	2.781	2.059	1.350	9/29/14	16:44	276	-2022	19
8.624	0.207	2.781	2.059	1.350	9/29/14	16:48	-160	-2989	21
8.508	0.210	2.769	2.059	1.345	9/29/14	16:51	88	-3866	17
8.517	0.189	2.753	2.054	1.340	9/29/14	16:56	33	-4573	21
8.519	**0.163**								
8.486	**0.272**								
5.911	0.480	2.511	1.287	1.950	9/29/14	17:07	-1001	-1601	18
8.257	0.178	2.638	1.952	1.352	9/30/14	8:21	253	-1921	8
8.239	0.212	2.642	1.954	1.352	9/30/14	8:25	-124	-3004	10
8.328	0.232	2.637	1.955	1.349	9/30/14	8:29	54	-3888	7
8.512	0.192	2.641	1.955	1.351	9/30/14	8:33	176	-4437	6
8.334	**0.249**								
8.079	0.129	2.640	1.972	1.338	9/30/14	8:51	607	456	-7
8.207	0.203	2.626	1.966	1.336	9/30/14	8:55	610	484	-7
8.089	0.189	2.621	1.961	1.337	9/30/14	9:00	612	506	-7
7.977	0.201	2.622	1.959	1.339	9/30/14	9:03	614	527	-8
8.088	**0.188**								
25.870	0.198	2.383	1.957	1.218	9/30/14	9:13	-5982	5234	-11
26.036	0.299	2.390	1.957	1.221	9/30/14	9:18	-5878	4901	-9
25.929	0.291	2.383	1.955	1.219	9/30/14	9:24	-5876	4809	-10
26.033	0.279	2.390	1.955	1.223	9/30/14	9:28	-5763	4782	-9
26.153	0.175	2.390	1.953	1.223	9/30/14	9:33	-5599	5137	-12
26.162	0.222	2.386	1.954	1.221	9/30/14	9:37	-5081	5259	-12
26.402	0.247	2.392	1.952	1.225	9/30/14	9:42	-4925	4877	-12
26.044	0.251	2.386	1.953	1.221	9/30/14	9:47	-4234	5118	-13
26.081	0.287	2.401	1.954	1.229	9/30/14	9:51	-4060	5058	-13
26.164	0.251	2.396	1.954	1.226	9/30/14	9:55	-4020	5056	-13
8.267	0.200	2.611	1.952	1.337	9/30/14	10:01	583	458	-9
8.231	0.226	2.617	1.956	1.338	9/30/14	10:05	585	486	-8
8.012	0.184	2.625	1.956	1.342	9/30/14	10:09	587	508	-9
8.245	0.233	2.624	1.957	1.341	9/30/14	10:13	591	533	-9
8.189	**0.238**								
8.138	**0.226**								
26.022	0.265	2.406	1.973	1.219	9/30/14	10:20	-1928	4930	2
25.831	0.148	2.422	1.979	1.224	9/30/14	10:25	-1799	4782	3
25.577	0.256	2.422	1.978	1.225	9/30/14	10:28	-1709	4684	3
25.990	0.285	2.402	1.966	1.222	9/30/14	10:33	-1604	5099	2
25.618	0.220	2.390	1.957	1.221	9/30/14	10:40	-1158	5241	1
25.839	0.173	2.411	1.967	1.226	9/30/14	10:44	-1230	5420	2
25.911	0.238	2.427	1.979	1.226	9/30/14	10:48	-1299	5547	3
26.131	0.257	2.444	1.983	1.232	9/30/14	10:54	1888	4514	-3
26.136	0.196	2.434	1.976	1.232	9/30/14	11:01	1766	4192	-5

26.208	0.192	2.415	1.965	1.229	9/30/14	11:04	1695	3907	-6
8.038	0.209	2.618	1.957	1.338	9/30/14	11:09	553	462	-9
8.345	0.224	2.645	1.967	1.345	9/30/14	11:12	558	488	-8
8.354	0.234	2.668	1.982	1.346	9/30/14	11:16	561	507	-8
8.283	0.238	2.675	1.986	1.347	9/30/14	11:20	567	531	-7
8.255	**0.296**								
8.222	**0.258**								
25.943	0.214	2.435	1.979	1.231	9/30/14	11:25	2553	4173	-7
25.998	0.214	2.412	1.965	1.228	9/30/14	11:30	2656	3984	-7
26.336	0.227	2.406	1.959	1.228	9/30/14	11:34	2864	4520	-7
26.150	0.175	2.438	1.981	1.230	9/30/14	11:40	4470	3587	-11
26.149	0.168	2.445	1.984	1.232	9/30/14	11:45	4503	3417	-11
26.021	0.218	2.450	1.982	1.236	9/30/14	11:49	4345	3083	-12
26.143	0.255	2.409	1.961	1.229	9/30/14	11:55	4941	2456	-15
26.246	0.234	2.396	1.950	1.229	9/30/14	12:00	4876	2060	-17
26.323	0.253	2.435	1.973	1.234	9/30/14	12:04	5089	1702	-17
26.026	0.245	2.427	1.981	1.225	9/30/14	12:12	-5215	3761	-3
25.898	0.178	2.407	1.967	1.224	9/30/14	12:17	-5166	3971	-3
25.567	0.227	2.380	1.949	1.221	9/30/14	12:20	-5130	4148	-5
8.302	0.198	2.586	1.939	1.333	9/30/14	12:25	535	531	-12
8.432	0.176	2.642	1.962	1.347	9/30/14	12:29	532	508	-11
8.406	0.193	2.655	1.978	1.342	9/30/14	12:32	533	483	-10
8.238	0.107	2.651	1.981	1.338	9/30/14	12:36	534	461	-10
8.345	**0.181**								
8.300	**0.247**								
26.127	0.209	2.362	1.935	1.221	9/30/14	12:52	-4787	2048	-10
26.126	0.246	2.416	1.963	1.231	9/30/14	12:56	-4868	1990	-9
26.165	0.252	2.438	1.976	1.234	9/30/14	12:59	-4966	1931	-8
25.910	0.211	2.403	1.974	1.217	9/30/14	13:07	1821	-515	-6
26.331	0.226	2.406	1.955	1.231	9/30/14	13:12	2228	-734	-7
25.979	0.250	2.380	1.944	1.224	9/30/14	13:19	3031	-511	-11
26.238	0.172	2.425	1.971	1.231	9/30/14	13:23	2837	-544	-9
26.286	0.285	2.428	1.974	1.230	9/30/14	13:28	4313	-673	-11
26.148	0.164	2.411	1.961	1.230	9/30/14	13:32	4159	-613	-12
25.961	0.267	2.370	1.932	1.227	9/30/14	13:36	4994	-784	-14
26.033	0.250	2.359	1.922	1.227	9/30/14	13:40	4795	-955	-15
8.346	0.274	2.639	1.965	1.343	9/30/14	13:46	506	458	-11
8.292	0.264	2.655	1.973	1.346	9/30/14	13:50	507	479	-11
8.348	0.167	2.660	1.974	1.348	9/30/14	13:53	509	507	-10
8.266	0.214	2.644	1.963	1.347	9/30/14	13:57	510	533	-11
8.320	**0.076**								
8.326	**0.127**								
23.708	0.229	2.339	1.909	1.225	9/30/14	14:04	-656	-1930	-5
23.550	0.259	2.388	1.932	1.236	9/30/14	14:09	-364	-1906	-6
23.318	0.204	2.416	1.967	1.228	9/30/14	14:17	6191	-2421	-4
23.262	0.263	2.403	1.957	1.228	9/30/14	14:22	6309	-3234	-3

23.433	0.192	2.346	1.916	1.225	9/30/14	14:28	5399	-3991	0
23.575	0.214	2.345	1.911	1.228	9/30/14	14:32	5436	-3450	-2
23.507	0.176	2.391	1.962	1.219	9/30/14	14:39	-347	-3830	10
23.464	0.233	2.389	1.965	1.216	9/30/14	14:45	-263	-4160	10
23.341	0.206	2.375	1.958	1.213	9/30/14	14:49	-1352	-3144	12
23.390	0.295	2.363	1.940	1.218	9/30/14	14:53	-1152	-3196	13
8.258	0.226	2.522	1.901	1.327	9/30/14	14:59	467	465	3
8.181	0.214	2.586	1.923	1.345	9/30/14	15:03	469	487	3
8.539	0.232	2.617	1.950	1.342	9/30/14	15:07	475	513	4
8.445	0.252	2.621	1.957	1.339	9/30/14	15:10	477	536	4
8.336	**0.299**								
8.336	**0.213**								
8.329	0.223	2.652	1.989	1.333	9/30/14	15:29	53	-355	6
8.317	0.214	2.675	2.002	1.336	9/30/14	15:32	59	-384	7
8.267	0.241	2.682	2.007	1.337	9/30/14	15:36	55	-331	7
8.081	0.219	2.682	2.006	1.337	9/30/14	15:40	62	-309	7
8.265	**0.212**								
27.082	0.249	2.402	1.977	1.215	9/30/14	15:50	570	-7813	17
26.937	0.237	2.422	1.983	1.221	9/30/14	15:54	887	-8000	18
27.010	0.167	2.453	2.001	1.226	9/30/14	15:59	523	-6315	13
27.206	0.248	2.452	2.002	1.225	9/30/14	16:03	593	-6896	15
26.901	0.243	2.448	1.996	1.226	9/30/14	16:08	2615	-5840	8
27.050	0.217	2.421	1.973	1.227	9/30/14	16:13	2989	-6065	8
25.812	0.224	2.418	1.983	1.219	9/30/14	16:19	-1716	-4533	17
25.793	0.236	2.441	1.999	1.221	9/30/14	16:24	-2278	-4448	20
25.564	0.229	2.419	1.995	1.213	9/30/14	16:32	-2845	-6418	21
25.701	0.198	2.380	1.967	1.210	9/30/14	16:36	-2009	-6822	18
25.459	0.262	2.370	1.951	1.215	9/30/14	16:41	-1993	-5047	18
25.475	0.190	2.420	1.983	1.220	9/30/14	16:46	-1521	-5268	17
8.139	0.209	2.659	1.994	1.334	9/30/14	16:50	56	-446	6
8.122	0.144	2.660	1.994	1.334	9/30/14	16:54	57	-472	6
8.158	0.244	2.651	1.985	1.335	9/30/14	16:57	56	-495	6
8.110	0.208	2.609	1.964	1.329	9/30/14	17:01	57	-520	5
8.134	**0.037**								
8.206	**0.206**								
8.464	0.282	2.577	1.930	1.336	9/30/14	17:33	-522	-203	-16
8.423	0.213	2.640	1.973	1.338	9/30/14	17:39	-526	-175	-13
8.131	0.194	2.650	1.982	1.337	9/30/14	17:42	-527	-149	-13
8.300	0.260	2.646	1.980	1.336	9/30/14	17:46	-530	-126	-13
8.356	**0.286**								

26.103	0.257	2.396	1.965	1.219	9/30/14	17:50	-4777	-811	-8
26.296	0.232	2.354	1.935	1.217	9/30/14	17:54	-4606	-992	-8
26.265	0.240	2.338	1.911	1.223	9/30/14	17:59	-2743	-1143	-11
26.273	0.187	2.396	1.952	1.227	9/30/14	18:04	-2824	-1189	-10
26.325	0.259	2.412	1.968	1.226	9/30/14	18:09	-155	-2908	-12
26.456	0.185	2.410	1.966	1.226	9/30/14	18:13	-169	-2784	-12
26.374	0.169	2.366	1.939	1.220	9/30/14	18:21	2097	-5183	-7
26.290	0.260	2.356	1.922	1.226	9/30/14	18:25	2240	-5442	-7
26.318	0.232	2.391	1.949	1.227	9/30/14	18:30	5933	-1030	1
26.333	0.196	2.395	1.959	1.222	9/30/14	18:35	5937	-937	1
26.698	0.291	2.389	1.950	1.225	9/30/14	18:43	3961	800	-15
26.442	0.233	2.387	1.940	1.230	9/30/14	18:47	4180	563	-15
8.201	0.192	2.582	1.933	1.336	9/30/14	18:51	-467	-119	-9
8.239	0.224	2.570	1.928	1.333	9/30/14	18:54	-465	-147	-9
8.097	0.252	2.569	1.928	1.333	9/30/14	18:58	-464	-172	-10
8.297	0.225	2.579	1.933	1.335	9/30/14	19:02	-464	-199	-9
8.207	**0.146**								
8.291	**0.275**								
26.519	0.181	2.372	1.936	1.225	9/30/14	19:06	4522	124	-11
26.610	0.279	2.384	1.937	1.231	9/30/14	19:10	4410	-122	-11
26.627	0.212	2.382	1.934	1.231	9/30/14	19:15	4674	1250	-12
26.602	0.270	2.376	1.933	1.229	9/30/14	19:19	4566	1570	-12
26.531	0.260	2.364	1.930	1.224	9/30/14	19:25	884	-6460	0
26.760	0.253	2.349	1.931	1.217	9/30/14	19:29	449	-6870	-1
8.366	0.191	2.569	1.931	1.331	9/30/14	19:34	-493	-200	-5
8.024	0.213	2.573	1.932	1.332	9/30/14	19:38	-493	-174	-6
7.970	0.201	2.581	1.933	1.335	9/30/14	19:41	-498	-146	-6
8.166	0.233	2.577	1.934	1.332	9/30/14	19:45	-497	-120	-5
8.178	**0.371**								
8.173	**0.253**								

7.957	0.238	2.680	2.005	1.337	9/30/14	20:08	-227	484	-17
8.280	0.213	2.689	2.009	1.339	9/30/14	20:12	-230	516	-16
7.999	0.206	2.690	2.009	1.339	9/30/14	20:15	-232	544	-16
8.144	0.238	2.692	2.010	1.339	9/30/14	20:19	-235	571	-16
8.067	**0.283**								
25.253	0.188	2.420	2.008	1.205	9/30/14	20:27	-666	1432	-15
24.715	0.175	2.461	2.009	1.225	9/30/14	20:31	-747	1480	-14
25.129	0.211	2.432	2.006	1.212	9/30/14	20:43	-1041	1476	-14
25.436	0.153	2.454	2.004	1.224	9/30/14	20:47	-981	1589	-15
25.118	0.195	2.409	2.003	1.203	9/30/14	20:53	-36	1397	-17
25.000	0.245	2.403	2.003	1.200	9/30/14	20:57	-30	1602	-17
25.587	0.286	2.333	2.001	1.166	9/30/14	21:04	513	1330	-18

25.018	0.244	2.404	1.999	1.203	9/30/14	21:08	614	1437	-18
25.389	0.196	2.433	1.998	1.218	9/30/14	21:13	2596	1254	-21
25.324	0.226	2.444	1.997	1.224	9/30/14	21:17	2675	1343	-22
25.611	0.216	2.339	1.995	1.173	9/30/14	21:22	4038	1159	-24
25.868	0.128	2.371	1.994	1.189	9/30/14	21:26	4260	1096	-25
8.099	0.201	2.660	1.992	1.335	9/30/14	21:31	-199	487	-18
8.026	0.228	2.664	1.991	1.338	9/30/14	21:35	-199	516	-18
7.988	0.225	2.662	1.990	1.338	9/30/14	21:38	-198	545	-17
8.044	0.158	2.661	1.989	1.338	9/30/14	21:42	-201	572	-17
8.051	**0.096**								
8.055	**0.210**								
18.534	0.269	2.457	1.983	1.239	9/30/14	21:52	1269	4987	-15
19.543	0.264	2.458	1.983	1.240	9/30/14	21:57	1170	5301	-14
20.011	0.199	2.459	1.982	1.240	9/30/14	22:01	1442	4813	-15
19.377	0.200	2.457	1.981	1.240	9/30/14	22:06	1181	5084	-14
19.287	0.275	2.451	1.980	1.238	9/30/14	22:10	1381	4915	-15
19.795	0.237	2.450	1.978	1.238	9/30/14	22:14	1204	4780	-15
19.187	0.232	2.445	1.977	1.237	9/30/14	22:18	1301	4983	-15
20.546	0.175	2.441	1.976	1.235	9/30/14	22:23	3135	4988	-16
20.189	0.143	2.439	1.973	1.236	9/30/14	22:28	3296	5157	-16
20.386	0.218	2.442	1.957	1.248	9/30/14	22:32	3272	4788	-17
8.411	0.259	2.627	1.966	1.336	9/30/14	22:39	-198	601	-18
8.208	0.237	2.627	1.963	1.338	9/30/14	22:43	-196	624	-18
8.101	0.176	2.621	1.959	1.338	9/30/14	22:46	-194	652	-18
8.190	0.206	2.615	1.954	1.338	9/30/14	22:50	-192	679	-18
8.264	**0.280**								
8.130	**0.255**								
19.629	0.195	2.393	1.940	1.233	9/30/14	22:58	-1696	5137	-11
18.457	0.208	2.355	1.914	1.230	9/30/14	23:08	-1726	4817	-12
20.428	0.270	2.352	1.906	1.234	9/30/14	23:12	-1702	5226	-11
19.976	0.259	2.313	1.878	1.231	9/30/14	23:24	-1659	5397	-12
20.681	0.197	2.438	1.982	1.230	9/30/14	23:38	-1729	5225	-11
18.332	0.192	2.452	1.984	1.236	9/30/14	23:42	-1758	4821	-11
8.195	0.222	2.645	1.984	1.333	9/30/14	23:49	-224	608	-8
8.120	0.224	2.654	1.982	1.339	9/30/14	23:53	-219	630	-7
8.052	0.161	2.649	1.980	1.338	9/30/14	23:57	-213	657	-8
8.304	0.260	2.648	1.977	1.340	10/1/14	0:00	-206	685	-7
8.173	**0.189**								
8.221	**0.259**								
20.502	0.291	2.460	2.000	1.230	10/1/14	0:09	-3605	5189	2
19.594	0.168	2.463	2.008	1.226	10/1/14	0:13	-3636	5525	2
19.343	0.192	2.432	1.984	1.226	10/1/14	0:19	-3666	5339	2
20.025	0.236	2.419	1.973	1.226	10/1/14	0:23	-3647	5198	2

18.551	0.191	2.412	1.966	1.227	10/1/14	0:28	-3515	5168	2
19.348	0.191	2.403	1.958	1.228	10/1/14	0:33	-3453	5136	2
20.055	0.294	2.370	1.949	1.216	10/1/14	0:42	-6236	5182	7
19.987	0.256	2.376	1.946	1.221	10/1/14	0:45	-6077	4943	7
19.805	0.261	2.377	1.944	1.223	10/1/14	0:51	-5695	5219	5
18.129	0.206	2.376	1.938	1.226	10/1/14	0:55	-5644	4849	6
7.788	0.153	2.556	1.930	1.324	10/1/14	1:03	-255	490	5
7.924	0.170	2.561	1.928	1.328	10/1/14	1:07	-255	517	5
8.014	0.262	2.565	1.926	1.332	10/1/14	1:11	-255	541	5
7.998	0.209	2.565	1.927	1.331	10/1/14	1:14	-258	567	6
7.902	**0.220**								
8.066	**0.314**								
7.986	0.153	2.677	2.020	1.326	10/1/14	1:27	-256	607	6
7.878	0.224	2.690	2.021	1.331	10/1/14	1:30	-253	632	7
7.876	0.265	2.695	2.022	1.333	10/1/14	1:34	-248	657	7
7.630	0.220	2.695	2.022	1.333	10/1/14	1:37	-242	684	7
9.668	**8.168**								
19.418	0.273	2.473	2.018	1.226	10/1/14	1:45	-5168	5021	9
19.664	0.219	2.465	2.017	1.222	10/1/14	1:51	-5101	5018	8
19.276	0.276	2.466	2.016	1.223	10/1/14	1:56	-5049	5199	8
19.257	0.262	2.472	2.016	1.226	10/1/14	2:00	-5236	4761	9
19.775	0.268	2.455	2.012	1.220	10/1/14	2:07	-4827	5057	8
18.335	0.203	2.467	2.013	1.225	10/1/14	2:11	-4790	4903	8
19.409	0.292	2.457	2.010	1.223	10/1/14	2:16	-4772	5089	8
18.380	0.262	2.453	2.009	1.221	10/1/14	2:20	-4739	5137	8
19.423	0.196	2.439	2.006	1.216	10/1/14	2:26	-4686	4372	8
20.190	0.282	2.439	2.004	1.217	10/1/14	2:30	-4796	4031	8
19.949	0.157	2.436	2.003	1.216	10/1/14	2:34	-4713	4556	7
19.624	0.220	2.447	2.009	1.218	10/1/14	2:40	-4690	4197	9
7.955	0.200	2.662	2.013	1.322	10/1/14	2:48	-343	495	4
8.072	0.190	2.672	2.017	1.325	10/1/14	2:51	-338	527	5
8.067	0.154	2.674	2.020	1.324	10/1/14	2:55	-332	552	4
8.254	0.228	2.676	2.020	1.325	10/1/14	2:59	-326	578	4
8.061	**0.245**								
7.967	**0.342**								
19.067	0.261	2.476	2.015	1.229	10/1/14	3:06	-6156	4425	-1
19.197	0.163	2.467	2.016	1.224	10/1/14	3:11	-6030	4639	-2
19.424	0.147	2.474	2.017	1.227	10/1/14	3:16	-5258	4287	-4
20.742	0.217	2.476	2.016	1.228	10/1/14	3:21	-5237	4094	-4
19.578	0.183	2.471	2.016	1.226	10/1/14	3:27	-5310	4171	-4
19.619	0.193	2.477	2.015	1.229	10/1/14	3:31	-5354	4059	-3
18.027	0.202	2.471	2.012	1.228	10/1/14	3:36	-5270	4471	-4
19.625	0.277	2.473	2.012	1.229	10/1/14	3:40	-5190	4453	-4
19.385	0.221	2.456	2.009	1.223	10/1/14	3:48	-3006	4340	3

16.929	0.199	2.459	2.009	1.224	10/1/14	3:52	-2921	4456	4
18.877	0.189	2.448	2.004	1.222	10/1/14	3:58	-2984	4407	3
19.090	0.163	2.450	2.003	1.224	10/1/14	4:02	-2955	4439	4
7.990	0.217	2.664	2.002	1.331	10/1/14	4:08	-367	495	-5
8.164	0.229	2.668	2.001	1.334	10/1/14	4:11	-359	525	-5
7.953	0.190	2.667	2.000	1.334	10/1/14	4:15	-352	553	-5
8.052	0.201	2.666	1.999	1.334	10/1/14	4:18	-346	581	-5
8.030	**0.166**								
8.051	**0.208**								
17.477	0.198	2.436	1.995	1.221	10/1/14	4:23	-2935	4472	3
17.968	0.175	2.439	1.991	1.225	10/1/14	4:29	-2871	4103	3
20.395	0.217	2.434	1.987	1.225	10/1/14	4:35	-756	4122	-1
19.785	0.251	2.430	1.985	1.225	10/1/14	4:40	-576	4023	-2
20.291	0.237	2.429	1.983	1.225	10/1/14	4:44	-771	3894	-1
19.505	0.326	2.431	1.983	1.226	10/1/14	4:48	-669	3864	-2
19.828	0.233	2.421	1.978	1.224	10/1/14	4:56	-158	-4327	-8
19.685	0.184	2.419	1.975	1.225	10/1/14	5:00	-125	-4100	-8
20.904	0.193	2.425	1.973	1.229	10/1/14	5:04	-173	-4786	-8
19.630	0.284	2.419	1.971	1.227	10/1/14	5:08	-57	-4743	-8
19.121	0.199	2.409	1.968	1.224	10/1/14	5:12	-166	-4696	-7
19.361	0.228	2.407	1.965	1.225	10/1/14	5:17	-124	-4490	-8
8.202	0.173	2.613	1.963	1.331	10/1/14	5:22	-393	501	-6
8.076	0.223	2.616	1.962	1.333	10/1/14	5:26	-385	529	-6
8.174	0.236	2.617	1.959	1.336	10/1/14	5:30	-377	554	-6
7.980	0.206	2.612	1.955	1.336	10/1/14	5:34	-371	580	-6
8.127	**0.194**								
8.065	**0.189**								
19.621	0.157	2.392	1.952	1.226	10/1/14	5:40	469	-4603	-10
20.241	0.265	2.391	1.950	1.226	10/1/14	5:43	499	-4724	-9
19.805	0.173	2.381	1.946	1.223	10/1/14	5:48	486	-4660	-9
19.324	0.189	2.362	1.940	1.218	10/1/14	5:58	-3866	-4303	-2
19.179	0.233	2.367	1.936	1.222	10/1/14	6:03	-3861	-4230	-1
20.804	0.217	2.360	1.934	1.220	10/1/14	6:08	-3854	-4450	-1
20.929	0.181	2.359	1.929	1.223	10/1/14	6:13	-3949	-4299	-1
20.654	0.317	2.349	1.926	1.220	10/1/14	6:17	-3905	-4454	-1
19.043	0.214	2.340	1.922	1.218	10/1/14	6:24	-6128	-3986	8
18.888	0.171	2.334	1.920	1.215	10/1/14	6:28	-6220	-4140	7
18.862	0.194	2.335	1.917	1.218	10/1/14	6:31	-6183	-4313	7
18.806	0.160	2.330	1.913	1.218	10/1/14	6:36	-6026	-3873	7
8.057	0.203	2.542	1.913	1.329	10/1/14	6:41	-424	508	3
8.098	0.211	2.544	1.912	1.330	10/1/14	6:45	-413	532	3
7.951	0.199	2.544	1.909	1.333	10/1/14	6:48	-405	556	3
8.083	0.260	2.544	1.907	1.334	10/1/14	6:52	-396	583	3
8.049	**0.115**								

8.103	**0.184**								
8.053	0.213	2.688	2.029	1.324	10/1/14	7:03	-452	517	4
8.116	0.167	2.712	2.034	1.333	10/1/14	7:07	-437	545	5
8.138	0.186	2.709	2.035	1.331	10/1/14	7:10	-427	572	5
7.922	0.241	2.704	2.035	1.329	10/1/14	7:14	-418	598	5
8.057	**0.194**								
26.231	0.239	2.471	2.028	1.219	10/1/14	7:20	-2810	-3343	9
26.397	0.195	2.476	2.027	1.222	10/1/14	7:24	-2791	-3105	10
26.334	0.271	2.468	2.025	1.219	10/1/14	7:28	-2652	-3345	9
26.530	0.251	2.467	2.024	1.219	10/1/14	7:32	-2582	-3331	9
26.659	0.226	2.463	2.023	1.217	10/1/14	7:37	-3466	-3301	11
26.422	0.177	2.456	2.022	1.215	10/1/14	7:41	-3527	-3344	11
26.622	0.164	2.465	2.021	1.220	10/1/14	7:45	-3344	-3524	11
26.531	0.172	2.471	2.018	1.225	10/1/14	7:54	-6101	-3314	0
26.347	0.228	2.480	2.017	1.229	10/1/14	7:57	-6095	-3054	2
20.116	0.187	2.472	2.016	1.226	10/1/14	8:04	-4184	-2336	-7
20.122	0.245	2.479	2.016	1.229	10/1/14	8:08	-4175	-1955	-6
19.971	0.184	2.470	2.014	1.227	10/1/14	8:13	-2310	-2491	-12
21.106	0.200	2.482	2.017	1.231	10/1/14	8:18	-2445	-2686	-11
21.088	0.227	2.475	2.018	1.227	10/1/14	8:22	-2388	-2645	-12
8.238	0.159	2.696	2.018	1.336	10/1/14	8:26	-481	524	-16
8.094	0.193	2.701	2.018	1.338	10/1/14	8:30	-467	549	-16
8.141	0.216	2.703	2.017	1.340	10/1/14	8:34	-456	572	-16
8.212	0.199	2.699	2.016	1.339	10/1/14	8:37	-444	596	-16
8.185	**0.129**								
8.107	**0.188**								

8.738	0.176	2.736	2.050	1.335	10/1/14	9:07	946	304	1
8.573	0.235	2.719	2.033	1.338	10/1/14	9:12	949	329	1
8.276	0.223	2.711	2.026	1.338	10/1/14	9:16	954	355	0
8.616	0.196	2.708	2.021	1.340	10/1/14	9:19	960	379	1
8.588	**0.379**								
19.512	0.161	2.455	2.012	1.220	10/1/14	9:24	-3388	-383	10
19.426	0.269	2.469	2.007	1.230	10/1/14	9:29	-3590	-281	1
19.556	0.242	2.462	2.007	1.227	10/1/14	9:33	-3233	-610	1
20.867	0.237	2.437	2.023	1.205	10/1/14	9:42	-7037	-987	6
20.851	0.218	2.454	2.013	1.219	10/1/14	9:46	-7211	-1138	-3
20.691	0.215	2.440	2.005	1.217	10/1/14	9:51	-7492	-634	-1
19.839	0.198	2.454	1.999	1.227	10/1/14	9:57	376	-1712	6
21.079	0.195	2.456	1.995	1.231	10/1/14	10:00	197	-1723	7
20.573	0.205	2.450	1.990	1.231	10/1/14	10:04	481	-1693	6
19.798	0.175	2.438	1.989	1.226	10/1/14	10:08	351	-1705	6
21.216	0.238	2.441	1.987	1.229	10/1/14	10:12	266	-1739	6

8.542	0.277	2.654	1.982	1.339	10/1/14	10:16	974	297	3
8.648	0.253	2.646	1.979	1.337	10/1/14	10:19	977	324	3
8.473	0.159	2.644	1.975	1.339	10/1/14	10:23	981	353	3
8.132	0.152	2.632	1.969	1.336	10/1/14	10:26	983	379	2
8.413	0.153	2.625	1.962	1.337	10/1/14	10:30	989	402	2
8.458	**0.356**								
8.515	**0.393**								
19.535	0.148	2.403	1.952	1.231	10/1/14	10:36	2192	-2511	2
21.260	0.200	2.404	1.950	1.233	10/1/14	10:40	2071	-2549	3
19.315	0.303	2.405	1.954	1.231	10/1/14	10:44	2136	-2532	2
21.364	0.214	2.401	1.948	1.233	10/1/14	10:47	2087	-2407	3
20.838	0.190	2.397	1.942	1.234	10/1/14	10:51	2391	-2550	2
21.080	0.234	2.400	1.936	1.240	10/1/14	10:55	5289	-1441	0
21.402	0.230	2.384	1.930	1.236	10/1/14	11:00	5124	-1422	5
19.595	0.244	2.352	1.925	1.222	10/1/14	11:06	-5784	-3653	-21
20.493	0.232	2.353	1.918	1.227	10/1/14	11:09	-5848	-3797	-22
19.991	0.276	2.333	1.917	1.217	10/1/14	11:13	-6117	-3578	-21
8.477	0.199	2.560	1.917	1.335	10/1/14	11:17	1005	289	3
8.173	0.229	2.566	1.918	1.338	10/1/14	11:21	1012	314	3
8.516	0.243	2.568	1.918	1.339	10/1/14	11:24	1016	341	3
8.393	0.273	2.567	1.919	1.338	10/1/14	11:27	1021	367	2
8.407	**0.277**								
8.431	**0.327**								
5.950	0.552	2.554	1.296	1.971	10/1/14	11:59	-95	356	-3
6.200	0.516	2.535	1.293	1.961	10/1/14	12:03	-582	91	0
5.944	0.541	2.524	1.288	1.960	10/1/14	12:06	324	108	-3
6.068	0.505	2.517	1.286	1.957	10/1/14	12:10	-339	637	-1
6.041	**0.241**								
11.092	0.491	2.724	1.282	2.124	10/1/14	12:15	-143	1519	1
10.902	0.480	2.710	1.282	2.114	10/1/14	12:19	86	1506	0
10.815	0.462	2.720	1.283	2.120	10/1/14	12:22	-15	1669	0
11.095	0.479	2.721	1.283	2.121	10/1/14	12:26	-139	1779	1
10.976	**0.281**								
4.733	0.344	2.834	1.280	2.214	10/1/14	12:30	46	-1039	0
4.739	0.350	2.821	1.279	2.205	10/1/14	12:35	727	-2013	-3
4.681	0.330	2.812	1.279	2.198	10/1/14	12:39	134	-2576	0
4.989	0.305	2.829	1.281	2.209	10/1/14	12:43	-922	-4484	1
4.786	**0.276**								
5.953	0.505	2.505	1.278	1.959	10/1/14	12:48	21	455	5

5.959	0.475	2.523	1.280	1.971	10/1/14	12:52	-280	269	1
5.835	0.496	2.503	1.279	1.957	10/1/14	12:56	-764	81	3
5.952	0.509	2.504	1.278	1.960	10/1/14	12:59	439	59	-3
5.925	**0.120**								
5.983	**0.215**								

6.365	0.504	2.458	1.270	1.935	10/1/14	13:18	-944	1127	-16
6.177	0.433	2.463	1.271	1.938	10/1/14	13:22	-911	1099	-10
6.401	0.432	2.438	1.270	1.920	10/1/14	13:25	-881	1131	-9
6.026	0.533	2.454	1.269	1.934	10/1/14	13:29	-957	1105	-9
6.267	**0.321**								
19.051	0.481	2.357	1.265	1.863	10/1/14	13:34	-4766	-670	-3
18.640	0.519	2.362	1.264	1.868	10/1/14	13:39	-4929	-610	-3
18.904	0.600	2.351	1.262	1.863	10/1/14	13:43	-4936	-486	-3
18.668	0.468	2.356	1.261	1.868	10/1/14	13:46	-4951	-373	-3
13.335	0.502	2.584	1.258	2.054	10/1/14	13:51	-4948	-337	-3
13.384	0.489	2.560	1.256	2.038	10/1/14	13:55	-4959	-287	-2
13.332	0.517	2.583	1.254	2.059	10/1/14	13:59	-4929	-241	-3
13.453	0.467	2.560	1.252	2.044	10/1/14	14:02	-4895	-217	-3
13.279	0.497	2.570	1.251	2.054	10/1/14	14:06	-4895	-183	-3
13.219	0.437	2.560	1.248	2.051	10/1/14	14:09	-4898	-132	-3
13.430	0.426	2.559	1.247	2.053	10/1/14	14:13	-4898	-87	-3
6.299	0.540	2.394	1.245	1.923	10/1/14	14:17	-976	1077	-10
6.221	0.480	2.397	1.245	1.925	10/1/14	14:21	-976	1049	-9
6.086	0.414	2.413	1.245	1.938	10/1/14	14:24	-978	1033	-10
5.905	0.472	2.404	1.244	1.932	10/1/14	14:28	-979	1015	-10
6.162	**0.336**								
6.205	**0.343**								
13.313	0.472	2.569	1.241	2.071	10/1/14	14:35	-4897	-61	-5
13.348	0.539	2.537	1.240	2.046	10/1/14	14:39	-4893	-19	-4
13.319	0.459	2.567	1.242	2.068	10/1/14	14:42	-4891	20	-3
13.522	0.465	2.538	1.241	2.044	10/1/14	14:46	-4888	55	-4
13.118	0.475	2.520	1.241	2.030	10/1/14	14:49	-4881	124	-3
13.277	0.385	2.545	1.241	2.051	10/1/14	14:54	-4834	246	-4
~~26.262~~	~~0.347~~	~~1.527~~	~~1.238~~	~~1.233~~	~~10/1/14~~	~~15:02~~	~~2089~~	~~-4931~~	~~6~~
18.558	0.404	2.407	1.293	1.861	10/1/14	15:08	2122	-4867	7
17.733	0.463	2.440	1.306	1.869	10/1/14	15:15	2113	-4806	8
13.130	0.448	2.658	1.308	2.031	10/1/14	15:18	2071	-4767	9
5.777	0.513	2.514	1.310	1.919	10/1/14	15:22	-1001	1010	6
5.734	0.501	2.513	1.310	1.918	10/1/14	15:26	-1001	1031	5
6.004	0.443	2.503	1.311	1.910	10/1/14	15:29	-998	1052	6
6.074	0.458	2.528	1.311	1.928	10/1/14	15:33	-1001	1081	6
5.873	**0.309**								

6.036	**0.399**								
19.043	0.555	2.422	1.309	1.850	10/1/14	15:37	2000	-4691	8
18.920	0.449	2.429	1.308	1.856	10/1/14	15:41	2051	-4744	10
18.602	0.543	2.454	1.308	1.876	10/1/14	15:45	1915	-4666	7
13.157	0.467	2.664	1.307	2.038	10/1/14	15:49	1876	-4669	7
13.290	0.433	2.651	1.305	2.031	10/1/14	15:54	1767	-4535	5
13.141	0.436	2.657	1.305	2.036	10/1/14	15:57	1672	-4420	5
13.209	0.489	2.654	1.304	2.034	10/1/14	16:01	1567	-4265	6
13.384	0.508	2.674	1.301	2.055	10/1/14	16:14	1394	-4233	5
12.829	0.407	2.678	1.302	2.057	10/1/14	16:18	1428	-4226	6
13.052	0.501	2.668	1.303	2.048	10/1/14	16:21	1465	-4222	5
5.576	0.493	2.521	1.302	1.936	10/1/14	16:26	-1025	1010	3
5.874	0.433	2.512	1.302	1.929	10/1/14	16:30	-1027	1036	4
5.850	0.477	2.491	1.302	1.913	10/1/14	16:33	-1025	1084	3
5.882	0.442	2.502	1.303	1.921	10/1/14	16:37	-1019	1118	4
5.919	0.450	2.496	1.303	1.915	10/1/14	16:41	-1072	1101	3
5.780	**0.318**								
5.847	**0.282**								
13.380	0.400	2.683	1.303	2.058	10/1/14	16:47	1505	-4218	5
13.277	0.473	2.655	1.303	2.038	10/1/14	16:51	1542	-4214	6
13.403	0.394	2.635	1.303	2.023	10/1/14	16:55	1549	-4185	5
~~16.639~~	~~0.242~~	~~2.355~~	~~1.302~~	~~1.809~~	~~10/1/14~~	~~16:59~~	~~1578~~	~~-4182~~	~~6~~
13.247	0.543	2.671	1.302	2.051	10/1/14	17:03	1604	-4182	5
13.288	0.397	2.673	1.302	2.053	10/1/14	17:07	1579	-4162	5
18.475	0.441	2.444	1.299	1.881	10/1/14	17:12	2426	-5180	7
18.808	0.605	2.420	1.298	1.864	10/1/14	17:16	2108	-5323	7
13.135	0.481	2.639	1.297	2.035	10/1/14	17:20	1632	-4185	5
13.086	0.462	2.656	1.298	2.047	10/1/14	17:24	1669	-4194	6
5.741	0.522	2.482	1.296	1.916	10/1/14	17:28	-960	1235	3
5.931	0.493	2.480	1.296	1.913	10/1/14	17:32	-908	1241	3
5.781	0.389	2.484	1.294	1.919	10/1/14	17:35	-896	1267	3
6.151	0.487	2.457	1.292	1.902	10/1/14	17:39	-862	1265	3
5.853	0.497	2.481	1.292	1.920	10/1/14	17:43	-882	1198	3
5.866	**0.315**								
5.830	**0.326**								
13.172	0.472	2.649	1.289	2.055	10/1/14	17:49	1713	-4207	5
13.248	0.419	2.610	1.287	2.028	10/1/14	17:52	1739	-4196	5
13.507	0.498	2.617	1.282	2.041	10/1/14	18:02	1231	-4084	4
13.427	0.474	2.608	1.281	2.036	10/1/14	18:07	1252	-4064	4
13.164	0.451	2.629	1.281	2.053	10/1/14	18:11	1270	-4045	4
13.190	0.479	2.650	1.280	2.070	10/1/14	18:16	1201	-4097	5
13.358	0.491	2.608	1.281	2.036	10/1/14	18:20	1177	-4111	4
12.907	0.458	2.614	1.279	2.043	10/1/14	18:25	987	-3809	5
13.255	0.462	2.613	1.280	2.042	10/1/14	18:29	1091	-3809	5

~~19.968~~	~~0.390~~	~~2.187~~	~~1.280~~	~~1.709~~	~~10/1/14~~	~~18:33~~	~~1114~~	~~-3801~~	~~4~~
18.723	0.495	2.381	1.279	1.862	10/1/14	18:37	1083	-3715	4
18.863	0.494	2.392	1.278	1.872	10/1/14	18:41	1103	-3663	5
6.034	0.549	2.457	1.275	1.926	10/1/14	18:47	-976	1172	2
5.976	0.464	2.444	1.275	1.917	10/1/14	18:50	-961	1189	3
6.189	0.508	2.435	1.274	1.911	10/1/14	18:54	-933	1191	3
5.768	0.464	2.444	1.273	1.919	10/1/14	18:57	-945	1168	2
6.000	**0.304**								
5.917	**0.335**								
13.556	0.433	2.586	1.270	2.036	10/1/14	19:03	-65	-2940	5
13.573	0.431	2.597	1.269	2.047	10/1/14	19:08	-138	-3202	5
13.538	0.421	2.580	1.268	2.035	10/1/14	19:13	-41	-3131	5
13.290	0.525	2.576	1.268	2.032	10/1/14	19:17	-5	-3126	5
13.343	0.478	2.591	1.267	2.045	10/1/14	19:20	-93	-3109	5
13.658	0.447	2.584	1.265	2.042	10/1/14	19:25	-90	-3200	5
13.457	0.394	2.577	1.263	2.039	10/1/14	19:29	-101	-3014	5
6.326	0.479	2.410	1.261	1.911	10/1/14	19:34	-1011	1249	2
6.147	0.503	2.405	1.260	1.909	10/1/14	19:37	-973	1267	2
5.962	0.483	2.422	1.259	1.924	10/1/14	19:41	-920	1278	3
6.244	0.550	2.399	1.256	1.910	10/1/14	19:45	-920	1304	3
6.180	**0.292**								
6.076	**0.339**								
5.893	0.499	2.474	1.275	1.941	10/1/14	20:15	-1263	419	-7
5.823	0.460	2.450	1.264	1.938	10/1/14	20:19	-1264	398	-7
5.704	0.444	2.441	1.256	1.943	10/1/14	20:23	-1286	356	-7
5.780	0.477	2.427	1.251	1.941	10/1/14	20:27	-1282	320	-7
5.819	**0.160**								
13.863	0.442	2.595	1.238	2.095	10/1/14	20:36	1036	-282	-10
13.906	0.532	2.530	1.236	2.048	10/1/14	20:41	1032	-311	-10
19.426	0.531	2.469	1.309	1.886	10/1/14	20:53	1041	-339	-10
19.037	0.555	2.505	1.311	1.911	10/1/14	20:57	1057	-373	-9
19.123	0.444	2.484	1.311	1.894	10/1/14	21:00	1068	-408	-9
19.108	0.507	2.490	1.311	1.899	10/1/14	21:04	1132	-483	-9
19.071	0.500	2.485	1.310	1.897	10/1/14	21:08	1176	-540	-9
19.063	0.554	2.439	1.307	1.865	10/1/14	21:12	1239	-576	-9
13.562	0.434	2.739	1.308	2.094	10/1/14	21:16	1266	-583	-9
13.579	0.394	2.747	1.306	2.104	10/1/14	21:20	1300	-640	-9
13.611	0.477	2.737	1.305	2.097	10/1/14	21:24	1317	-670	-9
19.103	0.469	2.463	1.303	1.891	10/1/14	21:28	1332	-691	-10
5.697	0.457	2.530	1.299	1.947	10/1/14	21:32	-1199	436	-8
5.554	0.504	2.524	1.298	1.944	10/1/14	21:36	-1287	475	-8

5.952	0.489	2.537	1.297	1.956	10/1/14	21:39	-1216	373	-8
5.772	0.535	2.527	1.295	1.951	10/1/14	21:43	-1288	260	-8
5.880	0.659	2.515	1.292	1.947	10/1/14	21:47	-1244	603	-9
5.771	**0.312**								
5.795	**0.239**								
19.451	0.474	2.440	1.289	1.892	10/1/14	21:52	1270	-841	-10
19.030	0.403	2.424	1.287	1.884	10/1/14	21:56	1320	-773	-10
18.890	0.390	2.436	1.285	1.896	10/1/14	22:00	1255	-1017	-10
19.675	0.491	2.422	1.283	1.888	10/1/14	22:04	1224	-1105	-10
19.235	0.544	2.410	1.281	1.881	10/1/14	22:08	1243	-1060	-10
13.663	0.458	2.684	1.280	2.097	10/1/14	22:12	1212	-1128	-10
19.387	0.619	2.282	1.279	1.784	10/1/14	22:17	1364	-1167	-10
19.365	0.511	2.419	1.279	1.892	10/1/14	22:20	1359	-1083	-10
19.298	0.491	2.421	1.276	1.897	10/1/14	22:25	1346	-1028	-9
13.702	0.516	2.683	1.276	2.102	10/1/14	22:28	1191	-1222	-10
5.916	0.568	2.480	1.271	1.952	10/1/14	22:37	-1265	615	-9
6.068	0.452	2.474	1.271	1.946	10/1/14	22:40	-1234	628	-8
5.981	0.486	2.475	1.271	1.947	10/1/14	22:44	-1256	641	-8
5.696	0.530	2.468	1.271	1.942	10/1/14	22:47	-1292	646	-8
5.915	**0.275**								
5.821	**0.324**								
19.688	0.479	2.395	1.267	1.890	10/1/14	22:57	1364	-336	-11
19.203	0.464	2.382	1.266	1.881	10/1/14	23:01	1442	-275	-11
19.452	0.508	2.386	1.265	1.886	10/1/14	23:05	1413	-332	-11
13.688	0.480	2.637	1.265	2.085	10/1/14	23:09	1443	-341	-11
13.812	0.492	2.646	1.260	2.099	10/1/14	23:17	1079	-1324	-11
~~16.092~~	~~0.285~~	~~2.425~~	~~1.260~~	~~1.925~~	~~10/1/14~~	~~23:23~~	~~1008~~	~~-1396~~	~~-10~~
13.798	0.477	2.643	1.259	2.100	10/1/14	23:27	984	-1395	-10
19.291	0.518	2.387	1.256	1.901	10/1/14	23:32	936	-1421	-10
19.210	0.488	2.332	1.255	1.859	10/1/14	23:36	892	-1494	-10
19.280	0.481	2.359	1.254	1.881	10/1/14	23:40	903	-1567	-10
5.769	0.571	2.441	1.253	1.949	10/1/14	23:45	-1208	510	-8
5.797	0.463	2.434	1.252	1.944	10/1/14	23:49	-1234	519	-8
5.911	0.452	2.434	1.251	1.945	10/1/14	23:52	-1208	560	-9
5.989	0.500	2.421	1.250	1.937	10/1/14	23:56	-1194	530	-9
5.847	**0.197**								
5.889	**0.225**								
19.436	0.490	2.515	1.326	1.896	10/2/14	0:10	860	-1670	-5
13.422	0.487	2.810	1.328	2.116	10/2/14	0:14	851	-1696	-5
13.664	0.473	2.798	1.329	2.106	10/2/14	0:18	842	-1719	-4
13.955	0.474	2.779	1.327	2.094	10/2/14	0:26	1612	1285	-6
19.292	0.517	2.502	1.327	1.886	10/2/14	0:30	1600	1253	-6
~~23.909~~	~~0.349~~	~~1.535~~	~~1.327~~	~~1.157~~	~~10/2/14~~	~~0:34~~	~~1599~~	~~1195~~	~~-5~~
19.161	0.564	2.513	1.326	1.895	10/2/14	0:39	1577	1116	-5

19.512	0.563	2.505	1.324	1.891	10/2/14	0:44	1674	987	-6
19.453	0.530	2.495	1.326	1.882	10/2/14	0:49	1675	858	-6
13.806	0.468	2.767	1.326	2.086	10/2/14	0:52	1695	840	-5
13.872	0.475	2.757	1.326	2.080	10/2/14	0:56	1719	825	-5
14.183	0.481	2.752	1.323	2.080	10/2/14	1:03	1853	407	-6
5.856	0.492	2.564	1.321	1.941	10/2/14	1:10	-1189	571	-18
5.628	0.501	2.575	1.321	1.949	10/2/14	1:13	-1173	586	-17
5.667	0.628	2.575	1.322	1.948	10/2/14	1:17	-1182	614	-17
5.920	0.440	2.566	1.321	1.943	10/2/14	1:21	-1181	635	-17
5.785	**0.259**								
5.812	**0.238**								
13.783	0.433	2.782	1.321	2.107	10/2/14	1:27	1859	352	-18
13.355	0.479	2.773	1.322	2.098	10/2/14	1:31	1880	337	-18
13.823	0.465	2.757	1.321	2.087	10/2/14	1:35	1881	287	-18
13.816	0.503	2.728	1.319	2.067	10/2/14	1:40	1890	242	-19
19.166	0.514	2.475	1.319	1.876	10/2/14	1:44	1863	210	-18
19.074	0.450	2.513	1.317	1.908	10/2/14	1:50	2000	46	-18
13.719	0.507	2.766	1.316	2.103	10/2/14	1:54	1995	5	-18
13.991	0.489	2.739	1.312	2.087	10/2/14	2:01	2189	-140	-19
13.800	0.429	2.760	1.312	2.103	10/2/14	2:05	2229	-226	-18
18.871	0.565	2.485	1.311	1.895	10/2/14	2:09	2187	-248	-18
5.428	0.488	2.558	1.307	1.957	10/2/14	2:15	-1335	505	-16
5.555	0.461	2.544	1.306	1.948	10/2/14	2:19	-1341	530	-15
5.678	0.436	2.545	1.304	1.951	10/2/14	2:22	-1345	548	-16
5.668	0.371	2.535	1.304	1.945	10/2/14	2:26	-1352	590	-15
5.551	**0.245**								
5.695	**0.316**								
19.164	0.527	2.480	1.302	1.905	10/2/14	2:32	2226	-283	-21
19.256	0.501	2.467	1.299	1.899	10/2/14	2:36	2417	-65	-21
19.585	0.554	2.449	1.297	1.889	10/2/14	2:40	2300	-31	-21
19.373	0.458	2.455	1.297	1.893	10/2/14	2:44	2336	-84	-21
13.939	0.480	2.671	1.296	2.062	10/2/14	2:48	2292	0	-21
19.082	0.469	2.470	1.297	1.904	10/2/14	2:53	2393	-242	-21
19.316	0.522	2.474	1.298	1.906	10/2/14	2:56	2437	-310	-20
13.933	0.475	2.658	1.297	2.050	10/2/14	3:00	2464	-313	-20
13.701	0.452	2.700	1.295	2.084	10/2/14	3:04	2499	-270	-20
13.796	0.483	2.695	1.292	2.085	10/2/14	3:09	2578	-267	-21
13.842	0.509	2.708	1.291	2.098	10/2/14	3:13	2558	-313	-21
19.107	0.450	2.432	1.289	1.887	10/2/14	3:17	2549	-339	-21
5.719	0.497	2.506	1.287	1.948	10/2/14	3:22	-1361	638	-18
5.880	0.482	2.502	1.285	1.947	10/2/14	3:26	-1370	668	-18
5.922	0.518	2.500	1.285	1.946	10/2/14	3:29	-1391	679	-18
5.716	0.453	2.504	1.285	1.949	10/2/14	3:33	-1367	697	-18
5.791	**0.203**								

5.666	**0.348**								
6.163	0.537	2.475	1.273	1.945	10/2/14	3:59	290	183	12
5.981	0.471	2.485	1.271	1.954	10/2/14	4:03	316	186	13
5.985	0.584	2.477	1.271	1.948	10/2/14	4:07	340	200	13
6.006	0.481	2.458	1.271	1.933	10/2/14	4:10	370	201	12
6.060	**0.190**								
11.671	0.502	2.647	1.267	2.089	10/2/14	4:19	-258	-829	11
11.805	0.490	2.654	1.265	2.098	10/2/14	4:23	-170	-841	12
11.811	0.490	2.632	1.258	2.093	10/2/14	4:27	-235	-879	12
17.175	0.425	2.381	1.261	1.889	10/2/14	4:31	-240	-902	12
17.209	0.556	2.386	1.262	1.891	10/2/14	4:36	-41	-1062	11
11.854	0.434	2.642	1.258	2.100	10/2/14	4:43	-710	-927	12
11.871	0.516	2.641	1.258	2.099	10/2/14	4:48	-761	-961	12
17.082	0.460	2.379	1.257	1.892	10/2/14	4:52	-790	-971	13
17.388	0.497	2.371	1.257	1.885	10/2/14	4:57	-856	-1092	13
17.015	0.511	2.399	1.257	1.908	10/2/14	5:01	-211	-309	12
17.269	0.508	2.387	1.258	1.897	10/2/14	5:06	-118	-272	13
17.374	0.526	2.387	1.260	1.896	10/2/14	5:10	-442	-206	14
6.085	0.508	2.463	1.261	1.954	10/2/14	5:15	243	296	13
6.074	0.583	2.462	1.262	1.951	10/2/14	5:18	263	323	13
6.178	0.507	2.459	1.263	1.948	10/2/14	5:22	296	319	13
6.226	0.452	2.462	1.261	1.953	10/2/14	5:26	305	299	12
6.130	**0.137**								
6.096	**0.183**								
11.825	0.558	2.666	1.271	2.098	10/2/14	5:35	-406	-2010	9
11.694	0.489	2.684	1.283	2.092	10/2/14	5:39	-438	-2029	10
16.783	0.500	2.444	1.288	1.897	10/2/14	5:43	-441	-2058	11
11.683	0.476	2.710	1.289	2.102	10/2/14	5:47	-473	-2061	11
11.869	0.469	2.684	1.283	2.092	10/2/14	5:52	-590	-2147	10
17.356	0.539	2.413	1.279	1.887	10/2/14	5:55	-616	-2145	11
17.289	0.524	2.408	1.276	1.888	10/2/14	5:59	-643	-2109	11
11.937	0.505	2.663	1.271	2.095	10/2/14	6:04	-430	-2171	11
16.827	0.565	2.395	1.268	1.889	10/2/14	6:08	-425	-2185	10
17.200	0.525	2.389	1.263	1.892	10/2/14	6:12	-458	-2310	10
17.217	0.596	2.385	1.263	1.888	10/2/14	6:16	-340	-2263	10
17.412	0.514	2.371	1.262	1.879	10/2/14	6:20	-305	-2254	10
6.082	0.512	2.442	1.257	1.943	10/2/14	6:26	332	306	17
6.175	0.431	2.425	1.255	1.933	10/2/14	6:29	339	343	17
6.392	0.523	2.439	1.255	1.944	10/2/14	6:33	359	330	17
6.283	0.501	2.430	1.256	1.936	10/2/14	6:37	368	312	17
6.203	**0.269**								
6.176	**0.220**								

17.096	0.514	2.348	1.254	1.872	10/2/14	6:43	-197	-2218	14
17.439	0.498	2.357	1.253	1.881	10/2/14	6:48	-130	-2370	13
11.873	0.463	2.602	1.252	2.079	10/2/14	6:53	-113	-2390	13
11.930	0.449	2.608	1.252	2.084	10/2/14	6:56	-9	-2447	13
11.870	0.524	2.781	1.338	2.078	10/2/14	7:09	-129	-2664	14
16.953	0.525	2.553	1.343	1.902	10/2/14	7:13	-158	-2670	15
16.936	0.596	2.551	1.345	1.897	10/2/14	7:17	-218	-2685	15
11.770	0.425	2.793	1.346	2.075	10/2/14	7:27	-1659	-4738	12
11.603	0.473	2.812	1.347	2.088	10/2/14	7:31	-1650	-4537	13
17.124	0.585	2.543	1.348	1.887	10/2/14	7:35	-1632	-4518	14
16.830	0.433	2.533	1.347	1.880	10/2/14	7:40	-1585	-4360	14
17.156	0.516	2.546	1.348	1.888	10/2/14	7:44	-1762	-4714	13
5.771	0.480	2.637	1.348	1.957	10/2/14	7:51	220	344	19
5.666	0.496	2.638	1.348	1.956	10/2/14	7:55	218	375	21
5.574	0.491	2.643	1.348	1.961	10/2/14	8:00	194	378	19
5.758	0.481	2.629	1.349	1.949	10/2/14	8:03	193	356	19
5.692	**0.183**								
5.963	**0.616**								

DTFA-Y	Mass	C-bkg	H1-bkg	Sample Name	16OH/16O	Mg/(Ca+Mg)	Fe/(Fe+Mg)
-4	898853	-2618332	-50299	Zero/	1.184E-04		
7	898853	-2618332	-50299	Zero/	1.130E-04		
-4	898853	-2618332	-50299	Zero/	1.142E-04		
-6	898853	-2618332	-50299	Zero/	1.121E-04		
-7	898853	-2618332	-50299	Zero/	1.138E-04		
-4	898853	-2618332	-50299	Zero/	1.093E-04		
7	898853	-2618332	-50299	Zero/	9.431E-05		
7	898853	-2618332	-50299	Zero/	9.668E-05		
1	898853	-2618332	-50299	Zero/	9.854E-05		
0	898853	-2618332	-50299	Zero/	9.416E-05		
4	898853	-2618332	-50299	Zero/	1.432E-04		
5	898853	-2618332	-50299	Zero/	1.459E-04		
~~8~~	~~898853~~	~~-2618332~~	~~-50299~~	~~Zero/~~	~~1.552E-04~~		
6	898853	-2618332	-50299	Zero/	1.446E-04		
5	898853	-2618332	-50299	Zero/	1.515E-04		
-2	898853	-2618332	-50299	Zero/	1.114E-04		
-3	898853	-2618332	-50299	Zero/	1.110E-04		
-2	898853	-2618332	-50299	Zero/	1.145E-04		
-3	898853	-2618332	-50299	Zero/	1.129E-04		
5	898853	-2618332	-50299	Zero/	1.216E-03		
4	898853	-2618332	-50299	Zero/	1.131E-03		
~~-1~~	~~898853~~	~~-2618332~~	~~-50299~~	~~Zero/~~	~~1.105E-03~~		
-5	898853	-2618332	-50299	Zero/	1.121E-03		
-4	898853	-2618332	-50299	Zero/	1.108E-03		
0	898853	-2618332	-50299	Zero/	1.143E-03		
3	898853	-2618332	-50299	Zero/	1.205E-03		
5	898853	-2618332	-50299	Zero/	1.305E-03		
4	898853	-2618332	-50299	Zero/	1.156E-03		
5	898853	-2618332	-50299	Zero/	1.219E-03		

3	898853	-2618332	-50299	Zero/	1.119E-03
2	898853	-2618332	-50299	Zero/	1.107E-03
-4	898853	-2618332	-50299	Zero/	1.123E-03
-6	898853	-2618332	-50299	Zero/	1.071E-03
5	898853	-2618332	-50299	Zero/	2.749E-03
-5	898853	-2603284	-50668	Zero/	6.341E-04
-6	898853	-2603284	-50668	Zero/	6.423E-04
-12	898853	-2603284	-50668	Zero/	6.041E-04
-15	898853	-2603284	-50668	Zero/	5.902E-04
-5	898853	-2603284	-50668	Zero/	1.430E-03
-5	898853	-2603284	-50668	Zero/	1.461E-03
-5	898853	-2603284	-50668	Zero/	1.471E-03
-6	898853	-2603284	-50668	Zero/	1.464E-03
-11	898853	-2603284	-50668	Zero/	1.172E-03
-11	898853	-2603284	-50668	Zero/	1.140E-03
-10	898853	-2603284	-50668	Zero/	1.181E-03
-10	898853	-2603284	-50668	Zero/	1.172E-03
-11	898853	-2603284	-50668	Zero/	1.171E-03
-9	898853	-2603284	-50668	Zero/	1.196E-03
-7	898853	-2603284	-50668	Zero/	1.189E-03
-5	898853	-2603284	-50668	Zero/	1.224E-03
-5	898853	-2603284	-50668	Zero/	1.207E-03
-4	898853	-2603284	-50668	Zero/	1.201E-03
-8	898853	-2603284	-50668	uwg2/	1.586E-03
-8	898853	-2603284	-50668	uwg2/	1.585E-03
-8	898853	-2603284	-50668	uwg2/	1.582E-03
-8	898853	-2603284	-50668	uwg2/	1.553E-03
-2	898853	-2603284	-50668	g6/	1.632E-03
-1	898853	-2603284	-50668	g6/	1.274E-03
-1	898853	-2603284	-50668	g6/	1.229E-03
-2	898853	-2603284	-50668	g6/	1.267E-03
-2	898853	-2603284	-50668	g6/	1.291E-03
-1	898853	-2603284	-50668	g6/	1.236E-03
-1	898853	-2603284	-50668	g6/	1.200E-03
-2	898853	-2603284	-50668	g6/	1.220E-03
-3	898853	-2603284	-50668	g6/	1.291E-03

-3	898853	-2603284	-50668	g6/	1.243E-03
-9	898853	-2603284	-50668	uwg2/	1.564E-03
-8	898853	-2603284	-50668	uwg2/	1.568E-03
-7	898853	-2603284	-50668	uwg2/	1.605E-03
-7	898853	-2603284	-50668	uwg2/	1.590E-03
-4	898853	-2603284	-50668	uwg2/	1.277E-03
-5	898853	-2603284	-50668	uwg2/	1.236E-03
-5	898853	-2603284	-50668	uwg2/	1.216E-03
-7	898853	-2603284	-50668	uwg2/	1.259E-03
-7	898853	-2603284	-50668	uwg2/	1.217E-03
-7	898853	-2603284	-50668	uwg2/	1.182E-03
-9	898853	-2603284	-50668	uwg2/	1.238E-03
-9	898853	-2603284	-50668	uwg2/	1.238E-03
-8	898853	-2603284	-50668	uwg2/	1.214E-03
-10	898853	-2603284	-50668	uwg2/	1.203E-03
-10	898853	-2603284	-50668	uwg2/	1.167E-03
-10	898853	-2603284	-50668	uwg2/	1.157E-03
-9	898853	-2603284	-50668	uwg2/	1.546E-03
-9	898853	-2603284	-50668	uwg2/	1.520E-03
-9	898853	-2603284	-50668	uwg2/	1.509E-03
-9	898853	-2603284	-50668	uwg2/	1.515E-03
-9	898853	-2603284	-50668	g6/	1.262E-03
-9	898853	-2603284	-50668	g6/	1.193E-03
-8	898853	-2603284	-50668	g6/	1.167E-03
-9	898853	-2603284	-50668	uwg2/	1.290E-03
-10	898853	-2603284	-50668	uwg2/	1.225E-03
-9	898853	-2603284	-50668	uwg2/	1.277E-03
-9	898853	-2603284	-50668	uwg2/	1.207E-03
-8	898853	-2603284	-50668	uwg2/	1.200E-03
-8	898853	-2603284	-50668	uwg2/	1.169E-03
-9	898853	-2603284	-50668	uwg2/	1.172E-03
-9	898853	-2603284	-50668	uwg2/	1.176E-03
-10	898853	-2603284	-50668	uwg2/	1.507E-03
-9	898853	-2603284	-50668	uwg2/	1.515E-03
-9	898853	-2603284	-50668	uwg2/	1.498E-03
-8	898853	-2603284	-50668	uwg2/	1.493E-03
-12	898853	-2603284	-50668	uwg2/	1.288E-03
-12	898853	-2603284	-50668	uwg2/	1.215E-03
-6	898853	-2603284	-50668	uwg2/	1.137E-03
-5	898853	-2603284	-50668	uwg2/	1.128E-03

-7	898853	-2603284	-50668	uwg2/	1.138E-03
-8	898853	-2603284	-50668	uwg2/	1.149E-03
-14	898853	-2603284	-50668	uwg2/	1.208E-03
-13	898853	-2603284	-50668	uwg2/	1.200E-03
-13	898853	-2603284	-50668	uwg2/	1.206E-03
-13	898853	-2603284	-50668	uwg2/	1.160E-03
-11	898853	-2603284	-50668	uwg2/	1.497E-03
-11	898853	-2603284	-50668	uwg2/	1.481E-03
-9	898853	-2603284	-50668	uwg2/	1.449E-03
-9	898853	-2603284	-50668	uwg2/	1.447E-03

-15	898853	-2603284	-50668	uwg2/	1.158E-03
-15	898853	-2603284	-50668	uwg2/	1.102E-03
-15	898853	-2603284	-50668	uwg2/	1.123E-03
-15	898853	-2603284	-50668	uwg2/	1.123E-03
-33	898853	-2603284	-50668	uwg2/	1.440E-03
-35	898853	-2603284	-50668	uwg2/	8.386E-04
-26	898853	-2603284	-50668	uwg2/	8.913E-04
-28	898853	-2603284	-50668	uwg2/	8.615E-04
-22	898853	-2603284	-50668	uwg2/	8.989E-04
-22	898853	-2603284	-50668	uwg2/	8.763E-04
-22	898853	-2603284	-50668	uwg2/	9.574E-04
-20	898853	-2603284	-50668	uwg2/	9.209E-04
-22	898853	-2603284	-50668	uwg2/	9.270E-04
-26	898853	-2603284	-50668	uwg2/	8.836E-04
-23	898853	-2603284	-50668	uwg2/	9.198E-04
-23	898853	-2603284	-50668	uwg2/	9.390E-04
-16	898853	-2603284	-50668	ugw2/	1.199E-03
-16	898853	-2603284	-50668	ugw2/	1.178E-03
-17	898853	-2603284	-50668	ugw2/	1.154E-03
-17	898853	-2603284	-50668	ugw2/	1.174E-03

-14	898853	-2603284	-50668	zero/	3.120E-04
-14	898853	-2603284	-50668	zero/	3.074E-04
-14	898853	-2603284	-50668	zero/	2.862E-04
-15	898853	-2603284	-50668	zero/	2.845E-04

-14	898853	-2603284	-50668	99V-3\G1.	2.680E-04
-14	898853	-2603284	-50668	99V-3\G1.	2.607E-04
-16	898853	-2603284	-50668	99V-3\G3.	2.783E-04
-16	898853	-2603284	-50668	99V-3\G3.	2.677E-04
-18	898853	-2603284	-50668	99V-3\G7.	2.621E-04
-18	898853	-2603284	-50668	99V-3\G7.	2.527E-04
-32	898853	-2603284	-50668	99V-3\G8.	2.413E-04
-35	898853	-2603284	-50668	99V-3\G8.	2.367E-04
-13	898853	-2603284	-50668	99V-3\G1(	2.424E-04
-13	898853	-2603284	-50668	99V-3\G1(	2.266E-04
-13	898853	-2603284	-50668	99V-3\G1	2.477E-04
-14	898853	-2603284	-50668	99V-3\G1	2.358E-04
-17	898853	-2603284	-50668	zero/	2.597E-04
-16	898853	-2603284	-50668	zero/	2.544E-04
-17	898853	-2603284	-50668	zero/	2.553E-04
-17	898853	-2603284	-50668	zero/	2.611E-04
-14	898853	-2603284	-50668	99V-3\G1	2.310E-04
-14	898853	-2603284	-50668	99V-3\G1	2.304E-04
-15	898853	-2603284	-50668	99V-3\G1	2.332E-04
-15	898853	-2603284	-50668	99V-3\G1	2.267E-04
-51	898853	-2603284	-50668	99V-3\G8.	2.264E-04
-63	898853	-2603284	-50668	99V-3\G8.	2.093E-04
-17	898853	-2603284	-50668	zero/	2.562E-04
-17	898853	-2603284	-50668	zero/	2.743E-04
-17	898853	-2603284	-50668	zero/	2.755E-04
-17	898853	-2603284	-50668	zero/	2.624E-04

-1	898853	-2603284	-50668	zero/	9.608E-04
-2	898853	-2603284	-50668	zero/	9.700E-04
-2	898853	-2603284	-50668	zero/	9.838E-04
-2	898853	-2603284	-50668	zero/	9.934E-04
-1	898853	-2603284	-50668	zero/	5.754E-03
-2	898853	-2603284	-50668	zero/	6.204E-03
-1	898853	-2603284	-50668	zero/	6.031E-03
-2	898853	-2603284	-50668	zero/	6.228E-03
-2	898853	-2603284	-50668	zero/	5.509E-03
-1	898853	-2603284	-50668	zero/	5.451E-03
-1	898853	-2603284	-50668	zero/	4.308E-03

-1	898853	-2603284	-50668	zero/	5.521E-03
-1	898853	-2603284	-50668	zero/	6.125E-03
-2	898853	-2603284	-50668	zero/	6.250E-03
-2	898853	-2603284	-50668	zero/	4.180E-03
-2	898853	-2603284	-50668	zero/	4.253E-03
-3	898853	-2603284	-50668	zero/	1.129E-03
-3	898853	-2603284	-50668	zero/	1.106E-03
-2	898853	-2603284	-50668	zero/	1.099E-03
-2	898853	-2603284	-50668	zero/	1.109E-03
3	898853	-2603284	-50668	zero/	8.947E-04
3	898853	-2603284	-50668	zero/	9.082E-04
2	898853	-2603284	-50668	zero/	9.515E-04
3	898853	-2603284	-50668	zero/	9.137E-04
2	898853	-2603284	-50668	zero/	9.045E-04
2	898853	-2603284	-50668	zero/	9.215E-04
2	898853	-2603284	-50668	zero/	9.056E-04
-1	898853	-2603284	-50668	zero/	9.054E-04
-1	898853	-2603284	-50668	zero/	8.960E-04
-1	898853	-2603284	-50668	zero/	8.918E-04
-4	898853	-2603284	-50668	zero/	1.166E-03
-3	898853	-2603284	-50668	zero/	1.145E-03
-4	898853	-2603284	-50668	zero/	1.131E-03
-4	898853	-2603284	-50668	zero/	1.145E-03
2	898853	-2603284	-50668	zero/	9.511E-04
1	898853	-2603284	-50668	zero/	9.718E-04
1	898853	-2603284	-50668	zero/	9.169E-04
2	898853	-2603284	-50668	zero/	9.686E-04
2	898853	-2603284	-50668	zero/	9.504E-04
2	898853	-2603284	-50668	zero/	9.060E-04
-4	898853	-2603284	-50668	uwg2/	1.128E-03
-4	898853	-2603284	-50668	uwg2/	1.119E-03
-4	898853	-2603284	-50668	uwg2/	1.115E-03
-4	898853	-2603284	-50668	uwg2/	1.118E-03
-2	898853	-2603284	-50668	uwg2/	6.728E-04
0	898853	-2603284	-50668	uwg2/	6.966E-04
0	898853	-2603284	-50668	uwg2/	7.187E-04
-1	898853	-2603284	-50668	uwg2/	7.152E-04

-1	898853	-2603284	-50668	uwg2/	7.111E-04
0	898853	-2603284	-50668	uwg2/	7.378E-04
-11	898853	-2603284	-50668	uwg2/	7.031E-04
-10	898853	-2603284	-50668	uwg2/	6.820E-04
-8	898853	-2603284	-50668	uwg2/	6.882E-04
-8	898853	-2603284	-50668	uwg2/	6.931E-04
-5	898853	-2603284	-50668	uwg2/	9.346E-04
-5	898853	-2603284	-50668	uwg2/	9.364E-04
-5	898853	-2603284	-50668	uwg2/	9.609E-04
-5	898853	-2603284	-50668	uwg2/	9.776E-04
-4	898853	-2603284	-50668	uwg2/	9.444E-04
-3	898853	-2603284	-50668	uwg2/	9.352E-04
-4	898853	-2603284	-50668	uwg2/	9.305E-04
-4	898853	-2603284	-50668	uwg2/	9.236E-04
-4	898853	-2603284	-50668	88-8 g2/	7.150E-04
-5	898853	-2603284	-50668	88-8 g2/	7.324E-04
-4	898853	-2603284	-50668	88-8 g2/	7.203E-04
-5	898853	-2603284	-50668	88-8 g2/	7.281E-04
-3	898853	-2603284	-50668	88-8 g2/	7.539E-04
-3	898853	-2603284	-50668	88-8 g2/	7.289E-04
-3	898853	-2603284	-50668	88-8 g2/	7.408E-04
-3	898853	-2603284	-50668	88-8 g2/	7.251E-04
-3	898853	-2603284	-50668	88-8 g2/	7.493E-04
-4	898853	-2603284	-50668	88-8 g2/	1.151E-03
-5	898853	-2603284	-50668	88-8 g2/	8.077E-04
-2	898853	-2603284	-50668	88-8 g2/	7.639E-04
-4	898853	-2603284	-50668	uwg2/	9.895E-04
-4	898853	-2603284	-50668	uwg2/	9.677E-04
-4	898853	-2603284	-50668	uwg2/	9.789E-04
-4	898853	-2603284	-50668	uwg2/	9.734E-04
-8	898853	-2603284	-50668	94I9-2(5)-4	8.077E-04
-8	898853	-2603284	-50668	94I9-2(5)-4	7.894E-04
-5	898853	-2603284	-50668	94I9-2(5)-4	7.786E-04
-5	898853	-2603284	-50668	94I9-2(5)-4	8.374E-04
-5	898853	-2603284	-50668	94I9-2(5)-4	7.661E-04
-5	898853	-2603284	-50668	94I9-2(5)-4	7.470E-04
-5	898853	-2603284	-50668	94I9-2(5)-4	8.229E-04
-5	898853	-2603284	-50668	94I9-2(5)-4	7.536E-04
0	898853	-2603284	-50668	94I9-2(5)-4	8.023E-04

-1	898853	-2603284	-50668	94I9-2(5)-4	8.189E-04
-1	898853	-2603284	-50668	94I9-2(5)-4	8.087E-04
-1	898853	-2603284	-50668	94I9-2(5)-4	7.817E-04
-4	898853	-2603284	-50668	uwg2/	1.001E-03
-4	898853	-2603284	-50668	uwg2/	9.877E-04
-4	898853	-2603284	-50668	uwg2/	9.958E-04
-4	898853	-2603284	-50668	uwg2/	9.805E-04
-1	898853	-2603284	-50668	94I9-2(5)-7	8.763E-04
0	898853	-2603284	-50668	94I9-2(5)-7	8.462E-04
1	898853	-2603284	-50668	94I9-2(5)-7	8.496E-04
1	898853	-2603284	-50668	94I9-2(5)-7	8.741E-04
1	898853	-2603284	-50668	94I9-2(5)-7	8.303E-04
0	898853	-2603284	-50668	94I9-2(5)-7	8.333E-04
-11	898853	-2603284	-50668	uwg2/	7.948E-04
-10	898853	-2603284	-50668	uwg2/	8.354E-04
-12	898853	-2603284	-50668	uwg2/	8.432E-04
-12	898853	-2603284	-50668	uwg2/	8.149E-04
-11	898853	-2603284	-50668	uwg2/	7.664E-04
-11	898853	-2603284	-50668	uwg2/	7.920E-04
-5	898853	-2603284	-50668	uwg2/	1.014E-03
-5	898853	-2603284	-50668	uwg2/	9.934E-04
-5	898853	-2603284	-50668	uwg2/	1.005E-03
-5	898853	-2603284	-50668	uwg2/	1.038E-03
-11	898853	-2603284	-50668	94I9-2(4)-7	8.198E-04
-12	898853	-2603284	-50668	94I9-2(4)-7	7.703E-04
-12	898853	-2603284	-50668	94I9-2(4)-7	7.822E-04
-9	898853	-2603284	-50668	94I9-2(4)-7	8.126E-04
-9	898853	-2603284	-50668	94I9-2(4)-7	7.938E-04
-8	898853	-2603284	-50668	94I9-2(4)-7	8.141E-04
-8	898853	-2603284	-50668	94I9-2(4)-7	8.125E-04
-9	898853	-2603284	-50668	94I9-2(4)-7	7.937E-04
-2	898853	-2603284	-50668	94I9-2(4)-7	7.571E-04
-1	898853	-2603284	-50668	94I9-2(4)-7	7.442E-04
-1	898853	-2603284	-50668	94I9-2(4)-7	7.493E-04
-3	898853	-2603284	-50668	94I9-2(4)-7	8.082E-04
-7	898853	-2603284	-50668	uwg2/	1.000E-03
-6	898853	-2603284	-50668	uwg2/	9.975E-04
-6	898853	-2603284	-50668	uwg2/	1.021E-03
-6	898853	-2603284	-50668	uwg2/	1.002E-03

-5	898853	-2603284	-50668	uwg2/	9.890E-04
-5	898853	-2603284	-50668	uwg2/	9.670E-04
-4	898853	-2603284	-50668	uwg2/	9.934E-04
-4	898853	-2603284	-50668	uwg2/	9.676E-04
-7	898853	-2603284	-50668	94I9-2(4)-	7.711E-04
-7	898853	-2603284	-50668	94I9-2(4)-	8.126E-04
-7	898853	-2603284	-50668	94I9-2(4)-	7.525E-04
-8	898853	-2603284	-50668	94I9-2(4)-	7.515E-04
-6	898853	-2603284	-50668	94I9-2(4)-	7.494E-04
-6	898853	-2603284	-50668	94I9-2(4)-	7.374E-04
-7	898853	-2603284	-50668	94I9-2(4)-	7.423E-04
-1	898853	-2603284	-50668	94I9-2(4)-	7.386E-04
-1	898853	-2603284	-50668	94I9-2(4)-	7.064E-04
-5	898853	-2603284	-50668	94I9-2(4)-	7.528E-04
-7	898853	-2603284	-50668	94I9-2(4)-	7.306E-04
-7	898853	-2603284	-50668	94I9-2(4)-	7.584E-04
-7	898853	-2603284	-50668	94I9-2(4)-	7.407E-04
-7	898853	-2603284	-50668	94I9-2(4)-	7.384E-04
-5	898853	-2603284	-50668	uwg2/	9.552E-04
-4	898853	-2603284	-50668	uwg2/	9.504E-04
-4	898853	-2603284	-50668	uwg2/	9.517E-04
-4	898853	-2603284	-50668	uwg2/	9.566E-04

-13	898853	-2603284	-50668	94I-9-2b\z	1.913E-04
-15	898853	-2603284	-50668	94I-9-2b\z	1.890E-04
-14	898853	-2603284	-50668	94I-9-2b\z	1.786E-04
-15	898853	-2603284	-50668	94I-9-2b\z	1.768E-04
-15	898853	-2603284	-50668	94I-9-2b\G	1.977E-04
-15	898853	-2603284	-50668	94I-9-2b\G	1.812E-04
-15	898853	-2603284	-50668	94I-9-2b\G	2.373E-04
-9	898853	-2603284	-50668	94I-9-2b\G	2.058E-04
-7	898853	-2603284	-50668	94I-9-2b\G	6.168E-04
-9	898853	-2603284	-50668	94I-9-2b\G	1.931E-04
-19	898853	-2603284	-50668	94I-9-2b\G	1.690E-04
-19	898853	-2603284	-50668	94I-9-2b\G	2.242E-04
-19	898853	-2603284	-50668	94I-9-2b\G	2.117E-04
-19	898853	-2603284	-50668	94I-9-2b\G	1.722E-04
-19	898853	-2603284	-50668	94I-9-2b\G	2.084E-04

-16	898853	-2603284	-50668	94I-9-2b\z	1.553E-04
-15	898853	-2603284	-50668	94I-9-2b\z	1.586E-04
-16	898853	-2603284	-50668	94I-9-2b\z	1.583E-04
-15	898853	-2603284	-50668	94I-9-2b\z	1.552E-04
-15	898853	-2603284	-50668	94I-9-2b\z	1.522E-04
-20	898853	-2603284	-50668	94I-9-2b\G	1.582E-04
-20	898853	-2603284	-50668	94I-9-2b\G	1.875E-04
-20	898853	-2603284	-50668	94I-9-2b\G	1.522E-04
-20	898853	-2603284	-50668	94I-9-2b\G	2.045E-04
-20	898853	-2603284	-50668	94I-9-2b\G	2.021E-04
-16	898853	-2603284	-50668	94I-9-2b\G	2.509E-04
-16	898853	-2603284	-50668	94I-9-2b\G	1.771E-04
-8	898853	-2603284	-50668	94I-9-2b\G	1.662E-04
-8	898853	-2603284	-50668	94I-9-2b\G	2.218E-04
-6	898853	-2603284	-50668	94I-9-2b\G	1.805E-04
-15	898853	-2603284	-50668	94I-9-2b\z	1.489E-04
-16	898853	-2603284	-50668	94I-9-2b\z	1.469E-04
-16	898853	-2603284	-50668	94I-9-2b\z	1.446E-04
-16	898853	-2603284	-50668	94I-9-2b\z	1.452E-04

-3	898853	-2619564	-50651		1.335E-03
-7	898853	-2619564	-50651		1.370E-03
-6	898853	-2619564	-50651		1.417E-03
-3	898853	-2619564	-50651		1.487E-03
0	898853	-2619564	-50651		1.470E-03
0	898853	-2619564	-50651	94I-9-2b\z	1.446E-03
1	898853	-2619564	-50651	94I-9-2b\z	1.436E-03
2	898853	-2619564	-50651	94I-9-2b\z	1.468E-03
-15	898853	-2619564	-50651	94I-9-2b\z	1.632E-03
-21	898853	-2619564	-50651	94I-9-2b\z	1.675E-03
-25	898853	-2619564	-50651	94I-9-2b\z	1.666E-03
-41	898853	-2619564	-50651	94I-9-2b\z	1.659E-03
-5	898853	-2619564	-50651	94I-9-2b\z	1.612E-03

-7	898853	-2619564	-50651	94I-9-2b\z	1.617E-03		
-9	898853	-2619564	-50651	94I-9-2b\z	2.187E-03		
-8	898853	-2619564	-50651	94I-9-2b\z	1.590E-03		

-16	898853	-2619564	-50651	zero/	5.793E-04		
-16	898853	-2619564	-50651	zero/	5.383E-04		
-16	898853	-2619564	-50651	zero/	5.196E-04		
-16	898853	-2619564	-50651	zero/	5.194E-04		
-16	898853	-2619564	-50651	99V-3\G1.	4.625E-04	**0.0**	**0.0**
-16	898853	-2619564	-50651	99V-3\G1.	4.600E-04	**0.0**	**0.0**
-16	898853	-2619564	-50651	99V-3\G1.	4.318E-04	**0.0**	**0.0**
-17	898853	-2619564	-50651	99V-3\G1.	4.428E-04	**0.0**	**0.0**
-17	898853	-2619564	-50651	99V-3\G1.	3.938E-04	**0.5**	**0.0**
-17	898853	-2619564	-50651	99V-3\G1.	3.925E-04	**0.5**	**0.0**
-18	898853	-2619564	-50651	99V-3\G1.	3.885E-04	**0.5**	**0.0**
-17	898853	-2619564	-50651	99V-3\G1.	3.803E-04	**0.5**	**0.0**
-18	898853	-2619564	-50651	99V-3\G1.	3.777E-04	**0.5**	**0.0**
-18	898853	-2619564	-50651	99V-3\G1.	3.736E-04	**0.5**	**0.0**
-18	898853	-2619564	-50651	99V-3\G1.	3.743E-04	**0.5**	**0.0**
-17	898853	-2619564	-50651	Carb Stan	4.430E-04		
-16	898853	-2619564	-50651	Carb Stan	4.410E-04		
-17	898853	-2619564	-50651	Carb Stan	4.349E-04		
-17	898853	-2619564	-50651	Carb Stan	4.452E-04		
-18	898853	-2619564	-50651	T1/	3.707E-04	**0.5**	**0.0**
-19	898853	-2619564	-50651	T1/	3.543E-04	**0.5**	**0.0**
-6	898853	-2619564	-50651	T1/	3.526E-04	**0.5**	**0.0**
-18	898853	-2619564	-50651	T1/	3.600E-04	**0.5**	**0.0**
-19	898853	-2619564	-50651	T1/	3.559E-04	**0.5**	**0.0**
-19	898853	-2619564	-50651	T1/	3.568E-04	**0.5**	**0.0**
~~-31~~	~~898853~~	~~-2619564~~	~~-50651~~	~~99V-3\G8.~~	~~1.999E-04~~		
-30	898853	-2619564	-50651	99V-3\G8.	4.798E-04	**0.0**	**0.0**
-29	898853	-2619564	-50651	99V-3\G8.	8.375E-04	**0.0**	**0.0**
-29	898853	-2619564	-50651	99V-3\G8.	3.091E-04	**0.5**	**0.0**
-16	898853	-2619564	-50651	Carb Stan	4.153E-04		
-17	898853	-2619564	-50651	Carb Stan	4.296E-04		
-16	898853	-2619564	-50651	Carb Stan	4.403E-04		
-17	898853	-2619564	-50651	Carb Stan	4.211E-04		

-28	898853	-2619564	-50651	99V-3\G8.	3.296E-04	**0.0**	**0.0**
-17	898853	-2619564	-50651	99V-3\G8.	3.371E-04	**0.0**	**0.0**
-28	898853	-2619564	-50651	99V-3\G8.	3.434E-04	**0.0**	**0.0**
-23	898853	-2619564	-50651	99V-3\G8.	3.082E-04	**0.5**	**0.0**
-28	898853	-2619564	-50651	99V-3\G8.	3.014E-04	**0.5**	**0.0**
-27	898853	-2619564	-50651	99V-3\G8.	2.967E-04	**0.5**	**0.0**
-26	898853	-2619564	-50651	99V-3\G8.	3.011E-04	**0.5**	**0.0**
-26	898853	-2619564	-50651	99V-3\G8.	3.129E-04	**0.5**	**0.0**
-26	898853	-2619564	-50651	99V-3\G8.	3.108E-04	**0.5**	**0.0**
-26	898853	-2619564	-50651	99V-3\G8.	3.026E-04	**0.5**	**0.0**
-17	898853	-2619564	-50651	Carb Stan	4.174E-04		
-17	898853	-2619564	-50651	Carb Stan	7.103E-04		
-16	898853	-2619564	-50651	Carb Stan	7.716E-04		
-17	898853	-2619564	-50651	Carb Stan	4.317E-04		
-17	898853	-2619564	-50651	Carb Stan	3.760E-04		
-26	898853	-2619564	-50651	T2/	3.199E-04	**0.5**	**0.0**
-26	898853	-2619564	-50651	T2/	2.974E-04	**0.5**	**0.0**
-26	898853	-2619564	-50651	T2/	3.021E-04	**0.5**	**0.0**
~~-26~~	~~898853~~	~~-2619564~~	~~-50651~~	~~T2/~~	~~3.859E-03~~	~~**0.5**~~	~~**0.0**~~
-26	898853	-2619564	-50651	T2/	2.917E-04	**0.5**	**0.0**
-26	898853	-2619564	-50651	T2/	3.331E-04	**0.5**	**0.0**
-32	898853	-2619564	-50651	99V-3\G8.	4.252E-04	**0.0**	**0.0**
-35	898853	-2619564	-50651	99V-3\G8.	3.087E-04	**0.0**	**0.0**
-26	898853	-2619564	-50651	T2/	3.004E-04	**0.5**	**0.0**
-26	898853	-2619564	-50651	T2/	2.924E-04	**0.5**	**0.0**
-17	898853	-2619564	-50651	Carb Stan	3.701E-04		
-17	898853	-2619564	-50651	Carb Stan	3.642E-04		
-17	898853	-2619564	-50651	Carb Stan	3.633E-04		
-17	898853	-2619564	-50651	Carb Stan	3.674E-04		
-16	898853	-2619564	-50651	Carb Stan	3.718E-04		
-26	898853	-2619564	-50651	T2/	2.977E-04	**0.5**	**0.0**
-27	898853	-2619564	-50651	T2/	3.035E-04	**0.5**	**0.0**
-25	898853	-2619564	-50651	T2/	3.915E-04	**0.5**	**0.0**
-26	898853	-2619564	-50651	T2/	3.178E-04	**0.5**	**0.0**
-26	898853	-2619564	-50651	T2/	2.853E-04	**0.5**	**0.0**
-26	898853	-2619564	-50651	T2/	2.875E-04	**0.5**	**0.0**
-26	898853	-2619564	-50651	T2/	3.058E-04	**0.5**	**0.0**
-24	898853	-2619564	-50651	T2/	2.890E-04	**0.5**	**0.0**
-25	898853	-2619564	-50651	T2/	2.880E-04	**0.5**	**0.0**

~~-24~~	~~898853~~	~~-2619564~~	~~-50651~~	~~T2/~~	~~1.990E-03~~	~~**0.0**~~	~~**0.0**~~
-24	898853	-2619564	-50651	T2/	3.635E-04	**0.0**	**0.0**
-24	898853	-2619564	-50651	T2/	3.257E-04	**0.0**	**0.0**
-17	898853	-2619564	-50651	Carb Stan	3.672E-04		
-17	898853	-2619564	-50651	Carb Stan	3.620E-04		
-17	898853	-2619564	-50651	Carb Stan	3.700E-04		
-17	898853	-2619564	-50651	Carb Stan	3.892E-04		
-21	898853	-2619564	-50651	99V-3\G7.	2.950E-04	**0.5**	**0.0**
-21	898853	-2619564	-50651	99V-3\G7.	2.861E-04	**0.5**	**0.0**
-21	898853	-2619564	-50651	99V-3\G7.	3.299E-04	**0.5**	**0.0**
-21	898853	-2619564	-50651	99V-3\G7.	3.129E-04	**0.5**	**0.0**
-21	898853	-2619564	-50651	99V-3\G7.	2.872E-04	**0.5**	**0.0**
-22	898853	-2619564	-50651	99V-3\G7.	2.920E-04	**0.5**	**0.0**
-21	898853	-2619564	-50651	99V-3\G7.	2.917E-04	**0.5**	**0.0**
-18	898853	-2619564	-50651	Carb Stan	3.580E-04		
-18	898853	-2619564	-50651	Carb Stan	4.338E-04		
-18	898853	-2619564	-50651	Carb Stan	3.739E-04		
-18	898853	-2619564	-50651	Carb Stan	3.554E-04		
-8	898853	-2619564	-50651	zero/	3.653E-04		
-9	898853	-2619564	-50651	zero/	1.799E-03		
-10	898853	-2619564	-50651	zero/	3.861E-04		
-10	898853	-2619564	-50651	zero/	3.569E-04		
-10	898853	-2619564	-50651	zero/	2.974E-04	**0.5**	**0.0**
-9	898853	-2619564	-50651	zero/	5.324E-04	**0.5**	**0.0**
-7	898853	-2619564	-50651	zero/	3.465E-04	**0.0**	**0.0**
-9	898853	-2619564	-50651	zero/	3.060E-04	**0.0**	**0.0**
-9	898853	-2619564	-50651	zero/	3.207E-04	**0.0**	**0.0**
-8	898853	-2619564	-50651	zero/	3.177E-04	**0.0**	**0.0**
-8	898853	-2619564	-50651	zero/	3.087E-04	**0.0**	**0.0**
-8	898853	-2619564	-50651	zero/	7.113E-04	**0.0**	**0.0**
-9	898853	-2619564	-50651	zero/	2.779E-04	**0.5**	**0.0**
-9	898853	-2619564	-50651	zero/	2.754E-04	**0.5**	**0.0**
-8	898853	-2619564	-50651	zero/	3.230E-04	**0.5**	**0.0**
-9	898853	-2619564	-50651	zero/	3.301E-04	**0.0**	**0.0**
-11	898853	-2619564	-50651	zero/	3.154E-04		
-10	898853	-2619564	-50651	zero/	6.158E-04		

-11	898853	-2619564	-50651	zero/	3.290E-04		
-10	898853	-2619564	-50651	zero/	9.070E-04		
-11	898853	-2619564	-50651	zero/	3.624E-04		
-9	898853	-2619564	-50651	T1/	3.112E-04	**0.0**	**0.0**
-9	898853	-2619564	-50651	T1/	3.123E-04	**0.0**	**0.0**
-9	898853	-2619564	-50651	T1/	3.069E-04	**0.0**	**0.0**
-9	898853	-2619564	-50651	T1/	3.278E-04	**0.0**	**0.0**
-9	898853	-2619564	-50651	T1/	5.682E-04	**0.0**	**0.0**
-9	898853	-2619564	-50651	T1/	2.746E-04	**0.5**	**0.0**
-10	898853	-2619564	-50651	T1/	2.034E-03	**0.0**	**0.0**
-9	898853	-2619564	-50651	T1/	3.055E-04	**0.0**	**0.0**
-9	898853	-2619564	-50651	T1/	3.105E-04	**0.0**	**0.0**
-10	898853	-2619564	-50651	T1/	2.708E-04	**0.5**	**0.0**
-11	898853	-2619564	-50651	zero/	3.427E-04		
-12	898853	-2619564	-50651	zero/	3.373E-04		
-12	898853	-2619564	-50651	zero/	3.449E-04		
-11	898853	-2619564	-50651	zero/	7.095E-04		
-9	898853	-2619564	-50651	T1/	3.157E-04	**0.0**	**0.0**
-10	898853	-2619564	-50651	T1/	5.564E-04	**0.0**	**0.0**
-10	898853	-2619564	-50651	T1/	3.145E-04	**0.0**	**0.0**
-10	898853	-2619564	-50651	T1/	2.748E-04	**0.5**	**0.0**
-10	898853	-2619564	-50651	T1/	3.887E-04	**0.5**	**0.0**
~~-10~~	~~898853~~	~~-2619564~~	~~-50651~~	~~T1/~~	~~1.433E-03~~	~~**0.5**~~	~~**0.0**~~
-10	898853	-2619564	-50651	T1/	2.725E-04	**0.5**	**0.0**
-9	898853	-2619564	-50651	T1/	3.107E-04	**0.0**	**0.0**
-9	898853	-2619564	-50651	T1/	7.727E-04	**0.0**	**0.0**
-9	898853	-2619564	-50651	T1/	3.021E-04	**0.0**	**0.0**
-12	898853	-2619564	-50651	zero/	3.176E-04		
-12	898853	-2619564	-50651	zero/	3.323E-04		
-12	898853	-2619564	-50651	zero/	3.973E-04		
-12	898853	-2619564	-50651	zero/	3.219E-04		
-9	898853	-2619564	-50651	T1/	2.962E-04	**0.0**	**0.0**
-9	898853	-2619564	-50651	T1/	2.502E-04	**0.5**	**0.0**
-10	898853	-2619564	-50651	T1/	2.530E-04	**0.5**	**0.0**
-10	898853	-2619564	-50651	T1/	2.610E-04	**0.5**	**0.0**
-10	898853	-2619564	-50651	T1/	2.847E-04	**0.0**	**0.0**
~~-10~~	~~898853~~	~~-2619564~~	~~-50651~~	~~T1/~~	~~1.395E-04~~	~~**0.0**~~	~~**0.0**~~
-9	898853	-2619564	-50651	T1/	2.848E-04	**0.0**	**0.0**

-10	898853	-2619564	-50651	T1/	2.908E-04	**0.0**	**0.0**
-10	898853	-2619564	-50651	T1/	2.843E-04	**0.0**	**0.0**
-10	898853	-2619564	-50651	T1/	2.534E-04	**0.5**	**0.0**
-11	898853	-2619564	-50651	T1/	2.507E-04	**0.5**	**0.0**
-10	898853	-2619564	-50651	T1/	1.053E-03	**0.5**	**0.0**
-9	898853	-2619564	-50651	zero/	3.344E-04		
-10	898853	-2619564	-50651	zero/	3.013E-04		
-10	898853	-2619564	-50651	zero/	3.096E-04		
-10	898853	-2619564	-50651	zero/	3.618E-04		
-8	898853	-2619564	-50651	T2-9/	3.856E-04	**0.5**	**0.0**
-8	898853	-2619564	-50651	T2-9/	2.457E-04	**0.5**	**0.0**
-8	898853	-2619564	-50651	T2-9/	5.131E-04	**0.5**	**0.0**
-9	898853	-2619564	-50651	T2-9/	3.481E-04	**0.5**	**0.0**
-8	898853	-2619564	-50651	T2-9/	6.029E-04	**0.0**	**0.0**
-7	898853	-2619564	-50651	T2-9/	2.763E-04	**0.0**	**0.0**
-8	898853	-2619564	-50651	T2-9/	2.591E-04	**0.5**	**0.0**
-8	898853	-2619564	-50651	T2-9/	2.495E-04	**0.5**	**0.0**
-8	898853	-2619564	-50651	T2-9/	2.438E-04	**0.5**	**0.0**
-8	898853	-2619564	-50651	T2-9/	3.934E-04	**0.0**	**0.0**
-9	898853	-2619564	-50651	zero/	2.903E-04		
-9	898853	-2619564	-50651	zero/	3.297E-04		
-9	898853	-2619564	-50651	zero/	2.933E-04		
-10	898853	-2619564	-50651	zero/	3.608E-04		
-7	898853	-2619564	-50651	T2-19/	2.813E-04	**0.0**	**0.0**
-9	898853	-2619564	-50651	T2-19/	2.946E-04	**0.0**	**0.0**
-9	898853	-2619564	-50651	T2-19/	2.694E-04	**0.0**	**0.0**
-8	898853	-2619564	-50651	T2-19/	2.743E-04	**0.0**	**0.0**
-9	898853	-2619564	-50651	T2-19/	3.992E-04	**0.5**	**0.0**
-8	898853	-2619564	-50651	T2-19/	4.516E-04	**0.0**	**0.0**
-8	898853	-2619564	-50651	T2-19/	2.727E-04	**0.0**	**0.0**
-8	898853	-2619564	-50651	T2-19/	5.744E-04	**0.5**	**0.0**
-9	898853	-2619564	-50651	T2-19/	2.433E-04	**0.5**	**0.0**
-8	898853	-2619564	-50651	T2-19/	2.449E-04	**0.5**	**0.0**
-8	898853	-2619564	-50651	T2-19/	2.509E-04	**0.5**	**0.0**
-8	898853	-2619564	-50651	T2-19/	2.723E-04	**0.0**	**0.0**
-10	898853	-2619564	-50651	zero/	2.880E-04		
-10	898853	-2619564	-50651	zero/	2.856E-04		
-10	898853	-2619564	-50651	zero/	2.838E-04		
-10	898853	-2619564	-50651	zero/	2.880E-04		

3	898853	-2619564	-50651	zero/	5.454E-04		
2	898853	-2619564	-50651	zero/	4.805E-04		
1	898853	-2619564	-50651	zero/	4.766E-04		
1	898853	-2619564	-50651	zero/	4.882E-04		
-1	898853	-2619564	-50651	zero/	4.453E-04	**0.5**	**0.0**
0	898853	-2619564	-50651	zero/	4.537E-04	**0.5**	**0.0**
0	898853	-2619564	-50651	zero/	4.390E-04	**0.5**	**0.0**
0	898853	-2619564	-50651	zero/	4.966E-04	**0.0**	**0.0**
-1	898853	-2619564	-50651	zero/	4.729E-04	**0.0**	**0.0**
-1	898853	-2619564	-50651	zero/	4.496E-04	**0.5**	**0.0**
-2	898853	-2619564	-50651	zero/	4.480E-04	**0.5**	**0.0**
-1	898853	-2619564	-50651	zero/	4.841E-04	**0.0**	**0.0**
-2	898853	-2619564	-50651	zero/	4.704E-04	**0.0**	**0.0**
1	898853	-2619564	-50651	zero/	5.279E-04	**0.0**	**0.0**
1	898853	-2619564	-50651	zero/	4.809E-04	**0.0**	**0.0**
2	898853	-2619564	-50651	zero/	4.886E-04	**0.0**	**0.0**
0	898853	-2619564	-50651	zero/	5.944E-04		
0	898853	-2619564	-50651	zero/	4.921E-04		
-1	898853	-2619564	-50651	zero/	4.927E-04		
0	898853	-2619564	-50651	zero/	5.986E-04		
-4	898853	-2619564	-50651	gr 1/	5.196E-04	**0.5**	**0.0**
-4	898853	-2619564	-50651	gr 1/	4.468E-04	**0.5**	**0.0**
-4	898853	-2619564	-50651	gr 1/	4.689E-04	**0.0**	**0.0**
-4	898853	-2619564	-50651	gr 1/	4.289E-04	**0.5**	**0.0**
-3	898853	-2619564	-50651	gr 1/	4.285E-04	**0.5**	**0.0**
-3	898853	-2619564	-50651	gr 1/	4.702E-04	**0.0**	**0.0**
-3	898853	-2619564	-50651	gr 1/	4.667E-04	**0.0**	**0.0**
-4	898853	-2619564	-50651	gr 1/	4.301E-04	**0.5**	**0.0**
-4	898853	-2619564	-50651	gr 1/	4.793E-04	**0.0**	**0.0**
-3	898853	-2619564	-50651	gr 1/	4.628E-04	**0.0**	**0.0**
-3	898853	-2619564	-50651	gr 1/	4.696E-04	**0.0**	**0.0**
-4	898853	-2619564	-50651	gr 1/	4.662E-04	**0.0**	**0.0**
1	898853	-2619564	-50651	zero/	5.023E-04		
-1	898853	-2619564	-50651	zero/	4.908E-04		
-1	898853	-2619564	-50651	zero/	4.883E-04		
-1	898853	-2619564	-50651	zero/	4.971E-04		

-4	898853	-2619564	-50651	gr 6/	5.527E-03	**0.0**	**0.0**
-4	898853	-2619564	-50651	gr 6/	4.691E-04	**0.0**	**0.0**
-4	898853	-2619564	-50651	gr 6/	4.365E-04	**0.5**	**0.0**
-5	898853	-2619564	-50651	gr 6/	4.334E-04	**0.5**	**0.0**
-4	898853	-2619564	-50651	gr 6/	4.176E-04	**0.5**	**0.0**
-3	898853	-2619564	-50651	gr 6/	5.534E-04	**0.0**	**0.0**
-3	898853	-2619564	-50651	gr 6/	4.303E-04	**0.0**	**0.0**
-11	898853	-2619564	-50651	gr 6/	3.793E-04	**0.5**	**0.0**
-10	898853	-2619564	-50651	gr 6/	3.693E-04	**0.5**	**0.0**
-10	898853	-2619564	-50651	gr 6/	4.067E-04	**0.0**	**0.0**
-9	898853	-2619564	-50651	gr 6/	4.051E-04	**0.0**	**0.0**
-11	898853	-2619564	-50651	gr 6/	4.029E-04	**0.0**	**0.0**
1	898853	-2619564	-50651	zero/	4.622E-04		
13	898853	-2619564	-50651	zero/	4.582E-04		
1	898853	-2619564	-50651	zero/	4.562E-04		
2	898853	-2619564	-50651	zero/	4.957E-04		

Note	Phase

bad grain

bad area of grain

test analysis

fo	1
fo	2
fo	3
fo	4
fo	5
fo	6
fo	7
fo	8
fo	9
fo	10

fo	11
fo	12
fo	13
fo	14
fo	15
fo	16
fo	17
fo	18
fo	19

fo	20
fo	21
fo	22
fo	23
fo	24
fo	25
fo	26
fo	27
fo	28
fo	29
fo	30
fo	31
fo	32
fo	33
fo	34
fo	35
fo	36
fo	37
fo	38
fo	39
fo	40
fo	41
fo	42
fo	43
fo	44
fo	45
fo	46
fo	47

fo	48
fo	49
fo	50
fo	51
fo	52
fo	53

fo	54
fo	55
fo	56
fo	57
fo	58
fo	59
fo	60
fo	61
fo	62
fo	63
fo	64
fo	65

fo	66
fo	67
fo	68
fo	69
fo	70
fo	71
fo	72
fo	73
fo	74
fo	75
fo	76
fo	77

fo	78
fo	79
fo	80
fo	81
fo	82
fo	83

fo	84
fo	85
fo	86
fo	87
fo	88
fo	89
fo	90

fo	91
fo	92
fo	93
fo	94
fo	95
fo	96
fo	97
fo	98
fo	99
fo	100
fo	101
fo	102
fo	103
fo	104
fo	105
fo	106
fo	107
fo	108
fo	109
fo	110
fo	111
fo	112
fo	113
fo	114
fo	115

fo	116
fo	117
fo	118
fo	119
fo	120
fo	121

fo	122
fo	123
fo	124
fo	125
fo	126
fo	127
fo	128
fo	129
fo	130
fo	131
fo	132
fo	133

fo	134
fo	135
fo	136
fo	137
fo	138
fo	139
fo	140
fo	141
fo	142

fo	143
fo	144
fo	145
fo	146
fo	147
fo	148
fo	149
fo	150
fo	151
fo	152
fo	153
fo	154
fo	155
fo	156
fo	157
fo	158
fo	159
fo	160
fo	161
fo	162
fo	163
fo	164
fo	165
fo	166
fo	167
fo	168
fo	169

fo	170
fo	171
fo	172
fo	173
fo	174
fo	175
fo	176
fo	177
fo	178
fo	179
fo	180
fo	181
fo	182
fo	183

fo	184
fo	185
fo	186
fo	187
fo	188
fo	189
fo	190
fo	191
fo	192
fo	193
fo	194

fo	195
fo	196
fo	197
fo	198
fo	199
fo	200
fo	201
fo	202
fo	203
fo	204

	cal	1
	cal	2
	cal	3
	cal	4
	dol	5
	dol	6
	dol	7
	dol	8
	dol	9
	dol	10
	dol	11
	dol	12
	dol	13
	dol	14
	dol	15
	dol	16
	dol	17
~~not calcite~~		~~18~~
	cal	19
	cal	20
	dol	21

	cal	22
	cal	23
	cal	24
	dol	25
	dol	26
	dol	27
	dol	28
	dol	29
	dol	30
	dol	31
	dol	32
	dol	33
	dol	34
~~**crack**~~	~~dol~~	~~35~~
	dol	36
	dol	37
	cal	38
	cal	39
	dol	40
	dol	41
	dol	42
	dol	43
	dol	44
	dol	45
	dol	46
	dol	47
	dol	48
	dol	49
	dol	50

~~grain boundary~~	~~cal~~	~~51~~
	cal	52
	cal	53
	dol	54
	dol	55
	dol	56
	dol	57
	dol	58
	dol	59
	dol	60
	dol	61
	dol	62
	cal	63
	cal	64
	cal	65
	cal	66
	cal	67
	cal	68
	dol	69
	dol	70
	dol	71
	cal	72

	cal	73
	cal	74
	cal	75
	cal	76
	cal	77
	dol	78
	cal	79
	cal	80
	cal	81
	dol	82
	cal	83
	cal	84
	cal	85
	dol	86
	dol	87
~~**crack**~~	~~dol~~	~~88~~
	dol	89
	cal	90
	cal	91
	cal	92
	cal	93
	dol	94
	dol	95
	dol	96
	cal	97
~~**inclusion**~~	~~cal~~	~~98~~
	cal	99

cal	100
cal	101
dol	102
dol	103
dol	104
dol	105
dol	106
dol	107
dol	108
cal	109
cal	110
dol	111
dol	112
dol	113
cal	114
cal	115
cal	116
cal	117
cal	118
dol	119
cal	120
cal	121
dol	122
dol	123
dol	124
dol	125
cal	126

dol	127
dol	128
dol	129
cal	130
cal	131
dol	132
dol	133
cal	134
cal	135
cal	136
cal	137
cal	138

dol	139
dol	140
cal	141
dol	142
dol	143
cal	144
cal	145
dol	146
cal	147
cal	148
cal	149
cal	150

cal	151
cal	152
dol	153
dol	154
dol	155
cal	156
cal	157
dol	158
dol	159
cal	160
cal	161
cal	162

	d18O VSMO\	d18Osims	bias	bias rel. to SCOL	Fo#
SCOL	5.32	9.693	4.350	**0**	**89**
NH-Ol	8.9	13.690	4.747	**0.20**	**100**
OR-Ol	5.88	9.586	3.684	**-0.66**	**60**

slope	**0.022**
intercept	**-1.966**

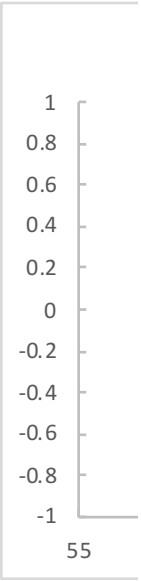

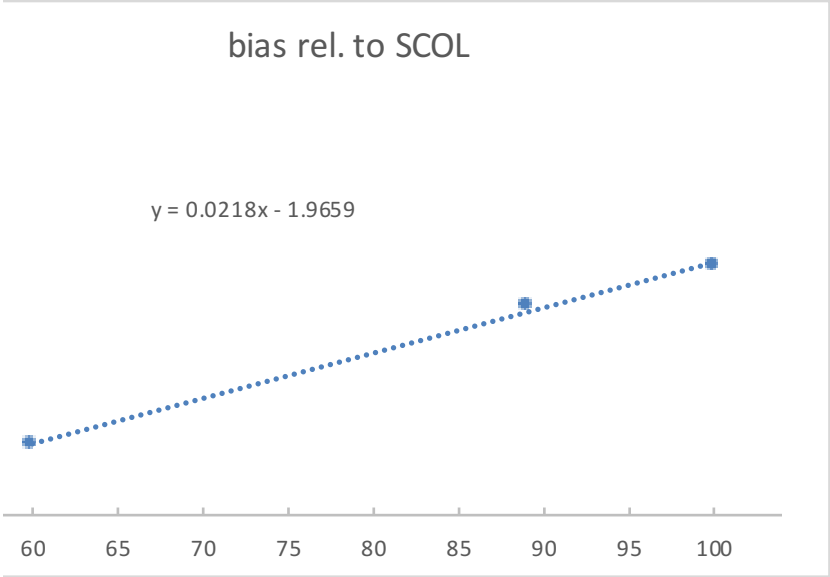
bias rel. to SCOL
y = 0.0218x - 1.9659
60
65
70
75
80
85
90
95
100

File	Comment	$\delta^{18}O$ ‰ VSMOW	2SD (ext.)	Mass Bias (‰)
	WI-STD-18			
20151019@1.asc	WI-STD-18 SCOL energy slit=5eV			
20151019@2.asc	WI-STD-18 SCOL			
20151019@3.asc	WI-STD-18 SCOL			
20151019@4.asc	WI-STD-18 SCOL Cs-Res=162			
20151019@5.asc	WI-STD-18 SCOL			
	average and 2SD			
20151019@6.asc	WI-STD-18 HN-OI g3			
20151019@7.asc	WI-STD-18 HN-OI g1			
20151019@8.asc	WI-STD-18 HN-OI g2 Cs-Res=163			
20151019@9.asc	WI-STD-18 HN-OI g4			
	average and 2SD	**8.90**		**4.75**
	bias relative to SCOL			**0.40**
	bias rel. to UWG-2			**1.85**
20151019@10.as	WI-STD-18 OR-OI g37			
20151019@11.as	WI-STD-18 OR-OI g36			
20151019@12.as	WI-STD-18 OR-OI g35			
20151019@13.as	WI-STD-18 OR-OI g34			
	average and 2SD	**5.88**		**3.68**
	bias relative to SCOL			**-0.66**
	bias rel. to UWG-2			**0.79**
20151019@14.as	WI-STD-18 SCOL			
20151019@15.as	WI-STD-18 SCOL Cs-Res=164			
20151019@16.as	WI-STD-18 SCOL			
20151019@17.as	WI-STD-18 SCOL			
	average and 2SD			
	bracket average and 2SD	**5.32**		**4.35**
	bias rel. to UWG-2			**1.45**

	Fo#	rel to UWG-2
SCOL	89	1.45
HN-OI	100	1.85
OR-OI	60	0.79

slope	0.026
intercept	-0.773

	E-Gun HV 9997=>9998			
20151020@18.as	WI-STD-18 SCOL			
20151020@19.as				
20151020@20.as	WI-STD-18 SCOL			
20151020@21.as	WI-STD-18 SCOL Cs-Res=167			
	average and 2SD	**5.32**		**4.16**
20151020@22.as	WI-STD-18 HN-OI g3	**8.90**		**4.33**

20151020@23.as	WI-STD-18 OR-OI g37	**5.88**		**3.98**
20151020@24.as	WI-STD-18 HN-OI g2 Cs-Res=168	**8.90**		**4.61**
	9-2bo			
20151020@25.as	9-2bo-UWG2			
20151020@26.as	9-2bo-UWG2			
20151020@27.as	9-2bo-UWG2			
20151020@28.as	9-2bo-UWG2			
	average and 2SD			
20151020@29.as	9-2bo-g9_6	**14.96**	**0.27**	4.67
20151020@30.as	9-2bo-g9_7 Cs-Res=169	**15.18**	**0.27**	4.67
20151020@31.as	9-2bo-g9_8	**16.35**	**0.27**	4.67
20151020@32.as	9-2bo-g9_9	**16.76**	**0.27**	4.67
20151020@33.as	9-2bo-g9_10	**16.36**	**0.27**	4.67
20151020@34.as	9-2bo-g9_11	**16.65**	**0.27**	4.67
20151020@35.as	9-2bo-g9_12 Cs-Res=170	**16.50**	**0.27**	4.67
20151020@36.as	9-2bo-g9_13	**15.88**	**0.27**	4.67
20151020@37.as	9-2bo-g9_14	**15.76**	**0.27**	4.67
20151020@38.as	9-2bo-g9_15	**14.85**	**0.27**	4.67
20151020@39.as	9-2bo-UWG2			
20151020@40.as	9-2bo-UWG2			
20151020@41.as	9-2bo-UWG2			
20151020@42.as	9-2bo-UWG2 Cs-Res=171			
	average and 2SD			
	bracket average and 2SD	**5.80**		**2.89**
20151020@43.as	9-2bo-g9_16	**14.68**	**0.19**	4.62
20151020@44.as	9-2bo-g9_17	**16.72**	**0.19**	4.62
20151020@45.as	9-2bo-g9_18	**15.33**	**0.19**	4.62
20151020@46.as	9-2bo-g9_19	**16.53**	**0.19**	4.62
20151020@47.as	9-2bo-g9_20	**15.79**	**0.19**	4.62
20151020@48.as	9-2bo-g9_20	**15.50**	**0.19**	4.62
20151020@49.as	9-2bo-g9_21 Cs-Res=172	**15.43**	**0.19**	4.62
20151020@50.as	9-2bo-g9_22	**16.73**	**0.19**	4.62
20151020@51.as	9-2bo-g9_23	**16.72**	**0.19**	4.62
20151020@52.as	9-2bo-g9_24	**16.64**	**0.19**	4.62
20151020@53.as	9-2bo-UWG2			
20151020@54.as	9-2bo-UWG2 Cs-Res=173			
20151020@55.as	9-2bo-UWG2			
20151020@56.as	9-2bo-UWG2 Cs-Res=175			
	average and 2SD			
	bracket average and 2SD	**5.80**		**2.84**
20151020@57.as	9-2bo-g9_25	**14.81**	**0.21**	4.66
20151020@58.as	9-2bo-g9_26	**15.49**	**0.21**	4.66
20151020@59.as	9-2bo-g9_27 Cs-Res=176	**15.32**	**0.21**	4.66
20151020@60.as	9-2bo-g9_28	**15.12**	**0.21**	4.66

20151020@61.as	9-2bo-g9_29	**15.05**	**0.21**	4.66
20151020@62.as	9-2bo-g9_30	**15.01**	**0.21**	4.66
20151020@63.as	9-2bo-g9_31	**14.85**	**0.21**	4.66
20151020@64.as	9-2bo-g9_32	**15.53**	**0.21**	4.66
20151020@65.as	9-2bo-g9_33	**14.73**	**0.21**	4.66
20151020@66.as	9-2bo-g9_34	**14.98**	**0.21**	4.66
20151020@67.as	9-2bo-UWG2 Cs-Res=177			
20151020@68.as	9-2bo-UWG2			
20151020@69.as	9-2bo-UWG2			
20151020@70.as	9-2bo-UWG2			
	average and 2SD			
	bracket average and 2SD	**5.80**		**2.88**
	WI-STD-74			
20151020@71.as	WI-STD-74 UWG-2 g1			
20151020@72.as	WI-STD-74 UWG-2 g1			
20151020@73.as	WI-STD-74 UWG-2 g2			
20151020@74.as	WI-STD-74 UWG-2 g3 Cs-Res=178			
	average and 2SD			
20151020@75.as	WI-STD-74 SCOL g1			
20151020@76.as	WI-STD-74 SCOL g2			
20151020@77.as	WI-STD-74 SCOL g2			
20151020@78.as	WI-STD-74 SCOL g1			
	average and 2SD	**5.32**		**4.19**
	bias rel. to UWG-2			**1.45**
20151020@79.as	WI-STD-74 UWG-2 g1			
20151020@80.as	WI-STD-74 UWG-2 g2			
20151020@81.as	WI-STD-74 UWG-2 g3			
20151020@82.as	WI-STD-74 UWG-2 g1			
	average and 2SD			
	bracket average and 2SD	**5.80**		**2.74**
	2ccn			
20151020@83.as	2ccn-UWG2			
20151020@84.as	2ccn-UWG2			
20151020@85.as	2ccn-UWG2			
20151020@86.as	2ccn-UWG2			
	average and 2SD			
20151020@87.as	2ccn-g12_1	**15.54**	**0.32**	4.56
20151020@88.as	2ccn-g12_2	**16.88**	**0.32**	4.56
20151020@89.as	2ccn-g12_3	**16.04**	**0.32**	4.56
20151020@90.as	2ccn-g12_4	**17.52**	**0.32**	4.56
20151020@91.as	2ccn-g12_5 Cs-Res=180	**17.08**	**0.32**	4.56
20151020@92.as	2ccn-g12_6	**17.04**	**0.32**	4.56
20151020@93.as	2ccn-g13_1	**15.64**	**0.32**	4.56
20151020@94.as	2ccn-g13_2	**16.89**	**0.32**	4.56

~~20151020@95.as~~	~~2ccn-g13_3~~	~~**11.86**~~	~~**0.32**~~	~~4.56~~
20151020@96.as	2ccn-g13_4	**16.77**	**0.32**	4.56
20151020@97.as	2ccn-UWG2			
20151020@98.as	2ccn-UWG2			
20151020@99.as	2ccn-UWG2			
20151020@100.a	2ccn-UWG2 Cs-Res=181			
	average and 2SD			
	bracket average and 2SD	**5.80**		**2.78**
20151020@101.a	2ccn-g1_1	**16.63**	**0.24**	4.41
~~20151020@102.a~~	~~2ccn-g1_2~~	~~**12.99**~~	~~**0.24**~~	~~4.41~~
20151020@103.a	2ccn-g7_1	**15.58**	**0.24**	4.41
20151020@104.a	2ccn-g7_2	**15.48**	**0.24**	4.41
20151020@105.a	2ccn-g7_3	**16.02**	**0.24**	4.41
20151020@106.a	2ccn-g7_4	**16.12**	**0.24**	4.41
20151020@107.a	2ccn-g8_1	**17.24**	**0.24**	4.41
~~20151020@108.a~~	~~2ccn-g8_2~~	~~**11.58**~~	~~**0.24**~~	~~4.41~~
20151020@109.a	2ccn-g8_3	**17.10**	**0.24**	4.41
20151020@110.a	2ccn-g8_4	**16.99**	**0.24**	4.41
20151020@111.a	2ccn-UWG2			
20151020@112.a	2ccn-UWG2			
20151020@113.a	2ccn-UWG2			
20151020@114.a	2ccn-UWG2			
	average and 2SD			
	bracket average and 2SD	**5.80**		**2.63**
20151020@115.a	2ccn-g9_1	**15.86**	**0.35**	4.41
~~20151020@116.a~~	~~2ccn-g9_2 Cs-Res=182~~	~~**13.34**~~	~~**0.35**~~	~~4.41~~
~~20151020@117.a~~	~~2ccn-g9_3~~	~~**12.03**~~	~~**0.35**~~	~~4.41~~
20151020@118.a	2ccn-g6_1	**15.81**	**0.35**	4.41
20151020@119.a	2ccn-g6_2	**15.43**	**0.35**	4.41
20151020@120.a	2ccn-g6_3	**15.40**	**0.35**	4.41
20151020@121.a	2ccn-g6_4	**17.06**	**0.35**	4.41
20151020@122.a	2ccn-g6_5	**15.65**	**0.35**	4.41
20151020@123.a	2ccn-g6_6	**16.27**	**0.35**	4.41
~~20151020@124.a~~	~~2ccn-g6_7~~	~~**13.98**~~	~~**0.35**~~	~~4.41~~
20151020@125.a	2ccn-UWG2			
20151020@126.a	2ccn-UWG2 Cs-Res=183			
20151020@127.a	2ccn-UWG2			
20151020@128.a	2ccn-UWG2			
	average and 2SD			
	bracket average and 2SD	**5.80**		**2.63**
20151020@129.a	2ccn-g14_1	**15.52**	**0.40**	4.46
20151020@130.a	2ccn-g14_2	**17.74**	**0.40**	4.46
20151020@131.a	2ccn-g14_3	**17.00**	**0.40**	4.46

20151020@132.a	2ccn-g14_4 Cs-Res=184	**17.12**	**0.40**	4.46
20151020@133.a	2ccn-g14_5	**15.56**	**0.40**	4.46
20151020@134.a	2ccn-g14_6	**15.97**	**0.40**	4.46
20151020@135.a	2ccn-g22_1	**17.47**	**0.40**	4.46
20151020@136.a	2ccn-g22_2	**17.28**	**0.40**	4.46
20151020@137.a	2ccn-g22_3	**15.62**	**0.40**	4.46
20151020@138.a	2ccn-g22_4	**17.27**	**0.40**	4.46
20151020@139.a	2ccn-UWG2			
20151020@140.a	2ccn-UWG2			
20151020@141.a	2ccn-UWG2			
20151020@142.a	2ccn-UWG2			
	average and 2SD			
	bracket average and 2SD	**5.80**		**2.68**
	Mass Calibration NMR=1007393		**E-Gun HV: 9998 => 9997**	
	2bbo			
20151020@143.a	2bbo-UWG2			
20151020@144.a	2bbo-UWG2			
20151020@145.a	2bbo-UWG2			
20151020@146.a	2bbo-UWG2			
	average and 2SD			
20151020@147.a	2bbo-g14_1	**16.60**	**0.22**	4.73
20151020@148.a	2bbo-g14_2	**15.46**	**0.22**	4.73
20151020@149.a	2bbo-g14_3	**15.51**	**0.22**	4.73
20151020@150.a	2bbo-g14_4 Cs-Res=186	**16.62**	**0.22**	4.73
20151020@151.a	2bbo-g8_1	**15.67**	**0.22**	4.73
20151020@152.a	2bbo-g8_2	**14.93**	**0.22**	4.73
20151020@153.a	2bbo-g8_3	**16.07**	**0.22**	4.73
20151020@154.a	2bbo-g8_4	**16.80**	**0.22**	4.73
20151020@155.a	2bbo-g8_5	**15.07**	**0.22**	4.73
20151020@156.a	2bbo-g8_6	**16.50**	**0.22**	4.73
20151020@157.a	2bbo-UWG2			
20151020@158.a	2bbo-UWG2			
20151020@159.a	2bbo-UWG2			
20151020@160.a	2bbo-UWG2			
	average and 2SD			
	bracket average and 2SD	**5.80**		**2.95**
20151020@161.a	2bbo-g28_1	**16.11**	**0.32**	4.74
20151020@162.a	2bbo-g28_2	**14.72**	**0.32**	4.74
20151020@163.a	2bbo-g28_3	**16.42**	**0.32**	4.74
20151020@164.a	2bbo-g29_1	**15.45**	**0.32**	4.74
20151020@165.a	2bbo-g29_2	**15.64**	**0.32**	4.74
20151020@166.a	2bbo-g11_1	**15.06**	**0.32**	4.74
20151020@167.a	2bbo-g11_2	**15.77**	**0.32**	4.74
20151020@168.a	2bbo-g21_1 Cs Res=187	**15.67**	**0.32**	4.74
20151020@169.a	2bbo-g21_2	**15.42**	**0.32**	4.74

20151020@170.a 2bbo-g21_3	**15.24**	**0.32**	4.74
20151020@171.a 2bbo-UWG2			
20151020@172.a 2bbo-UWG2			
20151020@173.a 2bbo-UWG2			
20151020@174.a 2bbo-UWG2			
average and 2SD			
bracket average and 2SD	**5.80**		**2.96**
2an			
20151020@175.a 2an-UWG2			
20151020@176.a 2an-UWG2			
20151020@177.a 2an-UWG2			
20151020@178.a 2an-UWG2			
average and 2SD			
20151020@179.a 2an-g1_1	**14.13**	**0.18**	4.82
20151020@180.a 2an-g1_2	**14.07**	**0.18**	4.82
20151020@181.a 2an-g1_3 Cs Res=188	**13.88**	**0.18**	4.82
20151020@182.a 2an-g1_4	**13.98**	**0.18**	4.82
20151020@183.a 2an-g2_1	**15.36**	**0.18**	4.82
20151020@184.a 2an-g2_2	**15.25**	**0.18**	4.82
20151020@185.a 2an-g3_1	**16.14**	**0.18**	4.82
20151020@186.a 2an-g3_2	**14.85**	**0.18**	4.82
20151020@187.a 2an-g3_3	**16.49**	**0.18**	4.82
20151020@188.a 2an-g3_4	**15.01**	**0.18**	4.82
20151020@189.a 2an-UWG2			
20151020@190.a 2an-UWG2			
20151020@191.a 2an-UWG2			
20151020@192.a 2an-UWG2			
average and 2SD			
bracket average and 2SD	**5.80**		**3.04**
20151020@193.a 2an-g4_1 Cs Res=190	**14.35**	**0.21**	4.80
20151020@194.a 2an-g4_2	**14.01**	**0.21**	4.80
20151020@195.a 2an-g5_1	**13.77**	**0.21**	4.80
20151020@196.a 2an-g5_2	**13.81**	**0.21**	4.80
20151020@197.a 2an-g6_1	**15.02**	**0.21**	4.80
20151020@198.a 2an-g6_2	**15.11**	**0.21**	4.80
20151020@199.a 2an-g7_1	**16.06**	**0.21**	4.80
20151020@200.a 2an-g7_2	**16.03**	**0.21**	4.80
20151020@201.a 2an-g7_3	**14.95**	**0.21**	4.80
20151020@202.a 2an-g8_1 Cs Res=191	**15.97**	**0.21**	4.80
20151020@203.a 2an-g8_2	**15.79**	**0.21**	4.80
20151020@204.a 2an-g8_3	**15.72**	**0.21**	4.80
20151020@205.a 2an-UWG2			
20151020@206.a 2an-UWG2			

20151020@207.a	2an-UWG2			
20151020@208.a	2an-UWG2			
	average and 2SD			
	bracket average and 2SD	**5.80**		**3.02**
20151020@209.a	2an-g9_1	**14.94**	**0.20**	4.78
20151020@210.a	2an-g9_2	**14.74**	**0.20**	4.78
20151020@211.a	2an-g10_1	**15.10**	**0.20**	4.78
20151020@212.a	2an-g10_2	**15.10**	**0.20**	4.78
20151020@213.a	2an-g10_3	**15.14**	**0.20**	4.78
20151020@214.a	2an-g10_4	**14.50**	**0.20**	4.78
20151020@215.a	2an-g11_1 Cs Res=192	**14.82**	**0.20**	4.78
20151020@216.a	2an-g11_2	**15.19**	**0.20**	4.78
20151020@217.a	2an-g12_1	**16.16**	**0.20**	4.78
20151020@218.a	2an-g12_2	**15.97**	**0.20**	4.78
20151020@219.a	2an-g13_1	**14.81**	**0.20**	4.78
20151020@220.a	2an-g13_2	**14.85**	**0.20**	4.78
20151020@221.a	2an-UWG2			
20151020@222.a	2an-UWG2			
20151020@223.a	2an-UWG2			
20151020@224.a	2an-UWG2			
	average and 2SD			
	bracket average and 2SD	**5.80**		**3.00**
	2ccn			
20151020@225.a	2ccn-UWG2			
20151020@226.a	2ccn-UWG2			
20151020@227.a	2ccn-UWG2			
20151020@228.a	2ccn-UWG2			
	average and 2SD			
20151020@229.a	2ccn-g12_7	**16.30**	**0.17**	4.54
20151020@230.a	2ccn-g12_8 Cs Res=193	**16.94**	**0.17**	4.54
20151020@231.a	2ccn-g12_9	**17.31**	**0.17**	4.54
20151020@232.a	2ccn-g12_10	**16.90**	**0.17**	4.54
20151020@233.a	2ccn-g12_11	**17.21**	**0.17**	4.54
20151020@234.a	2ccn-g12_12	**17.49**	**0.17**	4.54
20151020@235.a	2ccn-g12_13	**17.33**	**0.17**	4.54
20151020@236.a	2ccn-g12_14	**17.15**	**0.17**	4.54
20151020@237.a	2ccn-g12_15	**17.00**	**0.17**	4.54
20151020@238.a	2ccn-g12_16	**17.07**	**0.17**	4.54
20151020@239.a	2ccn-g12_17	**17.29**	**0.17**	4.54
20151020@240.a	2ccn-g12_18	**17.44**	**0.17**	4.54
20151020@241.a	2ccn-UWG2			
20151020@242.a	2ccn-UWG2			
20151020@243.a	2ccn-UWG2			
20151020@244.a	2ccn-UWG2			

	average and 2SD			
	bracket average and 2SD	**5.80**		**2.75**
20151020@245.a	2ccn-g12_19	**15.83**	**0.20**	4.56
20151020@246.a	2ccn-g12_20 Cs Res=194	**15.73**	**0.20**	4.56
20151020@247.a	2ccn-g12_21	**15.74**	**0.20**	4.56
20151020@248.a	2ccn-g12_22	**15.77**	**0.20**	4.56
20151020@249.a	2ccn-g12_23	**16.87**	**0.20**	4.56
20151020@250.a	2ccn-g12_24	**16.99**	**0.20**	4.56
20151020@251.a	2ccn-g12_25	**17.07**	**0.20**	4.56
20151020@252.a	2ccn-g12_26	**16.98**	**0.20**	4.56
20151020@253.a	2ccn-g12_27	**15.91**	**0.20**	4.56
20151020@254.a	2ccn-g12_28	**16.48**	**0.20**	4.56
20151020@255.a	2ccn-g12_29	**16.89**	**0.20**	4.56
20151020@256.a	2ccn-g12_30	**16.54**	**0.20**	4.56
20151020@257.a	2ccn-g12_UWG2			
20151020@258.a	2ccn-g12_UWG2			
20151020@259.a	2ccn-g12_UWG2			
20151020@260.a	2ccn-g12_UWG2			
	average and 2SD			
	bracket average and 2SD	**5.80**		**2.78**
20151020@261.a	2ccn-g12_31	**15.94**	**0.22**	4.56
20151020@262.a	2ccn-g12_32	**15.68**	**0.22**	4.56
20151020@263.a	2ccn-g12_33	**15.86**	**0.22**	4.56
20151020@264.a	2ccn-g12_34	**16.71**	**0.22**	4.56
20151020@265.a	2ccn-g12_35	**16.82**	**0.22**	4.56
20151020@266.a	2ccn-g12_36	**16.08**	**0.22**	4.56
20151020@267.a	2ccn-g12_37 Cs Res=195	**16.01**	**0.22**	4.56
20151020@268.a	2ccn-g12_38	**15.98**	**0.22**	4.56
20151020@269.a	2ccn-g12_39	**15.88**	**0.22**	4.56
20151020@270.a	2ccn-g12_40	**16.87**	**0.22**	4.56
20151020@271.a	2ccn-g12_41	**16.88**	**0.22**	4.56
20151020@272.a	2ccn-g12_42	**17.20**	**0.22**	4.56
20151020@273.a	2ccn-UWG2			
20151020@274.a	2ccn-UWG2			
20151020@275.a	2ccn-UWG2			
20151020@276.a	2ccn-UWG2			
	average and 2SD			
	bracket average and 2SD	**5.80**		**2.78**
20151020@277.a	2ccn-g22_5	**17.39**	**0.15**	4.57
20151020@278.a	2ccn-g22_6	**17.23**	**0.15**	4.57
20151020@279.a	2ccn-g22_7	**17.27**	**0.15**	4.57
20151020@280.a	2ccn-g22_8	**17.10**	**0.15**	4.57
20151020@281.a	2ccn-g22_9	**17.39**	**0.15**	4.57
20151020@282.a	2ccn-g22_10	**17.24**	**0.15**	4.57

20151020@283.a	2ccn-g22_11	**16.79**	**0.15**	4.57
20151020@284.a	2ccn-g22_12 Cs-Res=196	**15.69**	**0.15**	4.57
20151020@285.a	2ccn-g22_13	**15.80**	**0.15**	4.57
20151020@286.a	2ccn-g22_14	**15.80**	**0.15**	4.57
20151020@287.a	2ccn-g22_15	**16.91**	**0.15**	4.57
20151020@288.a	2ccn-UWG2			
20151020@289.a	2ccn-UWG2			
20151020@290.a	2ccn-UWG2			
20151020@291.a	2ccn-UWG2			
	average and 2SD			
	bracket average and 2SD	**5.80**		**2.78**
	Mass Calibration NMR=1007393			
	FC offset 64sec			
20151021@292.a	2ccn-UWG2			
20151021@293.a	2ccn-UWG2			
20151021@294.a	2ccn-UWG2			
20151021@295.a	2ccn-UWG2			
	average and 2SD			
20151021@296.a	2ccn-g22_16	**17.24**	**0.15**	4.26
20151021@297.a	2ccn-g22_17	**17.34**	**0.15**	4.26
20151021@298.a	2ccn-g22_18	**17.60**	**0.15**	4.26
20151021@299.a	2ccn-g22_19	**16.97**	**0.15**	4.26
20151021@300.a	2ccn-g22_20	**17.15**	**0.15**	4.26
20151021@301.a	2ccn-g22_21	**15.82**	**0.15**	4.26
20151021@302.a	2ccn-g22_22	**15.88**	**0.15**	4.26
20151021@303.a	2ccn-g22_23	**15.65**	**0.15**	4.26
20151021@304.a	2ccn-g22_24	**15.87**	**0.15**	4.26
20151021@305.a	2ccn-g22_25	**15.81**	**0.15**	4.26
20151021@306.a	2ccn-g22_26	**15.89**	**0.15**	4.26
20151021@307.a	2ccn-UWG2			
20151021@308.a	2ccn-UWG2			
20151021@309.a	2ccn-UWG2			
20151021@310.a	2ccn-UWG2			
	average and 2SD			
	bracket average and 2SD	**5.80**		**2.48**
20151021@311.a	2ccn-g14_7	**15.79**	**0.10**	4.28
20151021@312.a	2ccn-g14_8	**17.05**	**0.10**	4.28
20151021@313.a	2ccn-g14_9	**15.68**	**0.10**	4.28
20151021@314.a	2ccn-g14_10	**17.23**	**0.10**	4.28
20151021@315.a	2ccn-g14_11 Cs-Res=197	**16.63**	**0.10**	4.28
20151021@316.a	2ccn-g14_12	**17.01**	**0.10**	4.28
20151021@317.a	2ccn-g14_13	**17.06**	**0.10**	4.28
20151021@318.a	2ccn-g14_14	**16.99**	**0.10**	4.28
20151021@319.a	2ccn-g14_15	**16.14**	**0.10**	4.28
20151021@320.a	2ccn-g14_16	**17.05**	**0.10**	4.28

20151021@321.a	2ccn-g14_17	**17.05**	**0.10**	4.28
20151021@322.a	2ccn-g14_18	**17.48**	**0.10**	4.28
20151021@323.a	2ccn-UWG2			
20151021@324.a	2ccn-UWG2			
20151021@325.a	2ccn-UWG2			
20151021@326.a	2ccn-UWG2			
	average and 2SD			
	bracket average and 2SD	**5.80**		**2.50**
~~20151021@327.a~~	~~2ccn-g14_19~~	~~**11.24**~~	~~**0.20**~~	~~4.30~~
20151021@328.a	2ccn-g14_20	**15.55**	**0.20**	4.30
20151021@329.a	2ccn-g14_21 Cs-Res=198	**15.64**	**0.20**	4.30
20151021@330.a	2ccn-g14_22	**15.73**	**0.20**	4.30
20151021@331.a	2ccn-g14_23	**17.44**	**0.20**	4.30
20151021@332.a	2ccn-g14_24	**16.81**	**0.20**	4.30
20151021@333.a	2ccn-g14_25	**17.58**	**0.20**	4.30
20151021@334.a	2ccn-g14_26	**14.80**	**0.20**	4.30
20151021@335.a	2ccn-g14_27	**17.14**	**0.20**	4.30
20151021@336.a	2ccn-g14_28	**17.03**	**0.20**	4.30
20151021@337.a	2ccn-UWG2			
20151021@338.a	2ccn-UWG2			
20151021@339.a	2ccn-UWG2			
20151021@340.a	2ccn-UWG2			
	average and 2SD			
	bracket average and 2SD	**5.80**		**2.52**
	2bo			
20151021@341.a	2bo-UWG2			
20151021@342.a	2bo-UWG2			
20151021@343.a	2bo-UWG2			
20151021@344.a	2bo-UWG2			
	average and 2SD			
20151021@345.a	2bo-g7_1	**15.64**	**0.26**	4.64
20151021@346.a	2bo-g7_2	**15.65**	**0.26**	4.64
20151021@347.a	2bo-g7_3	**15.23**	**0.26**	4.64
20151021@348.a	2bo-g7_4	**16.02**	**0.26**	4.64
20151021@349.a	2bo-g7_5	**15.74**	**0.26**	4.64
20151021@350.a	2bo-g17_1	**15.55**	**0.26**	4.64
20151021@351.a	2bo-g17_2	**16.68**	**0.26**	4.64
20151021@352.a	2bo-g17_3	**16.93**	**0.26**	4.64
20151021@353.a	2bo-g11_1	**14.17**	**0.26**	4.64
20151021@354.a	2bo-g11_2 Cs-Res=199	**15.06**	**0.26**	4.64
20151021@355.a	2bo-g11_3	**15.08**	**0.26**	4.64
20151021@356.a	2bo-g11_4	**16.29**	**0.26**	4.64
20151021@357.a	2bo-UWG2			

20151021@358.a	2bo-UWG2			
20151021@359.a	2bo-UWG2			
20151021@360.a	2bo-UWG2			
	average and 2SD			
	bracket average and 2SD	**5.80**		**2.85**
20151021@361.a	2bo-g14_1	**15.98**	**0.21**	4.59
20151021@362.a	2bo-g14_2	**14.34**	**0.21**	4.59
20151021@363.a	2bo-g14_3	**15.05**	**0.21**	4.59
20151021@364.a	2bo-g14_4	**14.40**	**0.21**	4.59
20151021@365.a	2bo-g14_5	**15.26**	**0.21**	4.59
20151021@366.a	2bo-g14_6	**14.60**	**0.21**	4.59
20151021@367.a	2bo-g14_7	**14.87**	**0.21**	4.59
20151021@368.a	2bo-g11_5	**14.15**	**0.21**	4.59
20151021@369.a	2bo-g11_6	**14.27**	**0.21**	4.59
20151021@370.a	2bo-g11_7	**14.21**	**0.21**	4.59
20151021@371.a	2bo-UWG2			
20151021@372.a	2bo-UWG2			
20151021@373.a	2bo-UWG2			
20151021@374.a	2bo-UWG2			
	average and 2SD			
	bracket average and 2SD	**5.80**		**2.80**
20151021@375.a	2bo-g11_8	**15.11**	**0.19**	4.61
20151021@376.a	2bo-g11_9	**14.76**	**0.19**	4.61
20151021@377.a	2bo-g11_10	**14.87**	**0.19**	4.61
20151021@378.a	2bo-g11_11	**14.64**	**0.19**	4.61
20151021@379.a	2bo-g11_12	**14.24**	**0.19**	4.61
20151021@380.a	2bo-g11_13	**14.23**	**0.19**	4.61
20151021@381.a	2bo-g8_6	**15.14**	**0.19**	4.61
20151021@382.a	2bo-g8_7	**15.02**	**0.19**	4.61
20151021@383.a	2bo-g8_8	**15.56**	**0.19**	4.61
20151021@384.a	2bo-g8_9	**15.10**	**0.19**	4.61
20151021@385.a	2bo-g8_10	**16.79**	**0.19**	4.61
20151021@386.a	2bo-g8_11	**16.59**	**0.19**	4.61
20151021@387.a	2bo-UWG2			
20151021@388.a	2bo-UWG2			
20151021@389.a	2bo-UWG2			
20151021@390.a	2bo-UWG2			
	average and 2SD			
	bracket average and 2SD	**5.80**		**2.83**
20151021@391.a	2bo-g8_12	**16.82**	**0.18**	4.60
20151021@392.a	2bo-g8_13	**16.75**	**0.18**	4.60
20151021@393.a	2bo-g8_14	**16.01**	**0.18**	4.60
20151021@394.a	2bo-g8_15	**15.56**	**0.18**	4.60
20151021@395.a	2bo-g8_16	**15.46**	**0.18**	4.60

20151021@396.a 2bo-g8_17	**15.35**	**0.18**	4.60
20151021@397.a 2bo-g8_18	**15.30**	**0.18**	4.60
20151021@398.a 2bo-g8_19	**15.68**	**0.18**	4.60
20151021@399.a 2bo-g8_20	**15.36**	**0.18**	4.60
20151021@400.a 2bo-g8_21	**16.40**	**0.18**	4.60
20151021@401.a 2bo-g8_22	**15.43**	**0.18**	4.60
20151021@402.a 2bo-g8_23	**16.91**	**0.18**	4.60
20151021@403.a 2bo-UWG2			
20151021@404.a 2bo-UWG2			
20151021@405.a 2bo-UWG2			
20151021@406.a 2bo-UWG2			
average and 2SD			
bracket average and 2SD	**5.80**		**2.82**
20151021@407.a 2bo-g8_24	**16.98**	**0.21**	4.58
20151021@408.a 2bo-g8_25	**16.74**	**0.21**	4.58
20151021@409.a 2bo-g8_26	**16.78**	**0.21**	4.58
20151021@410.a 2bo-g8_27	**16.65**	**0.21**	4.58
20151021@411.a 2bo-g8_28	**16.83**	**0.21**	4.58
20151021@412.a 2bo-g8_29	**16.95**	**0.21**	4.58
20151021@413.a 2bo-g8_30	**16.90**	**0.21**	4.58
20151021@414.a 2bo-g8_31	**16.66**	**0.21**	4.58
20151021@415.a 2bo-g8_32	**16.70**	**0.21**	4.58
20151021@416.a 2bo-g8_33	**16.73**	**0.21**	4.58
20151021@417.a 2bo-g8_34	**15.11**	**0.21**	4.58
20151021@418.a 2bo-g8_35	**15.22**	**0.21**	4.58
20151021@419.a 2bo-UWG2			
20151021@420.a 2bo-UWG2			
20151021@421.a 2bo-UWG2			
20151021@422.a 2bo-UWG2			
average and 2SD			
bracket average and 2SD	**5.80**		**2.80**
20151021@423.a 2bo-g8_36	**16.50**	**0.15**	4.54
20151021@424.a 2bo-g8_37	**15.20**	**0.15**	4.54
20151021@425.a 2bo-g8_38	**17.01**	**0.15**	4.54
20151021@426.a 2bo-g8_39	**15.68**	**0.15**	4.54
20151021@427.a 2bo-g8_40	**16.96**	**0.15**	4.54
20151021@428.a 2bo-g8_41	**16.93**	**0.15**	4.54
20151021@429.a 2bo-g8_42	**16.91**	**0.15**	4.54
20151021@430.a 2bo-g8_43	**16.75**	**0.15**	4.54
20151021@431.a 2bo-g8_44	**16.97**	**0.15**	4.54
20151021@432.a 2bo-g8_45	**16.94**	**0.15**	4.54
20151021@433.a 2bo-g8_46	**16.77**	**0.15**	4.54
20151021@434.a 2bo-g8_47	**16.90**	**0.15**	4.54
20151021@435.a 2bo-UWG2			

20151021@436.a	2bo-UWG2			
20151021@437.a	2bo-UWG2			
20151021@438.a	2bo-UWG2			
	average and 2SD			
	bracket average and 2SD	**5.80**		**2.76**
	Mass Calibration NMR=1007406			
20151021@439.a	2b0-UWG2			
20151021@440.a	2b0-UWG2			
20151021@441.a	2b0-UWG2			
20151021@442.a	2b0-UWG2			
	average and 2SD			
20151021@443.a	2b0-g8_48	**16.98**	**0.19**	4.60
20151021@444.a	2b0-g8_49	**16.56**	**0.19**	4.60
20151021@445.a	2b0-g8_50	**16.79**	**0.19**	4.60
20151021@446.a	2b0-g8_51	**15.17**	**0.19**	4.60
20151021@447.a	2b0-g8_52	**16.83**	**0.19**	4.60
20151021@448.a	2b0-g8_53	**16.98**	**0.19**	4.60
20151021@449.a	2b0-g8_54	**15.47**	**0.19**	4.60
20151021@450.a	2b0-g8_55	**16.78**	**0.19**	4.60
20151021@451.a	2b0-g8_56	**16.32**	**0.19**	4.60
20151021@452.a	2b0-g8_57	**16.22**	**0.19**	4.60
20151021@453.a	2b0-g8_58	**16.70**	**0.19**	4.60
20151021@454.a	2b0-g8_59	**16.30**	**0.19**	4.60
20151021@455.a	2b0-g8_60	**16.09**	**0.19**	4.60
20151021@456.a	2b0-UWG2			
20151021@457.a	2b0-UWG2			
20151021@458.a	2b0-UWG2			
20151021@459.a	2b0-UWG2			
	average and 2SD			
	bracket average and 2SD	**5.80**		**2.81**
	2bbo			
20151021@460.a	2bbo-UWG2			
20151021@461.a	2bbo-UWG2			
20151021@462.a	2bbo-UWG2			
20151021@463.a	2bbo-UWG2			
20151021@464.a	2bbo-g28_4	**16.96**	**0.15**	4.58
20151021@465.a	2bbo-g28_5	**16.66**	**0.15**	4.58
20151021@466.a	2bbo-g28_6	**15.26**	**0.15**	4.58
20151021@467.a	2bbo-g28_7	**15.64**	**0.15**	4.58
20151021@468.a	2bbo-g28_8	**15.49**	**0.15**	4.58
20151021@469.a	2bbo-g28_9	**16.42**	**0.15**	4.58
20151021@470.a	2bbo-g28_10	**16.70**	**0.15**	4.58
20151021@471.a	2bbo-g28_11	**16.78**	**0.15**	4.58
20151021@472.a	2bbo-g28_12	**16.75**	**0.15**	4.58

20151021@473.a 2bbo-g28_13 Cs Res=203	**15.65**	**0.15**	4.58
20151021@474.a 2bbo-g28_14	**14.77**	**0.15**	4.58
20151021@475.a 2bbo-g28_15	**14.49**	**0.15**	4.58
20151021@476.a 2bbo-UWG2			
20151021@477.a 2bbo-UWG2			
20151021@478.a 2bbo-UWG2			
20151021@479.a 2bbo-UWG2			
average and 2SD			
bracket average and 2SD	**5.80**		**2.79**
20151021@480.a 2bbo-g28_16	**16.72**	**0.23**	4.44
20151021@481.a 2bbo-g28_17	**17.15**	**0.23**	4.44
20151021@482.a 2bbo-g28_18	**17.12**	**0.23**	4.44
20151021@483.a 2bbo-g28_19	**16.83**	**0.23**	4.44
20151021@484.a 2bbo-g28_20	**15.06**	**0.23**	4.44
20151021@485.a 2bbo-g28_21	**14.90**	**0.23**	4.44
20151021@486.a 2bbo-g28_22	**15.90**	**0.23**	4.44
20151021@487.a 2bbo-g28_23	**17.05**	**0.23**	4.44
20151021@488.a 2bbo-g28_24	**16.98**	**0.23**	4.44
20151021@489.a 2bbo-g28_25	**16.84**	**0.23**	4.44
20151021@490.a 2bbo-g28_26	**16.50**	**0.23**	4.44
20151021@491.a 2bbo-g28_27	**16.78**	**0.23**	4.44
20151021@492.a 2bbo-UWG2			
20151021@493.a 2bbo-UWG2			
20151021@494.a 2bbo-UWG2			
20151021@495.a 2bbo-UWG2			
average and 2SD			
bracket average and 2SD	**5.80**		**2.66**
20151021@496.a 2bbo-g28_28	**16.39**	**0.17**	4.39
20151021@497.a 2bbo-g28_29	**16.66**	**0.17**	4.39
20151021@498.a 2bbo-g28_30	**16.85**	**0.17**	4.39
20151021@499.a 2bbo-g28_31	**15.17**	**0.17**	4.39
20151021@500.a 2bbo-g28_32	**16.80**	**0.17**	4.39
20151021@501.a 2bbo-UWG2			
20151021@502.a 2bbo-UWG2			
20151021@503.a 2bbo-UWG2			
20151021@504.a 2bbo-UWG2			
average and 2SD			
bracket average and 2SD	**5.80**		**2.60**
20151021@505.a 2bbo-g14_5 Cs Res=204	**16.43**	**0.15**	4.45
20151021@506.a 2bbo-g14_6	**16.33**	**0.15**	4.45
20151021@507.a 2bbo-g14_7	**16.31**	**0.15**	4.45
20151021@508.a 2bbo-g14_8	**16.33**	**0.15**	4.45
20151021@509.a 2bbo-g14_9	**16.36**	**0.15**	4.45

20151021@510.a 2bbo-g14_10	**15.08**	**0.15**	4.45
20151021@511.a 2bbo-g14_11	**16.28**	**0.15**	4.45
20151021@512.a 2bbo-g14_12	**15.35**	**0.15**	4.45
20151021@513.a 2bbo-g14_13	**15.97**	**0.15**	4.45
20151021@514.a 2bbo-g14_14	**16.28**	**0.15**	4.45
20151021@515.a 2bbo-g14_15	**16.46**	**0.15**	4.45
20151021@516.a 2bbo-g14_16	**15.38**	**0.15**	4.45
20151021@517.a 2bbo-UWG2			
20151021@518.a 2bbo-UWG2			
20151021@519.a 2bbo-UWG2			
20151021@520.a 2bbo-UWG2			
average and 2SD			
bracket average and 2SD	**5.80**		**2.67**
20151021@521.a 2bbo-g14_17	**15.60**	**0.23**	4.43
20151021@522.a 2bbo-g14_18	**16.29**	**0.23**	4.43
20151021@523.a 2bbo-g14_19	**15.52**	**0.23**	4.43
20151021@524.a 2bbo-g14_20	**16.26**	**0.23**	4.43
20151021@525.a 2bbo-g14_21	**15.44**	**0.23**	4.43
20151021@526.a 2bbo-g14_22	**16.12**	**0.23**	4.43
20151021@527.a 2bbo-g14_23	**16.04**	**0.23**	4.43
20151021@528.a 2bbo-g14_24	**16.34**	**0.23**	4.43
20151021@529.a 2bbo-g14_25	**16.08**	**0.23**	4.43
20151021@530.a 2bbo-g14_26	**14.92**	**0.23**	4.43
20151021@531.a 2bbo-g14_27	**16.40**	**0.23**	4.43
20151021@532.a 2bbo-g14_28	**15.07**	**0.23**	4.43
20151021@533.a 2bbo-g14_29	**15.46**	**0.23**	4.43
20151021@534.a 2bbo-g14_30	**14.94**	**0.23**	4.43
20151021@535.a 2bbo-g14_31	**16.82**	**0.23**	4.43
20151021@536.a 2bbo-UWG2			
20151021@537.a 2bbo-UWG2			
20151021@538.a 2bbo-UWG2			
20151021@539.a 2bbo-UWG2			
average and 2SD			
bracket average and 2SD	**5.80**		**2.65**
20151021@540.a 2bbo-g14_32	**16.38**	**0.30**	4.43
20151021@541.a 2bbo-g14_33	**16.53**	**0.30**	4.43
20151021@542.a 2bbo-g14_34 Cs-Res=205	**14.92**	**0.30**	4.43
20151021@543.a 2bbo-g14_35	**16.43**	**0.30**	4.43
20151021@544.a 2bbo-g14_36	**15.09**	**0.30**	4.43
20151021@545.a 2bbo-g14_37	**14.64**	**0.30**	4.43
20151021@546.a 2bbo-g14_38	**16.00**	**0.30**	4.43
20151021@547.a 2bbo-g14_39	**15.65**	**0.30**	4.43
20151021@548.a 2bbo-g14_40	**16.21**	**0.30**	4.43
20151021@549.a 2bbo-g14_41	**14.75**	**0.30**	4.43
20151021@550.a 2bbo-g14_42	**15.61**	**0.30**	4.43

20151021@551.a 2bbo-g14_43	**16.31**	**0.30**	4.43
20151021@552.a 2bbo-g14_44	**15.18**	**0.30**	4.43
20151021@553.a 2bbo-g14_45	**16.16**	**0.30**	4.43
20151021@554.a 2bbo-UWG2			
20151021@555.a 2bbo-UWG2			
20151021@556.a 2bbo-UWG2			
20151021@557.a 2bbo-UWG2			
average and 2SD			
bracket average and 2SD	**5.80**		**2.65**
88-8			
20151021@558.a A10-UWG2			
20151021@559.a A10-UWG2			
20151021@560.a A10-UWG2			
20151021@561.a A10-UWG2			
20151021@562.a 88-8-g10_7	**14.72**	**0.21**	4.41
20151021@563.a 88-8-g10_8	**14.12**	**0.21**	4.41
20151021@564.a 88-8-g10_9	**13.96**	**0.21**	4.41
20151021@565.a 88-8-g10_10	**14.33**	**0.21**	4.41
20151021@566.a 88-8-g10_11	**14.63**	**0.21**	4.41
20151021@567.a 88-8-g10_12	**16.06**	**0.21**	4.41
20151021@568.a 88-8-g10_13	**15.99**	**0.21**	4.41
20151021@569.a 88-8-g10_14	**15.22**	**0.21**	4.41
20151021@570.a 88-8-g10_15	**15.41**	**0.21**	4.41
20151021@571.a 88-8-g10_16	**14.20**	**0.21**	4.41
20151021@572.a 88-8-g10_17	**14.86**	**0.21**	4.41
20151021@573.a 88-8-g10_18	**14.77**	**0.21**	4.41
20151021@574.a A10-UWG2			
20151021@575.a A10-UWG2			
20151021@576.a A10-UWG2			
20151021@577.a A10-UWG2			
average and 2SD			
bracket average and 2SD	**5.80**		**2.62**
20151021@578.a 88-8 g10_19 Cs Res=206	**14.63**	**0.22**	4.31
20151021@579.a 88-8 g10_20	**15.37**	**0.22**	4.31
20151021@580.a 88-8 g10_21	**15.95**	**0.22**	4.31
20151021@581.a 88-8 g10_22	**16.72**	**0.22**	4.31
20151021@582.a 88-8 g10_23	**15.00**	**0.22**	4.31
20151021@583.a 88-8 g10_24	**16.61**	**0.22**	4.31
20151021@584.a 88-8 g10_25	**16.79**	**0.22**	4.31
20151021@585.a 88-8 g10_26	**16.48**	**0.22**	4.31
20151021@586.a 88-8 g10_27	**14.29**	**0.22**	4.31
20151021@587.a 88-8 g10_28	**15.94**	**0.22**	4.31
20151021@588.a 88-8 g10_29	**15.86**	**0.22**	4.31
20151021@589.a 88-8 g10_30	**16.51**	**0.22**	4.31

20151021@590.a	A10-UWG2			
20151021@591.a	A10-UWG2			
20151021@592.a	A10-UWG2			
20151021@593.a	A10-UWG2			
	average and 2SD			
	bracket average and 2SD	**5.80**		**2.52**
20151021@594.a	88-8 g10_31	**14.35**	**0.19**	4.21
20151021@595.a	88-8 g10_32	**15.42**	**0.19**	4.21
20151021@596.a	88-8 g10_33	**16.66**	**0.19**	4.21
20151021@597.a	88-8 g10_34	**15.13**	**0.19**	4.21
20151021@598.a	88-8 g10_35	**16.16**	**0.19**	4.21
20151021@599.a	88-8 g10_36	**16.66**	**0.19**	4.21
20151021@600.a	88-8 g10_37	**16.48**	**0.19**	4.21
20151021@601.a	88-8 g10_38	**14.51**	**0.19**	4.21
20151021@602.a	88-8 g10_39	**14.42**	**0.19**	4.21
20151021@603.a	88-8 g10_40	**14.03**	**0.19**	4.21
20151021@604.a	88-8 g10_41	**14.22**	**0.19**	4.21
20151021@605.a	88-8 g10_42	**14.32**	**0.19**	4.21
20151021@606.a	A10-UWG2			
20151021@607.a	A10-UWG2			
20151021@608.a	A10-UWG2			
20151021@609.a	A10-UWG2			
	average and 2SD			
	bracket average and 2SD	**5.80**		**2.43**

$\delta^{18}O$ ‰ measured	2SE (int.)	^{16}O (Gcps)	IP (nA)	Yield (Gcps/nA)	Date	Time	X	Y	DTFA-X
	1.86nA w/o e-beam => e-beam offset=0.13nA								
7.846	0.573	1.066	1.721	0.620	10/19/15	16:20	-952	-202	3
9.723	0.217	2.644	1.660	1.592	10/19/15	16:38	-1093	14	0
9.675	0.188	2.661	1.647	1.616	10/19/15	16:42	-1097	-6	0
9.492	0.226	2.875	1.799	1.598	10/19/15	16:48	-1067	-3	1
9.743	0.179	2.893	1.818	1.591	10/19/15	16:52	-1140	-25	2
9.658	**0.229**								
13.627	0.238	2.596	1.817	1.429	10/19/15	16:56	-2537	-1313	-2
13.430	0.204	2.538	1.784	1.422	10/19/15	17:12	-4195	-1977	0
13.785	0.191	2.661	1.875	1.419	10/19/15	17:19	-2856	-3317	-5
13.917	0.231	2.598	1.856	1.400	10/19/15	17:23	-1203	-2198	-1
13.690	**0.420**								
9.825	0.160	3.157	1.822	1.733	10/19/15	17:27	980	-1654	0
9.477	0.161	3.138	1.794	1.749	10/19/15	17:31	590	-1818	1
9.356	0.188	3.097	1.768	1.751	10/19/15	17:35	588	-2284	1
9.685	0.168	3.052	1.740	1.754	10/19/15	17:40	1175	-2066	-1
9.586	**0.419**								
9.668	0.230	2.767	1.724	1.605	10/19/15	17:44	-1181	-146	-1
9.751	0.256	2.882	1.810	1.592	10/19/15	17:52	-1195	-193	-2
9.724	0.223	2.852	1.793	1.591	10/19/15	17:56	-1282	-245	0
9.768	0.203	2.811	1.775	1.583	10/19/15	18:00	-1336	-378	-1
9.728	**0.088**								
9.693	**0.177**								

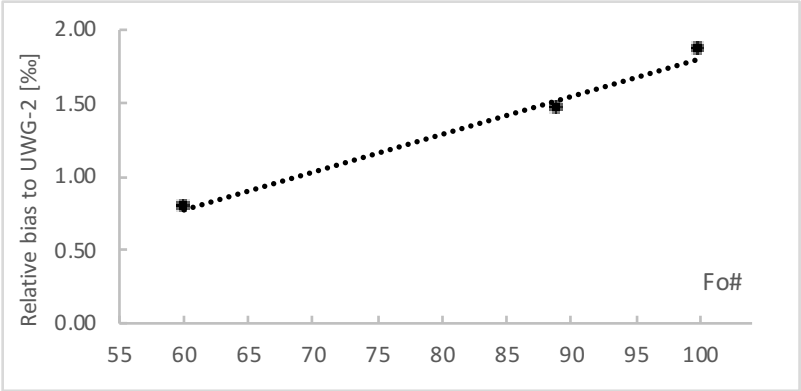

9.409	0.165	2.813	1.738	1.619	10/20/15	8:16	-1288	-289	0
9.584	0.195	2.816	1.759	1.601	10/20/15	8:20	-1292	-331	0
9.439	0.125	2.795	1.745	1.602	10/20/15	8:23	-1757	-295	2
9.587	0.250	2.883	1.798	1.603	10/20/15	8:28	-1675	-319	2
9.505	**0.188**								
13.273	0.185	2.592	1.808	1.434	10/20/15	8:32	-2835	-1398	5

9.888	0.164	3.118	1.797	1.735	10/20/15	8:36	999	-1693	-2
13.554	0.232	2.684	1.873	1.433	10/20/15	8:43	-2829	-3296	-2
8.929	0.181	2.793	1.806	1.547	10/20/15	9:09	-1297	61	-11
8.821	0.173	2.759	1.785	1.546	10/20/15	9:13	-1276	60	-12
8.782	0.235	2.732	1.767	1.546	10/20/15	9:18	-1251	59	-12
8.683	0.244	2.711	1.752	1.548	10/20/15	9:22	-1230	59	-12
8.804	**0.203**								
19.704	0.237	2.459	1.730	1.422	10/20/15	9:31	-2251	3238	-13
19.924	0.218	2.549	1.792	1.423	10/20/15	9:39	-2241	3249	-13
21.103	0.217	2.505	1.789	1.401	10/20/15	9:44	-2224	3243	-13
21.507	0.200	2.521	1.775	1.420	10/20/15	9:48	-2220	3265	-13
21.105	0.232	2.411	1.761	1.369	10/20/15	9:53	-2207	3249	-13
21.400	0.193	2.486	1.749	1.422	10/20/15	9:57	-2209	3277	-13
21.249	0.263	2.586	1.819	1.422	10/20/15	10:05	-2188	3255	-14
20.623	0.223	2.612	1.833	1.425	10/20/15	10:09	-2183	3241	-14
20.507	0.247	2.578	1.817	1.418	10/20/15	10:14	-2237	3229	-14
19.593	0.237	2.546	1.796	1.418	10/20/15	10:18	-2242	3267	-14
8.621	0.198	2.758	1.775	1.554	10/20/15	10:22	-1299	84	-13
8.504	0.165	2.730	1.761	1.551	10/20/15	10:26	-1275	86	-13
8.621	0.173	2.706	1.747	1.549	10/20/15	10:34	-1251	85	-13
8.684	0.229	2.805	1.809	1.550	10/20/15	10:42	-1230	85	-13
8.608	**0.150**								
8.706	**0.267**								
19.376	0.194	2.585	1.814	1.425	10/20/15	10:47	-2292	3229	-15
21.418	0.270	2.555	1.802	1.418	10/20/15	10:51	-2389	3151	-13
20.027	0.274	2.535	1.784	1.421	10/20/15	10:55	-2307	3218	-14
21.228	0.191	2.523	1.769	1.426	10/20/15	10:59	-2313	3205	-14
20.482	0.224	2.508	1.757	1.428	10/20/15	11:04	-2325	3193	-14
20.195	0.241	2.492	1.750	1.424	10/20/15	11:08	-2341	3189	-14
20.129	0.216	2.583	1.814	1.424	10/20/15	11:14	-2346	3174	-13
21.429	0.220	2.560	1.803	1.420	10/20/15	11:19	-2354	3162	-13
21.416	0.290	2.542	1.785	1.424	10/20/15	11:23	-2373	3163	-14
21.340	0.180	2.518	1.766	1.426	10/20/15	11:28	-2361	3143	-14
8.772	0.182	2.698	1.738	1.552	10/20/15	11:32	-1302	114	-13
8.561	0.164	2.751	1.772	1.552	10/20/15	11:40	-1284	112	-8
8.726	0.204	2.700	1.746	1.546	10/20/15	11:44	-1259	117	-8
8.767	0.206	2.799	1.812	1.545	10/20/15	11:53	-1237	119	-8
8.707	**0.198**								
8.657	**0.194**								
19.541	0.212	2.524	1.781	1.417	10/20/15	11:58	-2293	3299	-9
20.224	0.180	2.489	1.746	1.426	10/20/15	12:02	-2296	3395	-9
20.055	0.201	2.573	1.804	1.427	10/20/15	12:09	-2267	3399	-9
19.850	0.264	2.558	1.808	1.415	10/20/15	12:13	-2295	3315	-9

19.782	0.197	2.569	1.803	1.425	10/20/15	12:17	-2300	3380	-9
19.747	0.204	2.556	1.802	1.419	10/20/15	12:22	-2294	3352	-9
19.584	0.203	2.553	1.798	1.420	10/20/15	12:26	-2295	3339	-9
20.269	0.223	2.565	1.802	1.423	10/20/15	12:30	-2306	3370	-9
19.459	0.266	2.517	1.776	1.417	10/20/15	12:34	-2221	3404	-8
19.711	0.267	2.487	1.749	1.422	10/20/15	12:38	-2211	3325	-8
8.873	0.145	2.809	1.813	1.549	10/20/15	12:47	-1311	137	-7
8.573	0.150	2.814	1.820	1.546	10/20/15	12:50	-1286	137	-8
8.666	0.167	2.805	1.819	1.542	10/20/15	12:54	-1262	140	-8
8.644	0.156	2.793	1.812	1.541	10/20/15	12:58	-1239	143	-8
8.689	**0.258**								
8.698	**0.214**								
8.692	0.152	2.774	1.782	1.557	10/20/15	13:13	369	-2059	3
8.494	0.164	2.738	1.771	1.546	10/20/15	13:16	400	-2074	3
8.501	0.173	2.735	1.748	1.564	10/20/15	13:20	-78	-3177	5
8.428	0.176	2.830	1.807	1.566	10/20/15	13:25	641	-3695	0
8.529	**0.227**								
9.440	0.144	2.897	1.811	1.600	10/20/15	13:30	-1815	-382	-5
9.468	0.204	2.848	1.797	1.585	10/20/15	13:34	-3393	-790	1
9.604	0.136	2.838	1.789	1.586	10/20/15	13:37	-3222	-757	0
9.636	0.197	2.845	1.788	1.592	10/20/15	13:41	-1808	-295	-5
9.537	**0.195**								
8.714	0.206	2.755	1.780	1.548	10/20/15	13:45	270	-2124	4
8.434	0.199	2.765	1.772	1.560	10/20/15	13:49	-45	-3172	5
8.592	0.187	2.744	1.765	1.555	10/20/15	13:53	562	-3765	1
8.560	0.176	2.734	1.759	1.554	10/20/15	13:57	354	-2007	4
8.575	**0.230**								
8.552	**0.217**								
8.752	0.188	2.798	1.793	1.561	10/20/15	14:28	-2407	72	-3
8.850	0.236	2.815	1.811	1.554	10/20/15	14:32	-2377	73	-3
8.563	0.188	2.802	1.810	1.548	10/20/15	14:35	-2352	75	-4
8.569	0.231	2.769	1.795	1.543	10/20/15	14:39	-2327	76	-4
8.684	**0.283**								
20.176	0.202	2.534	1.773	1.429	10/20/15	14:46	-1174	-368	-2
21.523	0.171	2.536	1.770	1.433	10/20/15	14:50	-1106	-329	-2
20.681	0.234	2.522	1.762	1.432	10/20/15	14:54	-1192	-415	-2
22.169	0.208	2.498	1.749	1.428	10/20/15	14:59	-1322	-347	-2
21.719	0.188	2.605	1.838	1.417	10/20/15	15:06	-1332	-416	-2
21.687	0.208	2.637	1.856	1.421	10/20/15	15:12	-1088	-463	-2
20.271	0.191	2.591	1.821	1.423	10/20/15	15:19	-4986	126	-10
21.530	0.188	2.565	1.808	1.419	10/20/15	15:24	-4982	267	-11

~~16.482~~	~~0.194~~	~~2.471~~	~~1.793~~	~~1.378~~	~~10/20/15~~	~~15:28~~	~~-4855~~	~~116~~	~~-11~~
21.406	0.232	2.534	1.783	1.421	10/20/15	15:33	-4898	238	-11
8.596	0.136	2.743	1.768	1.552	10/20/15	15:39	-2400	95	-7
8.583	0.174	2.726	1.758	1.550	10/20/15	15:43	-2369	100	-7
8.560	0.180	2.709	1.750	1.548	10/20/15	15:47	-2343	102	-7
8.307	0.212	2.839	1.829	1.552	10/20/15	15:54	-2318	104	-8
8.512	**0.274**								
8.598	**0.317**								
21.116	0.229	2.571	1.844	1.394	10/20/15	15:58	-2406	-7980	-10
~~17.460~~	~~0.185~~	~~2.580~~	~~1.860~~	~~1.387~~	~~10/20/15~~	~~16:06~~	~~-2372~~	~~-7881~~	~~-19~~
20.062	0.209	2.607	1.842	1.415	10/20/15	16:12	-5089	-4106	-15
19.964	0.231	2.526	1.808	1.397	10/20/15	16:16	-5123	-4201	-15
20.507	0.235	2.532	1.787	1.417	10/20/15	16:20	-4998	-4068	-15
20.603	0.229	2.500	1.769	1.414	10/20/15	16:26	-5106	-4202	-15
21.729	0.179	2.529	1.760	1.437	10/20/15	16:32	-637	-3655	-14
~~16.046~~	~~0.212~~	~~2.525~~	~~1.770~~	~~1.426~~	~~10/20/15~~	~~16:36~~	~~-544~~	~~-3542~~	~~3~~
21.591	0.233	2.525	1.773	1.424	10/20/15	16:41	-709	-3806	3
21.480	0.212	2.525	1.772	1.425	10/20/15	16:45	-773	-3626	3
8.308	0.182	2.770	1.784	1.553	10/20/15	16:50	-2398	55	-1
8.425	0.121	2.760	1.783	1.548	10/20/15	16:54	-2368	54	-1
8.436	0.160	2.755	1.780	1.548	10/20/15	16:58	-2342	54	-1
8.364	0.159	2.724	1.767	1.542	10/20/15	17:02	-2316	54	-1
8.383	**0.119**								
8.447	**0.239**								
20.336	0.258	2.499	1.743	1.434	10/20/15	17:07	1376	-2656	-2
~~17.813~~	~~0.228~~	~~2.509~~	~~1.797~~	~~1.396~~	~~10/20/15~~	~~17:11~~	~~1417~~	~~-2535~~	~~-1~~
~~16.492~~	~~0.243~~	~~2.550~~	~~1.835~~	~~1.389~~	~~10/20/15~~	~~17:16~~	~~1415~~	~~-2554~~	~~-2~~
20.290	0.238	2.649	1.850	1.431	10/20/15	17:23	-5512	-1605	-10
19.913	0.175	2.624	1.863	1.408	10/20/15	17:27	-5542	-1741	-10
19.881	0.154	2.604	1.837	1.418	10/20/15	17:31	-5367	-1627	-11
21.545	0.224	2.534	1.783	1.421	10/20/15	17:39	-5425	-1706	-11
20.131	0.180	2.529	1.773	1.426	10/20/15	17:43	-5484	-1571	-11
20.749	0.239	2.512	1.767	1.421	10/20/15	17:48	-5381	-1655	-11
~~18.448~~	~~0.212~~	~~2.458~~	~~1.758~~	~~1.398~~	~~10/20/15~~	~~17:52~~	~~-5408~~	~~-1686~~	~~-11~~
8.616	0.189	2.707	1.748	1.549	10/20/15	17:57	-2396	31	-5
8.700	0.180	2.827	1.823	1.551	10/20/15	18:04	-2365	32	-4
8.542	0.173	2.802	1.818	1.541	10/20/15	18:07	-2341	33	-4
8.154	0.170	2.772	1.796	1.543	10/20/15	18:11	-2312	35	-5
8.503	**0.483**								
8.443	**0.350**								
20.046	0.168	2.504	1.773	1.413	10/20/15	18:21	-5114	663	-6
22.282	0.254	2.511	1.761	1.426	10/20/15	18:25	-5050	604	-6
21.531	0.205	2.480	1.739	1.426	10/20/15	18:29	-5085	729	-7

21.656	0.215	2.578	1.805	1.429	10/20/15	18:35	-5063	619	-7
20.086	0.216	2.571	1.821	1.412	10/20/15	18:39	-5074	634	-6
20.499	0.233	2.585	1.821	1.420	10/20/15	18:43	-5099	654	-6
22.007	0.187	2.582	1.813	1.424	10/20/15	18:48	-4929	4004	-16
21.811	0.267	2.564	1.807	1.419	10/20/15	18:52	-4922	4103	-17
20.147	0.199	2.549	1.797	1.419	10/20/15	18:57	-4887	3903	-16
21.803	0.228	2.546	1.790	1.422	10/20/15	19:01	-4939	3987	-16
8.747	0.169	2.749	1.777	1.547	10/20/15	19:05	-2397	11	-6
8.422	0.180	2.737	1.770	1.546	10/20/15	19:09	-2366	12	-7
8.338	0.197	2.731	1.764	1.548	10/20/15	19:13	-2337	14	-6
8.408	0.248	2.730	1.761	1.550	10/20/15	19:16	-2310	13	-6
8.479	**0.365**								
8.491	**0.397**								
	Cs-Res=185								
8.849	0.233	2.832	1.817	1.559	10/20/15	20:12	787	-1447	-6
8.936	0.206	2.794	1.795	1.556	10/20/15	20:15	811	-1449	-6
8.839	0.182	2.775	1.781	1.558	10/20/15	20:19	836	-1451	-7
8.786	0.204	2.768	1.772	1.562	10/20/15	20:23	862	-1456	-7
8.853	**0.124**								
21.407	0.192	2.539	1.760	1.443	10/20/15	20:28	1600	-6224	-3
20.258	0.207	2.523	1.750	1.441	10/20/15	20:33	1698	-6175	-3
20.310	0.165	2.501	1.742	1.435	10/20/15	20:37	1603	-6293	-3
21.425	0.225	2.620	1.823	1.437	10/20/15	20:43	1583	-6233	-3
20.472	0.227	2.626	1.842	1.426	10/20/15	20:52	1671	4655	-1
19.726	0.178	2.609	1.837	1.420	10/20/15	20:56	1684	4559	-1
20.878	0.234	2.614	1.831	1.428	10/20/15	21:00	1612	4728	-1
21.604	0.162	2.585	1.824	1.417	10/20/15	21:05	1287	4444	0
19.870	0.203	2.587	1.815	1.426	10/20/15	21:09	1379	4540	-1
21.311	0.232	2.588	1.823	1.419	10/20/15	21:14	1769	4615	0
8.659	0.215	2.847	1.825	1.560	10/20/15	21:20	779	-1470	-9
8.742	0.233	2.838	1.822	1.558	10/20/15	21:24	803	-1472	-9
8.624	0.185	2.828	1.820	1.554	10/20/15	21:28	832	-1474	-10
8.662	0.185	2.833	1.818	1.558	10/20/15	21:31	860	-1478	-10
8.672	**0.100**								
8.762	**0.220**								
20.930	0.230	2.565	1.801	1.424	10/20/15	21:40	1617	-2757	-8
19.528	0.198	2.556	1.795	1.424	10/20/15	21:44	1672	-2789	-7
21.245	0.183	2.573	1.789	1.438	10/20/15	21:51	1581	-2704	-8
20.261	0.204	2.526	1.768	1.429	10/20/15	22:05	742	795	-3
20.460	0.194	2.506	1.762	1.423	10/20/15	22:09	713	737	-3
19.872	0.149	2.497	1.754	1.423	10/20/15	22:18	-7667	-1801	-38
20.589	0.279	2.469	1.750	1.411	10/20/15	22:22	-7706	-1935	-38
20.491	0.190	2.631	1.842	1.429	10/20/15	22:31	-1521	-5465	-18
20.240	0.217	2.645	1.849	1.430	10/20/15	22:35	-1509	-5426	-18

20.052	0.163	2.642	1.847	1.430	10/20/15	22:39	-1425	-5470	-18
8.768	0.165	2.880	1.848	1.558	10/20/15	22:45	802	-1420	-5
8.798	0.185	2.890	1.862	1.552	10/20/15	22:49	826	-1421	-5
8.825	0.230	2.898	1.868	1.552	10/20/15	22:53	853	-1420	-5
9.133	0.202	2.887	1.867	1.547	10/20/15	22:57	879	-1423	-5
8.881	**0.339**								
8.776	**0.322**								
8.887	0.214	2.789	1.798	1.551	10/20/15	23:09	-359	-499	-20
8.988	0.154	2.760	1.779	1.551	10/20/15	23:13	-333	-502	-20
8.722	0.109	2.739	1.769	1.548	10/20/15	23:17	-310	-503	-21
8.838	0.169	2.736	1.762	1.553	10/20/15	23:21	-285	-504	-21
8.859	**0.221**								
19.015	0.231	2.541	1.732	1.467	10/20/15	23:34	-507	822	-21
18.955	0.200	2.523	1.727	1.461	10/20/15	23:39	-473	812	-21
18.768	0.203	2.655	1.813	1.464	10/20/15	23:46	-548	812	-21
18.870	0.227	2.675	1.830	1.462	10/20/15	23:50	-484	858	-21
20.256	0.224	2.627	1.831	1.434	10/20/15	23:57	-292	1699	-23
20.141	0.137	2.607	1.829	1.426	10/21/15	0:01	-289	1673	-23
21.032	0.216	2.604	1.816	1.434	10/21/15	0:06	474	1647	-24
19.741	0.262	2.587	1.806	1.432	10/21/15	0:10	447	1681	-24
21.392	0.199	2.572	1.801	1.428	10/21/15	0:15	454	1603	-23
19.900	0.171	2.572	1.794	1.434	10/21/15	0:20	518	1670	-24
8.856	0.198	2.743	1.775	1.546	10/21/15	0:25	-360	-477	-19
8.737	0.203	2.735	1.765	1.549	10/21/15	0:29	-335	-477	-19
8.933	0.258	2.692	1.738	1.549	10/21/15	0:33	-309	-478	-20
8.861	0.198	2.591	1.680	1.542	10/21/15	0:36	-283	-478	-20
8.847	**0.162**								
8.853	**0.180**								
19.216	0.179	2.676	1.840	1.454	10/21/15	0:59	540	2517	-26
18.877	0.247	2.657	1.833	1.449	10/21/15	1:04	532	2450	-26
18.636	0.197	2.659	1.824	1.458	10/21/15	1:10	449	2640	-26
18.670	0.172	2.644	1.817	1.455	10/21/15	1:14	476	2623	-26
19.886	0.228	2.571	1.799	1.429	10/21/15	1:23	-120	2770	-26
19.985	0.225	2.557	1.790	1.428	10/21/15	1:28	-122	2790	-26
20.931	0.223	2.538	1.764	1.438	10/21/15	1:41	-129	-1306	-17
20.910	0.196	2.513	1.753	1.433	10/21/15	1:46	-136	-1357	-17
19.816	0.223	2.496	1.745	1.430	10/21/15	1:50	-97	-1401	-17
20.844	0.222	2.622	1.833	1.430	10/21/15	1:59	-1328	-2582	-14
20.667	0.194	2.639	1.836	1.438	10/21/15	2:03	-1378	-2620	-14
20.596	0.166	2.618	1.835	1.427	10/21/15	2:08	-1421	-2641	-14
8.655	0.180	2.834	1.835	1.545	10/21/15	2:13	-366	-453	-18
8.944	0.147	2.816	1.824	1.543	10/21/15	2:17	-342	-455	-18

8.763	0.190	2.801	1.818	1.541	10/21/15	2:21	-313	-456	-19
8.912	0.166	2.795	1.810	1.544	10/21/15	2:25	-284	-456	-18
8.819	**0.269**								
8.833	**0.208**								
19.791	0.179	2.554	1.778	1.436	10/21/15	2:39	-1862	-2691	-15
19.590	0.232	2.536	1.775	1.429	10/21/15	2:44	-1837	-2708	-14
19.960	0.200	2.536	1.764	1.437	10/21/15	2:49	-1666	-2786	-14
19.955	0.175	2.521	1.759	1.433	10/21/15	2:53	-1670	-2809	-14
20.001	0.209	2.506	1.753	1.430	10/21/15	2:57	-1624	-2820	-14
19.351	0.224	2.501	1.746	1.433	10/21/15	3:01	-1699	-2763	-15
19.676	0.163	2.640	1.847	1.429	10/21/15	3:10	-2283	-2819	-15
20.052	0.224	2.636	1.855	1.421	10/21/15	3:15	-2319	-2786	-14
21.019	0.226	2.633	1.846	1.427	10/21/15	3:22	-2345	-3207	-14
20.826	0.238	2.625	1.841	1.426	10/21/15	3:26	-2365	-3239	-14
19.666	0.209	2.612	1.832	1.425	10/21/15	3:34	-2466	-3834	-15
19.708	0.197	2.606	1.825	1.428	10/21/15	3:39	-2488	-3828	-15
8.905	0.151	2.803	1.814	1.546	10/21/15	3:43	-364	-431	-18
8.788	0.183	2.794	1.808	1.545	10/21/15	3:47	-338	-431	-18
8.752	0.253	2.789	1.802	1.548	10/21/15	3:51	-310	-431	-19
8.829	0.221	2.782	1.797	1.548	10/21/15	3:55	-283	-431	-19
8.819	**0.131**								
8.819	**0.196**								
8.542	0.189	2.760	1.770	1.559	10/21/15	4:12	-2452	-28	-10
8.711	0.184	2.736	1.764	1.551	10/21/15	4:16	-2424	-30	-10
8.651	0.223	2.730	1.758	1.553	10/21/15	4:20	-2398	-30	-10
8.434	0.221	2.721	1.751	1.554	10/21/15	4:24	-2372	-30	-11
8.585	**0.245**								
20.914	0.193	2.492	1.740	1.432	10/21/15	4:35	-1205	-421	-9
21.550	0.167	2.598	1.818	1.429	10/21/15	4:42	-1213	-435	-8
21.926	0.155	2.601	1.839	1.414	10/21/15	4:47	-1227	-424	-8
21.515	0.255	2.641	1.863	1.417	10/21/15	4:52	-1230	-438	-9
21.828	0.310	2.613	1.850	1.413	10/21/15	4:56	-1254	-438	-8
22.100	0.234	2.584	1.834	1.409	10/21/15	5:01	-1274	-439	-8
21.943	0.213	2.577	1.822	1.414	10/21/15	5:05	-1275	-425	-8
21.759	0.277	2.570	1.812	1.418	10/21/15	5:10	-1289	-416	-9
21.615	0.209	2.554	1.804	1.416	10/21/15	5:15	-1310	-410	-8
21.683	0.204	2.541	1.796	1.415	10/21/15	5:19	-1313	-398	-8
21.906	0.231	2.530	1.788	1.415	10/21/15	5:23	-1318	-381	-8
22.053	0.217	2.521	1.782	1.415	10/21/15	5:27	-1331	-393	-9
8.546	0.167	2.762	1.773	1.558	10/21/15	5:33	-2457	-49	-10
8.499	0.175	2.740	1.766	1.551	10/21/15	5:37	-2427	-53	-10
8.607	0.210	2.727	1.760	1.549	10/21/15	5:40	-2400	-55	-10
8.556	0.214	2.750	1.764	1.558	10/21/15	5:44	-2374	-55	-11

8.552	**0.089**								
8.568	**0.174**								
20.457	0.201	2.484	1.751	1.419	10/21/15	5:50	-1169	-355	-8
20.359	0.233	2.617	1.839	1.423	10/21/15	5:58	-1175	-339	-8
20.372	0.286	2.635	1.856	1.420	10/21/15	6:02	-1194	-345	-8
20.400	0.229	2.613	1.853	1.410	10/21/15	6:07	-1205	-331	-9
21.502	0.152	2.615	1.849	1.414	10/21/15	6:11	-1225	-337	-9
21.628	0.204	2.609	1.842	1.416	10/21/15	6:15	-1243	-332	-8
21.707	0.207	2.608	1.845	1.414	10/21/15	6:19	-1258	-340	-8
21.618	0.226	2.599	1.832	1.419	10/21/15	6:24	-1233	-321	-8
20.540	0.256	2.574	1.816	1.418	10/21/15	6:28	-1187	-368	-8
21.112	0.208	2.569	1.810	1.420	10/21/15	6:34	-1153	-392	-8
21.529	0.235	2.568	1.806	1.422	10/21/15	6:38	-1130	-402	-8
21.178	0.205	2.639	1.841	1.433	10/21/15	6:43	-1215	-390	-8
8.559	0.181	2.868	1.848	1.552	10/21/15	6:48	-2465	-69	-10
8.623	0.255	2.858	1.845	1.549	10/21/15	6:51	-2439	-71	-10
8.525	0.192	2.847	1.842	1.546	10/21/15	6:55	-2410	-72	-11
8.824	0.270	2.813	1.823	1.543	10/21/15	6:59	-2384	-73	-10
8.633	**0.268**								
8.592	**0.204**								
20.577	0.198	2.550	1.797	1.419	10/21/15	7:04	-1148	-357	-8
20.310	0.250	2.525	1.776	1.422	10/21/15	7:09	-1147	-340	-9
20.496	0.229	2.508	1.762	1.424	10/21/15	7:13	-1131	-333	-9
21.345	0.193	2.499	1.751	1.427	10/21/15	7:17	-1133	-316	-8
21.463	0.217	2.493	1.741	1.432	10/21/15	7:22	-1137	-302	-9
20.715	0.215	2.476	1.734	1.428	10/21/15	7:27	-1121	-366	-8
20.641	0.205	2.593	1.823	1.423	10/21/15	7:35	-1108	-443	-8
20.610	0.201	2.623	1.840	1.425	10/21/15	7:40	-1100	-453	-8
20.516	0.219	2.628	1.844	1.425	10/21/15	7:44	-1101	-467	-8
21.513	0.178	2.616	1.844	1.419	10/21/15	7:48	-1177	-535	-8
21.524	0.218	2.617	1.843	1.420	10/21/15	7:53	-1136	-528	-8
21.841	0.261	2.613	1.840	1.420	10/21/15	7:58	-1190	-521	-8
8.679	0.153	2.836	1.831	1.549	10/21/15	8:03	-2470	-89	-10
8.531	0.129	2.824	1.824	1.548	10/21/15	8:07	-2447	-91	-10
8.520	0.257	2.807	1.818	1.544	10/21/15	8:11	-2420	-94	-10
8.501	0.194	2.839	1.833	1.549	10/21/15	8:14	-2395	-96	-10
8.558	**0.164**								
8.595	**0.220**								
22.036	0.231	2.635	1.862	1.415	10/21/15	8:25	-4950	4003	-14
21.878	0.163	2.604	1.843	1.413	10/21/15	8:29	-4953	4020	-13
21.910	0.202	2.572	1.818	1.414	10/21/15	8:34	-4969	4019	-13
21.745	0.266	2.524	1.789	1.411	10/21/15	8:38	-4969	4037	-14
22.035	0.225	2.499	1.762	1.418	10/21/15	8:42	-4996	4034	-14
21.887	0.201	2.473	1.746	1.417	10/21/15	8:46	-4986	4052	-14

21.433	0.297	2.465	1.733	1.422	10/21/15	8:51	-4920	4016	-13
20.326	0.252	2.586	1.824	1.418	10/21/15	9:00	-4901	4016	-13
20.437	0.196	2.598	1.836	1.415	10/21/15	9:04	-4895	4032	-13
20.439	0.162	2.597	1.839	1.412	10/21/15	9:08	-4878	4035	-13
21.550	0.192	2.602	1.834	1.418	10/21/15	9:13	-4879	4050	-13
8.653	0.181	2.830	1.825	1.551	10/21/15	9:19	-2466	-104	-7
8.705	0.185	2.810	1.818	1.546	10/21/15	9:22	-2443	-106	-7
8.593	0.191	2.802	1.813	1.546	10/21/15	9:26	-2420	-112	-7
8.610	0.208	2.790	1.806	1.545	10/21/15	9:30	-2395	-114	-7
8.640	**0.100**								
8.599	**0.153**								
8.187	0.185	2.779	1.794	1.548	10/21/15	9:55	-2465	-136	-7
8.374	0.176	2.781	1.800	1.545	10/21/15	9:59	-2444	-134	-6
8.224	0.197	2.793	1.807	1.546	10/21/15	10:03	-2421	-131	-7
8.286	0.154	2.779	1.802	1.543	10/21/15	10:07	-2398	-139	-7
8.268	**0.164**								
21.576	0.147	2.509	1.786	1.405	10/21/15	10:19	-4940	3967	-15
21.672	0.231	2.553	1.816	1.406	10/21/15	10:22	-4918	3967	-15
21.939	0.150	2.580	1.837	1.404	10/21/15	10:26	-4924	3949	-15
21.307	0.211	2.575	1.844	1.397	10/21/15	10:29	-4901	3948	-15
21.488	0.253	2.582	1.845	1.400	10/21/15	10:33	-4912	3932	-15
20.148	0.260	2.569	1.839	1.397	10/21/15	10:36	-4891	3932	-14
20.209	0.250	2.563	1.829	1.402	10/21/15	10:39	-4901	3916	-15
19.977	0.124	2.561	1.824	1.404	10/21/15	10:43	-4871	3909	-14
20.194	0.144	2.549	1.831	1.392	10/21/15	10:47	-4871	3923	-15
20.137	0.194	2.562	1.826	1.403	10/21/15	10:51	-4838	3980	-14
20.223	0.205	2.540	1.821	1.395	10/21/15	10:55	-4844	3943	-16
8.259	0.203	2.770	1.807	1.533	10/21/15	10:59	-2401	119	-7
8.250	0.180	2.747	1.793	1.532	10/21/15	11:03	-2370	121	-7
8.366	0.177	2.753	1.792	1.537	10/21/15	11:06	-2343	123	-7
8.393	0.245	2.733	1.788	1.528	10/21/15	11:10	-2319	127	-7
8.317	**0.146**								
8.292	**0.153**								
20.138	0.240	2.501	1.762	1.420	10/21/15	11:15	-5146	668	-12
21.406	0.204	2.475	1.756	1.409	10/21/15	11:19	-5128	659	-12
20.025	0.143	2.467	1.752	1.408	10/21/15	11:22	-5115	679	-12
21.579	0.211	2.459	1.745	1.410	10/21/15	11:26	-5108	697	-12
20.981	0.178	2.584	1.829	1.413	10/21/15	11:32	-5094	703	-12
21.358	0.268	2.583	1.836	1.407	10/21/15	11:36	-5105	722	-12
21.409	0.193	2.579	1.832	1.408	10/21/15	11:40	-5102	738	-12
21.347	0.243	2.550	1.816	1.404	10/21/15	11:44	-5076	694	-12
20.494	0.244	2.534	1.803	1.406	10/21/15	11:47	-5093	664	-12
21.399	0.212	2.530	1.795	1.409	10/21/15	11:51	-5082	683	-12

21.403	0.139	2.516	1.789	1.406	10/21/15	11:55	-5066	647	-12
21.832	0.186	2.510	1.782	1.409	10/21/15	11:59	-5046	618	-12
8.329	0.236	2.719	1.770	1.536	10/21/15	12:04	-2408	141	-4
8.334	0.127	2.708	1.765	1.534	10/21/15	12:08	-2376	145	-4
8.290	0.174	2.704	1.762	1.535	10/21/15	12:11	-2349	147	-4
8.277	0.252	2.696	1.760	1.532	10/21/15	12:14	-2325	150	-4
8.308	**0.057**								
8.312	**0.103**								
~~15.589~~	~~0.259~~	~~2.384~~	~~1.751~~	~~1.361~~	~~10/21/15~~	~~12:19~~	~~-5277~~	~~659~~	~~3~~
19.919	0.227	2.460	1.743	1.412	10/21/15	12:23	-5118	646	-12
20.008	0.213	2.589	1.833	1.412	10/21/15	12:29	-5114	633	-12
20.097	0.208	2.596	1.854	1.400	10/21/15	12:33	-5103	572	-12
21.816	0.259	2.599	1.859	1.398	10/21/15	12:37	-5100	590	-12
21.186	0.194	2.599	1.860	1.397	10/21/15	12:40	-5088	605	-12
21.953	0.195	2.599	1.858	1.399	10/21/15	12:44	-5072	594	-13
19.170	0.135	2.613	1.861	1.404	10/21/15	12:48	-5065	584	-13
21.518	0.180	2.619	1.863	1.405	10/21/15	12:52	-5032	659	-13
21.409	0.195	2.603	1.858	1.401	10/21/15	12:55	-5054	661	-13
8.272	0.180	2.824	1.843	1.533	10/21/15	13:00	-2476	-164	-8
8.253	0.257	2.808	1.836	1.530	10/21/15	13:05	-2454	-163	-8
8.353	0.206	2.802	1.838	1.525	10/21/15	13:08	-2433	-161	-8
8.566	0.180	2.812	1.843	1.526	10/21/15	13:11	-2409	-161	-8
8.361	**0.287**								
8.334	**0.200**								
8.847	0.170	2.795	1.841	1.518	10/21/15	13:18	-1306	40	-13
8.850	0.133	2.797	1.837	1.523	10/21/15	13:22	-1280	42	-13
8.734	0.180	2.793	1.831	1.525	10/21/15	13:25	-1254	39	-13
8.683	0.142	2.796	1.833	1.525	10/21/15	13:29	-1232	39	-13
8.779	**0.167**								
20.347	0.180	2.520	1.795	1.404	10/21/15	13:35	241	-4599	-12
20.357	0.222	2.509	1.786	1.405	10/21/15	13:39	374	-4553	-12
19.936	0.189	2.515	1.778	1.414	10/21/15	13:43	177	-4593	-12
20.734	0.205	2.492	1.773	1.405	10/21/15	13:46	52	-4615	-12
20.448	0.216	2.500	1.769	1.414	10/21/15	13:50	101	-4732	-12
20.263	0.191	2.475	1.768	1.400	10/21/15	14:00	1839	7303	-8
21.391	0.219	2.460	1.763	1.395	10/21/15	14:04	1863	7196	-9
21.642	0.208	2.443	1.754	1.393	10/21/15	14:08	1896	7406	-7
18.870	0.227	2.445	1.739	1.406	10/21/15	14:13	-1964	1476	-12
19.766	0.199	2.564	1.824	1.406	10/21/15	14:19	-1960	1560	-12
19.782	0.224	2.581	1.842	1.401	10/21/15	14:22	-1801	1440	-12
21.001	0.287	2.599	1.857	1.399	10/21/15	14:26	-1984	1474	-13
8.583	0.230	2.838	1.857	1.528	10/21/15	14:30	-1307	155	-13

8.542	0.145	2.821	1.851	1.524	10/21/15	14:34	-1285	158	-13
8.551	0.194	2.818	1.846	1.526	10/21/15	14:37	-1259	158	-13
8.571	0.188	2.809	1.842	1.525	10/21/15	14:41	-1236	160	-13
8.562	**0.037**								
8.670	**0.257**								
20.637	0.171	2.603	1.863	1.397	10/21/15	14:48	-7196	3198	-29
18.997	0.220	2.564	1.857	1.381	10/21/15	14:52	-7188	3098	-27
19.703	0.156	2.542	1.847	1.377	10/21/15	14:55	-7158	3110	-27
19.053	0.225	2.541	1.842	1.380	10/21/15	14:59	-7200	3182	-28
19.914	0.235	2.547	1.840	1.384	10/21/15	15:03	-7183	3140	-28
19.251	0.201	2.534	1.838	1.379	10/21/15	15:07	-7193	3165	-28
19.529	0.159	2.546	1.838	1.385	10/21/15	15:10	-7177	3121	-28
18.805	0.143	2.552	1.825	1.398	10/21/15	15:20	-1981	1485	-4
18.917	0.208	2.531	1.818	1.393	10/21/15	15:24	-1959	1488	-3
18.862	0.220	2.586	1.844	1.403	10/21/15	15:27	-1969	1500	-3
8.548	0.166	2.886	1.889	1.528	10/21/15	15:33	-1317	17	-19
8.828	0.220	2.902	1.898	1.529	10/21/15	15:36	-1293	19	-18
8.723	0.178	2.904	1.900	1.528	10/21/15	15:40	-1266	22	-18
8.611	0.178	2.887	1.896	1.523	10/21/15	15:43	-1242	20	-18
8.678	**0.247**								
8.620	**0.205**								
19.792	0.217	2.604	1.862	1.398	10/21/15	15:47	-1984	1545	-17
19.437	0.268	2.517	1.809	1.391	10/21/15	15:51	-1951	1550	-18
19.551	0.229	2.497	1.780	1.402	10/21/15	15:55	-1962	1538	-18
19.321	0.191	2.482	1.769	1.403	10/21/15	15:59	-1971	1524	-18
18.917	0.269	2.470	1.763	1.401	10/21/15	16:02	-1981	1514	-18
18.902	0.217	2.468	1.758	1.404	10/21/15	16:06	-1960	1512	-18
19.818	0.270	2.471	1.744	1.417	10/21/15	16:13	-487	2441	-22
19.694	0.224	2.457	1.739	1.413	10/21/15	16:16	-471	2435	-22
20.240	0.167	2.585	1.834	1.409	10/21/15	16:22	-489	2426	-22
19.783	0.206	2.615	1.854	1.410	10/21/15	16:26	-470	2424	-22
21.473	0.208	2.611	1.860	1.404	10/21/15	16:30	-488	2412	-22
21.271	0.276	2.627	1.866	1.408	10/21/15	16:33	-468	2408	-22
8.524	0.178	2.855	1.868	1.528	10/21/15	16:38	-1313	175	-19
8.636	0.195	2.858	1.871	1.528	10/21/15	16:42	-1288	179	-19
8.642	0.119	2.851	1.871	1.524	10/21/15	16:45	-1267	182	-19
8.630	0.190	2.856	1.876	1.522	10/21/15	16:49	-1245	184	-19
8.608	**0.112**								
8.643	**0.193**								
21.496	0.201	2.627	1.878	1.399	10/21/15	16:53	-486	2398	-22
21.426	0.210	2.618	1.874	1.397	10/21/15	16:56	-467	2393	-22
20.682	0.155	2.612	1.871	1.396	10/21/15	17:00	-486	2383	-22
20.232	0.259	2.607	1.869	1.395	10/21/15	17:03	-465	2379	-22
20.131	0.145	2.605	1.868	1.395	10/21/15	17:07	-493	2371	-22

20.024	0.163	2.595	1.861	1.395	10/21/15	17:10	-474	2365	-22
19.972	0.234	2.582	1.851	1.395	10/21/15	17:15	-458	2364	-22
20.355	0.201	2.581	1.840	1.403	10/21/15	17:19	-497	2596	-22
20.033	0.204	2.567	1.836	1.399	10/21/15	17:23	-509	2583	-22
21.077	0.165	2.587	1.838	1.407	10/21/15	17:27	-493	2573	-22
20.100	0.174	2.569	1.840	1.396	10/21/15	17:31	-512	2566	-22
21.595	0.166	2.578	1.838	1.403	10/21/15	17:34	-493	2557	-22
8.631	0.145	2.795	1.831	1.527	10/21/15	17:39	-1314	198	-19
8.545	0.205	2.781	1.825	1.524	10/21/15	17:42	-1289	202	-20
8.653	0.161	2.776	1.819	1.526	10/21/15	17:45	-1268	207	-19
8.829	0.212	2.742	1.813	1.512	10/21/15	17:49	-1246	210	-19
8.665	**0.238**								
8.636	**0.183**								
21.639	0.203	2.532	1.810	1.399	10/21/15	17:54	-510	2551	-22
21.400	0.254	2.534	1.810	1.400	10/21/15	17:57	-492	2543	-22
21.438	0.264	2.546	1.816	1.402	10/21/15	18:01	-511	2534	-22
21.302	0.221	2.546	1.811	1.406	10/21/15	18:05	-493	2527	-22
21.490	0.203	2.528	1.801	1.403	10/21/15	18:08	-511	2519	-22
21.603	0.194	2.520	1.794	1.405	10/21/15	18:12	-492	2511	-22
21.554	0.204	2.514	1.789	1.406	10/21/15	18:15	-511	2498	-22
21.314	0.213	2.535	1.793	1.414	10/21/15	18:19	-497	2492	-22
21.360	0.228	2.517	1.793	1.404	10/21/15	18:23	-508	2485	-22
21.386	0.265	2.515	1.784	1.410	10/21/15	18:26	-490	2477	-22
19.758	0.220	2.489	1.775	1.402	10/21/15	18:30	-508	2467	-22
19.873	0.142	2.484	1.766	1.407	10/21/15	18:34	-483	2466	-22
8.566	0.137	2.693	1.754	1.535	10/21/15	18:40	-1315	224	-19
8.636	0.212	2.686	1.756	1.530	10/21/15	18:44	-1291	229	-19
8.572	0.235	2.676	1.749	1.530	10/21/15	18:47	-1270	233	-20
8.472	0.163	2.797	1.828	1.531	10/21/15	18:53	-1247	236	-20
8.562	**0.135**								
8.613	**0.210**								
21.119	0.152	2.585	1.851	1.396	10/21/15	19:02	-328	2458	-22
19.810	0.197	2.607	1.861	1.400	10/21/15	19:06	-302	2472	-23
21.633	0.261	2.567	1.845	1.392	10/21/15	19:10	-338	2476	-22
20.289	0.247	2.557	1.827	1.400	10/21/15	19:13	-338	2436	-22
21.580	0.182	2.541	1.819	1.397	10/21/15	19:17	-355	2485	-22
21.550	0.211	2.532	1.816	1.394	10/21/15	19:21	-373	2498	-22
21.528	0.226	2.522	1.810	1.393	10/21/15	19:24	-390	2504	-22
21.367	0.216	2.535	1.807	1.403	10/21/15	19:27	-389	2520	-22
21.588	0.190	2.520	1.801	1.399	10/21/15	19:32	-477	2538	-22
21.563	0.189	2.519	1.799	1.400	10/21/15	19:35	-474	2559	-22
21.391	0.198	2.522	1.797	1.403	10/21/15	19:39	-459	2545	-22
21.519	0.267	2.515	1.795	1.401	10/21/15	19:43	-445	2560	-22
8.493	0.220	2.744	1.792	1.532	10/21/15	19:47	-1315	-8	-20

8.714	0.163	2.733	1.788	1.528	10/21/15	19:50	-1292	-6	-20
8.595	0.230	2.745	1.791	1.533	10/21/15	19:54	-1264	-4	-19
8.550	0.179	2.742	1.797	1.525	10/21/15	19:57	-1240	-5	-20
8.588	**0.188**								
8.575	**0.154**								

8.760	0.183	2.681	1.772	1.513	10/21/15	20:13	-1319	246	-20
8.480	0.204	2.722	1.777	1.531	10/21/15	20:16	-1294	250	-20
8.508	0.209	2.719	1.782	1.526	10/21/15	20:20	-1268	255	-20
8.682	0.218	2.704	1.775	1.523	10/21/15	20:23	-1245	258	-20
8.608	**0.271**								
21.650	0.150	2.469	1.768	1.396	10/21/15	20:28	-458	2567	-22
21.231	0.241	2.462	1.765	1.395	10/21/15	20:31	-443	2576	-22
21.463	0.206	2.467	1.761	1.401	10/21/15	20:36	-451	2534	-22
19.835	0.162	2.512	1.778	1.412	10/21/15	20:40	-601	2449	-22
21.499	0.248	2.441	1.746	1.398	10/21/15	20:45	-585	2443	-22
21.657	0.215	2.559	1.831	1.397	10/21/15	20:52	-583	2459	-22
20.135	0.236	2.561	1.842	1.391	10/21/15	20:56	-592	2474	-22
21.454	0.149	2.569	1.846	1.392	10/21/15	21:01	-576	2476	-22
20.987	0.278	2.581	1.851	1.394	10/21/15	21:05	-379	2406	-22
20.888	0.240	2.570	1.848	1.391	10/21/15	21:10	-394	2397	-22
21.372	0.229	2.566	1.843	1.392	10/21/15	21:15	-397	2412	-22
20.975	0.268	2.572	1.841	1.397	10/21/15	21:18	-411	2405	-23
20.760	0.168	2.568	1.844	1.393	10/21/15	21:23	-413	2424	-22
8.642	0.202	2.767	1.824	1.517	10/21/15	21:28	-1206	158	-19
8.706	0.153	2.771	1.826	1.518	10/21/15	21:31	-1180	158	-20
8.652	0.199	2.778	1.829	1.519	10/21/15	21:35	-1154	160	-20
8.609	0.147	2.757	1.820	1.515	10/21/15	21:38	-1130	158	-20
8.652	**0.081**								
8.630	**0.191**								

8.563	0.211	2.773	1.805	1.536	10/21/15	21:57	799	-1520	2
8.659	0.193	2.766	1.802	1.535	10/21/15	22:00	823	-1520	2
8.710	0.185	2.768	1.807	1.532	10/21/15	22:04	851	-1520	2
8.691	0.194	2.783	1.817	1.532	10/21/15	22:07	876	-1520	1
21.612	0.199	2.540	1.803	1.408	10/21/15	22:17	1593	-2716	4
21.311	0.223	2.527	1.796	1.407	10/21/15	22:20	1593	-2731	3
19.910	0.156	2.512	1.790	1.403	10/21/15	22:24	1608	-2734	4
20.289	0.137	2.492	1.783	1.398	10/21/15	22:28	1597	-2745	4
20.133	0.192	2.488	1.776	1.401	10/21/15	22:32	1614	-2743	4
21.069	0.163	2.530	1.801	1.405	10/21/15	22:36	1596	-2760	4
21.351	0.225	2.534	1.813	1.398	10/21/15	22:40	1606	-2772	4
21.429	0.200	2.465	1.766	1.395	10/21/15	22:43	1621	-2780	4
21.403	0.151	2.449	1.747	1.402	10/21/15	22:47	1603	-2790	3

20.303	0.285	2.578	1.844	1.398	10/21/15	22:55	1621	-2792	4
19.417	0.209	2.588	1.857	1.394	10/21/15	22:59	1616	-2808	4
19.133	0.201	2.587	1.860	1.391	10/21/15	23:03	1634	-2800	4
8.603	0.205	2.850	1.860	1.533	10/21/15	23:09	800	-1541	3
8.599	0.182	2.847	1.859	1.532	10/21/15	23:12	821	-1544	2
8.470	0.226	2.842	1.858	1.529	10/21/15	23:15	844	-1545	2
8.583	0.211	2.838	1.858	1.528	10/21/15	23:19	870	-1545	1
8.564	**0.126**								
8.610	**0.154**								
21.234	0.201	2.581	1.849	1.395	10/21/15	23:24	1581	-2751	4
21.672	0.210	2.571	1.844	1.394	10/21/15	23:27	1569	-2739	4
21.643	0.164	2.568	1.840	1.396	10/21/15	23:32	1571	-2723	4
21.344	0.160	2.569	1.837	1.398	10/21/15	23:36	1550	-2739	4
19.571	0.141	2.563	1.835	1.397	10/21/15	23:39	1542	-2723	4
19.407	0.210	2.559	1.832	1.397	10/21/15	23:44	1532	-2736	4
20.419	0.221	2.559	1.831	1.398	10/21/15	23:49	1625	-2730	4
21.572	0.212	2.551	1.825	1.398	10/21/15	23:53	1627	-2743	4
21.500	0.217	2.558	1.821	1.405	10/21/15	23:57	1643	-2730	4
21.354	0.195	2.561	1.820	1.407	10/22/15	0:01	1664	-2730	4
21.017	0.241	2.559	1.815	1.410	10/22/15	0:05	1668	-2716	4
21.295	0.274	2.511	1.809	1.388	10/22/15	0:10	1633	-2716	4
8.353	0.218	2.785	1.819	1.531	10/22/15	0:14	802	-1567	2
8.347	0.179	2.774	1.815	1.529	10/22/15	0:18	823	-1567	2
8.507	0.182	2.763	1.808	1.528	10/22/15	0:21	845	-1565	1
8.349	0.144	2.755	1.803	1.528	10/22/15	0:24	869	-1565	1
8.389	**0.157**								
8.476	**0.229**								
20.853	0.270	2.515	1.794	1.402	10/22/15	0:30	1644	-2764	4
21.118	0.180	2.511	1.791	1.402	10/22/15	0:34	1668	-2773	4
21.311	0.199	2.510	1.785	1.406	10/22/15	0:39	1682	-2756	4
19.625	0.197	2.484	1.780	1.396	10/22/15	0:43	1585	-2801	4
21.264	0.183	2.540	1.810	1.403	10/22/15	0:46	1562	-2795	4
8.573	0.214	2.708	1.768	1.531	10/22/15	0:54	807	-1592	2
8.365	0.208	2.688	1.754	1.532	10/22/15	0:57	828	-1592	1
8.407	0.189	2.673	1.746	1.531	10/22/15	1:01	852	-1595	1
8.458	0.256	2.669	1.741	1.533	10/22/15	1:04	873	-1596	1
8.451	**0.180**								
8.420	**0.170**								
20.958	0.240	2.608	1.852	1.408	10/22/15	1:18	1586	-6265	6
20.856	0.211	2.612	1.855	1.408	10/22/15	1:22	1593	-6279	6
20.838	0.206	2.601	1.855	1.403	10/22/15	1:26	1576	-6249	6
20.858	0.231	2.599	1.851	1.404	10/22/15	1:30	1561	-6237	5
20.886	0.206	2.593	1.849	1.402	10/22/15	1:34	1530	-6238	6

19.602	0.218	2.567	1.845	1.391	10/22/15	1:37	1505	-6241	6
20.802	0.260	2.571	1.840	1.397	10/22/15	1:42	1515	-6251	6
19.875	0.204	2.575	1.836	1.402	10/22/15	1:46	1650	-6206	6
20.494	0.230	2.573	1.833	1.404	10/22/15	1:50	1678	-6191	6
20.805	0.225	2.571	1.831	1.404	10/22/15	1:54	1647	-6190	6
20.987	0.214	2.566	1.826	1.405	10/22/15	1:58	1632	-6200	6
19.902	0.230	2.572	1.824	1.410	10/22/15	2:02	1653	-6220	6
8.479	0.166	2.783	1.820	1.529	10/22/15	2:08	814	-1615	2
8.583	0.206	2.776	1.819	1.527	10/22/15	2:11	834	-1617	2
8.530	0.175	2.772	1.816	1.527	10/22/15	2:15	857	-1617	1
8.491	0.268	2.769	1.815	1.526	10/22/15	2:18	880	-1619	1
8.521	**0.094**								
8.486	**0.152**								
20.105	0.220	2.548	1.810	1.407	10/22/15	2:22	1666	-6228	6
20.798	0.248	2.548	1.808	1.409	10/22/15	2:26	1678	-6239	6
20.019	0.262	2.555	1.809	1.412	10/22/15	2:29	1686	-6250	6
20.767	0.214	2.551	1.813	1.407	10/22/15	2:33	1678	-6173	6
19.941	0.207	2.549	1.809	1.409	10/22/15	2:37	1701	-6191	6
20.626	0.231	2.546	1.805	1.411	10/22/15	2:41	1615	-6244	6
20.540	0.198	2.536	1.802	1.407	10/22/15	2:44	1652	-6281	6
20.842	0.273	2.544	1.807	1.408	10/22/15	2:48	1633	-6254	6
20.585	0.185	2.550	1.814	1.406	10/22/15	2:52	1577	-6187	6
19.418	0.128	2.529	1.806	1.401	10/22/15	2:55	1613	-6167	6
20.903	0.201	2.520	1.794	1.405	10/22/15	2:59	1623	-6183	6
19.574	0.186	2.516	1.786	1.409	10/22/15	3:03	1605	-6153	6
19.965	0.263	2.518	1.781	1.414	10/22/15	3:08	1606	-6142	6
19.435	0.215	2.501	1.775	1.409	10/22/15	3:12	1578	-6171	6
21.324	0.294	2.475	1.769	1.399	10/22/15	3:16	1647	-6159	9
8.379	0.156	2.697	1.762	1.531	10/22/15	3:20	819	-1642	2
8.355	0.172	2.796	1.806	1.548	10/22/15	3:23	841	-1643	1
8.294	0.159	2.710	1.794	1.510	10/22/15	3:27	862	-1644	1
8.611	0.177	2.678	1.755	1.526	10/22/15	3:30	884	-1643	1
8.410	**0.278**								
8.465	**0.226**								
20.885	0.202	2.445	1.735	1.409	10/22/15	3:35	1629	-6166	6
21.040	0.181	2.444	1.731	1.412	10/22/15	3:39	1602	-6181	6
19.422	0.149	2.566	1.824	1.407	10/22/15	3:46	1594	-6170	6
20.934	0.175	2.594	1.842	1.408	10/22/15	3:51	1592	-6193	6
19.593	0.153	2.584	1.847	1.399	10/22/15	3:54	1624	-6153	6
19.140	0.217	2.590	1.847	1.402	10/22/15	3:58	1640	-6148	6
20.508	0.256	2.590	1.843	1.405	10/22/15	4:02	1655	-6148	6
20.150	0.267	2.591	1.842	1.407	10/22/15	4:06	1661	-6135	7
20.712	0.205	2.596	1.838	1.412	10/22/15	4:10	1669	-6145	6
19.246	0.192	2.572	1.834	1.402	10/22/15	4:14	1567	-6184	6
20.111	0.186	2.581	1.832	1.408	10/22/15	4:18	1566	-6196	6

20.815	0.220	2.575	1.830	1.408	10/22/15	4:22	1583	-6205	6
19.685	0.247	2.561	1.826	1.402	10/22/15	4:26	1549	-6200	5
20.662	0.190	2.555	1.822	1.403	10/22/15	4:30	1525	-6222	6
8.649	0.201	2.783	1.820	1.529	10/22/15	4:34	822	-1667	1
8.390	0.208	2.777	1.817	1.528	10/22/15	4:37	843	-1668	1
8.668	0.189	2.771	1.815	1.526	10/22/15	4:40	866	-1668	1
8.381	0.190	2.767	1.813	1.527	10/22/15	4:44	888	-1668	0
8.522	**0.316**								
8.466	**0.300**								
8.418	0.179	2.761	1.800	1.534	10/22/15	5:00	-288	274	-17
8.506	0.168	2.755	1.799	1.531	10/22/15	5:03	-266	271	-17
8.451	0.213	2.747	1.797	1.529	10/22/15	5:07	-240	268	-17
8.555	0.214	2.745	1.797	1.528	10/22/15	5:10	-214	266	-17
19.190	0.227	2.528	1.789	1.413	10/22/15	5:28	-1571	4930	-13
18.588	0.239	2.526	1.783	1.417	10/22/15	5:32	-1620	4669	-13
18.427	0.149	2.515	1.777	1.415	10/22/15	5:36	-1617	4720	-13
18.801	0.195	2.503	1.774	1.411	10/22/15	5:40	-1551	4816	-12
19.096	0.197	2.500	1.769	1.413	10/22/15	5:44	-1494	4802	-12
20.536	0.175	2.503	1.772	1.412	10/22/15	5:47	-1620	4829	-12
20.464	0.247	2.510	1.778	1.412	10/22/15	5:51	-1680	4844	-12
19.697	0.208	2.507	1.774	1.413	10/22/15	5:54	-1740	4846	-13
19.884	0.155	2.501	1.767	1.415	10/22/15	5:58	-1669	4777	-13
18.667	0.175	2.489	1.762	1.412	10/22/15	6:02	-1731	4735	-13
19.328	0.205	2.503	1.767	1.416	10/22/15	6:05	-1703	4666	-12
19.241	0.161	2.515	1.777	1.415	10/22/15	6:09	-1539	4675	-12
8.243	0.196	2.701	1.766	1.529	10/22/15	6:14	-299	254	-17
8.382	0.221	2.683	1.760	1.525	10/22/15	6:17	-272	249	-17
8.398	0.241	2.684	1.755	1.530	10/22/15	6:20	-245	246	-17
8.555	0.190	2.674	1.751	1.527	10/22/15	6:23	-216	243	-17
8.395	**0.255**								
8.439	**0.207**								
18.995	0.225	2.598	1.829	1.420	10/22/15	6:30	-1508	4754	-12
19.744	0.245	2.617	1.860	1.407	10/22/15	6:33	-1587	4799	-12
20.325	0.196	2.665	1.902	1.401	10/22/15	6:37	-1610	4965	-13
21.096	0.216	2.793	1.996	1.400	10/22/15	6:41	-1656	4932	-12
19.369	0.226	2.832	2.022	1.400	10/22/15	6:45	-1727	4936	-12
20.987	0.192	2.820	2.013	1.401	10/22/15	6:49	-1574	5085	-12
21.172	0.231	2.713	1.955	1.388	10/22/15	6:52	-1558	5147	-12
20.861	0.218	2.631	1.871	1.406	10/22/15	6:57	-1640	5085	-12
18.656	0.217	2.607	1.853	1.407	10/22/15	7:00	-1700	5071	-12
20.318	0.206	2.594	1.842	1.408	10/22/15	7:04	-1487	5049	-12
20.236	0.240	2.580	1.833	1.407	10/22/15	7:08	-1529	5067	-13
20.883	0.179	2.575	1.829	1.408	10/22/15	7:11	-1448	5127	-12

8.287	0.214	2.779	1.820	1.526	10/22/15	7:15	-302	233	-17
8.301	0.198	2.764	1.817	1.522	10/22/15	7:18	-278	229	-17
8.196	0.205	2.764	1.812	1.525	10/22/15	7:22	-249	223	-17
8.344	0.193	2.755	1.809	1.523	10/22/15	7:25	-222	219	-17
8.282	**0.125**								
8.338	**0.221**								
18.615	0.270	2.548	1.801	1.415	10/22/15	7:30	-1674	5171	-13
19.696	0.209	2.541	1.800	1.412	10/22/15	7:33	-1620	5157	-12
20.941	0.165	2.537	1.796	1.413	10/22/15	7:37	-1513	5133	-12
19.405	0.152	2.542	1.790	1.420	10/22/15	7:41	-1399	5267	-13
20.432	0.239	2.527	1.788	1.413	10/22/15	7:44	-1455	5226	-12
20.937	0.141	2.527	1.786	1.415	10/22/15	7:48	-1503	5178	-12
20.759	0.205	2.526	1.783	1.417	10/22/15	7:51	-1662	5039	-13
18.780	0.175	2.516	1.777	1.415	10/22/15	7:56	-1618	5206	-13
18.685	0.124	2.511	1.776	1.414	10/22/15	8:01	-1566	4713	-12
18.301	0.250	2.510	1.771	1.417	10/22/15	8:04	-1671	4692	-13
18.489	0.211	2.497	1.768	1.412	10/22/15	8:08	-1599	4753	-13
18.586	0.205	2.493	1.764	1.413	10/22/15	8:13	-1546	4840	-12
8.090	0.182	2.695	1.760	1.532	10/22/15	8:16	-306	211	-18
8.115	0.202	2.689	1.758	1.529	10/22/15	8:20	-281	205	-17
8.319	0.228	2.681	1.757	1.526	10/22/15	8:23	-254	202	-17
8.265	0.213	2.686	1.756	1.530	10/22/15	8:27	-227	196	-17
8.197	**0.224**								
8.240	**0.191**								

DTFA-Y	Mass	C-bkg	H1-bkg	Sample Name	$^{16}OH/^{16}O$	Fo#	Phase	Note
0	898615	-2624140	-54734	101/	1.91E-04			
0	898615	-2624140	-54734	101/	1.74E-04			
1	898615	-2624140	-54734	101/	1.86E-04			
0	898615	-2624140	-54734	101/	1.73E-04			
0	898615	-2624140	-54734	101/	1.93E-04			
-5	898615	-2624140	-54734	101/	1.38E-04			
-2	898615	-2624140	-54734	101/	1.47E-04			
-8	898615	-2624140	-54734	101/	1.43E-04			
-7	898615	-2624140	-54734	101/	1.42E-04			
-6	898615	-2624140	-54734	101/	2.68E-04			
-7	898615	-2624140	-54734	101/	2.26E-04			
-9	898615	-2624140	-54734	101/	2.26E-04			
-8	898615	-2624140	-54734	101/	2.32E-04			
-2	898615	-2624140	-54734	101/	1.83E-04			
-1	898615	-2624140	-54734	101/	1.76E-04			
-2	898615	-2624140	-54734	101/	1.72E-04			
-2	898615	-2624140	-54734	101/	1.74E-04			
0	898620	-2673420	-55420	101/	1.62E-04			
0	898620	-2673420	-55420	101/	1.61E-04			
-1	898620	-2673420	-55420	101/	1.60E-04			
-1	898620	-2673420	-55420	101/	1.57E-04			
-4	898620	-2673420	-55420	101/	1.29E-04			

-6	898620	-2673420	-55420	101/	2.57E-04		
-7	898620	-2673420	-55420	101/	1.37E-04		
-4	898620	-2673420	-55420	101/	1.66E-04		
-5	898620	-2673420	-55420	101/	1.75E-04		
-5	898620	-2673420	-55420	101/	1.76E-04		
-5	898620	-2673420	-55420	101/	1.78E-04		
2	898620	-2673420	-55420	101/	1.59E-04	**99**	fo
1	898620	-2673420	-55420	101/	1.73E-04	**99**	fo
1	898620	-2673420	-55420	101/	1.46E-03	**99**	fo
2	898620	-2673420	-55420	101/	2.32E-04	**99**	fo
2	898620	-2673420	-55420	101/	9.82E-04	**99**	fo
2	898620	-2673420	-55420	101/	2.55E-04	**99**	fo
1	898620	-2673420	-55420	101/	2.54E-04	**99**	fo
1	898620	-2673420	-55420	101/	2.56E-04	**99**	fo
1	898620	-2673420	-55420	101/	2.66E-04	**99**	fo
1	898620	-2673420	-55420	101/	2.55E-04	**99**	fo
-6	898620	-2673420	-55420	UWG2 std	1.85E-04		
-6	898620	-2673420	-55420	UWG2 std	1.84E-04		
-6	898620	-2673420	-55420	UWG2 std	2.02E-04		
-6	898620	-2673420	-55420	UWG2 std	1.88E-04		
1	898620	-2673420	-55420	G9/	1.54E-04	**99**	fo
1	898620	-2673420	-55420	G9/	2.11E-04	**99**	fo
1	898620	-2673420	-55420	G9/	1.82E-04	**99**	fo
1	898620	-2673420	-55420	G9/	2.22E-04	**99**	fo
1	898620	-2673420	-55420	G9/	2.10E-04	**99**	fo
1	898620	-2673420	-55420	G9/	1.87E-04	**99**	fo
1	898620	-2673420	-55420	G9/	2.36E-04	**99**	fo
1	898620	-2673420	-55420	G9/	2.70E-04	**99**	fo
1	898620	-2673420	-55420	G9/	2.38E-04	**99**	fo
0	898620	-2673420	-55420	G9/	2.49E-04	**99**	fo
-5	898620	-2673420	-55420	G9/	1.75E-04		
-6	898620	-2673420	-55420	G9/	1.98E-04		
-6	898620	-2673420	-55420	G9/	1.80E-04		
-6	898620	-2673420	-55420	G9/	1.80E-04		
1	898620	-2673420	-55420	G9/	1.61E-04	**99**	fo
2	898620	-2673420	-55420	G9/	2.39E-04	**99**	fo
2	898620	-2673420	-55420	G9/	1.80E-04	**99**	fo
1	898620	-2673420	-55420	G9/	1.76E-04	**99**	fo

1	898620	-2673420	-55420	G9/	2.32E-04	**99**	fo
1	898620	-2673420	-55420	G9/	1.76E-04	**99**	fo
1	898620	-2673420	-55420	G9/	1.92E-04	**99**	fo
2	898620	-2673420	-55420	G9/	2.76E-04	**99**	fo
2	898620	-2673420	-55420	G9/	3.20E-04	**99**	fo
2	898620	-2673420	-55420	G9/	2.91E-04	**99**	fo
-6	898620	-2673420	-55420	UWG2 std	1.67E-04		
-5	898620	-2673420	-55420	UWG2 std	1.72E-04		
-5	898620	-2673420	-55420	UWG2 std	1.81E-04		
-5	898620	-2673420	-55420	UWG2 std	1.74E-04		
2	898620	-2673420	-55420	UWG2 std	1.46E-03		
1	898620	-2673420	-55420	UWG2 std	1.54E-03		
0	898620	-2673420	-55420	UWG2 std	1.46E-03		
-3	898620	-2673420	-55420	UWG2 std	1.26E-03		
0	898620	-2673420	-55420	UWG2 std	1.40E-03		
3	898620	-2673420	-55420	UWG2 std	1.37E-03		
3	898620	-2673420	-55420	UWG2 std	1.39E-03		
0	898620	-2673420	-55420	UWG2 std	1.41E-03		
0	898620	-2673420	-55420	UWG2 std	1.39E-03		
-1	898620	-2673420	-55420	UWG2 std	1.37E-03		
-7	898620	-2673420	-55420	UWG2 std	1.32E-03		
0	898620	-2673420	-55420	UWG2 std	1.36E-03		
-6	898620	-2673420	-55420	UWG2 std	1.50E-04		
-6	898620	-2673420	-55420	UWG2 std	1.52E-04		
-6	898620	-2673420	-55420	UWG2 std	1.54E-04		
-7	898620	-2673420	-55420	UWG2 std	1.55E-04		
-10	898620	-2673420	-55420	UWG2 std	1.66E-04	**99**	fo
-10	898620	-2673420	-55420	UWG2 std	2.17E-04	**99**	fo
-9	898620	-2673420	-55420	UWG2 std	1.69E-04	**99**	fo
-9	898620	-2673420	-55420	UWG2 std	1.97E-04	**99**	fo
-11	898620	-2673420	-55420	UWG2 std	1.94E-04	**99**	fo
-10	898620	-2673420	-55420	UWG2 std	2.34E-04	**99**	fo
-8	898620	-2673420	-55420	UWG2 std	1.43E-04	**99**	fo
-7	898620	-2673420	-55420	UWG2 std	1.78E-04	**99**	fo

~~-7~~	~~898620~~	~~-2673420~~	~~-55420~~	~~UWG2 std~~	~~4.92E-03~~	~~**99**~~	~~fo~~	~~humite~~
-7	898620	-2673420	-55420	UWG2 std	2.05E-04	**99**	fo	
-6	898620	-2673420	-55420	2ccn-UWG	1.64E-04			
-7	898620	-2673420	-55420	2ccn-UWG	1.61E-04			
-6	898620	-2673420	-55420	2ccn-UWG	1.62E-04			
-7	898620	-2673420	-55420	2ccn-UWG	1.56E-04			
-72	898620	-2673420	-55420	2ccn-UWG	1.53E-04	**99**	fo	
~~-68~~	~~898620~~	~~-2673420~~	~~-55420~~	~~2ccn-UWG~~	~~3.94E-04~~	~~**99**~~	~~fo~~	~~humite~~
-5	898620	-2673420	-55420	2ccn-UWG	1.24E-04	**99**	fo	
-5	898620	-2673420	-55420	2ccn-UWG	1.36E-03	**99**	fo	
-6	898620	-2673420	-55420	2ccn-UWG	1.93E-03	**99**	fo	
-5	898620	-2673420	-55420	2ccn-UWG	2.38E-04	**99**	fo	
-15	898620	-2673420	-55420	2ccn-UWG	1.85E-04	**99**	fo	
~~-16~~	~~898620~~	~~-2673420~~	~~-55420~~	~~2ccn-UWG~~	~~4.51E-04~~	~~**99**~~	~~fo~~	~~humite~~
-18	898620	-2673420	-55420	2ccn-UWG	1.78E-04	**99**	fo	
-17	898620	-2673420	-55420	2ccn-UWG	1.97E-04	**99**	fo	
-8	898620	-2673420	-55420	2ccn-UWG	1.68E-04			
-8	898620	-2673420	-55420	2ccn-UWG	1.68E-04			
-8	898620	-2673420	-55420	2ccn-UWG	1.70E-04			
-7	898620	-2673420	-55420	2ccn-UWG	1.57E-04			
					1.633E-04			
-14	898620	-2673420	-55420	2ccn-UWG	1.43E-04	**99**	fo	
~~-13~~	~~898620~~	~~-2673420~~	~~-55420~~	~~2ccn-UWG~~	~~6.44E-03~~	~~**99**~~	~~fo~~	~~humite~~
~~-14~~	~~898620~~	~~-2673420~~	~~-55420~~	~~2ccn-UWG~~	~~5.40E-03~~	~~**99**~~	~~fo~~	~~humite~~
-5	898620	-2673420	-55420	2ccn-UWG	1.21E-04	**99**	fo	
-5	898620	-2673420	-55420	2ccn-UWG	8.74E-04	**99**	fo	
-6	898620	-2673420	-55420	2ccn-UWG	2.36E-04	**99**	fo	
-5	898620	-2673420	-55420	2ccn-UWG	1.87E-04	**99**	fo	
-4	898620	-2673420	-55420	2ccn-UWG	1.30E-04	**99**	fo	
-5	898620	-2673420	-55420	2ccn-UWG	3.21E-04	**99**	fo	
~~-5~~	~~898620~~	~~-2673420~~	~~-55420~~	~~2ccn-UWG~~	~~2.70E-03~~	~~**99**~~	~~fo~~	~~humite~~
-7	898620	-2673420	-55420	2ccn-UWG	1.54E-04			
-8	898620	-2673420	-55420	2ccn-UWG	1.61E-04			
-8	898620	-2673420	-55420	2ccn-UWG	1.58E-04			
-7	898620	-2673420	-55420	2ccn-UWG	1.60E-04			
-8	898620	-2673420	-55420	2ccn-UWG	2.93E-04	**99**	fo	
-8	898620	-2673420	-55420	2ccn-UWG	1.70E-04	**99**	fo	
-7	898620	-2673420	-55420	2ccn-UWG	2.13E-04	**99**	fo	

-8	898620	-2673420	-55420	2ccn-UWG	2.58E-04	**99**	fo
-8	898620	-2673420	-55420	2ccn-UWG	2.64E-03	**99**	fo
-8	898620	-2673420	-55420	2ccn-UWG	1.66E-04	**99**	fo
-5	898620	-2673420	-55420	2ccn-UWG	2.15E-04	**99**	fo
-5	898620	-2673420	-55420	2ccn-UWG	1.76E-04	**99**	fo
-5	898620	-2673420	-55420	2ccn-UWG	1.95E-04	**99**	fo
-6	898620	-2673420	-55420	2ccn-UWG	1.97E-04	**99**	fo
-8	898620	-2673420	-55420	2ccn-UWG	1.64E-04		
-8	898620	-2673420	-55420	2ccn-UWG	1.62E-04		
-8	898620	-2673420	-55420	2ccn-UWG	1.77E-04		
-7	898620	-2673420	-55420	2ccn-UWG	1.55E-04		

3	898618	-2673420	-55420	2ccn-UWG	2.09E-04		
3	898618	-2673420	-55420	2ccn-UWG	2.16E-04		
2	898618	-2673420	-55420	2ccn-UWG	2.19E-04		
2	898618	-2673420	-55420	2ccn-UWG	2.21E-04		
-24	898618	-2673420	-55420	2ccn-UWG	2.57E-04	**99**	fo
-23	898618	-2673420	-55420	2ccn-UWG	2.38E-04	**99**	fo
-26	898618	-2673420	-55420	2ccn-UWG	2.64E-04	**99**	fo
-25	898618	-2673420	-55420	2ccn-UWG	2.43E-04	**99**	fo
5	898618	-2673420	-55420	2ccn-UWG	2.05E-04	**99**	fo
4	898618	-2673420	-55420	2ccn-UWG	2.84E-04	**99**	fo
6	898618	-2673420	-55420	2ccn-UWG	2.46E-04	**99**	fo
4	898618	-2673420	-55420	2ccn-UWG	2.59E-04	**99**	fo
5	898618	-2673420	-55420	2ccn-UWG	2.12E-04	**99**	fo
5	898618	-2673420	-55420	2ccn-UWG	2.68E-04	**99**	fo
2	898618	-2673420	-55420	2bbo-UWC	2.39E-04		
1	898618	-2673420	-55420	2bbo-UWC	2.51E-04		
2	898618	-2673420	-55420	2bbo-UWC	2.51E-04		
2	898618	-2673420	-55420	2bbo-UWC	2.50E-04		
-5	898618	-2673420	-55420	2bbo-UWC	3.21E-04	**99**	fo
-4	898618	-2673420	-55420	2bbo-UWC	2.87E-04	**99**	fo
-5	898618	-2673420	-55420	2bbo-UWC	2.70E-04	**99**	fo
0	898618	-2673420	-55420	2bbo-UWC	2.27E-04	**99**	fo
-1	898618	-2673420	-55420	2bbo-UWC	2.34E-04	**99**	fo
23	898618	-2673420	-55420	2bbo-UWC	1.82E-04	**99**	fo
24	898618	-2673420	-55420	2bbo-UWC	1.88E-04	**99**	fo
-11	898618	-2673420	-55420	2bbo-UWC	2.01E-04	**99**	fo
-11	898618	-2673420	-55420	2bbo-UWC	2.53E-04	**99**	fo

-11	898618	-2673420	-55420	2bbo-UWC	2.29E-04	**99**	fo
2	898618	-2673420	-55420	2bbo-UWC	2.40E-04		
2	898618	-2673420	-55420	2bbo-UWC	2.34E-04		
2	898618	-2673420	-55420	2bbo-UWC	2.28E-04		
2	898618	-2673420	-55420	2bbo-UWC	2.17E-04		
-15	898618	-2673420	-55420	2bbo-UWC	1.80E-04		
-16	898618	-2673420	-55420	2bbo-UWC	1.87E-04		
-15	898618	-2673420	-55420	2bbo-UWC	1.89E-04		
-15	898618	-2673420	-55420	2bbo-UWC	1.91E-04		
-13	898618	-2673420	-55420	2bbo-UWC	9.79E-03	**99**	fo
-13	898618	-2673420	-55420	2bbo-UWC	9.85E-03	**99**	fo
-14	898618	-2673420	-55420	2bbo-UWC	9.92E-03	**99**	fo
-14	898618	-2673420	-55420	2bbo-UWC	9.77E-03	**99**	fo
-14	898618	-2673420	-55420	2bbo-UWC	2.59E-04	**99**	fo
-14	898618	-2673420	-55420	2bbo-UWC	2.54E-04	**99**	fo
-13	898618	-2673420	-55420	2bbo-UWC	2.25E-04	**99**	fo
-13	898618	-2673420	-55420	2bbo-UWC	8.55E-04	**99**	fo
-13	898618	-2673420	-55420	2bbo-UWC	2.23E-04	**99**	fo
-13	898618	-2673420	-55420	2bbo-UWC	1.96E-04	**99**	fo
-16	898618	-2673420	-55420	2an-UWG2	1.98E-04		
-16	898618	-2673420	-55420	2an-UWG2	2.05E-04		
-16	898618	-2673420	-55420	2an-UWG2	2.17E-04		
-16	898618	-2673420	-55420	2an-UWG2	1.97E-04		
-12	898618	-2673420	-55420	2an-UWG2	9.76E-03	**99**	fo
-13	898618	-2673420	-55420	2an-UWG2	9.80E-03	**99**	fo
-12	898618	-2673420	-55420	2an-UWG2	9.97E-03	**99**	fo
-12	898618	-2673420	-55420	2an-UWG2	1.03E-02	**99**	fo
-13	898618	-2673420	-55420	2an-UWG2	2.33E-04	**99**	fo
-12	898618	-2673420	-55420	2an-UWG2	2.43E-04	**99**	fo
-15	898618	-2673420	-55420	2an-UWG2	2.02E-04	**99**	fo
-14	898618	-2673420	-55420	2an-UWG2	2.04E-04	**99**	fo
-15	898618	-2673420	-55420	2an-UWG2	2.36E-04	**99**	fo
-14	898618	-2673420	-55420	2an-UWG2	2.83E-04	**99**	fo
-14	898618	-2673420	-55420	2an-UWG2	1.95E-04	**99**	fo
-14	898618	-2673420	-55420	2an-UWG2	1.94E-04	**99**	fo
-16	898618	-2673420	-55420	2an-UWG2	1.63E-04		
-16	898618	-2673420	-55420	2an-UWG2	1.67E-04		

-16	898618	-2673420	-55420	2an-UWG2	1.70E-04		
-16	898618	-2673420	-55420	2an-UWG2	1.59E-04		
-13	898618	-2673420	-55420	2an-UWG2	2.40E-04	**99**	fo
-12	898618	-2673420	-55420	2an-UWG2	2.18E-04	**99**	fo
-13	898618	-2673420	-55420	2an-UWG2	1.51E-04	**99**	fo
-13	898618	-2673420	-55420	2an-UWG2	2.12E-04	**99**	fo
-14	898618	-2673420	-55420	2an-UWG2	1.95E-04	**99**	fo
-12	898618	-2673420	-55420	2an-UWG2	2.25E-04	**99**	fo
-12	898618	-2673420	-55420	2an-UWG2	2.03E-04	**99**	fo
-12	898618	-2673420	-55420	2an-UWG2	1.74E-04	**99**	fo
-11	898618	-2673420	-55420	2an-UWG2	1.77E-04	**99**	fo
-12	898618	-2673420	-55420	2an-UWG2	2.59E-04	**99**	fo
-10	898618	-2673420	-55420	2an-UWG2	2.16E-04	**99**	fo
-10	898618	-2673420	-55420	2an-UWG2	2.09E-04	**99**	fo
-15	898618	-2673420	-55420	2an-UWG2	1.62E-04		
-16	898618	-2673420	-55420	2an-UWG2	1.63E-04		
-16	898618	-2673420	-55420	2an-UWG2	1.63E-04		
-16	898618	-2673420	-55420	2an-UWG2	1.57E-04		
-6	898618	-2673420	-55420	2an-UWG2	8.36E-05		
-6	898618	-2673420	-55420	2an-UWG2	8.61E-05		
-7	898618	-2673420	-55420	2an-UWG2	8.76E-05		
-7	898618	-2673420	-55420	2an-UWG2	8.83E-05		
-8	898618	-2673420	-55420	2an-UWG2	1.38E-04	**99**	fo
-9	898618	-2673420	-55420	2an-UWG2	1.83E-04	**99**	fo
-9	898618	-2673420	-55420	2an-UWG2	1.82E-04	**99**	fo
-9	898618	-2673420	-55420	2an-UWG2	1.52E-04	**99**	fo
-9	898618	-2673420	-55420	2an-UWG2	1.82E-04	**99**	fo
-9	898618	-2673420	-55420	2an-UWG2	1.52E-04	**99**	fo
-9	898618	-2673420	-55420	2an-UWG2	1.79E-04	**99**	fo
-8	898618	-2673420	-55420	2an-UWG2	1.44E-04	**99**	fo
-8	898618	-2673420	-55420	2an-UWG2	1.51E-04	**99**	fo
-9	898618	-2673420	-55420	2an-UWG2	1.51E-04	**99**	fo
-9	898618	-2673420	-55420	2an-UWG2	1.50E-04	**99**	fo
-8	898618	-2673420	-55420	2an-UWG2	1.57E-04	**99**	fo
-8	898618	-2673420	-55420	2ccn-UWG	1.05E-04		
-8	898618	-2673420	-55420	2ccn-UWG	9.98E-05		
-7	898618	-2673420	-55420	2ccn-UWG	9.42E-05		
-7	898618	-2673420	-55420	2ccn-UWG	9.24E-05		

-9	898618	-2673420	-55420	2ccn-g12x	1.18E-04	**99**	fo
-9	898618	-2673420	-55420	2ccn-g12x	1.20E-04	**99**	fo
-9	898618	-2673420	-55420	2ccn-g12x	1.29E-04	**99**	fo
-9	898618	-2673420	-55420	2ccn-g12x	7.49E-04	**99**	fo
-8	898618	-2673420	-55420	2ccn-g12x	1.54E-04	**99**	fo
-9	898618	-2673420	-55420	2ccn-g12x	1.51E-04	**99**	fo
-8	898618	-2673420	-55420	2ccn-g12x	1.62E-04	**99**	fo
-8	898618	-2673420	-55420	2ccn-g12x	1.64E-04	**99**	fo
-9	898618	-2673420	-55420	2ccn-g12x	1.56E-04	**99**	fo
-9	898618	-2673420	-55420	2ccn-g12x	1.38E-04	**99**	fo
-9	898618	-2673420	-55420	2ccn-g12x	1.54E-04	**99**	fo
-8	898618	-2673420	-55420	2ccn-g12x	1.98E-04	**99**	fo
-8	898618	-2673420	-55420	2ccn-UWG	1.05E-04		
-8	898618	-2673420	-55420	2ccn-UWG	1.05E-04		
-8	898618	-2673420	-55420	2ccn-UWG	1.09E-04		
-8	898618	-2673420	-55420	2ccn-UWG	1.13E-04		
-8	898618	-2673420	-55420	2ccn-g12x	1.47E-04	**99**	fo
-9	898618	-2673420	-55420	2ccn-g12x	1.30E-04	**99**	fo
-9	898618	-2673420	-55420	2ccn-g12x	1.21E-04	**99**	fo
-9	898618	-2673420	-55420	2ccn-g12x	2.87E-04	**99**	fo
-8	898618	-2673420	-55420	2ccn-g12x	1.92E-04	**99**	fo
-9	898618	-2673420	-55420	2ccn-g12x	1.39E-04	**99**	fo
-8	898618	-2673420	-55420	2ccn-g12x	1.12E-04	**99**	fo
-9	898618	-2673420	-55420	2ccn-g12x	1.07E-04	**99**	fo
-8	898618	-2673420	-55420	2ccn-g12x	1.11E-04	**99**	fo
-8	898618	-2673420	-55420	2ccn-g12x	1.48E-04	**99**	fo
-8	898618	-2673420	-55420	2ccn-g12x	2.20E-04	**99**	fo
-8	898618	-2673420	-55420	2ccn-g12x	1.37E-04	**99**	fo
-8	898618	-2673420	-55420	2ccn-UWG	1.04E-04		
-8	898618	-2673420	-55420	2ccn-UWG	1.01E-04		
-8	898618	-2673420	-55420	2ccn-UWG	1.01E-04		
-8	898618	-2673420	-55420	2ccn-UWG	9.30E-05		
-5	898618	-2673420	-55420	2ccn-UWG	1.36E-04	**99**	fo
-6	898618	-2673420	-55420	2ccn-UWG	1.41E-04	**99**	fo
-6	898618	-2673420	-55420	2ccn-UWG	1.50E-04	**99**	fo
-6	898618	-2673420	-55420	2ccn-UWG	1.53E-04	**99**	fo
-5	898618	-2673420	-55420	2ccn-UWG	1.50E-04	**99**	fo
-5	898618	-2673420	-55420	2ccn-UWG	1.80E-04	**99**	fo

-5	898618	-2673420	-55420	2ccn-UWG	1.66E-04	**99**	fo
-4	898618	-2673420	-55420	2ccn-UWG	1.07E-04	**99**	fo
-5	898618	-2673420	-55420	2ccn-UWG	9.68E-05	**99**	fo
-5	898618	-2673420	-55420	2ccn-UWG	1.09E-04	**99**	fo
-5	898618	-2673420	-55420	2ccn-UWG	2.00E-04	**99**	fo
-8	898618	-2673420	-55420	2ccn-UWG	1.22E-04		
-9	898618	-2673420	-55420	2ccn-UWG	1.03E-04		
-9	898618	-2673420	-55420	2ccn-UWG	1.04E-04		
-9	898618	-2673420	-55420	2ccn-UWG	1.04E-04		

-9	898620	-2664092	-54003	2ccn-UWG	8.18E-05		
-9	898620	-2664092	-54003	2ccn-UWG	8.34E-05		
-9	898620	-2664092	-54003	2ccn-UWG	8.34E-05		
-8	898620	-2664092	-54003	2ccn-UWG	8.28E-05		
-4	898620	-2664092	-54003	2ccn-UWG	1.82E-04	**99**	fo
-5	898620	-2664092	-54003	2ccn-UWG	1.68E-04	**99**	fo
-5	898620	-2664092	-54003	2ccn-UWG	1.89E-04	**99**	fo
-4	898620	-2664092	-54003	2ccn-UWG	1.77E-04	**99**	fo
-4	898620	-2664092	-54003	2ccn-UWG	1.57E-04	**99**	fo
-4	898620	-2664092	-54003	2ccn-UWG	1.09E-04	**99**	fo
-5	898620	-2664092	-54003	2ccn-UWG	1.27E-04	**99**	fo
-4	898620	-2664092	-54003	2ccn-UWG	1.79E-04	**99**	fo
-4	898620	-2664092	-54003	2ccn-UWG	2.00E-04	**99**	fo
-5	898620	-2664092	-54003	2ccn-UWG	1.05E-04	**99**	fo
-5	898620	-2664092	-54003	2ccn-UWG	2.80E-04	**99**	fo
-6	898620	-2664092	-54003	2ccn-UWG	7.80E-05		
-6	898620	-2664092	-54003	2ccn-UWG	8.03E-05		
-6	898620	-2664092	-54003	2ccn-UWG	8.28E-05		
-6	898620	-2664092	-54003	2ccn-UWG	7.84E-05		
-6	898620	-2664092	-54003	2ccn-UWG	8.62E-05	**99**	fo
-7	898620	-2664092	-54003	2ccn-UWG	1.38E-04	**99**	fo
-7	898620	-2664092	-54003	2ccn-UWG	1.08E-04	**99**	fo
-7	898620	-2664092	-54003	2ccn-UWG	1.39E-04	**99**	fo
-7	898620	-2664092	-54003	2ccn-UWG	2.03E-04	**99**	fo
-7	898620	-2664092	-54003	2ccn-UWG	1.41E-04	**99**	fo
-7	898620	-2664092	-54003	2ccn-UWG	1.46E-04	**99**	fo
-6	898620	-2664092	-54003	2ccn-UWG	1.57E-04	**99**	fo
-6	898620	-2664092	-54003	2ccn-UWG	2.19E-04	**99**	fo
-7	898620	-2664092	-54003	2ccn-UWG	1.58E-04	**99**	fo

-7	898620	-2664092	-54003	2ccn-UWG	2.07E-04	**99**	fo	
-6	898620	-2664092	-54003	2ccn-UWG	1.48E-04	**99**	fo	
-7	898620	-2664092	-54003	2ccn-UWG	8.23E-05			
-6	898620	-2664092	-54003	2ccn-UWG	8.06E-05			
-6	898620	-2664092	-54003	2ccn-UWG	8.10E-05			
-6	898620	-2664092	-54003	2ccn-UWG	8.09E-05			
~~-8~~	~~898620~~	~~-2664092~~	~~-54003~~	~~2ccn-g14/~~	~~4.42E-03~~	~~**99**~~	~~fo~~	~~humite~~
-7	898620	-2664092	-54003	2ccn-g14/	1.36E-04	**99**	fo	
-6	898620	-2664092	-54003	2ccn-g14/	1.05E-04	**99**	fo	
-6	898620	-2664092	-54003	2ccn-g14/	4.58E-04	**99**	fo	
-8	898620	-2664092	-54003	2ccn-g14/	1.24E-04	**99**	fo	
-7	898620	-2664092	-54003	2ccn-g14/	2.45E-04	**99**	fo	
-7	898620	-2664092	-54003	2ccn-g14/	1.45E-04	**99**	fo	
-7	898620	-2664092	-54003	2ccn-g14/	7.19E-04	**99**	fo	
-8	898620	-2664092	-54003	2ccn-g14/	2.15E-04	**99**	fo	
-7	898620	-2664092	-54003	2ccn-g14/	1.69E-04	**99**	fo	
-9	898620	-2664092	-54003	2ccn-UWG	8.27E-05			
-9	898620	-2664092	-54003	2ccn-UWG	7.81E-05			
-9	898620	-2664092	-54003	2ccn-UWG	7.70E-05			
-9	898620	-2664092	-54003	2ccn-UWG	8.57E-05			
-7	898620	-2664092	-54003	UWG2 std	9.55E-05			
-7	898620	-2664092	-54003	UWG2 std	9.66E-05			
-8	898620	-2664092	-54003	UWG2 std	9.96E-05			
-8	898620	-2664092	-54003	UWG2 std	1.00E-04			
-22	898620	-2664092	-54003	UWG2 std	6.98E-05	**99**	fo	
-22	898620	-2664092	-54003	UWG2 std	7.96E-05	**99**	fo	
-22	898620	-2664092	-54003	UWG2 std	7.42E-05	**99**	fo	
-22	898620	-2664092	-54003	UWG2 std	7.61E-05	**99**	fo	
-23	898620	-2664092	-54003	UWG2 std	1.29E-04	**99**	fo	
37	898620	-2664092	-54003	UWG2 std	6.51E-05	**99**	fo	
35	898620	-2664092	-54003	UWG2 std	1.29E-04	**99**	fo	
40	898620	-2664092	-54003	UWG2 std	1.51E-04	**99**	fo	
-3	898620	-2664092	-54003	2bo-g17/	1.75E-04	**99**	fo	
-4	898620	-2664092	-54003	2bo-g17/	1.56E-04	**99**	fo	
-4	898620	-2664092	-54003	2bo-g17/	1.85E-04	**99**	fo	
-4	898620	-2664092	-54003	2bo-g17/	1.62E-04	**99**	fo	
-6	898620	-2664092	-54003	UWG2 std	8.09E-05			

-6	898620	-2664092	-54003	UWG2 std	8.63E-05		
-6	898620	-2664092	-54003	UWG2 std	8.72E-05		
-6	898620	-2664092	-54003	UWG2 std	8.85E-05		
-21	898620	-2664092	-54003	2bo-g11/	7.82E-05	**99**	fo
-21	898620	-2664092	-54003	2bo-g11/	1.72E-04	**99**	fo
-20	898620	-2664092	-54003	2bo-g11/	1.98E-04	**99**	fo
-21	898620	-2664092	-54003	2bo-g11/	1.45E-04	**99**	fo
-21	898620	-2664092	-54003	2bo-g11/	1.47E-04	**99**	fo
-20	898620	-2664092	-54003	2bo-g11/	1.69E-04	**99**	fo
-20	898620	-2664092	-54003	2bo-g11/	2.10E-04	**99**	fo
-5	898620	-2664092	-54003	2bo-g11/	1.98E-04	**99**	fo
-4	898620	-2664092	-54003	2bo-g11/	1.92E-04	**99**	fo
-4	898620	-2664092	-54003	2bo-g11/	1.90E-04	**99**	fo
-6	898620	-2664092	-54003	UWG2 std	1.06E-04		
-6	898620	-2664092	-54003	UWG2 std	1.07E-04		
-6	898620	-2664092	-54003	UWG2 std	1.26E-04		
-7	898620	-2664092	-54003	UWG2 std	1.15E-04		
-3	898620	-2664092	-54003	2bo-g11/	1.69E-04	**99**	fo
-3	898620	-2664092	-54003	2bo-g11/	2.02E-04	**99**	fo
-2	898620	-2664092	-54003	2bo-g11/	1.62E-04	**99**	fo
-3	898620	-2664092	-54003	2bo-g11/	1.91E-04	**99**	fo
-3	898620	-2664092	-54003	2bo-g11/	2.12E-04	**99**	fo
-4	898620	-2664092	-54003	2bo-g11/	2.12E-04	**99**	fo
1	898620	-2664092	-54003	2bo-g11/	8.60E-05	**99**	fo
1	898620	-2664092	-54003	2bo-g11/	9.06E-05	**99**	fo
0	898620	-2664092	-54003	2bo-g11/	1.09E-04	**99**	fo
0	898620	-2664092	-54003	2bo-g11/	9.78E-05	**99**	fo
0	898620	-2664092	-54003	2bo-g11/	1.50E-04	**99**	fo
-1	898620	-2664092	-54003	2bo-g11/	1.45E-04	**99**	fo
-5	898620	-2664092	-54003	UWG2 std	1.08E-04		
-6	898620	-2664092	-54003	UWG2 std	9.19E-05		
-6	898620	-2664092	-54003	UWG2 std	8.72E-05		
-6	898620	-2664092	-54003	UWG2 std	8.57E-05		
0	898620	-2664092	-54003	2bo-g8/	1.47E-04	**99**	fo
0	898620	-2664092	-54003	2bo-g8/	1.47E-04	**99**	fo
0	898620	-2664092	-54003	2bo-g8/	1.50E-04	**99**	fo
-1	898620	-2664092	-54003	2bo-g8/	1.71E-04	**99**	fo
0	898620	-2664092	-54003	2bo-g8/	6.85E-04	**99**	fo

0	898620	-2664092	-54003	2bo-g8/	1.83E-04	**99**	fo
0	898620	-2664092	-54003	2bo-g8/	2.09E-04	**99**	fo
2	898620	-2664092	-54003	2bo-g8/	3.87E-04	**99**	fo
1	898620	-2664092	-54003	2bo-g8/	3.04E-04	**99**	fo
0	898620	-2664092	-54003	2bo-g8/	1.37E-04	**99**	fo
0	898620	-2664092	-54003	2bo-g8/	2.03E-04	**99**	fo
1	898620	-2664092	-54003	2bo-g8/	1.67E-04	**99**	fo
-5	898620	-2664092	-54003	UWG2 std	8.97E-05		
-5	898620	-2664092	-54003	UWG2 std	9.28E-05		
-6	898620	-2664092	-54003	UWG2 std	8.84E-05		
0	898620	-2664092	-54003	UWG2 std	8.77E-05		
1	898620	-2664092	-54003	2bo-g8/	1.67E-04	**99**	fo
1	898620	-2664092	-54003	2bo-g8/	1.68E-04	**99**	fo
2	898620	-2664092	-54003	2bo-g8/	1.60E-04	**99**	fo
2	898620	-2664092	-54003	2bo-g8/	1.71E-04	**99**	fo
2	898620	-2664092	-54003	2bo-g8/	1.37E-04	**99**	fo
2	898620	-2664092	-54003	2bo-g8/	1.48E-04	**99**	fo
3	898620	-2664092	-54003	2bo-g8/	1.42E-04	**99**	fo
2	898620	-2664092	-54003	2bo-g8/	1.46E-04	**99**	fo
2	898620	-2664092	-54003	2bo-g8/	1.40E-04	**99**	fo
2	898620	-2664092	-54003	2bo-g8/	1.64E-04	**99**	fo
2	898620	-2664092	-54003	2bo-g8/	2.55E-04	**99**	fo
2	898620	-2664092	-54003	2bo-g8/	1.64E-04	**99**	fo
-5	898620	-2664092	-54003	UWG2 std	9.06E-05		
-6	898620	-2664092	-54003	UWG2 std	8.86E-05		
-5	898620	-2664092	-54003	UWG2 std	8.83E-05		
-5	898620	-2664092	-54003	UWG2 std	8.60E-05		
1	898620	-2664092	-54003	2bo-g8/	1.34E-04	**99**	fo
1	898620	-2664092	-54003	2bo-g8/	1.36E-04	**99**	fo
0	898620	-2664092	-54003	2bo-g8/	1.29E-04	**99**	fo
0	898620	-2664092	-54003	2bo-g8/	1.89E-04	**99**	fo
1	898620	-2664092	-54003	2bo-g8/	1.24E-04	**99**	fo
0	898620	-2664092	-54003	2bo-g8/	1.39E-04	**99**	fo
0	898620	-2664092	-54003	2bo-g8/	1.45E-04	**99**	fo
1	898620	-2664092	-54003	2bo-g8/	1.49E-04	**99**	fo
2	898620	-2664092	-54003	2bo-g8/	2.13E-04	**99**	fo
1	898620	-2664092	-54003	2bo-g8/	2.05E-04	**99**	fo
1	898620	-2664092	-54003	2bo-g8/	1.73E-04	**99**	fo
1	898620	-2664092	-54003	2bo-g8/	1.65E-04	**99**	fo
-6	898620	-2664092	-54003	UWG2 std	9.57E-05		

-6	898620	-2664092	-54003	UWG2 std	8.89E-05		
-6	898620	-2664092	-54003	UWG2 std	9.17E-05		
-6	898620	-2664092	-54003	UWG2 std	8.63E-05		

-5	898614	-2664092	-54003	/	9.08E-05		
-5	898614	-2664092	-54003	/	9.98E-05		
-5	898614	-2664092	-54003	/	9.68E-05		
-5	898614	-2664092	-54003	/	9.12E-05		
2	898614	-2664092	-54003	2bo-g8/	1.91E-04	**99**	fo
2	898614	-2664092	-54003	2bo-g8/	1.59E-04	**99**	fo
2	898614	-2664092	-54003	2bo-g8/	2.10E-04	**99**	fo
3	898614	-2664092	-54003	2bo-g8/	1.62E-04	**99**	fo
3	898614	-2664092	-54003	2bo-g8/	1.57E-04	**99**	fo
2	898614	-2664092	-54003	2bo-g8/	2.76E-04	**99**	fo
2	898614	-2664092	-54003	2bo-g8/	1.85E-04	**99**	fo
1	898614	-2664092	-54003	2bo-g8/	1.50E-04	**99**	fo
1	898614	-2664092	-54003	2bo-g8/	1.60E-04	**99**	fo
1	898614	-2664092	-54003	2bo-g8/	1.64E-04	**99**	fo
2	898614	-2664092	-54003	2bo-g8/	1.45E-04	**99**	fo
2	898614	-2664092	-54003	2bo-g8/	1.60E-04	**99**	fo
1	898614	-2664092	-54003	2bo-g8/	1.44E-04	**99**	fo
-5	898614	-2664092	-54003	UWG2 std	7.65E-05		
-5	898614	-2664092	-54003	UWG2 std	7.25E-05		
-6	898614	-2664092	-54003	UWG2 std	7.28E-05		
-5	898614	-2664092	-54003	UWG2 std	7.40E-05		

2	898614	-2664092	-54003	UWG2 std	8.42E-05		
3	898614	-2664092	-54003	UWG2 std	8.67E-05		
1	898614	-2664092	-54003	UWG2 std	8.81E-05		
1	898614	-2664092	-54003	UWG2 std	8.93E-05		
-6	898614	-2664092	-54003	UWG2 std	1.57E-04	**99**	fo
-5	898614	-2664092	-54003	UWG2 std	1.76E-04	**99**	fo
-5	898614	-2664092	-54003	UWG2 std	1.07E-04	**99**	fo
-5	898614	-2664092	-54003	UWG2 std	4.87E-04	**99**	fo
-5	898614	-2664092	-54003	UWG2 std	1.30E-04	**99**	fo
-5	898614	-2664092	-54003	UWG2 std	1.79E-04	**99**	fo
-4	898614	-2664092	-54003	UWG2 std	2.08E-04	**99**	fo
-5	898614	-2664092	-54003	UWG2 std	5.12E-04	**99**	fo
-6	898614	-2664092	-54003	UWG2 std	1.62E-04	**99**	fo

-5	898614	-2664092	-54003	UWG2 std	1.76E-04	**99**	fo
-4	898614	-2664092	-54003	UWG2 std	1.94E-04	**99**	fo
-4	898614	-2664092	-54003	UWG2 std	2.01E-04	**99**	fo
1	898614	-2664092	-54003	2bbo-UWC	1.12E-04		
1	898614	-2664092	-54003	2bbo-UWC	1.05E-04		
2	898614	-2664092	-54003	2bbo-UWC	1.01E-04		
1	898614	-2664092	-54003	2bbo-UWC	1.03E-04		
-4	898614	-2664092	-54003	2bbo-g28/	2.10E-04	**99**	fo
-4	898614	-2664092	-54003	2bbo-g28/	1.79E-04	**99**	fo
-4	898614	-2664092	-54003	2bbo-g28/	2.53E-04	**99**	fo
-5	898614	-2664092	-54003	2bbo-g28/	1.64E-04	**99**	fo
-5	898614	-2664092	-54003	2bbo-g28/	1.87E-04	**99**	fo
-5	898614	-2664092	-54003	2bbo-g28/	1.88E-04	**99**	fo
-4	898614	-2664092	-54003	2bbo-g28/	2.08E-04	**99**	fo
-4	898614	-2664092	-54003	2bbo-g28/	2.16E-04	**99**	fo
-5	898614	-2664092	-54003	2bbo-g28/	2.04E-04	**99**	fo
-4	898614	-2664092	-54003	2bbo-g28/	1.60E-04	**99**	fo
-4	898614	-2664092	-54003	2bbo-g28/	1.59E-04	**99**	fo
-4	898614	-2664092	-54003	2bbo-g28/	1.52E-03	**99**	fo
2	898614	-2664092	-54003	2bbo-UWC	1.11E-04		
1	898614	-2664092	-54003	2bbo-UWC	1.08E-04		
1	898614	-2664092	-54003	2bbo-UWC	1.11E-04		
1	898614	-2664092	-54003	2bbo-UWC	1.11E-04		
-4	898614	-2664092	-54003	2bbo-g28/	3.66E-04	**99**	fo
-4	898614	-2664092	-54003	2bbo-g28/	2.20E-04	**99**	fo
-4	898614	-2664092	-54003	2bbo-g28/	1.88E-04	**99**	fo
-5	898614	-2664092	-54003	2bbo-g28/	2.04E-04	**99**	fo
-5	898614	-2664092	-54003	2bbo-g28/	1.50E-04	**99**	fo
1	898614	-2664092	-54003	2bbo-UWC	1.06E-04		
1	898614	-2664092	-54003	2bbo-UWC	1.01E-04		
1	898614	-2664092	-54003	2bbo-UWC	9.94E-05		
1	898614	-2664092	-54003	2bbo-UWC	9.63E-05		
-25	898614	-2664092	-54003	2bbo-UWC	1.43E-04	**99**	fo
-26	898614	-2664092	-54003	2bbo-UWC	1.35E-04	**99**	fo
-26	898614	-2664092	-54003	2bbo-UWC	1.48E-04	**99**	fo
-26	898614	-2664092	-54003	2bbo-UWC	1.53E-04	**99**	fo
-18	898614	-2664092	-54003	2bbo-UWC	1.43E-04	**99**	fo

-19	898614	-2664092	-54003	2bbo-UWC	1.68E-04	**99**	fo
-19	898614	-2664092	-54003	2bbo-UWC	1.49E-04	**99**	fo
-18	898614	-2664092	-54003	2bbo-UWC	1.42E-04	**99**	fo
-18	898614	-2664092	-54003	2bbo-UWC	1.45E-04	**99**	fo
-18	898614	-2664092	-54003	2bbo-UWC	1.56E-04	**99**	fo
-18	898614	-2664092	-54003	2bbo-UWC	1.50E-04	**99**	fo
-18	898614	-2664092	-54003	2bbo-UWC	1.04E-04	**99**	fo
7	898614	-2664092	-54003	2bbo-UWC	1.12E-04		
7	898614	-2664092	-54003	2bbo-UWC	9.63E-05		
7	898614	-2664092	-54003	2bbo-UWC	1.07E-04		
7	898614	-2664092	-54003	2bbo-UWC	9.63E-05		
-18	898614	-2664092	-54003	2bbo-g14/	9.89E-05	**99**	fo
-18	898614	-2664092	-54003	2bbo-g14/	1.46E-04	**99**	fo
-18	898614	-2664092	-54003	2bbo-g14/	1.31E-04	**99**	fo
-18	898614	-2664092	-54003	2bbo-g14/	1.76E-04	**99**	fo
-18	898614	-2664092	-54003	2bbo-g14/	1.50E-04	**99**	fo
-19	898614	-2664092	-54003	2bbo-g14/	1.70E-04	**99**	fo
-20	898614	-2664092	-54003	2bbo-g14/	1.56E-04	**99**	fo
-18	898614	-2664092	-54003	2bbo-g14/	1.45E-04	**99**	fo
-17	898614	-2664092	-54003	2bbo-g14/	1.97E-04	**99**	fo
-17	898614	-2664092	-54003	2bbo-g14/	1.76E-04	**99**	fo
-17	898614	-2664092	-54003	2bbo-g14/	1.73E-04	**99**	fo
-17	898614	-2664092	-54003	2bbo-g14/	1.56E-04	**99**	fo
-17	898614	-2664092	-54003	2bbo-g14/	1.36E-04	**99**	fo
-18	898614	-2664092	-54003	2bbo-g14/	1.92E-04	**99**	fo
-17	898614	-2664092	-54003	2bbo-g14/	1.71E-04	**99**	fo
7	898614	-2664092	-54003	2bbo-UWC	9.94E-05		
7	898614	-2664092	-54003	2bbo-UWC	9.26E-05		
7	898614	-2664092	-54003	2bbo-UWC	9.42E-05		
7	898614	-2664092	-54003	2bbo-UWC	9.45E-05		
-17	898614	-2664092	-54003	2bbo-g14/	1.79E-04	**99**	fo
-17	898614	-2664092	-54003	2bbo-g14/	2.20E-04	**99**	fo
-18	898614	-2664092	-54003	2bbo-g14/	1.96E-04	**99**	fo
-18	898614	-2664092	-54003	2bbo-g14/	1.81E-04	**99**	fo
-18	898614	-2664092	-54003	2bbo-g14/	1.98E-04	**99**	fo
-17	898614	-2664092	-54003	2bbo-g14/	1.91E-04	**99**	fo
-17	898614	-2664092	-54003	2bbo-g14/	1.50E-04	**99**	fo
-17	898614	-2664092	-54003	2bbo-g14/	1.67E-04	**99**	fo
-17	898614	-2664092	-54003	2bbo-g14/	1.43E-04	**99**	fo
-18	898614	-2664092	-54003	2bbo-g14/	2.05E-04	**99**	fo
-17	898614	-2664092	-54003	2bbo-g14/	2.14E-04	**99**	fo

-18	898614	-2664092	-54003	2bbo-g14/	1.95E-04	**99**	fo
-18	898614	-2664092	-54003	2bbo-g14/	1.76E-04	**99**	fo
-19	898614	-2664092	-54003	2bbo-g14/	2.57E-04	**99**	fo
6	898614	-2664092	-54003	2bbo-UWC	9.43E-05		
6	898614	-2664092	-54003	2bbo-UWC	9.14E-05		
6	898614	-2664092	-54003	2bbo-UWC	9.38E-05		
6	898614	-2664092	-54003	2bbo-UWC	9.02E-05		
11	898614	-2664092	-54003	2bbo-UWC	8.42E-04		
11	898614	-2664092	-54003	2bbo-UWC	8.66E-04		
10	898614	-2664092	-54003	2bbo-UWC	8.75E-04		
10	898614	-2664092	-54003	2bbo-UWC	8.84E-04		
13	898614	-2664092	-54003	2bbo-UWC	6.93E-04	**99**	fo
12	898614	-2664092	-54003	2bbo-UWC	7.42E-04	**99**	fo
13	898614	-2664092	-54003	2bbo-UWC	7.41E-04	**99**	fo
13	898614	-2664092	-54003	2bbo-UWC	7.26E-04	**99**	fo
13	898614	-2664092	-54003	2bbo-UWC	7.41E-04	**99**	fo
13	898614	-2664092	-54003	2bbo-UWC	7.22E-04	**99**	fo
12	898614	-2664092	-54003	2bbo-UWC	7.38E-04	**99**	fo
12	898614	-2664092	-54003	2bbo-UWC	7.35E-04	**99**	fo
13	898614	-2664092	-54003	2bbo-UWC	7.50E-04	**99**	fo
13	898614	-2664092	-54003	2bbo-UWC	7.52E-04	**99**	fo
13	898614	-2664092	-54003	2bbo-UWC	7.52E-04	**99**	fo
13	898614	-2664092	-54003	2bbo-UWC	7.64E-04	**99**	fo
10	898614	-2664092	-54003	A10-UWG/	9.69E-04		
10	898614	-2664092	-54003	A10-UWG/	9.99E-04		
9	898614	-2664092	-54003	A10-UWG/	1.01E-03		
10	898614	-2664092	-54003	A10-UWG/	1.00E-03		
12	898614	-2664092	-54003	88-8 g10/	7.49E-04	**99**	fo
12	898614	-2664092	-54003	88-8 g10/	7.58E-04	**99**	fo
12	898614	-2664092	-54003	88-8 g10/	7.21E-04	**99**	fo
12	898614	-2664092	-54003	88-8 g10/	7.11E-04	**99**	fo
12	898614	-2664092	-54003	88-8 g10/	7.14E-04	**99**	fo
11	898614	-2664092	-54003	88-8 g10/	7.24E-04	**99**	fo
12	898614	-2664092	-54003	88-8 g10/	7.42E-04	**99**	fo
12	898614	-2664092	-54003	88-8 g10/	7.61E-04	**99**	fo
13	898614	-2664092	-54003	88-8 g10/	7.54E-04	**99**	fo
13	898614	-2664092	-54003	88-8 g10/	7.40E-04	**99**	fo
12	898614	-2664092	-54003	88-8 g10/	7.54E-04	**99**	fo
13	898614	-2664092	-54003	88-8 g10/	7.60E-04	**99**	fo

10	898614	-2664092	-54003	A10-UWG/	9.83E-04		
9	898614	-2664092	-54003	A10-UWG/	1.01E-03		
9	898614	-2664092	-54003	A10-UWG/	1.02E-03		
10	898614	-2664092	-54003	A10-UWG/	1.01E-03		
13	898614	-2664092	-54003	88-8 g10/	7.59E-04	**99**	fo
12	898614	-2664092	-54003	88-8 g10/	7.60E-04	**99**	fo
12	898614	-2664092	-54003	88-8 g10/	7.62E-04	**99**	fo
12	898614	-2664092	-54003	88-8 g10/	7.57E-04	**99**	fo
13	898614	-2664092	-54003	88-8 g10/	7.60E-04	**99**	fo
12	898614	-2664092	-54003	88-8 g10/	7.66E-04	**99**	fo
13	898614	-2664092	-54003	88-8 g10/	7.75E-04	**99**	fo
13	898614	-2664092	-54003	88-8 g10/	7.87E-04	**99**	fo
12	898614	-2664092	-54003	88-8 g10/	7.76E-04	**99**	fo
13	898614	-2664092	-54003	88-8 g10/	7.97E-04	**99**	fo
13	898614	-2664092	-54003	88-8 g10/	7.72E-04	**99**	fo
13	898614	-2664092	-54003	88-8 g10/	7.81E-04	**99**	fo
9	898614	-2664092	-54003	A10-UWG/	9.98E-04		
9	898614	-2664092	-54003	A10-UWG/	1.04E-03		
9	898614	-2664092	-54003	A10-UWG/	1.05E-03		
9	898614	-2664092	-54003	A10-UWG/	1.03E-03		

1
2
3
4
5
6
7
8
9
10

11
12
13
14
15
16
17
18
19
20

21
22
23
24

25
26
27
28
29
30

31
32
33
34
35
36
37
38

39

40
~~41~~
42
~~43~~
44
~~45~~
46
~~47~~
48
~~49~~

50
~~51~~
52
~~53~~
54
~~55~~
56
~~57~~
58
~~59~~

60
61
62

63
64
65
66
67
68
69

70
71
72
73
74
75
76
77
78
79

80
81
82
83
84
85
86
87
88

89

90
91
92
93
94
95
96
97
98
99

100
101
102
103
104
105
106
107
108
109
110
111

112
113
114
115
116
117
118
119
120
121
122
123

124
125
126
127
128
129
130
131
132
133
134
135

136
137
138
139
140
141
142
143
144
145
146
147

148
149
150
151
152
153
154
155
156
157
158
159

160
161
162
163
164
165

166
167
168
169
170

171
172
173
174
175
176
177
178
179
180
181

182
183
184
185
186
187
188
189
190
191

192
193

~~194~~
195
~~196~~
197
~~198~~
199
~~200~~
201
~~202~~
203

204
205
206
207
208
209
210
211
212
213
214
215

216
217
218
219
220
221
222
223
224
225

226
227
228
229
230
231
232
233
234
235
236
237

238
239
240
241
242

243
244
245
246
247
248
249

250
251
252
253
254
255
256
257
258
259
260
261

262
263
264
265
266
267
268
269
270
271
272
273

274
275
276
277
278
279
280
281
282
283
284
285
286

287
288
289
290
291
292
293
294
295

296
297
298

299
300
301
302
303
304
305
306
307
308
309
310

311
312
313
314
315

316
317
318
319
320

321
322
323
324
325
326
327

328
329
330
331
332
333
334
335
336
337
338
339
340
341
342

343
344
345
346
347
348
349
350
351
352
353

354
355
356

357
358
359
360
361
362
363
364
365
366
367
368

369
370
371
372
373
374
375
376
377
378
379
380

381
382
383
384
385
386
387
388
389
390
391
392

	d18O VSMOW	d18Osims	bias	bias rel. to SCOL	Fo#
SCOL	5.32	9.693	4.350	**0**	**89**
NH-Ol	8.9	13.690	4.747	**0.40**	**100**
OR-Ol	5.88	9.586	3.684	**-0.66**	**60**

slope	**0.026**
intercept	**-2.225**

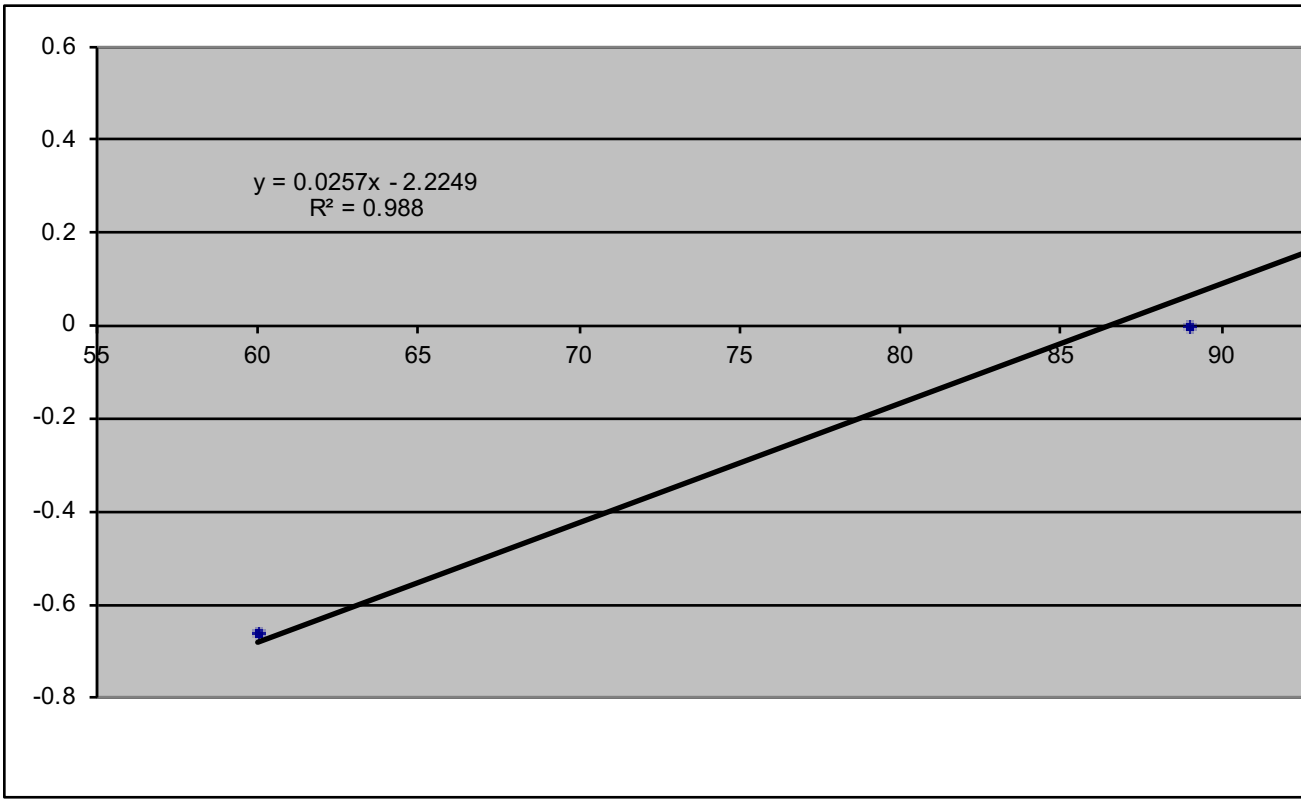

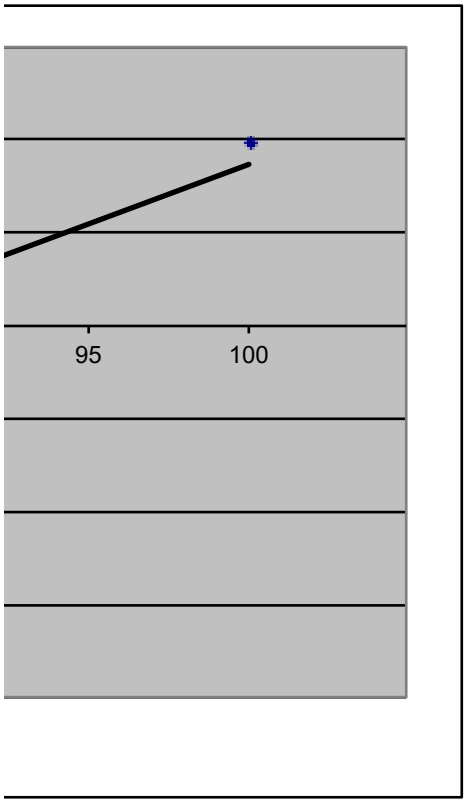
95
100